Novel family of CB2R agonists regulates inflammatory responses

A thesis submitted for the degree of Doctor of Philosophy in Pathology

University of Oxford

Trinity term 2012

Ivy Christou

Sir William Dunn School of Pathology and Lincoln College

Acknowledgments

First I would like to thank my supervisor Professor David Greaves for the opportunity to work in his laboratory and to develop as a scientist. I appreciate your support, your time for the many useful one-to-one, the free reign to follow my own ideas and for the many in vivo experiments we did as a team. I would like to also thank you for improving my teaching and presentation skills and for the opportunity to teach undergraduates and an NYU professor!

I would also like to thank British Heart Foundation for my studentship that enabled me to pursue a PhD debt-free and Lincoln college for accepting me as a graduate, for funding my attendance to an international conference and for encouraging a very social MCR. I would also like to thank Dr Angela Russell and Matteo Giannella-Borradori for the successful collaboration leading to Chapter 3 of my thesis, a patent and a MedChem paper. I would also like to thank Dr Eileen McNeil for her very helpful technical advice and guidance throughout my PhD. Moreover I would like to thank Nigel Rust for his help with flow cytometry experiments and Denise Jeffs for her help with the mouse work. I would also like to thank Dr Wei Zhi Wang for her kind gift of mouse brain cDNA.

To previous and current members of the Greaves lab – Gemma White the Great, for the patience to teach me techniques, for countless advice in all matters and for the funny chats; Rosie Hart for her friendly welcome in the lab and for the advice in flow cytometry and cytotoxicity experiments; Fernando Martinez-Estrada and Thomas Tan for their great advice regarding macrophages and antibodies respectively; Asif Iqbal and Daniel Regan-Komito, that introduced the “friendly banter at your workplace” and kindly proof-read my thesis chapters.

My great friends Maria, Elena, Abie and Costas; thank you for your support, friendship and love whether things are going good or bad and for the laughter every time we meet that makes everything look better. Last but not least, my friends from Oxford – Kristin, you have been the best housemate and an amazing friend; Ntina and Elena thank you for the great times out, the unforgettable game nights and the continuous support.

To Jon – for being everything I wished for; thank you for your love, your friendship, the support in all matters throughout my PhD and for being my partner in crime in all our travelling and adventures.

My family – my sister Elena, my parents Popi and Vassilis and my grandparents. Thank you all for letting me dream big, for supporting and encouraging my aspirations, for being there no matter what, for your advice in all matters and for your unconditional love.

ABSTRACT

Novel family of CB2R agonists regulates inflammatory responses

Ivy Christou, Lincoln College & Sir William Dunn School of Pathology

Submitted for the degree of D.Phil of Pathology, Trinity Term 2012

Inflammation is a multifactorial response towards noxious stimuli, however appropriate regulation and resolution of inflammation is crucial for the prevention of chronic inflammatory diseases such as atherosclerosis. The endocannabinoid (eCB) system is an endogenous immunomodulatory system which consists of a series of lipophilic ligands that signal via two G-protein-coupled receptors. Cannabinoid receptor 1 (CB1R) is mainly expressed in the central nervous system and its activation has psychoactive effects. Cannabinoid receptor 2 (CB2R) is mainly expressed on leukocytes and receptor activation has anti-inflammatory actions in mouse models of atherosclerosis and chronic inflammatory pain. It is considered that CB2R activation is involved in modulation of the recruitment of inflammatory cells, especially monocytes/macrophages; however the exact mechanism of action has not been fully elucidated. We hypothesised that activation of CB2R modulates monocyte/ macrophage recruitment and signalling, thus providing a homeostatic mechanism to limit macrophage activation in inflammatory responses.

The high lipophilicity of cannabinoid ligands and their lack of selectivity for CB2R over CB1R limits CB2R drug development. In collaboration with Dr Angela Russell, we used virtual screening and a CB2R cAMP assay that we validated to discover a novel CB2R agonist, 3-((2'-Cyanobenzyl)thio)-5*H*-[1,2,4]triazino[5,6-*b*]indole, (DIAS2). In collaboration with Dr Russell's group who did chemical synthesis, we extended this novel scaffold to include over 80 compounds. Using the same hCB2R cAMP screening assay we demonstrated that 16 compounds with the same scaffold are at active at CB2R in the nanomolar range. At least 3 compounds, including DIAS2, were found to be ≥ 300-fold selective for CB2R over CB1R in cAMP assays and radioligand binding studies. In the inflammatory model of zymosan-induced peritonitis, DIAS2 dose-dependently inhibited inflammatory monocyte recruitment by 50% at highest dose of 5 mg/kg with no effect on neutrophils. In further zymosan-induced peritonitis experiments 5 mg/kg of DIAS2 and a structurally-similar CB2R agonist from the same family of triazino-indoles inhibited monocyte recruitment while a different CB2R agonist (JWH-133) at 5 mg/kg did not inhibit monocyte recruitment. Analysis of peritoneal exudates showed that the inhibition of monocyte recruitment was not associated with changes in the levels of JE, MIP-1α and nitric oxide but was associated with increased levels of the chemokine KC. Using in vitro cell biology approaches, we demonstrated that 10μM dose of both DIAS2 and JWH-133 reduced forskolin-induced cAMP production in primary murine macrophages. Also 2.5 to 10 μM of JWH-133 and HU-308 dose-dependently induced primary murine macrophage chemotaxis which could be blocked a CB2R antagonist (SR 144528, 1 μM) while DIAS2 at doses up to 10 μM was not a chemoattractant. Accordingly HU-308 and JWH-133 were at least 3-fold more efficacious than DIAS2 at recruiting β-arrestin to the murine CB2R. Moreover in studies with primary murine macrophages 10 μM dose of JWH-133 and HU-308 induced ERK1/2 and Akt phosphorylation within 30 minutes, while 2-AG (an endogenous eCB ligand) and DIAS2 at 10 μM had no such effect.

In summary, we have discovered a novel family CB2R agonists and demonstrated that some devoid of chemotactic active CB2R agonists can reduce monocyte recruitment *in vivo* while other chemoattractant CB2R agonists have no *in vivo* anti-inflammatory effect. We propose that non-chemotactic CB2R agonists represent a new class of anti-inflammatory drugs with a novel mode of action.

Abbreviations

Δ9-THC – Δ9-tetrahydrocannabinol

2-AG – 2-Arachidonyl glycerol

AA – Arachidonic acid

AC – Adenylate cyclase

AEA – Arachidonyl ethanolamide

ANOVA – Analysis of variance

ApoE – Apolipoprotein E

ATP – Adenosine triphosphate

BCA – Bicinchoninic acid

BMDM – Bone marrow derived macrophages

Bp – base pair

BSA – Bovine serum albumin

cAMP – cyclic adenosine monophosphate

CB1R – Cannabinoid receptor 1

CB2R – Cannabinoid receptor 2

cDNA – complementary deoxyribonucleic acid

CFA – Complete Freund ’s adjuvant

CHO – Chinese hamster ovary

CNS – Central Nervous system

CTG – CellTiter-Glo ®

DAPI – 4’,6- diamidino-2-phenylindole

DAMPs – Damage associated molecular patterns

DMSO – Dimethyl sulfoxide

D-PBS – Dulbecco’s phosphate buffered saline

dNTPs – deoxynucleotide triphosphates

eCB – Endocannabinoid system

ECM – Extracellular matrix

EDTA – Ethylenediaminetetracetic acid

EGF – Epidermal growth factor

ELISA – Enzyme linked immunosorbent assay

ERK – Extracellular signal-regulated kinase

FAAH – Fatty-acid amide hydrolase

FACS – Fluorescence activated cell sorting

FCS – Foetal calf serum

FITC – Fluorescein isothiocyanate

fMLP – N-formyl-metionyl-leucine-phenylalanine

GAPDH – Glyceraldehyde 3-phosphate dehydrogenase

GPCR – G-protein coupled receptor

Hck – Haemopoietic cell kinase

HEPES – 4-(2-hydroxyethyl)-piperazine-1-ethanesulfonic acid

HP-β-cyclodextrin – 2-hydroxypropyl cyclodextrin

HRP – Horseradish peroxidase

HTS – High throughput screen

ICAM-1 – Intracellular adhesion molecule-1

IBMX – 1-Methyl-3-isobutylxanthine

IFN – Interferon

Ig – immunoglobulin

IL – Interleukin

i.p. – intraperitoneal

KC – Keratinocyte chemoattractant

KO – Knockout

LDL – Low density lipoprotein

LPI – L-alpha-lysophosphatidylinositol

LPS – Lipopolysaccharide

LTB4 – Leukotriene B4

MAGL – Monoacylglycerol lipase

MAPK – Mitogen activated protein kinase

MCP – Monocyte chemoattractant protein

M-CSF – Macrophage-colony stimulating factor

MIP – Macrophage inflammatory protein

MMLV – Moloney murine leukaemia virus

mRNA – Messenger ribonucleic acid

NF- κB – Nuclear factor-κB

NO – Nitric oxide

Ox-LDL – Oxidised low density lipoprotein

PAMPs – Pathogen associated molecular patterns

PBMC – Peripheral blood mononuclear cell

PCR – Polymerase chain reaction

pDCs – Plasmacytoid dendritic cells

PE – phycoerythrin

PECs – Peritoneal exudate cell

PECAM-1 – Platelet endothelial cell adhesion molecule-1

PI3K – phosphoinositide 3 kinase

PKA – Protein kinase A

PKC – Protein kinase C

PPAR-γ – Peroxisome proliferator-activated receptor-γ

RLU – Relative luminescence units

RPM – Revolutions per minute

RPMI – Roswell Park Memorial Institute medium

PRR – Pattern recognition receptors

ROS – Reactive oxygen species

RT – Room temperature

SD – Standard deviation

SDS-PAGE – Sodium dodecyl sulphate polyacrylamide gel electrophoresis

SEM – Standard error of mean

TBS – Tris buffered saline

TGF – Transforming growth factor

TLR – Toll-like receptor

TNF – Tumour necrosis factor

TRPV1 – Transient receptor potential cation channel subfamily V 1

VCAM-1 – Vascular cell adhesion molecule-1

VLA-4 – Very late antigen-4

VLDL – Very low density lipoprotein (VLDL

VSMCs – Vascular smooth muscle cells

WT – Wild-type

Table of Contents

Table of contents: Figures and Tables

CHAPTER 1 : INTRODUCTION

1.1 Inflammation

The role of the immune system is to defend the body against infections that can occur when bacteria, parasites, fungi or viruses enter the organism. Two phases characterise the body's response to an infection. The first and fastest line of defence is the innate response since it can occur immediately. Prolonged infection (days) leads to activation of the adaptive immune system. Inflammation is the body's response to tissue injury. This injury can be induced by a wide range of stimuli, from live micro-organisms to toxic chemicals and sharp instruments. The cardinal signs of acute inflammation are redness, swelling, heat and pain and the different signs of inflammation suggest a complex interplay of several systems which include many cells types, several receptors and many signalling pathways (Ryan *et al.*, 1977). The usual outcome of inflammation is removal of the injurious stimulant leading to tissue healing.

Initiation of the inflammatory response in the tissue occurs when resident macrophages recognise the pathogen and accordingly release pro-inflammatory cytokines such as interleukin-1β (IL-1β), IL-6 and tumour-necrosis factor-α (TNF-α) as well as chemokines such as IL-8 (CXCL8) (Beutler *et al.*, 2003). The cytokines released during inflammation promote endothelial activation leading to pronounced up-regulation of the surface expression of intracellular-adhesion molecule-1 (ICAM-1) (Dustin *et al.*, 1986), P-selectin, E-selectin and vascular cell adhesion molecule-1

(VCAM-1) (Iiyama *et al.*, 1999). Up regulation of the previously mentioned endothelial-selectins and leukocyte-expressed adhesion molecules, such as L-selectin and very late antigen 4 (VLA-4), leads to leukocytes transiently rolling on the endothelium (Ley *et al.*, 1995; Ley *et al.*, 2007). In later stages of the inflammatory response, further activation of the leukocytes by chemokines leads to integrin clustering which can now interact with their endothelium-expressed ligands leading to reduction of rolling, strong cell adhesion and arrest on the endothelium (Ley *et al.*, 2007; Williams *et al.*, 2011). This adhesion process is followed by leukocyte transmigration through blood vessel walls and finally migration into the tissue towards a chemokine gradient. As well as promoting leukocyte adhesion, chemokines (cytokines inducing cell migration) induce inflammatory cell recruitment down the chemokine gradient.

Key cell types involved in co-ordinating inflammatory responses will be discussed below.

1.1.1 Neutrophils

Neutrophils are a type of polymorphonuclear cells first described by Ehrlich (Ehrlich *et al.*, 1956) and are characterised by a multilobed nucleus surrounded by a granule laden cytoplasm. Neutrophils are the most abundant leukocytes in the blood (~60%), they originate from the bone marrow and they have a short life span. The main functions of neutrophils are bacterial phagocytosis and lysis accompanied by release of inflammatory mediators to promote their bactericidal actions.

During inflammation neutrophils are the first cells to be recruited from the blood in order to deal with the pathogen. In order to recruit neutrophils, activated resident macrophages release chemokines including IL-8 (the mouse homologues are KC (CXCL1 in the mouse) and macrophage inflammatory protein (MIP)-2 (MIP-2 also named as CXCL2 in the mouse)) which recruit cells via the chemokine receptors CXCR1 and CXCR2 (Rovai *et al.*, 1998), while simultaneous production of the inhibitory cytokine IL-10 regulates the inflammatory cell influx (Ajuebor *et al.*, 1999; Cailhier *et al.*, 2005). Moreover, activation of the complement system in the plasma by bacteria leads to a cascade of reactions and the release of the C5a fragment which is a potent chemoattractant for neutrophils (Damerau *et al.*, 1978). Following phagocytosis of pathogens, neutrophils release the contents of at least three types of storage granules into the intracellular phagolysosome containing the pathogen (Smith, 1994). The released granule contents include oxygen free radicals, lactoferrin, lysozyme and other bactericidal proteins such as LL-37 (Borregaard *et al.*, 1997). The variety of granules enables the neutrophil to effectively lyse and eliminate both Gram-negative and Gram-positive bacteria.

Due to their short life span, neutrophils require the help of recruited monocytes to further eliminate pathogens and resolve the on-going inflammatory process. Using mouse models of acute inflammation it has been demonstrated that neutrophils contribute to the production of TNF-α and of the chemokines KC, MIP-1α (CCL3) and RANTES (CCL5) (García-Ramallo *et al.*, 2002). Production of these mediators contributes on maintaining endothelium adhesiveness for the monocytes while the chemokines produced promote monocyte influx to the site. Apart from the release of

chemokines, some bactericidal proteins released also have monocyte chemoattractant abilities. For example LL-37 has been demonstrated to mobilise monocytes in the subcutaneous air pouch model of inflammation (Soehnlein *et al.*, 2008). Moreover exposure of lysophosphatidylcholine by apoptotic neutrophils in turn leads to further monocyte recruitment (Peter *et al.*, 2008). Therefore simultaneous to their bactericidal actions, neutrophils promote the recruitment of monocytes for the second phase of the innate response.

Sometimes the neutrophil cytotoxic contents can be released extra-cellularly and lead to tissue injury. For example in the case of rheumatoid arthritis, it has been demonstrated that neutrophil-derived leukotriene B4 (LTB4) had a crucial role in cartilage destruction and the inflammation of the arthritic joint (Chen *et al.*, 2006). Phagocytosis of apoptotic neutrophils in a non-phlogistic manner is essential to prevent tissue damage from uncontrolled release of the neutrophil's content. Effective clearance of apoptotic neutrophils is an anti-inflammatory process since macrophages release products such as tumour-growth factor-β (TGF-β) and IL-10 which are involved in resolution of inflammation and healing (Savill *et al.*, 2002; Serhan *et al.*, 2005; Soehnlein *et al.*, 2010). Several mediators have been shown to promote macrophage phagocytosis of apoptotic neutrophils, these include the glucocorticoids (Liu *et al.*, 1999), the lipoxins (Maderna *et al.*, 2009a) and annexin-1 (Scannell *et al.*, 2007).

1.1.2 Macrophages and monocytes

Metchnikoff was the first to observe mononuclear phagocytes in the blood and tissue (Metchnikoff, 1905). He considered the cells from the two locations to be functionally identical and gave them the term “macrophages”. Metchnikoff proposed that macrophages were the cells responsible for pathogen clearance in both invertebrates and vertebrates. It is now known that both neutrophils and macrophages can phagocytose pathogens and although neutrophils are more efficient bactericidal cells, macrophages can more effectively deal with immune-evasive bacteria and simultaneously modulate and co-ordinate the neutrophil-initiated immune response (Silva, 2010). Apart from pathogens, macrophages are responsible for the scavenging and clearance of debris and dead cells at the inflammatory site. Moreover they are also involved in initiation of the adaptive immune response, angiogenesis, dealing with cancerous cells as well as secreting a vast array of products upon activation in order to regulate their tissue microenvironment. Macrophages are present in locations such as the peritoneum, the pleura, lungs (alveolar macrophages), lymph nodes, spleen, gut, brain (microglia) and liver (Kupffer cells). They are therefore permanently and strategically located within tissues in order to initiate and orchestrate the inflammatory response.

Identification of the origin of the blood mononuclear phagocyte (monocyte) and their differentiation into the large tissue phagocyte (macrophage) was the aim of many elegant studies. A definitive study by Clark and Clark in amphibians was a key demonstration that when the monocyte leaves the bloodstream to enter a tissue it

develops into a macrophage (Clark *et al.*, 1930). They injected carmine granules into the bloodstream of tadpoles which monocytes then phagocytosed and became pigmented. Fat was then injected into the tissue. Tissue resident macrophages were observed ingesting fat globules but most importantly carmine-containing monocytes were observed emerging from the vessels into the tissue and also ingesting the fat. The monocytes were observed to gradually disintegrate the fat globules and become permanently enlarged while retaining their pigmentation. Regarding the organ origin of the monocyte itself, a pioneering study using tritiated-thymidine to label cell populations and X-ray radiation or splenectomy, demonstrated that monocyte progenitors mainly originate from the bone marrow (van Furth *et al.*, 1968). Only monocyte progenitors in the bone marrow can rapidly proliferate while circulating blood monocytes and peritoneal macrophages are terminally differentiated (van Furth *et al.*, 1968). Overall these studies were crucial for demonstrating convincingly what is now a well-accepted process in most species, thus during injury monocytes progenitors migrate from the bone marrow to the blood and are then actively recruited to tissues where they differentiate into macrophages.

Macrophages can be activated by a range of stimuli and they rely on their pattern recognition receptors (PRR) to identify conserved non-self motifs such as pathogen associated molecular patterns (PAMPs) and self-derived damage-associated molecular patterns (DAMPs). PRRs include the family of the Toll-like receptors and the related families of NOD-like receptors and RIG-I-like receptors. Toll-like receptors (TLR) are involved in the recognition of microbial PAMPs, which range from bacterial and yeast cell wall components such as lipopolysaccharides (LPS) and

zymosan respectively, to double stranded RNA and unmethylated DNA from bacteria and viruses (Kawai *et al.*, 2011). The intracellular NOD-like receptors can identify products from damaged cells, such as ATP, as well as microbial peptidoglycan breakdown products (Creagh *et al.*, 2006). On the other hand, RIG-I-like receptors are intracellular receptors that can identify virally-derived nucleic acids (Kato *et al.*, 2005). Overall, macrophages have the capacity to respond to a variety of danger-signals and mount crucial specialized responses to deal with the presented danger.

Following TLR activation, production of interferon (IFN)-γ from either Th1 lymphocytes (adaptive immunity) or natural killer cells (innate immunity), is crucial for rapid priming of macrophages which is needed for potent microbicidal and inflammatory activity of macrophages (Dalton *et al.*, 1993; Hu *et al.*, 2008; Schultz *et al.*, 1983). The activation state of the macrophage that consists of IFN-γ priming and TLR activation is known as “classical” or “M1”. M1-macrophages have an inflammatory role and the capacity to release a variety of pro-inflammatory cytokines and chemokines with the aim to participate in Th1-mediated responses to eliminate viruses and bacteria (Mantovani *et al.*, 2002; Mills *et al.*, 2000).

Separating the macrophage phenotypes into different activation states depending on cytokine stimulus is an extensively researched area. Two main macrophage activation subtypes have been identified while a few others are still debated due to possible macrophage plasticity (Table 1) (Mosser *et al.*, 2008; Murray *et al.*, 2011). M1-macrophages have the ability to release a vast diversity of secreted factors with

different roles in inflammation. M1-macrophages can produce the pro-inflammatory cytokines IL-6, TNF-α and IL-12. Notably TLR activation only releases the pro-protein of the other key inflammatory cytokine IL-1β and simultaneous activation of NOD-like receptor, one part of the inflammasome complex, is needed for the proteolytic cleavage of pro-IL-1β and release of active IL-1β (Agostini *et al.*, 2004). TNF-α and IL-6 are involved in autocrine activation of macrophages while TNF-α and IL-1β also induce endothelial activation and increase vascular permeability. Moreover IL-1β, IL-12 and IL-6 are involved in differentiation and/or activation of T lymphocytes (T cells) in adaptive immunity (Kopf *et al.*, 2010) . Reactive oxygen species (ROS) and nitric oxide (NO) have a key a role in killing pathogens either by directly oxidizing the pathogen's membrane or promoting the acidic conditions in the cell's phagosome enabling membrane penetration and destruction of the pathogen (Wink *et al.*, 2011). M1-macrophages also release chemokines such as IL-8 and monocyte chemoattractant protein-1 (MCP-1, CCL2), which are involved in adhesion and recruitment of monocytes, neutrophils and T-cells.

Macrophages	Functions/Diseases	Stimulus	Products
M1 macrophages (classical)	Crucial inflammatory role in clearance of bacteria and viruses Prolonged inflammation involved in the pathogenesis of atherosclerosis and rheumatoid arthritis	PAMPs from bacteria and viruses + IFN-γ from Th1 cells/ Natural killer cells OR DAMPs from within organism such as ATP	TNF-α
			IL-1β
			IL-6
			IL-12
			Nitric oxide
			Chemokines: IL-8, MCP-1, RANTES
M2 macrophages (alternative) (also suggested to be named as M2a)	1) Protective for parasite and allergic responses 2) Modulation of M1-macrophage responses in chronic inflammatory diseases 3) Tissue repair and remodelling Overactivation linked with pathogenesis of chronic airway disease such as asthma and Chronic Obstructive Pulmonary Disease	Th2-related responses: IL-4 and IL-13	Low levels of IL-10
			Low levels of TGF-β
			Proline (collagen precursor)
			Fibronectin
			IL-1R antagonist
			Polyamines (arginase enzymatic pathway)
M2b-macrophages (Regulatory)	Immunosuppression	IL-10 TGF-β Glucocorticoids Apoptotic cells	IL-10 (high levels)
			TGF-β
			Annexin-1 (mainly Glucocorticoids)

Table 1. Different macrophage activation states have distinct functions

Macrophages can be activated by a range of stimuli and can adopt distinct phenotypes according to their activation. Following activation with PAMPs/DAMPs in the presence of IFN-γ, macrophages acquire a highly inflammatory and cytotoxic phenotype in order to terminate the pathogenic insult. Macrophage activation by Th2 related cytokines IL-4 and IL-13, leads to an alternative activation status which promotes tissue repair and protects against allergens and parasites. Little is known about the third macrophage phenotype which is considered regulatory and encompasses several unrelated anti-inflammatory stimuli such as glucocorticoids and IL-10. Importantly macrophages can distinguish between several stimuli and accordingly produce minute or high amounts of some of their products (Byers *et al.*, 2011; Gordon, 2003; Mosser *et al.*, 2008).

Apart from “classical” inflammatory macrophages, a second established macrophage phenotype when the cells are activated with IL-4 and IL-13 produced by Th2 cells or eosinophils, is known as “M2” or “alternative”. M2-macrophages have a regulatory role in association with Th2 cells in responses against parasites, allergy and tissue remodelling (Gordon *et al.*, 2010; Varin *et al.*, 2009). For example, M2-macrophages can modulate inflammation due to their higher production of the anti-inflammatory cytokine IL-10 (Schebesch *et al.*, 1997) while activation of monocytes and macrophages with IL-4 reduced their LPS-induced expression of IL-6 and IL-1β (Cheung *et al.*, 1990; Hart *et al.*, 1995). Additionally, M2-macrophages have increased expression of arginase which is involved in diverting the essential precursor L-Arginine away from the NO production pathway (Munder *et al.*, 1998). Importantly, activation of macrophages with IL-4 and IL-13 inhibits IFN-γ mediated killing of intracellular pathogens such as *Mycobacterium tuberculosis* and thus modulates macrophage antimicrobial activity (Harris *et al.*, 2007). M2-macrophages are also involved in tissue remodelling by the production of extracellular matrix (ECM) components such as fibronectin (Gratchev *et al.*, 2001). For further information on other less defined macrophage activation states please refer to Table 1.

In summary, neutrophils and macrophages are crucially involved in the initiation and progression of inflammatory responses. Regulation of particularly macrophage activation could inhibit chronic inflammation which is involved in the pathogenesis of many inflammatory diseases such as atherosclerosis.

1.2 The endocannabinoid system and immune regulation

1.2.1 The endocannabinoid system

The endocannabinoid system (eCB) is an endogenous signalling system that has a modulating role in pain perception, food intake, energy metabolism, intestinal motility, immune responses and mood (Grant *et al.*, 2005; Howlett *et al.*, 2002). The eCB consists of at least two distinct membrane receptors, along with the endocannabinoid ligands, the endocannabinoid membrane transporter and endocannabinoid metabolizing enzymes (Figure 1.1).

1.2.1.1 **Receptors of the endocannabinoid system**

For hundreds of years, cannabis has been a popular drug that has been used both recreationally and medicinally for the treatment of pain (Mikuriya, 1969). Decades of experimental studies starting from the 1940's identified the phytocannabinoid Δ9-tetrahydrocannabinol (Δ9-THC) to be the psychoactive component of *Cannabis sativa* (also known as marijuana) responsible for dependence and sedation (Pertwee, 2006). Although the existence of cannabinoid receptors was a highly debated subject, pioneering studies from the lab of Howlett in the 1980's demonstrated that cannabinoids, both the phytocannabinoid Δ9-THC and its synthetic analog CP-55940, could regulate cyclic adenosine monophosphate (cAMP) production via adenylate cyclase (Howlett, 1987) thus indicating the presence of G protein-coupled receptors (GPCRs).

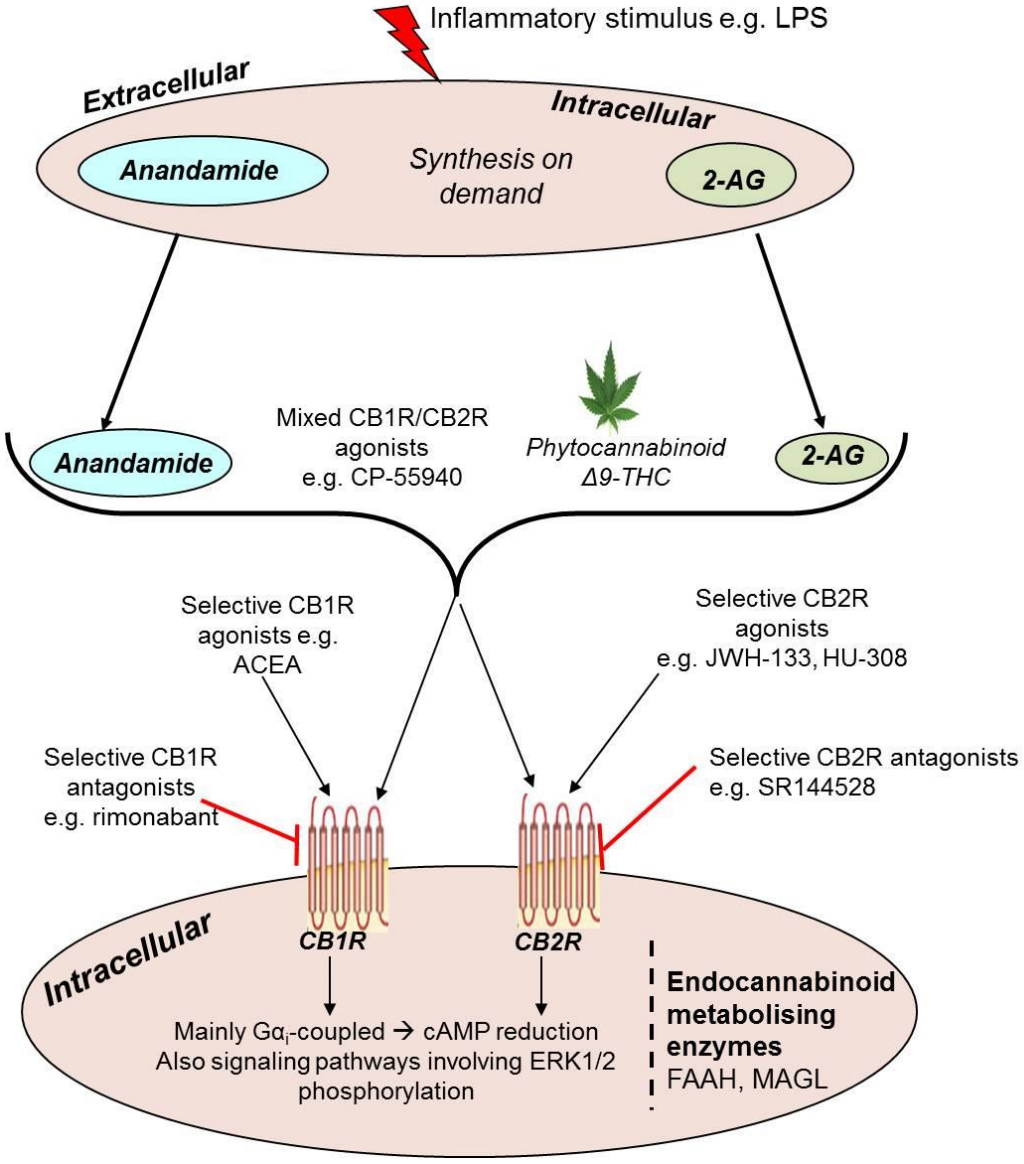

Figure 1.1: A general overview of the endocannabinoid system
Upon receiving an inflammatory stimulus, cells with the capacity to produce endocannabinoid receptor ligands such as tissue resident or recruited macrophages synthesise 2-AG and/or anandamide on demand. Once the ligands are released in the extracellular environment they can activate the endocannabinoid GPCRs CB1R and CB2R, which are mainly expressed in the CNS and immune system respectively. In inflammatory conditions target cells could be the endothelial cells or recruited monocytes/macrophages. Both CB1R and CB2R are $G\alpha_i$-coupled receptors and their activation reduces the cellular cAMP levels and thus inhibits the cAMP-dependent signalling pathways within the cell. Another cannabinoid-mediated signalling pathway is regulation of the ERK1/2 phosphorylation. Endogenous ligands can be degraded by the metabolising enzymes FAAH and MAGL, whose expression is cell dependent and can be modulated by inflammation.

The two well established cannabinoid receptors (CBR) are CB1R and CB2R and they are seven-transmembrane GPCRs. In 1990, CB1R was the first cannabinoid receptor to be identified and cloned from the brain with Δ9-THC demonstrating a CB1R-dependent down-regulation of cAMP production (Matsuda *et al.*, 1990). Subsequently, a second cannabinoid receptor (CB2R) which also had the ability to bind to Δ9-THC and CP-55940, was identified and cloned from splenic macrophages (Munro *et al.*, 1993). Like other $G\alpha_i$-protein coupled receptors, activation of CB1R and CB2R by their specific ligands leads to inhibition of the enzyme adenylate cyclase (AC), which is responsible for the production of cAMP, and thus activation of the receptors by ligands leads to down-regulation of intracellular cAMP levels (Matsuda *et al.*, 1990; Slipetz *et al.*, 1995). Interestingly in some yet not understood situations CB1R can become coupled to $G\alpha_s$-proteins (Glass *et al.*, 1997). Cannabinoid receptor activation has also been linked with other downstream pathways such as activation of the signalling pathways of phosphoinositide3-kinase (PI3K) and mitogen-activated protein kinase (MAPK) and regulation of extracellular signal-regulated kinases (ERK) 1/2 phosphorylation (Howlett *et al.*, 2004).

It has been consistently shown that CB1R is mainly distributed at different brain regions and at the presynaptic terminals of neuronal subpopulations in the central nervous system (CNS), mainly at the hippocampus and cerebellum (Herkenham *et al.*, 1990; Iversen, 2003). Conversely CB2R is mainly expressed in immune cells with CB2R mRNA identified in B lymphocytes (B cells), natural killer cells, monocytes and peripheral macrophages, neutrophils and T cells in this order of expression (Galiegue *et al.*, 1995). Specifically in macrophage populations, CB2R mRNA has

been found in peritoneal macrophages, splenic macrophages and microglia. However CB1R and CB2R expression is not exclusive to the aforementioned locations. CB1R mRNA is weakly expressed on macrophages and B-cells and in comparison to CB2R is of the range of 1-10% (Di Marzo *et al.*, 1999; Galiegue *et al.*, 1995). Regarding the presence of CB2R in the CNS, recent studies have demonstrated that the receptor is indeed expressed at locations such as the brain stem, hippocampus, neurons, glial cells and cerebellum (Onaivi *et al.*, 2012), albeit to a lesser extent than in immune cells. The discrepancies between CB2R expression data are likely due to the recent identification of a second isoform of CB2R (CB2A isoform) which has higher expression in the brain rather than the periphery while the second and most-studied isoform (CB2B isoform) has higher expression in the peripheral tissues rather than the brain (Liu *et al.*, 2009). It should be noted that identifying the protein expression of the receptors in some species has proven challenging due to the lack of high quality specific anti-CB1R and anti-CB2R antibodies.

1.2.1.2 **Endocannabinoid ligands**

Five endogenous endocannabinoid ligands have been identified while related endogenous lipids are constantly being discovered. The two main, most abundant and hence best studied eCB ligands are arachidonylethanolamide (anandamide, AEA) and 2-arachidonoylglycerol (2-AG) (Pacher *et al.*, 2006). The other endocannabinoids are virodhamine, noladin ether and arachidonoyl dopamine. At basal conditions in tissues and bodily fluid, 2-AG and AEA have been found in

nanomolar to micromolar concentrations at plasma, adipose, heart, spleen and brain tissue of several species (Zoerner *et al.*, 2011). In all locations studied it has been found consistently that 2-AG was present at substantially higher concentrations than AEA.

Perhaps to facilitate internal regulation within the system, the two ligands do not have identical pharmacology. AEA binds both CB1R and CB2R although with marginally higher affinity for CB1R over CB2R (Bayewitch *et al.*, 1995; Gonsiorek *et al.*, 2000). Intriguingly AEA is a full agonist at the CB1R but inconsistent results exist on whether it is a full or weak partial agonist at the CB2R (Felder *et al.*, 1995; Gonsiorek *et al.*, 2000). The inconsistent results seen with AEA and CB2R may be due to differences in the extent of the cell's receptor reserve since CB2R activation by AEA was only seen in systems with high receptor expression (Gonsiorek *et al.*, 2000). This could suggest low efficiency of the receptor-to-response coupling induced by AEA and that AEA will only be biologically active at CB2R when receptor levels are high. On the other hand, 2-AG has been demonstrated to be a full agonist in both binding and activation of hCB2R and hCB1R (Mechoulam *et al.*, 1995). However, 2-AG is 20-fold less potent than AEA in CB1R activation assays (Gonsiorek *et al.*, 2000). Overall, AEA and 2-AG are the main ligands for CB1R and CB2R respectively but similar to the chemokine network redundancy also occurs within the eCB.

Evidence exists that the eCB ligands act at receptors other than the CB1R and CB2R cannabinoid receptors. For example, AEA has been reported to activate peroxisome

proliferator-activated receptor-γ (PPAR-γ) and the transient receptor potential cation channel subfamily V 1 (TRPV1) (Bouaboula *et al.*, 2005; Ross, 2003). 2-AG is also a promiscuous ligand that can activate GABA(A) receptors (Sigel *et al.*, 2011) and α3-glycine receptors (Lozovaya *et al.*, 2011; Xiong *et al.*, 2012). The possibility of a third cannabinoid receptor has not been ruled out either. GPR55 is considered a putative cannabinoid-like receptor that can be activated by many synthetic cannabinoid ligands, for example the CB1R antagonist rimonabant, but conflicting data exists on whether activation of GPR55 by AEA and 2-AG can modulate downstream signalling pathways including GTPγS binding and ERK1/2 phosphorylation (Ross, 2009; Sharir *et al.*, 2010). In conclusion, the promiscuity of the cannabinoid ligands, both endogenous and synthetic, can make it difficult to conclusively interpret without appropriate controls which of their many physiological actions are due to CB1R and CB2R.

In a process similar to on demand synthesis of proglastandins and leukotrienes, both 2-AG and AEA are synthesised upon stimulation and then released into the extracellular environment. 2-AG and AEA can be synthesised by a variety of cells in response to inflammatory stimuli. Strong evidence exists that macrophages and platelets are capable of producing both ligands in response to LPS (Di Marzo *et al.*, 1999; Pestonjamasp *et al.*, 1998; Varga *et al.*, 1998). Other studies have also demonstrated that microglia can produce 2-AG, but not AEA, in response to ATP (Witting *et al.*, 2004), while stimulation of human umbilical vein endothelial cells with thrombin also induces 2-AG release (Sugiura *et al.*, 1998). Microglia cannot produce AEA in response to inflammation, suggesting that the presence of a potent CB1R

ligand might be counterproductive during CNS inflammation due to its misleading side-effects of hedonia. In summary, the endocannabinoid ligands 2-AG and AEA are present in tissues during homeostasis and importantly the ligands levels can be further increased in response to inflammation.

In addition to synthesis on demand, the endocannabinoid system has the ability to regulate the duration of its activation by regulating the extracellular levels of its endogenous ligands. Membrane endocannabinoid transporters exist on cells such as macrophages and are responsible for sequestering the endocannabinoid ligands back into the cell where they can be degraded by metabolising enzymes. Monoacylglycerol lipase (MAGL) is the main metabolising enzyme of 2-AG (Dinh *et al.*, 2002) but can also degrade AEA (Di Marzo *et al.*, 1999). Fatty-acid amide hydrolase (FAAH) is the main metabolising enzyme of AEA (Cravatt *et al.*, 1996) but can also degrade 2-AG (Goparaju *et al.*, 1998). Importantly, MAGL and FAAH are both present in macrophages and inflammatory treatments such as LPS can specifically down-regulate MAGL expression on these cells (Di Marzo *et al.*, 1999). Platelets, which as previously mentioned can produce 2-AG, also express MAGL but not FAAH (Di Marzo *et al.*, 1999). Thus, the cells capable of endocannabinoid ligand production also have endogenous regulating mechanisms in the form of metabolising enzymes in order to control the levels of CB1R and CB2R ligands during homeostasis and inflammation.

The metabolic products of 2-AG and AEA degradation are not inert lipids. On the contrary, 2-AG is hydrolysed into arachidonic acid (AA) and glycerol (Dinh *et al.*, 2002), while AEA is metabolised into arachidonic acid and ethanolamine (Cravatt *et al.*, 2002). Therefore endocannabinoid ligands can be considered AA precursors since their degradation leads to AA production. In turn, AA can be metabolised by the enzymes cyclooxygenase and lipoxygenase, leading to the release of prostaglandins, thromboxanes, prostacyclins and leukotrienes (LTs) which are key inducers of inflammation, fever and pain. In support of this concept, a recent study has demonstrated that human neutrophils responded to a metabolic product of 2-AG and this was identified to be LTB4 (Chouinard *et al.*, 2011). In summary, metabolism of endocannabinoid ligands regulates not only the endocannabinoid system but also impacts other signalling systems in inflammation biology, such as the AA pathway.

1.2.2 The role of the endocannabinoid system in homeostasis

Identification of the receptors and the endocannabinoid ligands in the brain and immune cells prompted researchers to investigate the role of the eCB at these locations. Since both 2-AG and AEA are expressed in brain and lymphoid tissues the output from eCB activation relies on the receptor expression at the site.

1.2.2.1 **Role of CB1R**

CB1R is widely expressed in the brain regions including the nucleus accumbens and the ventral tegmental area which are considered to be central brain reward circuits

(Lupica *et al.*, 2004). Marijuana is the most commonly used recreational drug due to its psychological euphoric and hallucinogenic effects and these effects are due to CB1R activation since they were blocked by the CB1R antagonist rimonabant (Huestis *et al.*, 2001). Apart from the euphoric effects, CB1R activation is involved in the behavioural process of physical dependence and self-administration (addiction) induced not only by cannabinoid drugs but also by morphine (Ledent *et al.*, 1999). CB1R knockout mice are healthy and fertile but have hypoalgesia and reduced locomotor activity in formalin tests as well as increased mortality rate (Zimmer *et al.*, 1999). CB1R knockout mice also have significantly lower body weight and less adipose tissue fat than wild type (WT) mice (Ravinet Trillou *et al.*, 2004).

CB1R is highly expressed in the nervous system both centrally and peripherally. CB1R activation by 2-AG, AEA or the phytocannabinoid Δ9-THC leads to hypothermia, catalepsy, hypomotility and analgesia (Ledent *et al.*, 1999; Mechoulam *et al.*, 1995; Smith *et al.*, 1994). A test comprising of these four behavioural changes is known as the “tetrad test” and is still used today for screening of compounds with activity at CB1R. Multiple studies have demonstrated that CB1R activation has a key analgesic role in nociceptive pain (mechanically induced) (Clayton *et al.*, 2002) and in heat-induced hyperalgesia (Johanek *et al.*, 2001). Moreover in inflammatory conditions such as the carrageenan paw oedema model, both CB1R and CB2R have been shown to have an analgesic effect by reducing inflammation-induced hypersensitivity (Clayton *et al.*, 2002). A pivotal study by Agarwal *et al.* (2007) demonstrated that specific activation of CB1R expressed in the periphery, and not in the CNS, has a dominant role in cannabinoid-induced analgesia in neuropathic and

inflammatory pain. In conclusion, targeting the peripheral CB1R has potential for discovering novel analgesics with no side-effects linked with activation of the receptor in the CNS.

Apart from its effects on the brain and neurons, CB1R activation has been linked with obesity. This was demonstrated by the finding that CB1R activation leads to defective leptin signalling to regulate food intake (Di Marzo *et al.*, 2001). Leptin is responsible for sending information to the hypothalamus regarding energy levels and increased leptin levels lead to suppressed appetite and increased energy usage (Morris *et al.*, 2009). CB1R activation has been demonstrated to enhance lipogenesis and increase appetite which in turn induces an increase in the fat mass and gain of weight (Cota *et al.*, 2003). Moreover activation of CB1R in mice increased the expression of lipogenic transcription factors and the synthesis of fatty acids in the liver. A positive feedback loop between high fat diet and AEA and CB1R receptor levels was also demonstrated (Osei-Hyiaman *et al.*, 2005). Sanofi-Aventis's potent selective CB1R antagonist (rimonabant) was therefore tested in clinical trials with obese patients and was shown to be effective in inducing weight loss within 12 months in the RIO-Europe study (Van Gaal *et al.*, 2005). This trial suggested that rimonabant could be used in the clinic to treat obese patients.

A follow up trial (CRESCENDO) with the compound aimed to test its effects on improving cardiovascular outcomes in a bigger cohort of obese patients. However the trial and the drug had to be abruptly terminated due to increased suicide rates

and other serious psychiatric side-effects such as anxiety and depression and the drug was withdrawn from the market (Topol *et al.*, 2010). This is not completely unexpected since a variety of pre-clinical models have demonstrated that CB1R antagonists increase anxiety and depression-like symptoms (McLaughlin *et al.*, 2012; Moreira *et al.*, 2009) while low doses of CB1R agonists had anxiolytic effects (Patel *et al.*, 2006). Overall CB1R activation does lead to obesity however CB1R also has an important role in positive/rewarding emotions which excludes CNS-penetrant CB1R antagonists as appropriate treatment for obesity.

Relative to the studies demonstrating CB1R effects on neurons, brain and lipogenesis, very few studies have demonstrated an immunoregulatory role of the receptor. Low levels of CB1R mRNA have been found in macrophages and T cells. CB1R was shown not to affect peritoneal macrophage chemotaxis to the chemotactic peptide N-formyl-metionyl-leucine-phenylalanine (fMLP) or chemokines (Raborn *et al.*, 2008; Sacerdote *et al.*, 2000). Also CB1R inhibition in human macrophages induced a modest (~25%) inhibition of LPS-induced cytokines such IL-1β, IL-6 and TNF-α (Sugamura *et al.*, 2009), while stimulation of the macrophage cell line RAW264.8 with AEA induced a modest increase (~20%) of ROS in a CB1R-dependent manner (Han *et al.*, 2009). In microglia, which also express low levels of the CB1R, the receptor was involved in inhibition of LPS-induced NO production by the mixed CB1R/CB2R agonist CP-55940 (Cabral *et al.*, 2001). CB1R was also expressed on infiltrating T lymphocytes in the animal model of multiple sclerosis, experimental autoimmune encephalomyelitis (EAE), however this expression was not linked to a functional effect of the receptor at either the steady state of the disease or

suppression of the disease induced by Δ9-THC. Instead, CB1R expression in neurons was partially involved in the Δ9-THC inhibitory effects on the disease's progression (Maresz *et al.*, 2007). These data suggest that CB1R can have an indirect role on immune responses via its expression on neurons. Currently no consistent data exist to support an immunoregulatory role of CB1R in immune cells.

1.2.2.2 **Role of CB2R**

High level expression of the CB2R was first found in immune cells (Galiegue *et al.*, 1995), while lower expression of the receptor was recently identified in the brain (Onaivi *et al.*, 2012), endothelial cells (Rajesh *et al.*, 2007) and vascular smooth muscle cells (Rajesh *et al.*, 2008). The action of the receptor can only be conclusively addressed in studies performed following the availability of the specific CB2R antagonist SR144528 or where CB2R knockout mice were used. CB2R knockout mice have been available since 2000 and they are healthy under normal and unchallenged circumstances (Buckley *et al.*, 2000). Nonetheless, CB2R knockout mice have altered immune responses as observed for the many healthy chemokine receptor knockout mice which are normal under homeostatic conditions (Haringman *et al.*, 2004; Power, 2003).

<u>CB2R and lymphocytes: B cells and T cells</u>

In leukocytes the expression of CB2R at both protein and mRNA level is highest in B-lymphocytes while lower expression of the receptor is also found in T-lymphocytes

(Carayon *et al.*, 1998; Galiegue *et al.*, 1995). This has led to rigorous studies regarding the role of the receptor on lymphocytes. Early findings demonstrated that Δ9-THC, AEA and the mixed CB1/CB2 agonist CP-55940 could inhibit in a dose-dependent manner the mitogen-induced proliferation of B cells and the CD3-induced proliferation of T cells when used in the micromolar range (Schwarz *et al.*, 1994). Moreover, they demonstrated that AEA but not CP-55940 could also induce lymphocyte apoptosis. Conversely, other studies demonstrated that nanomolar concentrations of Δ9-THC and CP-55940 dose-dependently increased proliferation of B cells in response to immunoglobulin cross-linking and CD40 ligation and these responses are CB2R-dependent (Carayon *et al.*, 1998; Derocq *et al.*, 1995). Overall, these studies suggest that the CB2R has a role in lymphocyte proliferation in a bi-phasic manner.

Apart from a role for CB2R in lymphocyte proliferation, it has been demonstrated that CB2R activation can lead to recruitment of B cells. However CB2R does not regulate the migration of B cells to other chemoattractants such as CXCL13 and sphingosine-1-phosphate (Basu *et al.*, 2011b). The opposite applies for peripheral blood T-cells where CB2R agonists were unable to induce chemotaxis but were able to inhibit T cell chemotaxis to CXCL12 (Coopman *et al.*, 2007). However Δ9-THC has been reported to induce calcium flux in T-cells in a CB2R-dependent manner (Rao *et al.*, 2004). It is therefore possible that in T-cells CB2R levels are not high enough to induce chemotaxis but are adequate to release calcium thus interfering with other simultaneous chemokine responses which also require calcium.

The availability of CB2R knockout mice has allowed investigation into the role of CB2R in lymphocyte physiology *in vivo*. Interestingly, in the spleen of CB2R knockout (KO) mice the numbers of marginal zone B cells and memory CD4+ T cells were significantly reduced compared to WT mice (Pereira *et al.*, 2009b; Ziring *et al.*, 2006). In the same studies, B cell numbers were also reduced in the peripheral blood of CB2R KO mice. Conversely no differences were seen in naïve CD4+, naïve CD8+ T cells or follicular B cells in KO mice compared to WT. Further studies were able to demonstrate that in the spleen, CB2R is crucial for homing and retention of marginal zone B cells (Basu *et al.*, 2011b) while the entry and crawling of immature B cells in the sinusoids of the bone marrow was also a CB2R-dependent process (Pereira *et al.*, 2009b). B cells from CB2R KO mice were not functionally defective since the proliferation, turn-over and BCR signalling where similar in WT animals. These findings suggest that CB2R is important for positioning of marginal zone B cells within lymphoid tissue but is dispensable for B cell functions under homeostatic or T cell dependent humoral conditions.

Marginal zone B cells have a crucial T cell-independent role in immunity since they can rapidly differentiate to plasma cells in response to blood-borne pathogens. Importantly in CB2R KO mice immunized with the T cell-independent antigen Pneumovax 23 (combination of polysaccharides from different strains of *Streptococcus pneumoniae)* marginal zone B cells produced significantly less IgM antibody (Basu *et al.*, 2011b). Therefore this study suggests that CB2R orchestrates a T cell-independent humoral response against pathogens by enabling activation of marginal zone B cells due to their appropriate homing and retention. Alternatively, it

has also been found that CB2R activation in B cells enhanced immunoglobulin class switching from IgM to IgE in response to IL-4 (Agudelo *et al.*, 2008). On the whole, CB2R activation is crucially involved in the humoral responses regulated by B cells and this effect may be due to combinatory actions on homing and class switching.

The immunoregulatory role of CB2R on macrophages and monocytes

As previously mentioned, mRNA expression of the $G\alpha_i$-coupled CB2R has been identified on monocytes and macrophages (Galiegue *et al.*, 1995). Although CB2R shares little homology with chemokine receptors, the role of CB2R in macrophage and monocyte chemotaxis has been investigated. Studies have demonstrated that the endocannabinoid ligand 2-AG, but not CP-55940 or AEA, can induce chemotaxis of human monocytes and promyelocytic cell line (monocyte-like cell line) HL-60 in a CB2R-dependent manner (Kishimoto *et al.*, 2003). Similar to the actions of 2-AG, the CB2R-selective agonists JWH-133 and JWH-015 were also shown to be weak chemoattractant of human monocytes with Akt and ERK1/2 phosphorylation involved in their chemotactic effect on monocytes (Montecucco *et al.*, 2008). Moreover in HL-60 cells, 2-AG and CP-55940 were both shown to induce rapid actin polymerization via CB2R, in a pathway involving activation of PI3K and an unspecified tyrosine kinase (Gokoh *et al.*, 2005). The cannabinoid effects on actin polymerization are crucial since regulation of actin polymerization is key for controlling shape changes required for leukocyte chemotaxis (Jones, 2000). Overall, the published literature suggests that CB2R activation is involved in monocyte and macrophage chemotactic responses.

Apart from inducing chemotaxis, CB2R activation has also been demonstrated to *reduce* chemotaxis to other chemoattractants. For example, *in vitro* and *in vivo* administration of CP-55940 could reduce migration of macrophages to fMLP in a CB2R-dependent manner (Sacerdote *et al.*, 2000). Moreover CB2R activation by Δ9-THC, CP-55940 or a synthetic CB2R agonist could reduce macrophage chemotaxis in response to the chemokine RANTES (CCL5) (Raborn *et al.*, 2008). Supporting evidence in human monocytes indicated that overnight stimulation with 20 μM of the synthetic CB2R agonist JWH-015 inhibited monocyte chemotaxis to MCP-1 and MIP-1α (CCL3) (Montecucco et al., 2008). The authors also demonstrated that JWH-015 inhibited by 30% of protein levels of CCR2 and CCR1 by PI3K and ERK1/2 dependent pathway. Overall, these data suggest that CB2R activation could reduce chemotaxis to other chemokines and these effects could be due to signalling pathways involving PI3K, ERK1/2 or actin remodelling.

Interestingly the endocannabinoid ligand 2-AG (but not AEA) and CP-55940 were shown to induce MCP-1 and IL-8 production via CB2R in HL-60 cells (Jbilo *et al.*, 1999; Kishimoto *et al.*, 2004). It is therefore possible that continuous MCP-1 production by CB2R activation could induce desensitization of the MCP-1 receptor CCR2 and this in turn would make the receptor unavailable to all its other chemotactic ligands such as monocyte chemoattractant protein-3 (MCP-3) (Jia *et al.*, 2008).

Complex and incomplete data from the 1990's exist regarding the role of cannabinoid receptors in macrophages stimulated with TLR agonists, mainly due to previous lack of availability of specific CB1R and CB2R antagonists and good anti-CB1R and CB2R antibodies. In human monocytes Δ9-THC increased LPS-induced TNF-α, IL-8 and IL-6 production while AEA decreased TNF-α when used in the micromolar range and had no effect on IL-6 and IL-8 production (Berdyshev *et al.*, 1997). Conversely in mouse macrophages, the phytocannabinoid Δ9-THC and AEA were shown to reduce LPS-induced NO and IL-6 production while 2-AG was only able to reduce IL-6 production (Chang *et al.*, 2001). Moreover treatment of mouse macrophages with 2-AG and Δ9-THC for 10-24 hours reduced LPS-induced TNF-α production (Gallily *et al.*, 2000; Zheng *et al.*, 1996). From these studies it is difficult to make definitive conclusions about the involvement the cannabinoid receptors in modulating macrophage inflammatory response. It is possible that non-cannabinoid receptors were involved in the observed effects or that the long incubation periods with the cannabinoids could have induced cell death (Zhu *et al.*, 1998).

So far studies have only investigated the specific involvement of CB2R (using antagonists) in macrophages activated with LPS. In one of these studies, CB2R activation by micromolar concentrations of the non-specific CB1R/CB2R agonists WIN-55212 and CP-55940, led to a reduction of LPS-induced NO production but CB2R agonists only had an effect when high doses of the TLR agonist were used (Ross *et al.*, 2000). In the second study, "classically"-activated (LPS/IFN-γ) thioglycollate-elicited macrophages were treated with the CB2R-specific agonist JWH-133. In a CB2R-dependent manner, JWH-133 was shown to dose-dependently

inhibit the production of IL-12p40 and this anti-inflammatory effect involved signalling via ERK1/2 and the production of IL-10 (Correa *et al.*, 2005). Since IL-12 is important for Th1 cell differentiation which in turn produces IFN-γ (major activator of classical macrophages as previously mentioned), it is possible that CB2R activation is involved in resolving inflammation by preventing the further induction of "classical" macrophages. However further studies including specific antagonists or CB2R knockout mice are needed to conclusively assess this.

Lack of evidence for CB2R role in neutrophil functions

CB2R mRNA has been identified in neutrophils (Galiegue *et al.*, 1995) but conflicting data exist on whether these cells express any CB2R at protein level (Deusch *et al.*, 2003; Graham *et al.*, 2010). It has been demonstrated that Δ9-THC has no effects on neutrophil chemotaxis and phagocytosis (Deusch *et al.*, 2003). Alternatively CP-55940 was reported to induce respiratory burst in neutrophils but this was due to indirect effects involving metabolic products of arachidonic acid (Kraft *et al.*, 2005). In a similar manner, 2-AG induced myeloperoxidase release and calcium mobilization in human neutrophils, however this was due to hydrolysis of 2-AG and the de novo synthesis of bioactive LTB4, a potent stimulator of neutrophils (Chouinard *et al.*, 2011). Overall, CB2R activation is not involved in neutrophil functions.

1.3 Atherosclerosis and the endocannabinoid system

1.3.1 Atherosclerosis pathology

Atherosclerosis is a multifactorial disease associated with chronic inflammation and deregulation of lipid metabolism and is the main cause of death in developed countries. Atherosclerosis is characterised by the formation of arterial lesions, also known as atherosclerotic plaques (Ross, 1999). A stable atherosclerotic plaque can cause flow-limiting arterial stenosis but this is not life-threatening. Conversely once the plaque is destabilised and then ruptured, its thrombogenic lipid core is exposed to circulating blood which in turn leads to thrombus formation. Depending on the site of plaque rupture, arterial occlusion can cause ischaemic stroke, myocardial infarction, heart failure or abdominal aneurysm (Hansson *et al.*, 2006). Possible therapeutic treatments could include prevention of further monocyte recruitment into the advanced plaque or promotion of pathways involved in plaque stability.

Atherosclerotic lesions are composed of accumulated lipids, inflammation and cell death (Hansson *et al.*, 2006). Accumulation of modified low-density lipoprotein (LDL) in the subendothelial space of the arterial wall activates vascular cells including vascular smooth muscle cells (VSMCs) and endothelial cells to release pro-inflammatory mediators and chemokines. Chemokines recruit monocytes into the lipid-rich site, which in turn differentiate into macrophages (Gerrity, 1981). Macrophages engulf modified LDL via their scavenger receptors and the prolonged intracellular accumulation of phorbol esters induces their transformation into foam cells (Kruth, 2001). Foam cells have the capability to release a plethora of pro-

inflammatory cytokines and chemokines thus exacerbating the inflammation further and promoting atherosclerosis. Moreover in advanced atherosclerosis, *in situ* macrophage apoptosis is one of the reasons for promoting the increase of lesion size (Gautier *et al.*, 2009).

Other cell types are also involved in the development of atherosclerosis. Activation of endothelial cells by altered shear stress, stenosis or age-related arterial stiffening increases endothelial permeability which allows increased leukocyte extravasation (Huynh *et al.*, 2011). Pro-inflammatory mediators such as TNF-α and modified LDL can also activate endothelial cells and upregulate their surface expression of adhesion molecules, such as P-selectin, E-selectin, ICAM-1 and platelet endothelial cell adhesion molecule-1 (PECAM-1), thus promoting the firm adhesion of inflammatory leukocytes (Galkina *et al.*, 2007). For example soluble ICAM-1 levels were strongly associated with the severity of atherosclerotic plaques in patients (van der Meer *et al.*, 2002). In atherosclerotic plaques, endothelial cell dysfunction is responsible for decreased release of NO which has a crucial role in vasodilatation and inhibition of both platelet aggregation and modification of LDL (Davignon *et al.*, 2004).

As the lesion progresses, migration of VSMCs which produce elastin, collagen and other extracellular matrix components, contributes to the production of a fibrous cap and hence stabilises the plaque (Clarke *et al.*, 2006). Moreover apoptosis of VSMCs in the plaque promotes the recruitment of macrophages due to the release of

chemokines (Schaub *et al.*, 2000). Pro-inflammatory chemokines found in the plaque, such as fractalkine, have been shown to have anti-apoptotic and pro-survival functions towards VSMCs (White *et al.*, 2010), this in turn could have a crucial effect on the fine balance between stabilising the atherosclerotic plaque and excessive vessel stenosis responsible for angina.

Together with chronic inflammation, adaptive immunity also contributes to the development of atherosclerosis. Oxidised-LDL (ox-LDL) is recognised by dendritic cells and then presented to naïve T cells. Depending on the cytokines present in the micro-environment, naïve T helper cells can differentiate into different subsets which can release different sets of cytokines. These subsets are Th1, Th2 and Th17. Th1-cells have been consistently shown to have a proatherosclerotic role mainly due to the release of pro-inflammatory cytokines such as IFN-γ and TNF-α (Lahoute *et al.*, 2011). Blocking either IFN-γ or TNF-α significantly reduces the progression of atherosclerosis by reducing lesion size (Branen *et al.*, 2004; Gupta *et al.*, 1997). The influence of Th2 cells and Th17 cells on atherosclerosis is still debated due to conflicting results. Regarding Th2 cells, the current understanding is that they have an anti-atherogenic role in early lesion development but they enhance plaque progression in advanced stages of atherosclerosis (Davenport *et al.*, 2003; Huber *et al.*, 2001). Overall many factors and adaptive immune cell types contribute to the complex process of atherogenesis and the development of the atherosclerotic lesion.

One therapeutic approach considered for the treatment of atherosclerosis is modulation of lipid metabolism. Many studies over the past 20 years have demonstrated that the levels of total cholesterol are positively associated with ischaemic heart disease (Prospective Studies *et al.*, 2007), while decreases in LDL cholesterol are associated with reductions in cardiovascular morbidity and mortality (Gotto *et al.*, 2012). Statins, which are inhibitors of the enzyme HMG-CoA reductase that is responsible for cholesterol synthesis in the liver, have been successful lipid-lowering drugs since apart from reducing LDL, they have demonstrated a significant reduction of cardiovascular incidents (Ridker *et al.*, 2008). Nonetheless, twenty years since the discovery of statins, no other therapeutic breakthrough has been achieved in the area of atherosclerosis.

1.3.1.1 **Animals models of atherosclerosis**

A variety of animal species have been used to model human atherosclerosis and to study the pathogenesis of the disease. There are two mouse models of atherosclerosis that are widely used and they have helped elucidate the pathophysiology of the disease. One of them uses Apolipoprotein E (ApoE) knockout mice while the other is genetic ablation of the LDL receptor (LDLR) thus creating LDLR knockout mice. Other animal models include the use of rabbits and pigs. Pigs naturally develop atherosclerosis similar to humans and plaque progression can be enhanced when the pigs are placed on a high fat diet (Reiser *et al.*, 1959; Reitman *et al.*, 1982). Rabbits are sensitive to cholesterol changes thus they readily develop fibro-fatty atherosclerotic lesions following cholesterol feeding (Clarkson *et al.*, 1926).

Despite the similarities of the pig and rabbit atherosclerosis models with human disease, mouse models have been more popular due to the ease of genetic modifications and lower maintenance cost (Getz *et al.*, 2012).

ApoE knockout mice

Lipoproteins are water-soluble complexes of lipids and proteins and their core contains hydrophobic lipids such as triglycerides and cholesterol. These lipids are essential for the cells' energy needs and membrane structures. The proteins associated with lipoproteins are known as apolipoproteins and they bind lipids such as cholesterol in order to aid their transport across the blood and lymphatics. Several classes of apolipoproteins exist and they have different physicochemical properties, functions and distribution. Apolipoprotein E is a blood plasma protein and it binds lipoproteins such as chylomicrons, LDL and very low density lipoprotein (VLDL) (Mahley *et al.*, 2009). ApoE is a high affinity ligand of the receptor systems involved in lipoprotein clearance, including the LDLR, the VLDL receptor, the LDL-receptor-related protein and proteoglycans. Once ApoE is bound to the receptors the apolipoprotein undergoes receptor-mediated endocytosis and lysosomal hydrolysis releases lipids into the cell. A mutation in one of the four ApoE isoforms leads to Type III dyslipoproteinemia which is associated with increased triglycerides and cholesterol in the blood leading to early development of atherosclerosis (Schneider *et al.*, 1981).

ApoE knockout mice were first described in 1992 (Zhang *et al.*, 1992). Within 3 months of normal chow diet (low cholesterol, low fat) these mice have intermediate cholesterolemia and prominent atherosclerotic lesions with foam-cell depositions. Lesions develop in the aorta and the carotid arteries. By 8 months advanced atherosclerotic lesions with fibrotic caps and induced arterial stenosis are observed. When these mice are fed a western diet their plasma cholesterol levels are even higher and the atherosclerotic lesions are larger with faster progression (Breslow, 1996). The main atherogenic stimuli in these mice are the remnants of VLDL and chylomicrons which become oxidised once they penetrate the endothelial layer and reach the arterial intima. The size of lesions and hence atherogenesis in ApoE knockout mice, refers to the average lesion area (stained with Sudan VI or oil red O for lipid content) in the heart and adjacent aorta.

LDLR knockout mice

The LDLR regulates plasma cholesterol levels by removing cholesterol-rich LDL from plasma. Once inside cells, LDL-derived cholesterol has several functions but it also regulates the expression of LDLR depending on the cell's metabolic needs. Patients with familial hypercholesterolemia have mutations in the LDLR gene resulting in high plasma levels of LDL, early atherosclerosis and increased incidence of cardiovascular events (Goldstein *et al.*, 1987). Therefore one of the advantages of this model is the proximity to a human gene mutation related to atherosclerosis.

LDLR knockout mice are mildly hypercholesterolemic and on normal chow diet they rarely develop arterial lesions due to liver production of truncated lipoproteins that contain high levels of ApoE. When the LDLR knockout mice are fed on high-fat (western-type) diet they become highly hypercholesterolemic with plasma LDL accumulation and atherosclerotic plaques with many foam cells are observed in the aortas (Ishibashi *et al.*, 1994). The main atherogenic stimuli in these mice are the remnants of LDL and intermediate density lipoproteins. A disadvantage of this model is the reliance on high-fat diet which can induce variability between animals and between different laboratories since different high fat diet recipes exist.

1.3.1.2 **Monocyte recruitment and macrophage apoptosis in atherosclerosis**

In 1856, Rudolph Virchow was the first to propose that injury to the arterial wall could induce the formation of atherosclerotic lesions and importantly that inflammatory responses had a causative role in the initial vessel injury (Virchow, 1856). The field has since progressed to understand in further detail the involvement of inflammatory cells in atherosclerosis.

The role of monocytes and monocyte-derived macrophages in the progression of atherosclerosis has been demonstrated in both mouse models of atherosclerosis by ablation of macrophage-colony stimulating factor (M-CSF). M-CSF is a cytokine involved specifically in the production, differentiation and function of monocytes and macrophages (Hamilton, 2008). M-CSF knockout mice have reduced blood

monocyte numbers and diminished peritoneal macrophages (Wiktor-Jedrzejczak *et al.*, 1982). In both LDLR and ApoE knockouts, simultaneous ablation of M-CSF led to a significant reduction of lesion size (at least 80% reduction) compared to single knockout control mice (de Villiers *et al.*, 1998; Rajavashisth *et al.*, 1998).

During atherosclerosis, monocyte recruitment from the bone marrow to the blood and then into the atherosclerotic lesion is dependent on many processes. The adhesion cascade and the chemokine system play a major role in this recruitment. Recruitment of leukocytes to the vessel wall is the first step for the development of atherosclerosis. In ApoE knockout mice, P-selectin and to a smaller extent E-selectin are critical for monocyte rolling on activated endothelium (An *et al.*, 2008; Collins *et al.*, 2000) while VCAM-1 and ICAM-1 are involved in firm adhesion (Ramos *et al.*, 1999). Importantly deficiency of either P-selectin or VCAM-1 leads to significant reduction of atherosclerotic lesion size in both ApoE and LDLR knockout mice (Collins *et al.*, 2000; Cybulsky *et al.*, 2001).

Several chemokines are involved in the recruitment of monocytes into plaques. Moreover two subsets of monocytes have been identified and their expression pattern of chemokine receptors is different. These subsets are $CCR2^{+}CX_3CR1^{+}$Ly-$6C^{high}$ and $CCR2^{-}CX_3CR1^{++}$Ly-$6C^{low}$ monocytes. During atherosclerosis both subsets are recruited into lesions but the $Ly6C^{high}$ monocyte subset recruitment is 20-fold higher and monitoring demonstrated that it is the $Ly6C^{high}$ subset that subsequently differentiates into lesional macrophages (Swirski *et al.*, 2007; Tacke *et al.*, 2007).

The Ly6C^{high} subset relies on CCR2, CCR5 and CX_3CR1 to be recruited into lesions while Ly6C^{low} monocytes are recruited in a CCR5 and not CX_3CR1 dependent manner (Tacke *et al.*, 2007).

According to the relative expression of the chemokine receptors CX_3CR1 and CCR2, Ly6C^{high} and Ly6C^{low} monocytes correspond to the two human monocyte subsets: CD14^{hi}CD16^{-} and CD14^{+}CD16^{+} monocytes (Geissmann *et al.*, 2003). Although monocyte subsets in human and mouse are not identical, they share a pattern of chemokine receptor expression that suggests similar recruitment pathways. Overall, monocyte recruitment is crucial for the development of atherosclerosis and chemokine receptor blockade could have a different effect on each monocyte subset.

Macrophage/foam cells numbers in the atherosclerotic plaques are predictive of disease progression. The number of macrophages is reliant on the recruitment of monocytes by factors previously mentioned while insufficient data exist for the chemotaxis of macrophages from the subendothelial space to the arterial intima which is the core of the atherosclerotic lesion. It has been suggested that macrophage numbers in the plaque are also reliant on the ability of cells to egress from the plaque into the circulation (Feig *et al.*, 2009). Netrin-1, a laminin-related molecule, has been identified to inhibit macrophage egress (van Gils *et al.*, 2012) while CCR7 has been shown to regulate the egress of monocyte-derived antigen-presenting cells from the plaque (Feig *et al.*, 2010). Moreover, induction of macrophage apoptosis could also reduce their numbers in the plaque (Potteaux *et*

al., 2011). Interestingly it has been reported that induction of macrophage apoptosis in early plaque reduces disease progression while induction of macrophage apoptosis in advanced lesions promotes atherosclerosis due to triggering of monocyte recruitment (Gautier *et al.*, 2009).

1.3.2 The endocannabinoid system and atherosclerosis

1.3.2.1 **The role of CB2R in atherosclerosis**

The blood levels of both the endocannabinoid ligands 2-AG and AEA are increased in patients with coronary artery atherosclerosis compared with patients with no atherosclerosis, suggesting the activation of the eCB system in the disease's pathophysiology (Sugamura *et al.*, 2009). The role of the CB2R in atherosclerosis was first demonstrated by a pivotal study by Steffens *et al.* (2005). In ApoE knockout mice fed on high-fat diet, a low oral dose of the phytocannabinoid Δ9-THC (1 mg/kg day in 5.5% milk for 6 weeks) reduced the size (by 40%) of both early and existing atherosclerotic lesions in a CB2R-dependent manner since it was reversed by the CB2R antagonist SR144528 (experimental details and data shown in Figure 1.2). Moreover immunohistochemistry studies identified the receptor in human and mouse atherosclerotic plaques as well as on macrophages and T cells recruited into mouse atherosclerotic lesions. In the same study the mechanism was suggested to be inhibition of macrophage chemotaxis, since peritoneal macrophages stimulated with IFN-γ or TNF-α *in vitro* underwent increased chemotaxis to 1nM MCP-1 and this enhancement in chemotaxis was inhibited by Δ9-THC. Δ9-THC effect was via CB2R since it was blocked by 1 μM SR 144528 (CB2R antagonist).

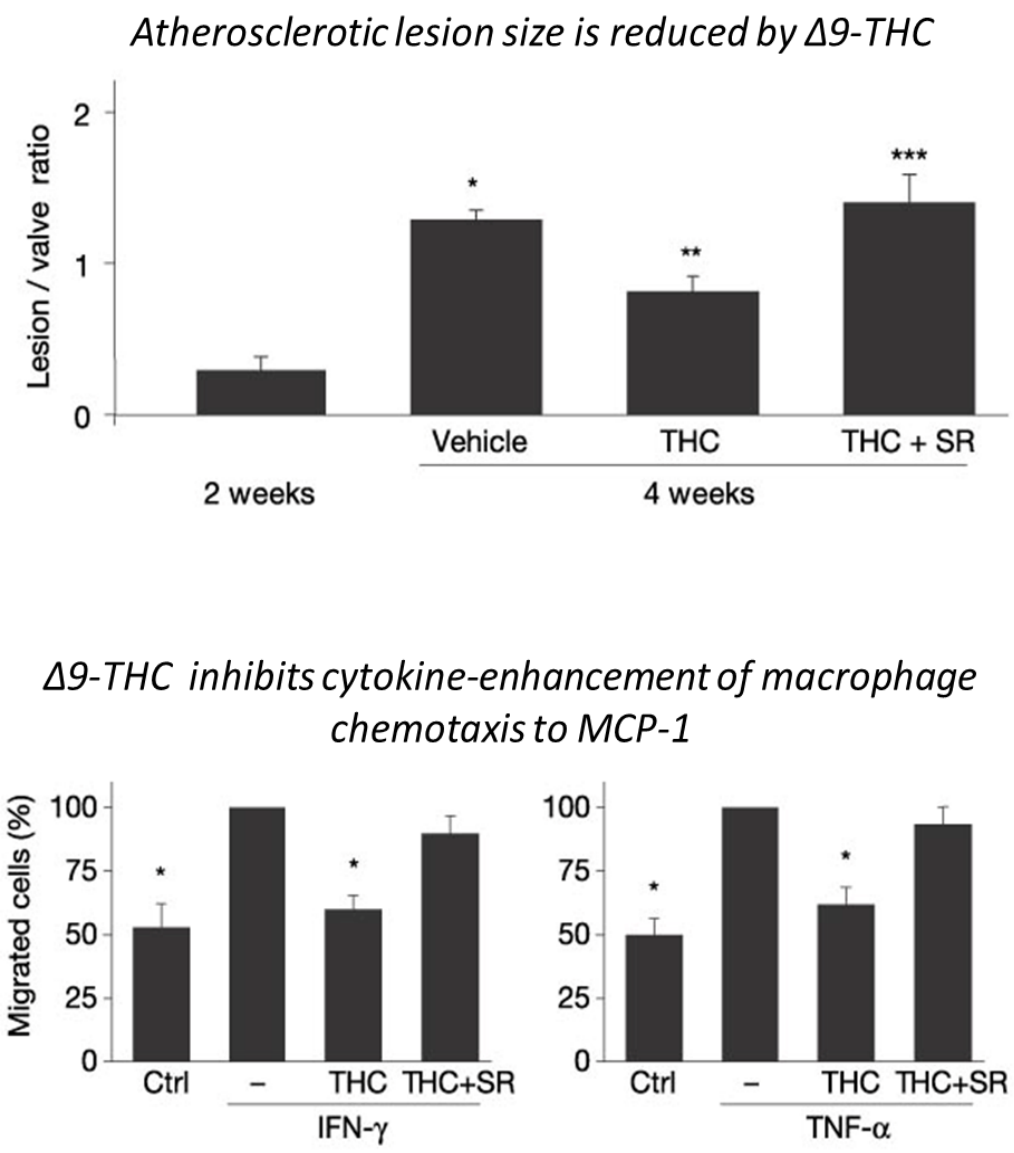

Figure 1.2: Pioneering demonstration of the atheroprotective effects of the phytocannabinoid Δ9-THC

Steffens *et al*., 2005 were the first to demonstrate that oral administration of the phytocannabinoid Δ9-THC (1 mg/kg daily for 6 weeks while mice were maintained on high-fat diet) reduced atherosclerotic lesion development in ApoE knockout mice. The atheroprotective effects of Δ9-THC were reversed by oral administration of the CB2R antagonist SR144528 (0.7 mg/kg in methanol, daily for 2 weeks in 4 week model) indicating the involvement of CB2R. The authors suggested that one mechanism of action for Δ9-THC was to inhibit the augmentation of macrophage chemotaxis to 1 nM MCP-1 in response to pro-inflammatory cytokines IFN-γ and TNF-α (Reproduced from Steffens et al. 2005).

In support of the authors *in vitro* data, mice treated with Δ9-THC had reduced macrophage content in lesions. Overall this study suggested an anti-atherosclerotic role for CB2R via inhibition of inflammatory responses.

Subsequent studies published after the start of my doctorate, aimed to expand this observation regarding the role of CB2R and identify further insights regarding the mechanism of action. In support of the findings of Steffens *et al.* (2005), the mixed CB1R/CB2R agonist WIN-55212 inhibited lesion development (by 30% at 1 mg/kg daily i.p. injections for 8 weeks) and reduced macrophage content and activation of nuclear factor-κB (NF-κB) in the plaques of ApoE knock-out mice fed on high-fat diet. These effects were shown to involve CB2R (Zhao *et al.*, 2010a). Interestingly in the same study, 24h activation of ApoE knockout peritoneal macrophages with LPS or ox-LDL led to increased secretion of IL-6, TNF-α and MCP-1. Pre-stimulation with 10 μM WIN-55212 inhibited the up-regulation of these proteins in a CB2R-dependent manner however no cytotoxicity assays were performed. In a separate study, treatment of ApoE knockout mice with WIN-55212 again reduced atherosclerotic lesion size along with a reduced expression of P-selectin, VCAM-1 and ICAM-1 in the aortas (Zhao *et al.*, 2010b). These studies support a role for CB2R in modulation of atherosclerosis development. A possible mechanism of action is down-regulation of adhesion molecules, pro-inflammatory cytokines and chemokines thus affecting both adhesion and chemotaxis of monocytes into the plaque.

CB2R has been demonstrated to modulate adhesion molecule expression on endothelial cells. Specifically endothelial cells activated with TNF-α have up-regulated expression of VCAM-1 and ICAM-1 leading to increased adhesion of monocytes to the endothelium (Chen *et al.*, 1995; Doherty *et al.*, 1989). Two different CB2R agonists (HU-308 and JWH-133) have been demonstrated to dose-dependently (0.5 to 4 μM range) decrease the enhancement of these adhesion molecules on endothelial cells in a CB2R-dependement manner. The two CB2R agonists used at 3 μM were also shown to decrease the adhesion of monocytes to the aortic endothelium (Rajesh *et al.*, 2007). These findings favour a CB2R-dependent mechanism that acts to reduce recruitment of monocytes by reducing their adhesion to endothelium.

Only one study so far has used ApoE/CB2R double knockout mice (Hoyer *et al.*, 2011). In this study, simultaneous ablation of CB2R in ApoE knockout mice did not increase lesion size compared to ApoE knockout mice despite the 30% relative increase in lesional macrophage numbers and increased vascular superoxide production in the plaques of $ApoE^{-/-}CB2R^{-/-}$ mice. Specific ablation of CB2R in myeloid cells (bone marrow transplantation) of ApoE knockout mice also increased macrophage numbers but again had no effect of lesion size compared to control ApoE knockouts. However treatment of ApoE knockout mice with 10 mg/kg JWH-133 decreased (by 40%) atherosclerotic lesion size and macrophage numbers while improving impaired endothelium-dependent vasorelaxation usually observed in ApoE mice, effects not seen in the $ApoE^{-/-}CB2R^{-/-}$ mice (Hoyer *et al.*, 2011). Moreover in the same study, treatment of ApoE knockout mice with JWH-133 decreased vascular

superoxide production in a CB2R dependent manner. Similar effects were recently reported in macrophages where CB2R knockdown by genetic ablation indicated a CB2R-mediated reduction of ROS produced by activation of an artificially over-expressed CB1R (Han *et al.*, 2009). Taken together, these data suggest that stimulation of CB2R by endogenous mediators is not adequate to affect atherosclerosis. This is most likely due to insufficient production of endogenous ligands which in combination with their low potency (micromolar range) may struggle to provide sufficient receptor coverage in the several cell targets of CB2R that are involved in modulating atherosclerosis. Instead activation of the receptor with an agonist of higher affinity and potency (nanomolar range) compared to 2-AG, such as JWH-133, appears to be adequate to observe an anti-inflammatory effect.

Conflicting data exist for the role of CB2R in atherosclerosis and these conflicting data arise from the use of the second mouse model of atherosclerosis, the LDLR knockout mice. In LDLR knockout mice fed on high-fat diet, neither administration of JWH-133 (5 mg/kg) nor simultaneous genetic ablation of CB2R in LDLR knockout mice modulated atherosclerotic lesion size at the aortic arch and root (Netherland *et al.*, 2010; Willecke *et al.*, 2011). JWH-133 administration had no effect on macrophage or T cell numbers in the plaque but $CB2R^{-/-}LDLR^{-/-}$mice did exhibit an increased macrophage content in their atherosclerotic lesions compared to LDLR knockout mice (Netherland *et al.*, 2010; Willecke *et al.*, 2011) echoing findings in $CB2R^{-/-}ApoE^{-/-}$mice (Hoyer *et al.*, 2011). Interestingly the level of apoptosis and collagen content in the lesions was decreased in $CB2R^{-/-}LDLR^{-/-}$mice compared to LDLR knockout mice. A third study in LDLR knockout mice demonstrated that

ablation of CB2R only in myeloid cells increased lesion size in the aortic arch but had no effect on the total lesion area at the aortic root (Delsing *et al.*, 2011). From these studies it seems that CB2R has a greater role in atherosclerosis resulting from deficiency of ApoE than LDLR knockout. Nevertheless it has to been taken into consideration that LDLR knockout mice develop faster and more advanced lesions than ApoE knockout mice (Ma *et al.*, 2012). Studies in both ApoE and LDLR knockout mice showed a role for CB2R in regulating macrophage numbers in atherosclerotic plaques and hence validate our efforts to study the anti-inflammatory effect effects of novel CB2R agonists.

Ox-LDL effects on macrophages and CB2R regulation

Uptake of ox-LDL by scavenger receptors on macrophages triggers the release of ROS, TNF-α and IL-6 via NF-κB activation and ERK1/2 phosphorylation (Janabi *et al.*, 2000). In macrophages, increasing doses of ox-LDL induced the release of both 2-AG and AEA and increased the mRNA of both CB1R and CB2R (Jiang *et al.*, 2009). Also ox-LDL-induced production of ROS and TNF-α in macrophages can be inhibited by the non-selective CB1R/CB2R agonist WIN-55212 via CB2R activation. CB2R activation by WIN-55212 inhibited the activation of NF-κB and the phosphorylation of ERK1/2 induced by ox-LDL suggesting this to be one potential mode of action (Hao *et al.*, 2010). Prolonged exposure of macrophages to high doses of ox-LDL can induce significant apoptosis and death (Wintergerst *et al.*, 2000) likely due to increased endoplasmic reticulum stress (Tabas, 2004). Despite the role of CB2R in inhibiting ox-LDL-induced cytokine release, the presence of CB2R on

macrophages increases the susceptibility of the cells to apoptosis induced by high doses of ox-LDL but has no effect on responses to low doses of ox-LDL (Freeman-Anderson *et al.*, 2008). The mechanism involved in this action was that ox-LDL induced down-regulation of Akt phosphorylation was more prominent in WT than CB2R knockout macrophages, thus endogenous CB2R activation was involved in inhibition of Akt phosphorylation.

Taken as a whole these published data on the role of CB2R in atherogenesis suggest that CB2R can have an anti-inflammatory effect on early or intermediate atherosclerotic lesions where the presence of other factors like ox-LDL are not at cytotoxic concentrations (Figure 1.3). In advanced stages of atherosclerosis associated with extremely high lipid accumulation, CB2R could promote damage by participating in pathophysiological mechanisms promoting cell apoptosis and death. Alternatively in advanced lesions the combination of a CB2R agonist with lipid lowering drugs like statins may maintain its anti-inflammatory effects.

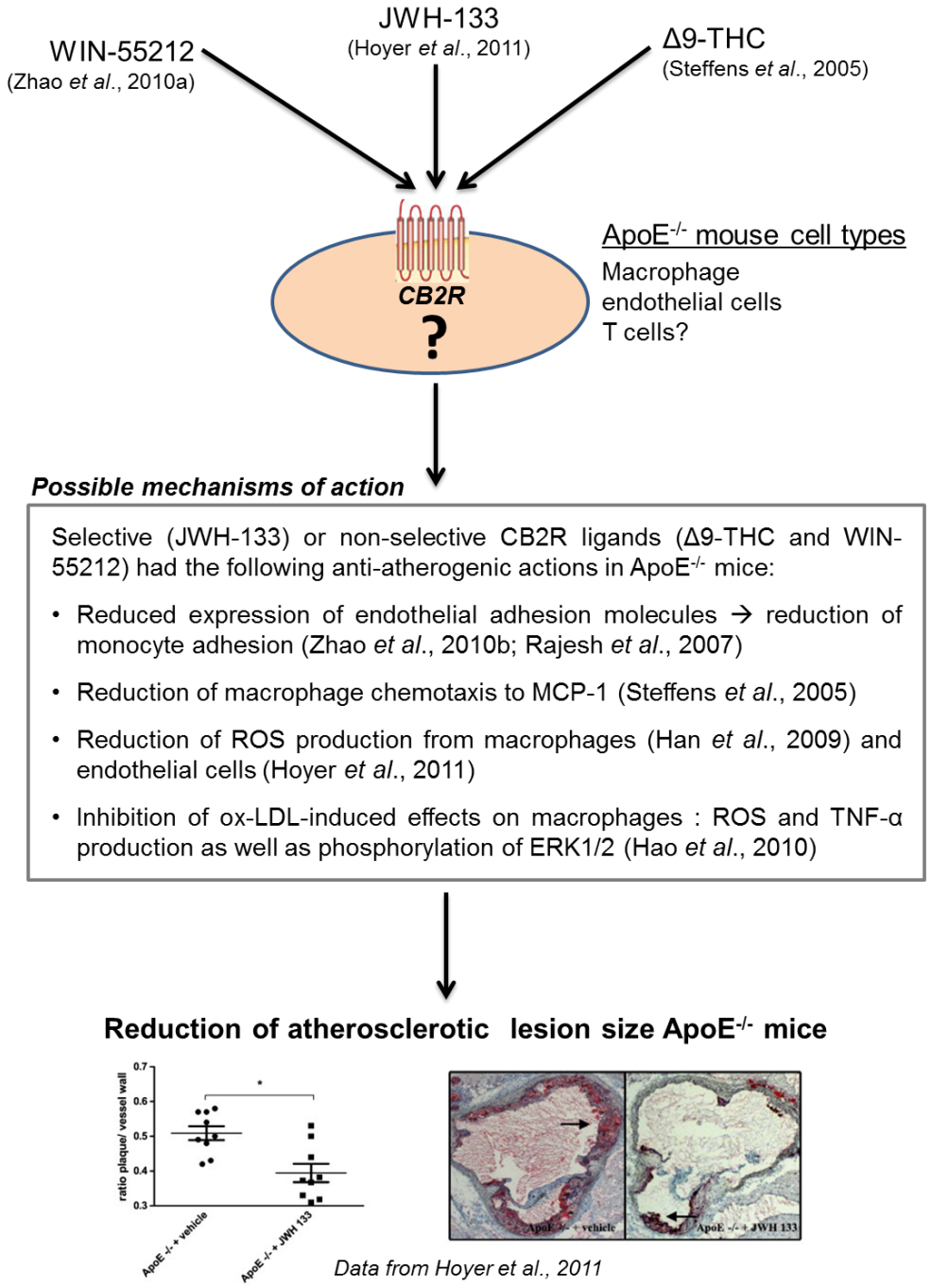

Data from Hoyer et al., 2011

Figure 1.3: Possible mode of action of CB2R in atherosclerosis summarized from multiple primary papers

Data from Hoyer et al., 2011 : Reprinted from J Mol Cell Cardiol., 51(6), Hoyer FF, Steinmetz M, Zimmer S, Becker A, Lutjohann D, Buchalla R, et al. (2011): Atheroprotection via cannabinoid receptor-2 is mediated by circulating and vascular cells in vivo. Pages 1007-1014. Copyright 2011, with permission from Elsevier.

1.3.2.2 **CB1R and atherosclerosis?**

The role of CB1R in atherosclerosis has not been investigated as thoroughly as the role of CB2R. No CB1R specific agonists or CB1R knockouts have been used. The only data available are from the use of the specific CB1R antagonist rimonabant. Daily administration of 50 mg/kg rimonabant to LDLR knockout mice reduced atherosclerotic lesion size and weight gain (Dol-Gleizes *et al.*, 2009). However in a Phase-II clinical trial, administration of rimonabant for 30 months to obese patients reduced body weight but had no effect on the carotid intima-media thickness thus blocking CB1R is not sufficient to modify the progression of atherosclerosis (O'Leary *et al.*, 2011).

1.4 Analgesic role of CB2R in pain

Recent studies have demonstrated that CB2R is not expressed only on immune cells. CB2R expression has been shown on neurons both in the periphery and the CNS (Wotherspoon *et al.*, 2005) as well as on glial cells and microglia in the brain (Onaivi *et al.*, 2006; Yiangou *et al.*, 2006). Importantly factors involved in driving neuropathic pain can up-regulate the expression of CB2R. For example, induction of nerve injury up-regulated the expression of CB2R in the spinal cord and dorsal root ganglia (Hervera *et al.*, 2010). Moreover the receptor is also up-regulated in activated microglia (Maresz *et al.*, 2005).

Like CB1R mentioned above, CB2R has also been linked with analgesia. Importantly CB2R activation and analgesia is devoid of psychiatric effects making it a more marketable target. 50 mg/kg of HU-308, a highly selective CB2R agonist, induced analgesia at the second phase of formalin-induced pain in a CB2R-dependent manner while having no detectable activity on the tetrad test for CB1R activity (Hanus *et al.*, 1999). CB2R activation with HU-308 reduced pain to non-noxious stimuli (allodynia) in animal models of post-operative pain and this was reversible with a CB2R antagonist (LaBuda *et al.*, 2005). Another selective CB2R agonist A-796260 from Abbott Laboratories was shown at 11 mg/kg to significantly inhibit neuropathic pain following nerve constriction injury, inflammatory pain induced from Complete Freund's Adjuvant (CFA) and reduce the activity-induced pain in osteoarthritic rats (Yao *et al.*, 2008). Other CB2R agonists have since then been demonstrated to inhibit neuropathic and inflammatory pain (Cheng *et al.*, 2007).

The mechanism of action for reduction of pain from CB2R agonists is highly debated and until recently remained elusive. CB2R activation may be involved in the inhibition of sensory nerve depolarization to prevent action potential transmission and neuron to neuron communication (Jhaveri *et al.*, 2007). Alternatively CB2R activation may be involved in regulation of cytokines released from microglia since JWH-133 dose-dependently (0.1 to 5 μM range) inhibited the LPS-induced release of the pro-inflammatory cytokine IL-12 and augmented the release of the anti-inflammatory cytokine IL-10 (Correa *et al.*, 2005). Activated microglia have been previously associated with the development of neuropathic pain and are responsible for release of inflammatory mediators such as TNF-α, IL-6, IL-1β and fractalkine which are

essential for the communication of microglia with neurons (Clark *et al.*, 2012; Schomberg *et al.*, 2012). Therefore the role of CB2R in reducing pain could be via inhibition of neuronal signal transmission or inflammatory cytokine release by microglia or both.

So far only one CB2R agonist has been tested in clinical trials. GW842166X is a selective CB2R agonist that behaves as a full agonist in a hCB2R cAMP assay but displays low affinity for the receptor (K_i= 2 μM) (Yao *et al.*, 2008). The only published data available demonstrate that the compound was able to inhibit CFA-induced hyperalgesia to weight bearing (inflammatory pain model) (Giblin *et al.*, 2007). GW842166X was administered to patients undergoing tooth extraction but demonstrated no effect on post-surgery nociceptive pain (Ostenfeld *et al.*, 2011). The lack of analgesic effect could be due to low affinity of the compound for the CB2R or due to wrong choice of application since more studies are needed regarding the mechanism of CB2R action.

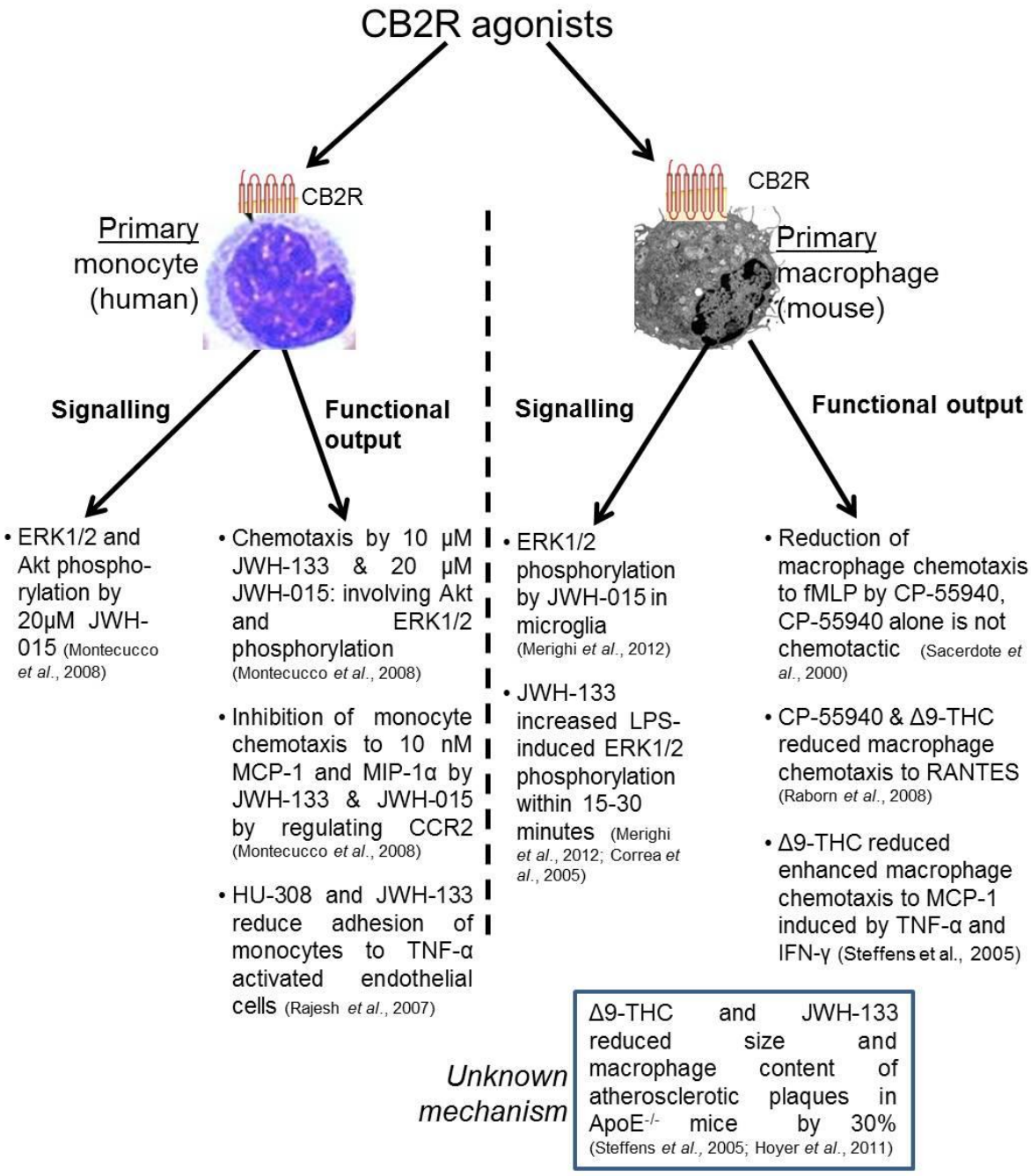

Figure 1.4: Key pathways studied in the literature about the immunological role of CB2R

This figure outlines the pathways studied in primary (physiological levels of the CB2R and physiological coupling) monocytes and macrophages. In this thesis signalling pathways and chemotaxis as a functional output were investigated with only selective CB2R agonists in primary murine macrophages.

1.5 Original hypothesis and thesis aims

Consideration of the published literature suggested that the endocannabinoid system has clear modulatory effects on macrophage, monocyte and microglia inflammatory responses. At the start of this thesis, Steffens *et al.* (2005) reported that Δ9-THC reduced atherosclerotic lesion size and macrophage content of lesions (Figure 1.2). These observations led to the hypothesis that specific activation of CB2R could regulate inflammatory responses by affecting recruitment of monocytes and macrophages; however the mechanism was and still is unclear (Figure 1.4). Moreover limitations for *in vivo* studies exist due to the high lipophilicity of currently available compounds targeting the cannabinoid receptors. Both cannabinoid receptors have highly hydrophobic pockets and their lipid ligands access the receptor binding pockets via the lipid bilayer (Hurst *et al.*, 2010). Identification of novel selective CB2R agonists would enable us to use these compounds in *in vivo* inflammation models at doses reflecting their activity rather than their solubility.

Aims:

- Identify novel selective CB2R agonists using virtual screening (Chapter 3)
- Use identified CB2R agonists in *in vivo* inflammation models (Chapter 4)
- Elucidate the signalling pathways activated by CB2R that are involved in regulating macrophage/monocyte recruitment in inflammation (Chapter 5)

CHAPTER 2 : METHODS

2.1 Animals

All animal experiments were performed with ethical approval from the Sir William Dunn School of Pathology Local Ethical Review committee and in accordance with the UK Home Office Regulations (Guidance of the Operation of Animals, Scientific Procedures Act, 1986. The mice used for all experiments were male C57BL/6J mice, 8-10 weeks old from Harlan Laboratories (Bicester, UK). When designing animal experiments attention was paid to integrate the principles of 3Rs (Reduction, Refinement and Replacement) (www.nc3rs.org.uk).

2.2 Materials

Materials for cell culture and *in vivo* experiments

- Dulbecco's phosphate buffered saline (PBS), Roswell Park Memorial Institute (RPMI) 1640 with L-Glutamine, foetal calf serum (FCS), penicillin/streptomycin and 4-(2-hydroxyethyl)-piperazine-1-ethanesulfonic acid (HEPES) were purchased from PAA laboratories (Yeovil, UK).
- 2-mercaptoethanol, ethylenediaminetetracetic acid (EDTA), bovine serum albumin (BSA), trypan blue 0.4%, dimethyl sulfoxide (DMSO), IBMX, forskolin from *Coleus forskohlii,* zymosan A from *Saccharomyces cerevisiae*, Cremophor®-EL, absolute ethanol (200 proof) and (2-hydroxypropyl)-β-cyclodextrin were purchased from Sigma-Aldrich (Gillingham, UK).

- Biogel P100 gel (polyacrylamide beads) was purchased from Bio-Rad (Hemel, Hampstead, UK). Saline 0.9% was purchased from Fisher Scientific (Thermo Scientific, Loughborough, UK). OptiMEM® was purchased from Invitrogen (Paisley, UK).
- Mouse brain cDNA (made from a mixture of E18, P0 and P8 mouse brains) was a kind gift of Dr Wei Zhi Wang from the department of Biochemistry, University of Oxford.

Compound	*Company*	*Stock*	*Storage*
HU-308	Tocris Bioscience	100 mM DMSO	-20^{o}C
JWH-133	Tocris Bioscience	100 mM DMSO	-20^{o}C
2-AG	Tocris Bioscience	100 mM DMSO	-80^{o}C
SR-144528	Cayman Chemical	40 mM DMSO	-20^{o}C
ACEA	Tocris Bioscience	100 mM DMSO	-20^{o}C
Δ9-THC	Sigma-Aldrich	79.5 mM ethanol (provided in solution)	-20^{o}C
L-α-Lysophosphatidyl-inositol (LPI) sodium salt from soybean	Sigma-Aldrich	20 mM DMSO	-20^{o}C
SAR compounds	Were synthesised by Matteo Gianella-Borradori (Department of Chemistry, Oxford)	10 mM DMSO	Room temperature (RT) for up to a week

Table 2.1 Cannabinoid ligands used in this thesis
All cannabinoids aliquots were warmed up at 37^{o}C for 15 minutes prior use to enhance solubility.

Tocris Bioscience (R&D Systems Europe, Abingdon, UK), Cayman Chemical (Cambridge, UK). Sigma-Aldrich (Gillingham, UK)

Table 2.2: Reagents and antibodies used in flow cytometry in this thesis

Reagent/Antigen	*Company*	*Clone*	*Dilution*	*Isotype*
Rabbit serum	Sigma-Aldrich	---	5%	
FcR II/III block	AbD Serotec	---	1:150	
Mouse gamma globulin	Jackson ImmunoResearch laboratories	---	1:100	
7/4 (FITC) (Ly-6B.2 alloantigen)	AbD Serotec	7/4	1:80	Rat IgG_{2a}
Ly6G (PE)	BD Biosciences	1A8	1:80	Rat IgG_{2a}
Ly6C (PerCP)	eBioscience	HK1.4	1:100	Rat IgG_{2c}
CD11b (APC)	AbD Serotec	M1/70.15	1:80	Rat IgG_{2b}
B220 (APC) (CD45R)	eBioscience	RA3-6B2	1:160	Rat IgG_{2a}
F4/80 (APC)	AbD Serotec	CI:A3-I	1:160	Rat IgG_{2b}
Rat IgG_{2a}	eBioscience	---	accordingly	
Formaldehyde solution (36.5%)	Sigma-Aldrich	---	Final: 1-2%	

AbD Serotec (Oxford, UK), BD Biosciences (Oxford, UK), eBioscience (Hatfield, UK), Jackson ImmunoResearch laboratories (Suffolk, UK), Sigma-Aldrich (Gillingham, UK)

Reagent/Antigen	*Company*	*Dilution*	*Species*
Complete Mini, EDTA free, protease inhibitor cocktail	Roche	1 tablet in 10 ml	
Phosphatase inhibitor cocktail 2	Sigma	1: 100	
BCA (bicinchoninic acid) protein assay kit	Thermo Scientific	Solution A : B 50 : 1	
Hybond-C extra nitrocellulose membrane	GE Healthcare		
Whatman filter paper	Sch & Sch		
ColorPlus prestained protein marker (7-175 kDa)	NEB		
Phospho-MAPK 44/42	CST	1:1000	Rabbit
Total ERK 2	Santa Cruz	1:1000	Rabbit
Phospho-Akt (Ser473)	CST	1:1000	Rabbit
Total Akt	CST	1:1000	Rabbit
Hck	R&D	1 µg/ml	Rat IgG_{2a}
anti-rabbit IgG-HRP	Bio-Rad	1 : 4000	Goat
anti-rat IgG-HRP	CST	1: 2000	Goat
Dried non-fat milk	Marvel	5 % w/v	
Tween® 20	Sigma	0.05 %	
SuperSignal West Pico	Thermo Scientific	Solution A : B	

Chemiluminescent Substrate		1 : 1	
Super RX medical X-ray film	Fuji (distributor: Thermo Scientific		

Table 2.3: Reagents and antibodies used for western blots in this thesis
Roche (Burgess Hill, UK), Sigma-Aldrich (Gillingham, UK), Thermo Scientific (Loughborough, UK), GE Healthcare (Chalfont St Giles, UK), Sch & Sch: Schleicher & Schuell (Dassell, Germany), NEB: New England Biolabs (Hitchin, UK), CST: Cell signalling technology (distributor: NEB, Hitchin, UK), Santa-Cruz (Heidelberg, Germany), R&D (R&D Systems Europe, Abingdon, UK), Bio-Rad laboratories (Hemel, Hampstead, UK), Marvel milk was from a local supermarket, Hck: hemopoietic cell kinase, HRP: horseradish peroxidase

Primers for polymerase chain reactions (PCR)

Primers were designed using the freely available Autoprime (Germany) with Guanine cytosine (GC) contents of 45-55%, at most 3 consecutive guanines, PCR amplicon lengths: 100-200 base pairs (bp) and total primers length between 19-24 bp. The primers were then blasted on the National Centre for Biotechnology information (NCBI) to confirm target genes.

CB1R (forward, FP): AAGGCCAGCGTTCAGCAA

CB1R (reverse, RP): ATCCTCCACACTCCCCTCTTC (primer pair used at 53^{o}C)

CB2R (FP): TCTGGGTGCCTGCCTTTG

CB2R (RP): AGCGCCTTGAACCTCCATCT (primer pair used at 59^{o}C)

GPR55 (FP): TTCACCAAGCAGCACAAAGG

GPR55 (RP): GCCATTTCCCTCCAGGAACT (primer pair used at 58^{o}C)

GAPDH (FP): ATGTTTGTGATGGGTGTGAAC

GAPDH (RP): CTGTGGTCATGAGCCCTTC (primer pair used at 58^{o}C)

Reagent	*Company*	*Dilution*
Random primers	Invitrogen	0.5 µg per µg of RNA, 1 µl/sample
M-MLV RT buffer (x5)	Promega	5 µl per sample
M-MLV reverse transcriptase (RT) enzyme	Promega	200 units per µg of RNA, 1 µl/sample
Deoxynucleotide (dNTPs) mix	Sigma-Aldrich	10 mM stock, 1.25 µl/sample
rRNasin RNase inhibitor	Promega	40 units/µl, 1 unit/µl
PCR tubes	Thermo Scientific	
SYBR green	Qiagen	
qRT-PCR tubes	Corbett Research	
Custom primers	EuroFins	300 nM final

Table 2.4: Reagents used in RT-PCR in this thesis
Promega (Southampton Science Park, UK), Qiagen (Manchester, UK), Sigma-Aldrich (Gillingham, UK), Thermo Scientific (Loughborough, UK)

2.3 Isolation of Biogel-elicited macrophages

There are several ways to obtain primary murine macrophages in adequate numbers for tissue culture experiments. These include bone-marrow derived macrophages (BMDM) and Biogel or thioglycollate-elicited macrophages (Davies *et al.*, 2005). Unlike BMDM, elicited macrophages are typically more activated since they were actively recruited in the cavity due to the eliciting stimulus and are therefore better suited for functional assays. In the first description of the Biogel-elicitation method, injection of 45-90µm Biogel P100 polyacrylamide beads leads to the recruitment of phagocytes (both neutrophils and macrophages) which are unable to phagocytose beads bigger than the cells' size (Fauve *et al.*, 1983). In our studies, 1 ml of 2% Biogel P100 beads (2% w/v beads in PBS, the solution was then autoclaved for sterility) were injected intraperitoneally to male 8-12 week old C57BL/6J mice using a 26G x ½" needle. Four days later the mice were culled with CO_2 asphyxiation and 10 ml of PBS/ 2mM EDTA were injected in the peritoneal cavity. A 19G x2" needle was

then used to massage the peritoneal cavity and to collect the cells into ice cold 15 ml polypropylene tubes. The cells were then centrifuged at 4^{o}C, 1000 rpm for 5 minutes and the pellets were resuspended in culture media to be used immediately in assays or FACS buffer 1 for flow cytometric analysis. Representative flow cytometry plot of the peritoneal cell exudates (PECs) are shown below (Figure 2.1). Biogel-elicited PECs consist of approximately 50-55% monocytes/macrophages, 35-40% neutrophils and 10% other cells. The cellular composition of Biogel-elicited PECs in our studies is in line with the percentages reported in other studies (Fauve *et al.*, 1983; Hart *et al.*, 2010).

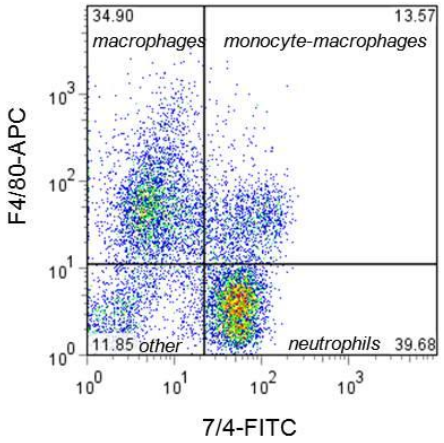

Figure 2.1: Characteristic Biogel-elicited PECs FACS plot

2.4 Isolation of human CD14^{+} monocytes

Healthy donor blood was collected by the National Health Service Blood and Transplant (NHSBT) and was processed into component donation leukocyte cones according to institutional guidelines. The blood was collected into 50 ml tubes, topped up to 40 ml with PBS and then separated into 4 tubes. Then the blood was underlayered with Ficoll-Paque Plus (GE Healthcare) and the tubes were centrifuged

2200 rpm, 30 minutes, slow acceleration, no deceleration. The plasma layer was aspirated and the white interface of peripheral blood mononuclear cells (PBMC) was collected into fresh tubes. The PBMCs were washed twice with PBS. The required number of PBMCs was added to a separate tube, washed with MACS buffer (Appendix 1). The cells were then resuspended with 80 µl MACS buffer per 10^7 cells and 20 µl of CD14 Microbeads (Miltenyi Biotech, Church lane Bisley, UK) were added per 10^7 cells. The cells and beads were mixed well and incubated at 4^oC, in the dark, for 15 minutes. Cells were washed with 2 ml MACS buffer per 10^7 cells and the pellet was resuspended 500 µl MACS buffer per 10^8 cells. LS columns (Miltenyi Biotech) were placed in the magnetic field of a MACS separator (Miltenyi Biotech) and were rinsed first with MACS buffer before the cell suspension was added. The column was then washed three times with 3 ml MACS buffer. The column was then removed from the magnetic field, 5 ml of MACS buffer were added to the column and the cells were immediately flushed into a new tube. The cells were then washed with chemotaxis buffer and immediately used. Characteristic flow cytometry plots of the PBMCs and $CD14^+$ monocytes are shown in Figure 2.2.

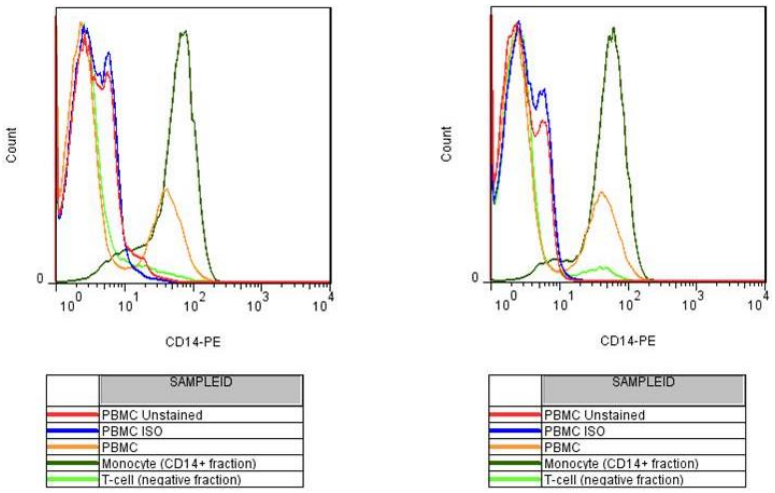

Figure 2.2: FACS plots from 2 donors for CD14 isolation indicating purity

2.5 Bone marrow isolation and culture of bone-marrow derived macrophages (BMDM)

Femurs and tibia of mice were collected from male C57BL/6J mice and cleaned from muscle and fur. The bones were then severed at each end and flushed with cold PBS. The clumps were dispersed by pipetting and the cells were passed through a 70μm cell strainer and then centrifuged for 5 minutes at 1000 rpm. The pellet from each mouse was re-suspended in BMDM-media (Appendix 1), counted and 4 million cells were then added per 9 cm petri dish (Sterilin, Cambridge UK) in 10 ml BMDM media. On the day 3, the media in each petri dish were topped up with 5 ml BMDM media. On day 7 the cells were detached with 5 ml cold PBS/ 10 mM EDTA, counted and used as needed.

2.6 Virtual screening

Virtual screening was performed in collaboration with Dr Russell's group (Department of Chemistry, University of Oxford, UK). HU-308 was selected as the ligand for ligand-based virtual screening for the reasons explained in Chapter 3. Forty conformers (spatial arrangements of atoms around single chemical bonds) for HU-308 and each compound in the medicinal chemistry library (20,000 compounds, two million conformers in total) were created using the programme *OMEGA* (OpenEye Scientific Software, Santa Fe, USA). The limitations used for the creation of conformers were: Comment energy true, verbose true, maxconfs 40 (or 100), maxrot 25, rms 0.5 (conformers designed with >0.5 similarity to lower energy conformation).

The conformers of HU-308 were screened against the conformers of the library using the programme *Rapid Overlay of Chemical Structures* (ROCS) (OpenEye Scientific Software, Santa Fe, USA). The limitations used for the alignment of conformers were: mcquery true, verbose true. The ranking of the library compound conformers was assigned according to their similarities to any of the HU-308 conformers. The top 500 ranks in the colour score (similarities in electrostatic forces), shape Tanimoto score (shape similarities) and combo score (a combination of colour and shape Tanimoto score) were identified by the programme ROCS.

2.7 β-arrestin interaction with GPCR assays

Ligand activation of GPCRs can lead to the activation of G-protein independent signalling pathways as well as G-protein-dependent signalling pathways. Depending on the receptor and the ligand, receptor activation induces the recruitment of specific G-protein receptor kinases which phosphorylate C-terminal serine/threonine residues to recruit β-arrestin proteins. β-arrestin proteins activate several downstream pathways including receptor desensitization, endocytosis and MAPK activation (Kovacs *et al.*, 2009).

In the DiscoveRx assays that I used in this thesis a GPCR is linked with a fragment of the enzyme β-galactosidase (β-gal) as a peptide tag format. Upon activation of the GPCR by a ligand, the complementary fragment of β-gal is recruited to the receptor and the β-gal enzyme is completed and this renders it active. Addition of substrate

(within detection reagents solution) leads to the generation of a chemiluminescent signal. Such assays allow the investigation of the alternative, G-protein-independent, β-arrestin pathway induced by receptor activation (Yan *et al.*, 2002).

The cells used in this assay were part of individual PathHunter^{TM} eXpress β-arrestin kits (DiscoveRx Corporation, Birmingham, UK). Specifically the cells used were: CHO-K1 mCNR2, CHO-K1 hGPR55, and human-embryonic kidney cells (HEK)-hCXCR2. 4150 growth-arrested cells (50 µl/well) were plated in half-area opaque clear-bottom 96-well plates (Corning) in provided PathHunter® Cell Plating 0 Reagent for 48 hours at 37^{o}C, 5% CO_2. Two days later the solutions were prepared containing 11 times the desired concentration in PathHunter® Cell Plating 0 Reagent. Then compounds or solvent (0.5% DMSO) were added in 5 µl volume to the wells and the plates were then incubated for 90 minutes at 37^{o}C, 5% CO_2. After the incubation step, working “detection reagent solution” was prepared according to manufacturer’s instructions with provided components and added to each well (27.5 µl). The plates were then incubated 90 minutes at RT in the dark, luminescence signal was measured using a standard luminometer (spectral range 250-850 nm) and raw data as Relative luminescence units (RLU) were exported to Excel for further analysis.

2.8 CB1R and CB2R cAMP assays on transfected cells

GPCR receptors characteristically exist in association with an inactive complex of three G-protein and guanosine diphosphate (GDP). Upon receptor activation by a ligand, conformational change of the receptor enables the receptor to act as a catalyst for the exchange of GDP for guanosine triphosphate (GTP). Acquiring of GTP activates the G-protein complex and leads its dissociation to Gα and Gβ/γ protein subunits which activate distinct signalling pathways. In the case of CB1 and CB2 cannabinoid receptors, the G-protein complex includes a Gαi-protein subunit, which when dissociated from the receptor exerts an inhibitory effect on the enzyme adenylate cyclase, leading to the conversion of ATP to cAMP. cAMP has many functions in a cell mainly by regulating protein kinases involved in regulation of many functions including cell differentiation, energy metabolism and regulation of mediator release depending on the cell type.

In the DiscoveRx cAMP assays, specific amounts of cAMP in the cells will pre-conjugated with β-galactosidase enzyme donor (ED). Within the activated and then lysed cells, the foskolin-induced cAMP and the conjugated cAMP-ED will compete for binding to the anti-cAMP antibody. In the presence of forskolin the increased amount of unconjugated cAMP will displace the ED-conjugated cAMP from the antibody, which will then be available to conjugate with the enzyme acceptor and thus form an active β-galactosidase enzyme. The active enzyme will be able to hydrolyse the substrate and produce a chemiluminescent signal. On the other hand, if the cells are activated by Gαi-coupled receptor agonist, the cAMP produced by forskolin will be

reduced therefore the conjugated cAMP will bind to the antibody and the uncompleted enzyme will not be able to hydrolyse the substrate.

Chinese hamster ovary (CHO)-K1 cells over-expressing either hCB1R or hCB2R were used as part of individual cAMP Hunter^{TM} eXpress kits from DiscoveRx (DiscoveRx, catalog number 95-0060E2CP2M). 15,600 cells (50 µl/well) were plated in half-area opaque clear-bottom 96-well plates (Corning, Birmingham, UK) in provided OCC2 media. The cells were incubated for 18 to 24 hours in 37^{o}C, 5% CO_2. The following day solutions were prepared four times the desired concentration in the provided "Cell Assay Buffer" and in the presence of 80 µM forskolin in 4% DMSO (provided in kit, reconstituted as 2 mM solution in DMSO, as optimized by company desired concentration on cells is 20 µM, final DMSO concentration 1%). The media was then aspirated from the cells and replaced with 22.5 µl of anti-cAMP antibody solution (1:3 dilution of anti-cAMP antibody with cell assay buffer, both provided with the kit). The compounds or solvent (0.2% DMSO) were then added to the cells at 7.5 µl/well for thirty minutes at 37^{o}C, 5% CO_2. To generate a cAMP standard curve, cAMP standard (250 µM provided with kit) was diluted 1:4 in cell assay buffer to generate highest final concentration of 5.2 µM in the final volume of 90 µl. Three-fold serial dilutions were also prepared. 7.5 µl of cAMP standard were added in empty wells and 22.5 µl of cAMP antibody solution was added on top. Detection limit of this assay was 2 nM of cAMP. During the incubation period the provided detection reagents were prepared as follows and then gently mixed: 3.8 ml Lysis Buffer, 1 ml Substrate Reagent 1, 0.2 ml Substrate Reagent 2. 5 ml of Reagent D were added to the mixed substrate solution and were again gently mixed.

Following the thirty minute incubation, 30 µl of the multi-component detection reagent mentioned above (patented) were added to all wells and incubated for one hour at RT in the dark. One hour later, 30 µl/well of the provided Reagent A (ready to use) were added to each well and incubated for three hours at RT in the dark. Three hours later the luminescence signal (spectral range 250 – 850 nm) correlated to total cAMP was recorded using a standard luminometer (Perkin-Elmer, Seer Green, UK).

The luminescence values of the wells containing cells incubated only with forskolin and solvent were normalised as 100%. The dose-response curves were expressed as a percentage of the forskolin and solvent wells. Once the dose-response curves were transformed to percentages, then the agonist doses needed to inhibit by 50% the induction of cAMP by forskolin (EC_{50} values) were identified using GraphPad prism non-linear regression curve fit (4 PL parameters). EC_{50} values from pooled experiments were obtained by plotting together dose-response curves from each experiment and then re-calculating the EC_{50} values. Detection limit of this assay was 2 nM cAMP so exact cAMP levels of unstimulated cells could not be extrapolated. Data are presented indicating the detection limit for two reasons: 1) the background cAMP levels could not be accurately detected to be subtracted and 2) any screened compounds non-specifically inhibiting the signal of detection reagents (rather than having CB2R-mediated effects) could be detected as they would inhibit the luminescence signal beyond the cAMP detection limit, for example SAR59 (page 98). Additionally non-specific action of CB2R agonists in the hCB2R cAMP assay was excluded by using active CB2R agonists in the similar hCB1R cAMP assay and observing no modulation of forskolin-induced cAMP production.

2.9 Radioligand binding assays

Radioligand binding assays were contracted to CEREP (Celle l'Evescault, France) where membranes from CHO-cells expressing either hCB1R or hCB2R were used to assess binding to the two cannabinoid receptors. Competition binding studies were performed by incubating membranes expressing hCB1R or hCB2R with the unlabelled compounds and tritiated CP-55940 (0.5 nM) or WIN-55212 (0.8 nM) respectively, for two hours at 37^{o}C. For CB1R and CB2R, non-specific binding was assessed using WIN-55212 at 10 and 5 μM respectively. Two hours later, the binding of tritiated ligands was assessed by scintillation counting. The competition binding data for each compound are expressed as the percentage of the remaining bound tritiated ligand after the compound's incubation with the membrane. EC_{50} values were identified using GraphPad prism non-linear regression curve fit. K_i values (equilibrium dissociation constants for each compound, reflecting affinity) were calculated from CEREP using the Cheng-Prusoff equation and the K_d value (equilibrium dissociation constant for each radioligand).

2.10 cAMP assay on primary murine Biogel-elicited macrophages

The media used throughout the cAMP studies with primary murine macrophages was chemotaxis buffer (Appendix 1). The forskolin concentration was chosen from published cAMP studies using primary murine peritoneal macrophages (Chang *et al.*, 1984). 4-day Biogel-PECs (isolated as detailed in section 2.3) were plated at 100,000 PECs/well of a 96-well plate and incubated in 37^{o}C, 5% CO_2 for 1 hour. The

cells were washed three times with warm PBS and the media was replaced for 2-3 hours to allow the cells to rest. 45 minutes prior cell stimulation the media was aspirated and replaced with 36 µl media. IBMX (100 µM) or solvent (0.2% ethanol) was then added to the cells for 20 minutes. Then 50 µM forskolin or solvent (0.25% DMSO) were added in 5 µl volume and the cells were incubated for 5 minutes at 37^{o}C. The cannabinoids or solvent (0.15% DMSO) or chemokines were added in a 5 µl volume for 5 minutes at 37^{o}C.

To terminate the assay, media were aspirated and replaced with 60 µl of the provided lysis buffer of cAMP-Screen® kit (Invitrogen). The cells were lysed for 30 minutes at 37^{o}C, while cAMP standards were prepared in lysis buffer ranging from 0.006 to 6000 pM. Lysates (60 µl) or standards (60 µl) were added in the pre-coated plate and then 30 µl of diluted cAMP-AP conjugate (provided undiluted, diluted in provided Conjugate Dilution Buffer) was added to each well, followed by gentle shaking of the plate for 2 minutes. Subsequently 60 µl of the provided anti-cAMP antibody was added per well and the plate was again shaken for 2 minutes. The plate was incubated for 30 minutes at RT in the dark, shaken briefly, and then incubated for 1 hour at RT. The plate was then washed 6 times with the provided Wash Buffer. Finally 100 µl of provided Substrate CSPD/ Sapphire-II RTU was added per well and the plate was incubated for 45 minutes, at RT, in the dark. The luminescence signal inversely correlated to total cAMP production was measured using a standard luminometer (spectral range 250 - 850 nm) and the cAMP concentration for each sample was extrapolated from the standard curve.

2.11 Zymosan-induced peritonitis

Zymosan-induced peritonitis was performed as previously described (White et al., 2011). Briefly, male C57BL/6 mice were injected intraperitoneally (i.p.) with 10 or 30 µg of zymosan or solvent (PBS) at 25 ml/kg. The kinetics of inflammatory cell recruitment in this zymosan dose are shown in Figure 4.1A & B. All i.p. injections in zymosan-induced peritonitis were performed with 0.5 ml 29G insulin syringes (BD Biosciences, Oxford, UK).

2.11.1 Studies using SigmaSolve and Tocrisolve™-100

Two hours after zymosan injection, the mice were injected i.p. with compounds dissolved in 1:1:18 ethanol: Cremophor®-EL: saline 0.9% (solution named as Sigmasolve in this thesis) or Tocrisolve™ -100 (75% water / 25% soya oil, Tocris Bioscience, Abingdon, UK) or for each case the solvent alone and administered at 25 ml/kg. The mice were culled four hours after zymosan and the peritoneal cavity was lavaged with 5ml of cold PBS/2mM EDTA.

2.11.2 Studies using DextrinSolve

Four hours after zymosan administration, the mice were injected i.p. with the compounds or the solvent (45% w/v (2-Hydroxypropyl)-β-Cyclodextrin dissolved in PBS, Appendix 1) at 5 ml/kg. Six hours after zymosan administration, the mice were sacrificed and the peritoneal cavity was lavaged with 5 ml of cold PBS/2mM EDTA. As shown in Figure 4.1B, without taking into account a possible solvent effect, at the time of compound administration the neutrophils were at peak and monocyte influx

was being initiated. Within 6 hours, the monocyte numbers would have reached ~EC_{30-40} of their maximum numbers in this model. Peritoneal exudates were immediately analysed by flow cytometry while cell-free supernatants were stored in -80^{o}C for later detection of sample analytes.

2.11.3 Flow cytometric analysis of zymosan-induced peritonitis samples

Total peritoneal cell counts were obtained by counting with a haemocytometer in the presence of 50% trypan blue 0.4% solution. Peritoneal exudates (350 µl) were added to 5 ml polypropylene flow cytometry tubes (Elkay, Basingstoke, UK) and then topped up with FACS Buffer 1 and centrifuged at 4^{o}C, 5 minutes, 1000 rpm. The pellets were resuspended in 50 µl FACS Buffer 2 with added FcR-II/III block and mouse gamma globulin and incubated on ice for fifteen minutes. Peritoneal cells were then stained with Ly6G, 7/4, Ly6C, CD11b and B220 (for details on reagents and antibodies refer to Table 2.2). The cells were then topped up with FACS buffer 1 and fixed with 1 % formaldehyde for at least one hour at 4^{o}C. Analysis was performed using a Dako Cyan ADP flow cytometer (Beckman Coulter Ltd, High Wycombe, UK). Using FlowJo software (Tree Star incorporation, Ashland, USA) the percentages of cells were obtained as follows. Cell doublets were excluded in analysis by gating around the one main peak in the Pulse width, then debris was excluded in the plot of forward and side scatter. After these exclusions, neutrophils were gated as Ly6G^{++}7/4^{++} while monocytes were gated as Ly6G^{-}7/4^{++} (as shown in Figure 4.2). To distinguish plasmacytoid dendritic cells (pDCs) and peritoneal B-cells in some experiments, the Ly6G^{-}7/4^{-} cell populations (Gautier *et al.*, 2012) were gated

as shown in Figure 4.13 and then pDCs were gated as $Ly6G^{-}7/4^{-}B220^{+}Ly6C^{+}$ while B-cells were gated as $Ly6G^{-}7/4^{-}B220^{+}Ly6C^{-}$ (Hochrein *et al.*, 2002; Nikolic *et al.*, 2002). To obtain total numbers in the peritoneal cavity, percentages of the different cell types were multiplied with total peritoneal cell counts.

2.12 Enzyme-linked immunosorbent assays (ELISA) for analysis of peritoneal samples

MaxiSorp Nunc 96-well immunoplates (Thermo Scientific, Loughborough, UK) were coated overnight at RT with 100 µl of primary antibody according to manufacturer's instructions. The next day the plates were washed three times with ELISA wash buffer (Appendix 1), tapped dry and then blocked with 300 µl/ well Reagent diluent (1 % BSA in PBS) for one hour at RT. The plates were washed three times with ELISA wash buffer, tapped dry and then 100 µl of neat or diluted (in Reagent Diluent) sample along with an analyte standard curve was added to the wells for 2 hours at RT. The plates were washed three times with ELISA wash buffer, tapped dry and then 100 µl/well of secondary antibody were added according to manufacturer's instructions for 2 hours at RT. The plates were washed three times with ELISA wash buffer, tapped dry and then 100 µl of Steptavidin-HRP were added per well according to manufacturer's instructions for 20 minutes at RT in the dark. The plates were then washed three times with ELISA wash buffer, tapped dry and then 50 µl of QS-1 step ultra TMB solution (Thermo Scientific, Loughborough, UK) were added to each well. The plates were gently tapped and allowed to equilibrate for 20 minutes at RT in the dark. 3M-H_2SO_4 (50 µl) was added to each well and gently tapped to stop the

reaction. The optical density (OD) in each plate was read at 450 nm using a microplate plate reader (BioTek, Potton, UK). Log OD values for the standard curve were plotted against Log concentration values and the concentration of the samples was extrapolated from the linear part of the curve.

Analyte	Company	Species	Detection Limit (in pg/ml)	
			Lower	Upper
KC	R&D	mouse	15.6	1000
MIP-1α	R&D	Mouse	7.8	500
TNF-α	R&D	Mouse	31.3	2000
JE	R&D	Mouse	3.9	250

Table 2.5: Reagents and antibodies used in ELISA assays
R&D (R&D Systems Europe, Abingdon, UK)

2.13 Nitrite/Nitrate detection in supernatants

Once nitric oxide (NO) is produced and released in solution, it can react with either molecular oxygen to form nitrite or oxyhemoglobin and superoxide anion to form nitrate. Both nitrite and nitrate are metabolically stable products and can be detected in solution. In tissue-culture experiments due to the prolonged incubations in the presence of oxygen, NO is readily converted to nitrite which can be detected by the colorimetric Griess assay (Griess, 1879). However, in *in vivo* tissue samples, NO remains mainly in the form nitrate, and nitrates in samples have to be enzymatically reduced to nitrite in order to be detected by Griess assay. Alternatively, semi-automated NO-analysers can be used to detect nitrate/nitrite. In these analysers vanadium (III) chloride in hydrochloric acid is used in order to convert both nitrate and nitrite to NO. Then reaction of NO with ozone leads to the release of nitrogen dioxide

(NO_2) and excitation of NO_2-electrons leads to light emission detectable by a photomultiplier tube.

Peritoneal exudate supernatants (50 µl) were added to a purge chamber of boiling 10 ml 97% vanadium (III) chloride (Sigma Aldrich, Gillingham, UK) in 1 N HCl maintained at 90-95°C and under a helium atmosphere. Nitric oxide, nitrate and nitrite was liberated from the samples into the gaseous headspace and conducted to the NO analyzer (Sievers Instruments Inc, Boulder, Colorado, USA) where it reacted with ozone to produce a chemiluminescent signal in the 650 to 800 nm range. The signal was graphically shown as a peak in the provided programme eDAQ. Then all the peaks were manually highlighted and the area under the curve was estimated by the programme. The amount of light was directly proportional to the NO concentration and samples concentration was extrapolated from the linear part of a sodium nitrate (Sigma Aldrich, Gillingham, UK) standard curve (dissolved in double-distilled water). Each sample was assessed in duplicate.

2.14 Polymerase-chain reaction (PCR) for mRNA detection

2.14.1 Cell treatment and lysis

2% Biogel beads were injected i.p. in mice and four days later the peritoneal cavity was lavaged with 10 ml of cold PBS/ 2mM EDTA. The media used throughout the mRNA studies was OptiMEM® (Appendix 1). To obtain a macrophage population enriched by adhesion, 1.6 million PECs ($0.8x10^6$ cells/ml) were plated per well of a 6-well plate and incubated in 37^oC, 5% CO_2 for one hour. The beads and non-

adherent cells were removed by three washes with pre-warmed PBS. 2 ml OptiMEM® was then added to the wells and the cells were allowed to rest for 2 hours at 37^{o}C, 5% CO_2. The media was then aspirated and replaced with 1 ml Trizol® (Invitrogen) and incubated for 2-3 minutes. Following thorough mixing by pipetting across the well, the lysates were transferred to eppendorf tubes and frozen at -80 ^{o}C.

2.14.2 Ribonucleic acid (RNA) isolation, purification and quantitation

The tubes were thawed, placed on ice and chloroform (200 µl) was added. The tubes were vortexed for 30 seconds and allowed to stand at 4^{o}C for 10 minutes, followed by centrifugation at 12,000 rpm for 20 minutes at 4^{o}C. The colourless phase was carefully collected and transferred to a new tube. An equal volume of 70% ethanol was added and immediately mixed. Total RNA was purified using an RNeasy mini kit (Qiagen) according to manufacturer's instructions for purification of RNA from animal cells. Genomic deoxyribonucleic acid (DNA) was removed by on-column DNase digestion using an RNase-Free DNase set (Qiagen) according to manufacturer's instructions. The concentration of purified RNA was measured using a Nanodrop ND-1000 Spectrophotometer at 240 nM (Thermo Fisher Scientific).

2.14.3 Reverse transcription (RT) reaction

RNA was transcribed to complementary DNA (cDNA) as follows. Random primers (0.5 µg per µg of RNA, 1 µl/sample) were mixed with 1 µg of RNA and made to total volume of 15 µl with nuclease-free water in PCR tubes. The mixture was heated for

5 minutes at 70^{o}C to melt the secondary structure within the template, and then was immediately cooled at 4^{o}C for 5 minutes. Then the following mastermix (10 µl per RNA sample) was prepared: M-MLV RT buffer x5 (5 µl/ sample), M-MLV RT enzyme (200 units per µg of RNA, 1 µl/sample), dNTPs mix (1.25 µl/sample) and rRNasin RNase inhibitor (1 unit/µl of reaction). The mastermix was then added to the tube with the RNA and primers and the total volume was made up to 25 µl with nuclease-free water. At this stage for negative RT controls the volume of the RT enzyme was replaced with water. The reactions were incubated at 37^{o}C for 60 minutes, then 15 minutes at 70^{o}C to inactivate the enzyme using a PTC 100 programmable Thermal Controller (MJ Research Inc). The samples were then stored at 20^{o}C.

2.14.4 Traditional agarose gel PCR

The cDNA was mixed with 5x Orange G loading dye and 20 µl sample was loaded to a 2% agarose gel prepared in 0.5X TBE and containing 0.5 µg/ml ethidium bromide. For quantification purposes a DNA ladder was also added to the gel. The gel was run for 40 minutes at 100V and then the DNA bands were quantified under UV light using Gel Doc 2000 (Bio-Rad).

2.14.5 qRT-PCR

qRT-PCR was performed using SYBR green, a double-stranded DNA binding dye. In qRT-PCR tubes, 9 µl of the following mastermix was added for each reaction on ice: 2X QuantiTect SYBR green PCR mastermix, forward primer (300-500nM), reverse

primer (300-500nM) and nuclease free water. 1 µl of cDNA (of +/- RT) was added in each tube and reactions containing water instead of cDNA were used as negative controls. The cDNA was amplified using Rotor-Gene RG-3000 (Qiagen) with the following conditions (per cycle) for 40 cycles:

1. 95 ºC, 15 min (hold step) (for activation of DNA polymerase)
2. 94 ºC, 15 s (for denaturing)
3. X (specific for each primer)ºC, 30 s (for annealing)
4. 72 ºC, 30 s (extension)

2.15 Cytotoxicity assays on primary murine macrophages

Biogel-elicited PECs were plated at 75,000 cells/well of a 96-well plate in chemotaxis buffer (Appendix 1). The cells were incubated for 1 hour at 37^{o}C, 5 % CO_2 and then washed three times with pre-warmed PBS. The media was replaced and the cells rested until activation. Compounds or solvent were prepared in the assay media. The media on the cells was aspirated and replaced with the treatments for 5 hours. After 5 hours, the treatments were aspirated, the cells were washed twice with media and then 30 µl of media was added per well. Successively 30 µl of CTG CellTiter-Glo® (CTG) (Promega) was added per well and the plate was shaken for 2 minutes in the dark. The solutions were transferred in a white opaque 96-well plate (Greiner Bio-one Ltd, Brunel way, UK) and allowed to equilibrate in the dark for 10 minutes at RT. The luminescence signal was then read using a luminometer. Cell survival was expressed as a percentage of the signal in the media-treated cells.

2.16 Chemotaxis studies using modified Boyden chamber

Chemotaxis is a term referring to a specific cell migration towards a chemical concentration gradient (directional locomotion). Boyden (1962) was the first to describe a method specialised to detect chemotaxis towards soluble factors since previous studies were only capable to detect chemotaxis towards bacterial clamps using photomicrographic traces (Harris, 1953). Boyden's chamber was divided into two compartments separated by a filter membrane of a specific pore size. Leukocytes (rabbit polymorphonuclear cells) were added at the upper compartment while the soluble factor was added at the bottom compartment. After an optimised incubation time, the membrane was fixed, stained and cleared. The stained migrated cells attached to the membrane were then counted microscopically (Boyden, 1962). Although this technique was optimised for each cell type and modified from one chamber to 96-well format, it played a fundamental role in the discovery of several chemotactic factors, including chemokines and the bacterial chemotactic peptide fMLP (Becker, 1983; Rollins, 1997).

2.16.1 Chemotaxis for murine Biogel-elicited PECs

4-day Biogel-elicited PECs were collected as previously mentioned, washed once with pre-warmed chemotaxis buffer and then resuspended at 5 million cells/ml in chemotaxis buffer. For studies with the CB2R antagonist SR144528 the cells were incubated at RT for 30 minutes with the antagonist or solvent (0.1 % DMSO). For the studies with cannabinoid agonist pre-treatment, the cells were pre-treated with JWH-133, DIAS2 or solvent (0.1 % DMSO) for 3 hours at 37^{o}C, 5 % CO_2. Dilutions of

chemokines or cannabinoids (solvent 0.3 % DMSO) were prepared in chemotaxis buffer. 325 µl of solutions were added to the wells of 96-well Neuroprobe ChemoTx plate (8 µm pore, 5.7mm diameter filter sites, Receptor technologies, Leamington Spa, UK) in triplicate (for chemokines) or quadruplicate (for cannabinoids). The filter was then gently placed on top of the solution dome and 80 µl of cell suspensions (400,000 cells/well) were accordingly placed on the filter sites. The plates were then incubated for 3 hours (for studies with cannabinoid agonist pre-treatment) or 4 hours (for all other studies) at 37^{o}C, 5 % CO_2. The cells were then removed from the top of the filter, which was then wiped clean and rinsed with PBS. The filter was then fixed with 1 % formalin in PBS for 10 minutes. Following another rinse with PBS, the filter was stained in the dark with DAPI (Roche) dissolved 1 µg/ml in water for 10 minutes. The filter was again rinsed with PBS and then sets of six filter sites were cut and mounted onto slides using fluorescent mounting medium (Sigma-Aldrich) and left overnight at 4^{o}C. The following day, the DAPI-stained nuclei were detected using an Axiovert 200 fluorescent inverted microscope (Zeiss, Welwyn garden City, UK). Two random images were taken per filter site. The *Metamorph* programme (Molecular Devices, Wokingham, UK) was used to count the nuclei in each image. Chemotaxis index was calculated as the ratio of migrated cells in wells with test compounds over the average number of migrated cells in the media/solvent well.

2.16.2 Chemotaxis for human monocytes isolated with CD14 positive selection

Human monocytes were isolated with CD14 positive selection as previously described. 325 µl of solutions were added to the wells of 96-well Neuroprobe ChemoTx plate (5 µm pore, 5.7mm diameter filter sites, Receptor technologies) in triplicate (for chemokines) or quadruplicate (for cannabinoids). The filter was then gently placed on top of the solution dome and 80 µl of cell suspensions (300,000 cells/well) were accordingly placed on the filter sites. The plates were then incubated for 2 hours at 37^{o}C, 5 % CO_2. In initial attempts both the cells attached to the filter and the cells migrated into the bottom well were assessed but it was found that cells were detaching were readily detaching from the filter within the two hours endpoint. To assess whether the cells had migrated into the bottom well, after the 2 hour incubation the filter was removed and the bottom well was mixed well. Then 50 µl of the solution in the bottom well was mixed with 50 µl of CTG in a white opaque 96-well plate. The plate was shaken for 2 minutes and allowed to equilibrate for 10 minutes (in the dark), at room temperature, before the luminescence was read using a luminometer. Chemotaxis index was calculated as the ratio of the luminescent signal in wells with test compounds over the average luminescent signal in the media/solvent well since it was demonstrated that the number of cells correlates with luminescence signal with sensitivity down to 100 cells (Figure 2.3).

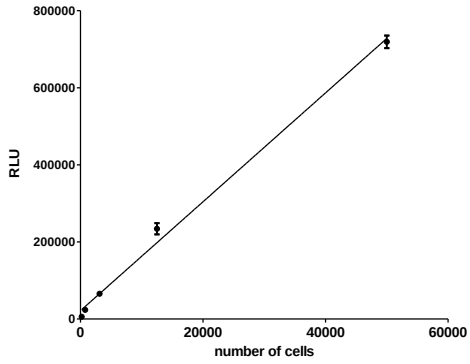

Figure 2.3: CTG detects cell number in a linear manner

2.17 Western-blot studies

2.17.1 Stimulation of cells

2% Biogel beads were injected i.p. in mice and four days later the peritoneal cavity was lavaged with 10 ml of cold PBS/ 2mM EDTA. The media used throughout the western blot studies was chemotaxis buffer (Appendix 1). Two million PECs ($1x10^6$ cells/ml) were plated per well of a 6-well plate and incubated in 37^oC, 5% CO_2 for one hour. The beads and non-adherent cells were removed by three washes with pre-warmed PBS. 2 ml chemotaxis buffer was then added to the wells and the cells were allowed to rest for 2 hours at 37^oC, 5% CO_2. One hour before stimulation, the media was aspirated and replaced with 1 ml chemotaxis buffer. Then 200 µl of treatments or solvent (0.3% DMSO for cannabinoids) were added to allocated wells for 5, 10, 20 or 30 minutes. After the incubations, the media was tipped off and the wells were gently tapped dry and placed in -80^oC.

2.17.2 Preparation of cell lysates

Cells were lysed by addition of 180 µl of Western Blot lysis buffer (Appendix 1) with added Phosphatase and Protease inhibitors (Appendix 1) and then manual disruption of cells in the wells using a 2 ml syringe plunger. The lysates were then spinned for 10 minutes, 13000 rpm at 4^{o}C and after the spin the supernatants were collected in new tubes. 10 µl of the lysate supernatants were reserved for the BCA assay while 4x Laemmli Buffer (Appendix 1) was added 1:4 to the rest of the lysates. The samples were then boiled for 5 minutes at 95^{o}C and stored at -80^{o}C or loaded to the gel.

2.17.3 BCA assay for protein concentration

The BCA assay (Table 2.3) is used to measure the protein concentration within each sample, which is necessary to ensure equal sample loading. In a 96-well plate, 190 µl of a solution containing a mixture of provided solution A and B (Table 2.3) was added to 10 µl samples (samples were diluted 1:5 in PBS). A BSA standard curve was included to extrapolate the protein concentration within the sample. The plate was incubated at 37^{o}C for 30 minutes. The samples were then read at 630nM using a microplate reader and a BSA standard curve was generated as shown in Figure 2.4. Sample concentrations were extrapolated from the linear part of the standard curve.

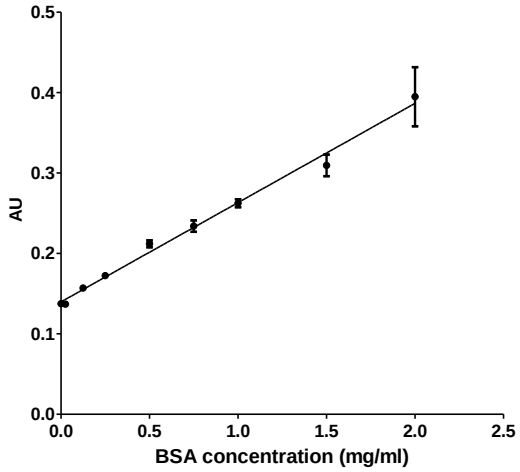

Figure 2.4: Representative graph of BCA assay for determining protein concentration

2.17.4 Sodium dodecyl sulphate polyacrylamide gel electrophoresis (SDS-PAGE)

SDS-PAGE was used in order to discriminate by size (molecular weight in kilo Daltons (kDa)) the denatured proteins within a sample and identify the exact size by comparing the protein size with a broad-range protein marker. A 10% running gel was used for separation with an upper layer of a 4% stacking gel. Samples were thawed and 30 µg were loaded on the SDS-PAGE gels, which were then run for 55 minutes at 150V in 1x Running buffer (Appendix 1) within a Mini Protean II electrophoresis cell (Bio-Rad, Hemel, Hampstead, UK).

2.17.5 Western blotting and development

Following the electrophoretic separation of proteins, samples were transferred from the gels onto nitrocellulose membranes by filling a Mini Protean II electrophoresis cell (Bio-Rad, Hemel, Hampstead, UK) with 1x Transfer buffer (Appendix 1) and run for two hours at 200 mA. In order to block non-specific binding, the nitrocellulose membranes were blocked for 1.5h at RT by slow rocking in 5% milk in TBS-T (Appendix 1). Following blocking, the membranes were washed with TBS-T twice for 1 minute and 3 times for 5 minutes. Membranes were then incubated overnight at 4^{o}C in the presence of the primary antibody diluted in 5 % milk/TBS-T (for pERK1/2 and total ERK2) or 5 % BSA/TBS-T (for pAkt and total Akt). The following day, the membranes were again washed with TBS-T twice for 1 minute and three times for 5 minutes. The secondary antibody diluted in 5 % milk/TBS-T was added to the membranes, which were then rocked slowly for 1.5h at RT. Membranes were washed twice with TBS-T for 1 minute and three times for five minutes. After the final wash the membranes were incubated for 5 minutes with 1 ml of SuperSignal West Pico Chemiluminescent Substrate (Table 2.3) and then exposed to X-ray film between 2 and 120 minutes. The film was processed using a Compact X4 X-ray film processor (Xograph, Tetbury, UK). The membranes were then stored at -20^{o}C in order to be tested for equal sample loading.

2.17.6 Stripping of western blot membranes

The membranes were washed twice for 1 minute with TBS-T and then placed in Stripping Buffer (Appendix 1) for 30 minutes at 50^{o}C. The membranes were then

washed 4 times with TBS-T for 5 minutes. The membranes were then re-blocked with 5 % milk/TBS-T and the same western blot protocol was repeated as above.

2.18 Phosphoarray assay

4-day murine Biogel-elicited macrophages were stimulated with solvent (0.3 % DMSO) or 10 μM of cannabinoid ligands JWH-133 and DIAS2 for 20 minutes (incubation times and compound concentration were selected from results in this thesis in Figure 5.8). The kit used a human phospho-kinase array kit (R&D) with most antibodies in this array cross-reacting with mouse species. The cells were lysed with the provided lysis buffer and then 330 μg of the lysates (concentration found by BCA assay) was loaded per membrane and the protocol was performed according to manufacturer's instructions were. Although no loading control was incorporated in the membrane, positive detection controls where included in each membrane at the top and bottom left-hand corner. Following film development, bands' intensity was analysed using by densitometry using ImageJ and the treatments' (JWH-133 and DIAS2) effect was normalised against the solvent.

2.19 Statistical analysis

Treatment groups were tested for normality using the D'Agostino Pearson omnibus test. Differences between normally distributed groups were tested with one-way Analysis of Variance (ANOVA) or two-way ANOVA followed by Dunnett's multiple comparisons test.

CHAPTER 3 : Discovery and characterisation of a novel class of CB2R agonists

3.1 Introduction

Targeting the cannabinoid CB2R has therapeutic potential in inflammatory diseases. Importantly, no psychoactive side-effects are expected with this therapeutic target, unlike targeting CB1R (Basu *et al.*, 2011a; Guindon *et al.*, 2008). Despite the inherent lipophilic nature of the endogenous ligands of the cannabinoid receptors, both cannabinoid receptors are druggable and selective CB1R and CB2R agonists and antagonists have been identified in the past 15 years (Di Marzo, 2009). The CB1R antagonist rimonabant had even reached the market as an orally available anti-obesity drug before being withdrawn for increasing suicidal rates and depression (Topol *et al.*, 2010). As I discuss below, abundant evidence exists that it is feasible to identify novel specific CB2R agonists with the potential to reach the market as a therapy for inflammation and pain.

3.1.1 Drug discovery challenges for CB2R agonists

A limited number of CB2R agonists have been identified so far and examples of CB2R agonists widely used as experimental tool compounds are shown in Figure 3.1. Despite the relative success in identifying selective CB2R agonists that have high efficacy in pre-clinical *in vivo* disease models and no activity in the CB1R-detecting tetrad test (da Silva *et al.*, 2011; Hanus *et al.*, 1999), only one compound

HU-308

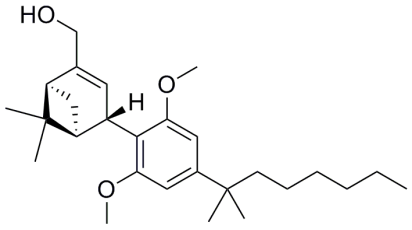

AM-1241

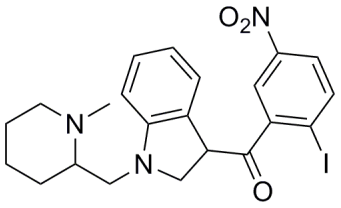

GW-405833

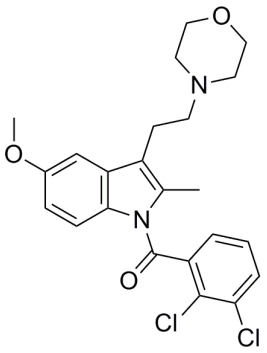

JWH-133

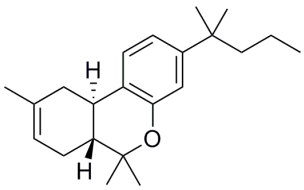

CB2R agonists	Affinity at hCB1R (nM)	Affinity at hCB2R (nM)	Selectivity for CB2R/CB1R (from affinity values)
HU-308	>10000	22.7	>440
GW-405833	4772	3.9	1200
JWH-133	677	3.4	200
AM-1241	280	3.4	82

Figure 3.1: Known selective CB2R agonists from the literature
CB2R was first identified on immune cells in 1993 (Munro *et al*., 1993) and many studies have since demonstrated its immunoregulatory effects (Howlett *et al*., 2002). Due to the therapeutic potential of a selective CB2R agonist, considerable effort has been made from both academic and industrial groups to identify such compounds. In this figure only selected examples of each structural class which are widely used and commercially available CB2R agonists are shown and the affinity values shown were obtained with radiolabelled ligand binding.

from GW Pharmaceuticals/GlaxoSmithKline (GW842166X) reached Phase-I clinical trials (Ostenfeld *et al.*, 2011). Several reasons may exist for this limited number of compounds that have progressed into the clinical arena. A possible reason could be the high lipophilicity of compounds such as HU-308, which is an undesirable physicochemical property since it can lead to low systemic exposure due to poor aqueous solubility and hence reduced *in vivo* activity (Di *et al.*, 2003). This is a problem not just for cannabinoid receptors but for all receptors with lipid ligands, for example the PPAR-γ receptors (Abdelrahman *et al.*, 2005; Shearer *et al.*, 2007). On the other hand, AM-1241, a widely used selective CB2R agonist (Malan *et al.*, 2001) demonstrated peculiar "protean agonist" pharmacology at the human CB2R. More specifically, AM-1241 in systems with low constitutive activity behaved as an agonist while in systems with high hCB2R expression and high constitutive activity of the receptor AM-1241 behaved as an inverse agonist (Yao *et al.*, 2006). A key challenge to advance CB2R agonists to the clinic is to expand our understanding of the complexity of CB2R pharmacology (Atwood *et al.*, 2012a) and identify novel chemical scaffolds which can be modified to reduce their lipophilicity and improve their pharmacokinetic properties *in vivo*.

Discovery of synthetic cannabinoid receptor ligands dates back to the 1980's predating even the discovery of the cannabinoid receptors themselves. Structure-activity-relationship (SAR) studies on the structure of Δ9-THC led to discovery of the more potent cannabimimetic analog CP-47497 (Weissman *et al.*, 1982), which was the prototype for the widely used non-selective cannabinoid receptor agonist CP-55940 (Devane *et al.*, 1988; Felder *et al.*, 1995; Melvin *et al.*, 1993). The first

selective CB2R agonists were the Δ8-THC (another component of *Cannabis sativa* similar to Δ9-THC) analogs L759633 and L759656, with selectivity at CB2R over CB1R of 163 and 414 fold respectively (Gareau *et al.*, 1996; Ross *et al.*, 1999), followed by the discovery of HU-308 with CB2R selectivity over 450 fold (Hanus *et al.*, 1999). On the whole, these studies were able to discover non-selective and selective CB2R agonists mainly by performing SAR studies on the molecule of Δ9-THC.

3.1.2 High-through put screening for the discovery of novel CB2R agonists

Several high-through put screens (HTS) exist for discovering novel GPCR ligands depending on the pharmacology and coupling of the receptor. In the cannabinoid area, radioligand binding studies with radiolabelled ligands have been used by pharmaceutical companies such as Merck (Hagmann, 2008; Vachal *et al.*, 2009) and Eli Lilly (Hollinshead *et al.*, 2012) to identify novel CB2R agonists. HTS calcium flux assays have been used for CB1R drug discovery within a chemical library (Szabo *et al.*, 2009) and a calcium-flux based HTS assay was also used to screen for cannabinoid ligands within a marine natural product extract library (Pereira *et al.*, 2009a). Additionally, use of a cAMP assay has been recently reported for the HTS of CB2R agonists (Zindell *et al.*, 2011).

Virtual screening is a computational method of compound screening from a chemical library in order to identify relevant compounds in a fast and cost-effective manner. Two main types of virtual screening are ligand-based virtual screening and structure-based virtual screening (Sukumar *et al.*, 2011). In ligand-based virtual screening, active known molecules are used as a target for identifying similar compounds within the library (Ripphausen *et al.*, 2011). Similarities in electrostatic forces and shape make the predominant contributions to the compound's similarity score with the known molecules (Kitchen *et al.*, 2004). A study using such a virtual screening approach used one set of CB2R agonists (including JWH-133, HU-308, AM-1241 and GW405833) and a second set of a CB2R antagonist (AM-630) to create two common-feature pharmacophore models before screening for similar compounds in a 1,000,000 compound library (Markt *et al.*, 2009). Following data mining for structure similarities and physicochemical property filtering, 14 compounds were screened for biological activity using a human CB2R cAMP assay. The authors identified one partial agonist, one antagonist and one inverse agonist all with affinity K_i between 1-2 μM and 3 novel scaffolds (Markt *et al.*, 2009). Thus, apart from time and cost-effectiveness advantages, ligand-based virtual screening can lead to the discovery of new chemical scaffolds whose discovery via traditional SAR studies on known molecules may never have happened.

Alternatively, virtual screening docking experiments use modelling of known GPCR receptor crystal structures, such as the rhodopsin receptor, to map the active site of the target receptor (Jorgensen, 2004). Protein-ligand docking is performed to identify hits with optimal positioning in the modelled receptor active site (Dias *et al.*, 2008).

For example, in the case of CB1R, a combination of mutagenesis studies and homology receptor studies have been used in drug discovery to identify synthetic ligands (Shim, 2010). Similar studies have been performed for CB2R. For example, in a study where a combination of common-feature pharmacophore modelling and a model of CB2R using rhodopsin as a template were used, 86 hits from a 50,000 compound library were screened in GTPγ-S assay leading to the identification of one novel CB2R agonist (Salo *et al.*, 2005). In summary, virtual screening can aid the identification of novel chemical scaffolds but docking experiments, which rely on homology models and not the actual structure of CB2R, may be a less effective method for detecting novel CB2R ligands.

3.1.3 Rationale

We reasoned that choosing one highly selective CB2R agonist (HU-308), instead of a compound set, for ligand-based virtual screening could provide a specific pharmacophore basis for identifying compounds with similar biological activity. Moreover, instead of performing traditional SAR studies on the structure of HU-308, virtual screening could rapidly identify distinct chemical scaffolds from the compounds present in a chemical library. HU-308 is also highly lipophilic and has poor in vivo availability. The ultimate goal of these experiments would be to identify selective CB2R agonists with novel chemical scaffolds and improved physicochemical properties compared to HU-308.

Two strategies are possible for testing the activity of novel compounds identified from virtual screening. The first one is radioligand binding studies for detection of ligand affinity for the receptor (Ekins *et al.*, 2007) and the other one is cell-based second messenger assays (such as cAMP and β-arrestin) for detection of ligand efficacy in inducing that particular pathway via the receptor (Kenakin, 2009; Williams, 2004). Affinity mainly reflects the strength of binding of the ligand for the receptor and does not provide information on the ligand's efficacy or agonist/antagonist nature. In theory, the ligand's affinity is only strongly correlated with the ligand's potency and efficacy to activate downstream signalling pathway when high receptor levels are present (Kenakin, 1985). On the other hand, second messenger assays provide direct information about the compounds efficacy in stimulating pathways downstream of the receptor. For these reasons and since we were specifically interested in identifying CB2R agonists and not antagonists, we opted to use second messenger assays for initial screening and then confirm by radioligand binding that the compounds were indeed acting via CB2R.

3.1.4 Experimental aims of this chapter

The aims of this chapter were to use virtual screening to identify novel compounds with similarity to HU-308, to expand the chemical family by SAR studies and pharmacologically characterize the active members of the discovered class in CB2R, CB1R and GPR55 assays. The chapter includes experiments to:

1. Identify and validate a suitable second messenger assay for screening potential CB2R ligands
2. Perform ligand-based virtual screening using HU-308 as bait and test the top 100 hits
3. Perform SAR studies to better characterise this novel chemical scaffold
4. Pharmacologically test the selectivity of the compounds for human CB2R
5. Demonstrate activity of lead compound in a second messenger assay on primary murine macrophages

Collaborators: Dr Angela J Russell and Matteo Gianella-Borradori (PhD student in Russell group) from the department of chemistry at the University of Oxford. Virtual screening (Aim 2) was performed with the help of Dr Russell. For the SAR studies needed to expand the chemical scaffold (Aim 3) Matteo Gianella-Borradori designed and synthesised the compounds.

3.2 Results

3.2.1 Identifying a suitable assay for screening

Two second messenger assays were tested for their ability to detect CB2R agonists. β-arrestin recruitment following receptor activation is a feature of many GPCRs so one of the assays tested was detection of β-arrestin recruitment following activation of mCB2R. From the commercially available compounds tested, only JWH-133 dose-dependently recruited β-arrestin with an EC_{50} of 1 μM while HU-308, 2-AG and Δ9-THC had no effect in this assay (Figure 3.2A). The second assay tested was a cellular cAMP assay since receptor-mediated inhibition of cAMP levels is a feature of all Gαi-coupled receptors. In the hCB2R-cAMP assay all agonists tested were able to decrease forskolin-induced cAMP production. Accordingly HU-308, JWH-133 and 2-AG had an EC_{50} of 36 nM, 38 nM and 1400 nM respectively in this assay (Figure 3.2B). The cAMP assay was selected as the screening assay for potential CB2R agonists since it ubiquitously detected all the tested CB2R ligands.

3.2.2 Virtual screening with HU-308 as template

Ligand-based virtual screening was performed with HU-308 as a template. HU-308 was selected due to its high selectivity for CB2R since it does not bind hCB1R at doses up to 10 μM (Hanus et al., 1999). Forty conformers (lowest energy conformations that the compound can exist in) of HU-308 were screened against a hundred conformers for every compound in the 20,000 compound library (i.e 2 million conformers in total) using the programme ROCS (Figure 3.3).

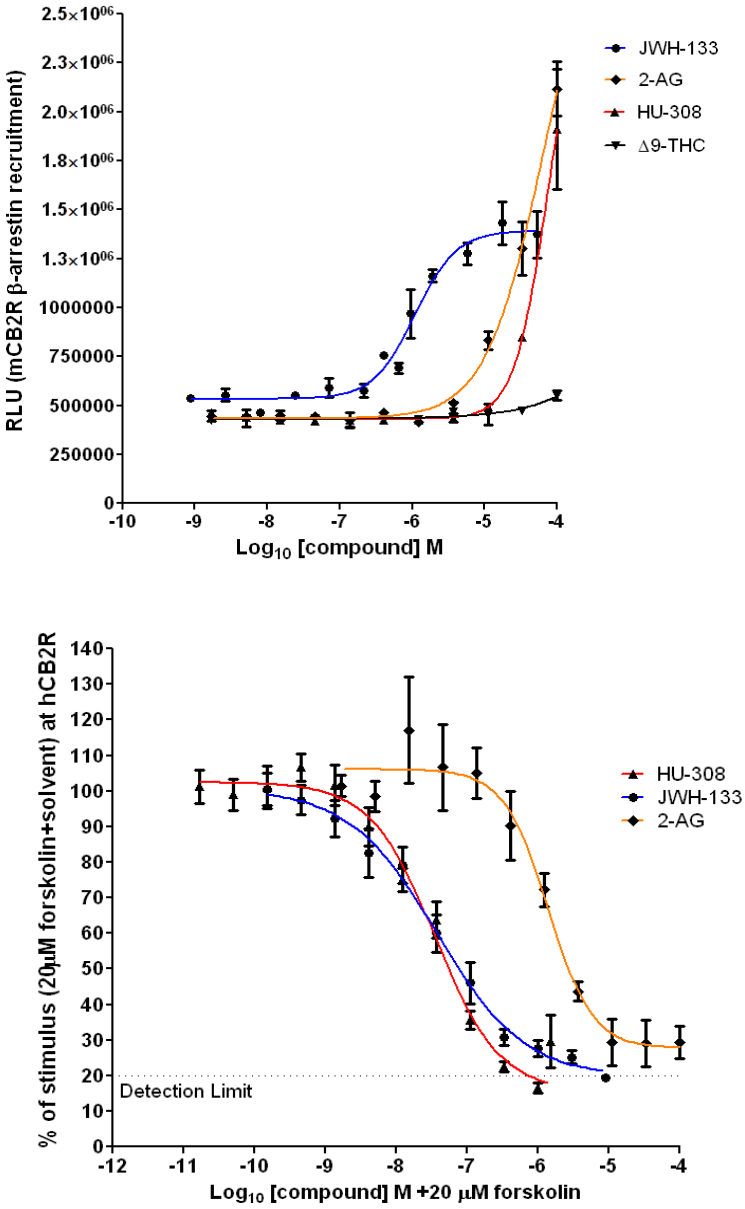

Figure 3.2: Comparing β-arrestin recruitment with cAMP assay for the screening of CB2R agonists

A) CHO-K1 mCB2R β-arrestin cells (DiscoveRx) were stimulated with compounds or solvent (0.5% DMSO) for 90 minutes followed by lysis of the cells according to manufacturer's protocol and detection of luminescence signal 90 minutes later. At this stage (revisited in Chapter 5) data were performed once, 2 technical replicates, error bars=standard deviation (SD). JWH-133 had an EC_{50} of 1 μM. B) CHO-K1 hCB2R cells (DiscoveRx) were stimulated for 30 minutes with compounds or solvent (0.2% DMSO) in the presence of 20 μM forskolin (1% DMSO). The cells were then lysed according to manufacturer's protocol and luminescence signal was detected four hours later. HU-308, JWH-133 and 2-AG had an EC_{50} of 36 nM, 38 nM and 1400 nM respectively. Pooled data of 3 independent experiments, 2 technical replicates, error bars=standard error of mean (SEM).

Compound	Combo score	Colour score	Shape Tanimoto score
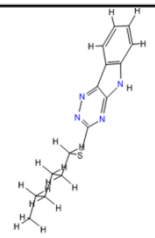	1.217 *Rank:1*	0.504 *Rank: 1*	0.713 Rank: 29
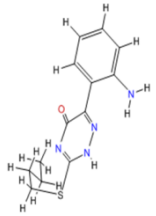	1.19 *Rank:2*	0.493 *Rank: 2*	0.697 Rank: 74
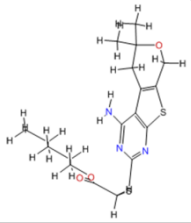	1.1 Rank: 26	0.36 Rank: 383	0.75 *Rank: 1*
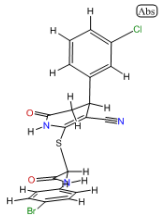	1.079 Rank: 62	0.336 Rank: 456	0.743 *Rank: 2*

Figure 3.3: Ligand-based virtual screening using HU-308: Top 2 hits from combo, colour and shape Tanimoto score

HU-308 was selected as the ligand for the virtual screening due to its high selectivity for CB2R over CB1R (>440 fold). 40 conformers of HU-308 were aligned against 100 conformers of each compound in the 20,000 compound library and compared for similarities using the programme ROCS. The program gave by default top 500 hits according to shape similarity (Shape Tanimoto score), electrostatic properties (Colour score) and a combination of both scores (Combo score). The top 2 hits from each scoring list are shown here as examples and the compounds are shown as the 2D conformation with the most similarity to HU-308.

The ranking of the library compound conformers was assigned according to their similarities to any of the HU-308 conformers. The top 500 ranks in the colour score (similarities in electrostatic forces), shape Tanimoto score (shape similarities) and combo score (a combination of colour and shape Tanimoto score) were identified by the programme. In Figure 3.3 the top 2 compounds for each score are shown. From these top 500 hits in each category the aim was to screen the top 60 in the combo score and the top 30 in the colour and shape Tanimoto score. By high-through-put screening only compounds with high chemical similarity to HU-308 (thus high score assigned by ROCS) we could identify a novel compound with CB2R activity, then by using SAR studies we could expand its scaffold into a chemical family. Taking into account compounds appearing to top ranks in more than one score and unavailability of six compounds in the library, ninety four compounds were screened in total in the cAMP assay.

3.2.3 Discovery of novel CB2R agonist using the optimised hCB2R cAMP assay

In $G\alpha_i$-cAMP assays, cAMP levels are raised by activation of AC by forskolin and activation of the $G\alpha_i$-coupled receptor leads to inhibition of AC and reduction of cAMP levels (Figure 3.4C, forskolin and $G\alpha_i$ actions in pink and blue arrows respectively). We designed the cAMP screening plates to include both a positive control (HU-308) and a cAMP standard curve to assess the sensitivity of the assay and serve as a cell-independent control for luminescence detection (Figure 3.4A and B).

A

cAMP standard curve (single points)										
HU-308 dose-response curve (single points) + 20 µM forskolin										
Forskolin + solvent	3µM of A	1µM of A	3µM of B	1µM of B						Forskolin + solvent

B

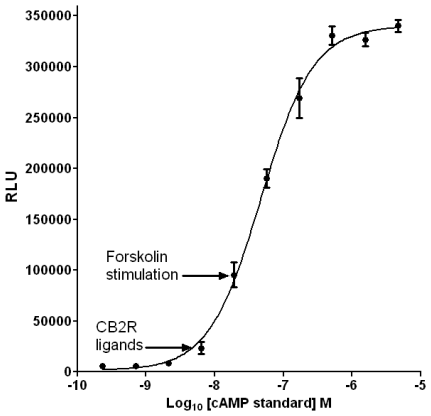

C

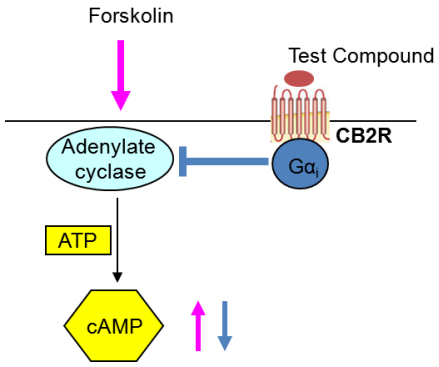

Figure 3.4: Screening plate layout, cAMP assay principle and standard curve

96-well screening plates were set up to include a positive control (HU-308) and a cAMP standard curve in each plate. The goal of our screen was to identify potent agonists with an activity plateau at 1 and 3 µM. For this reason, compounds were screened in these doses in duplicate and in the presence of 20 µM forskolin. Moreover, a confidence interval of 2 SD from the mean value of the stimulus was applied to identify hits. A) Screening plate layout, B) Representative cAMP standard curve pooled from 2 plates in the same assay, C) cAMP assay principle.

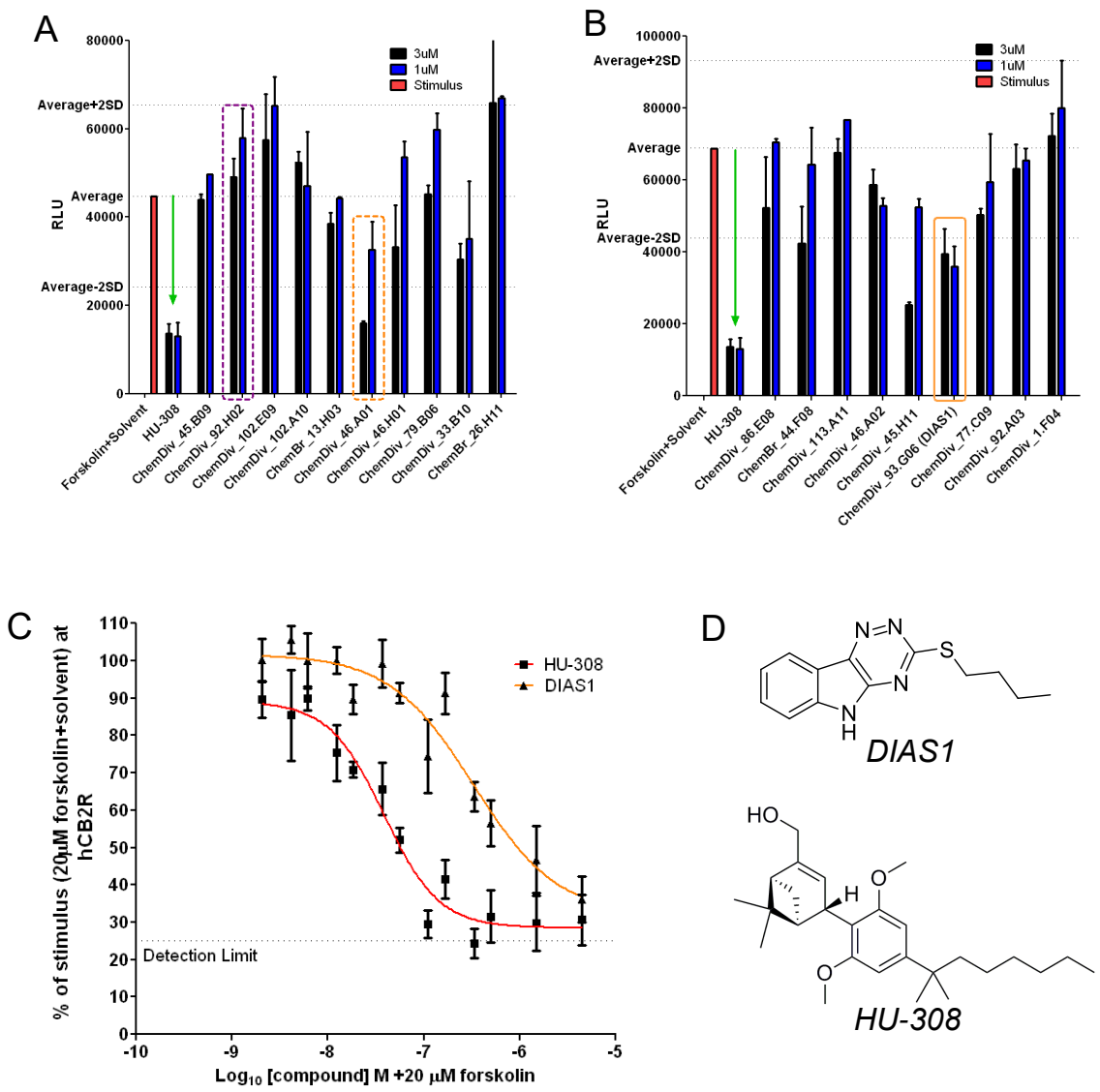

Figure 3.5: Examples of screening plates and identification of DIAS1 from the first round of virtual screening

CHO-K1 hCB2R cells were stimulated with compounds in the presence of forskolin as in Figure 3.2. From the 94 library compounds screened in the hCB2R cAMP assay, only one compound (DIAS1, combo rank 16) inhibited at 1 and 3 µM the forskolin-induced cAMP production and was validated further. A) and B) Screening plate examples, error bars=SD from 2 technical replicates. C) HU-308 and DIAS1 dose-response curve with EC_{50} of 37 and 320 nM in the hCB2R cAMP assay. Pooled data of 3 independent experiments, error bars=SEM, D) Structures of DIAS1 and HU-308.

Since the aim was to discover potent CB2R agonists with activity in the nanomolar range, thus similar potency to other CB2R agonists, like HU-308 which exhibit E_{max} at at 1 and 3 μM (Figure 3.2B), all 94 compounds were tested at 1 and 3 μM doses since potent. From the 94 compounds tested in the cAMP assay, only one compound (named DIAS1) exhibited a plateau at these 2 doses (Figure 3.5A and B). DIAS1 and HU-308 dose-dependently decreased cAMP production with an EC_{50} of 320 and 37 nM respectively (Figure 3.5C) and its structure is shown in Figure 3.5D. Apart from DIAS1, the rest of the tested compounds were either inactive or active only at the 3 μM dose (highlighted examples in Figure 3.5A and B).

The tri-cyclic core of DIAS1 was entered back into the library to identify more available compounds in the same library with the same core. Taking into account compound availability and an ideal molecular weight under 400, from the thirty seven compounds identified 30 compounds were eventually screened in the cAMP assay. One compound (named DIAS2), out of the 30 screened, inhibited cAMP production at 1 and 3 μM (Figure 3.6A). DIAS2 dose-dependently decreased forskolin-induced cAMP production with an EC_{50} of 110 nM (Figure 3.6B) and its structure is shown in Figure 3.6C. Compared to HU-308, DIAS2 was 3-fold less potent however it was 3-fold more potent than the initial virtual screening hit (DIAS1).

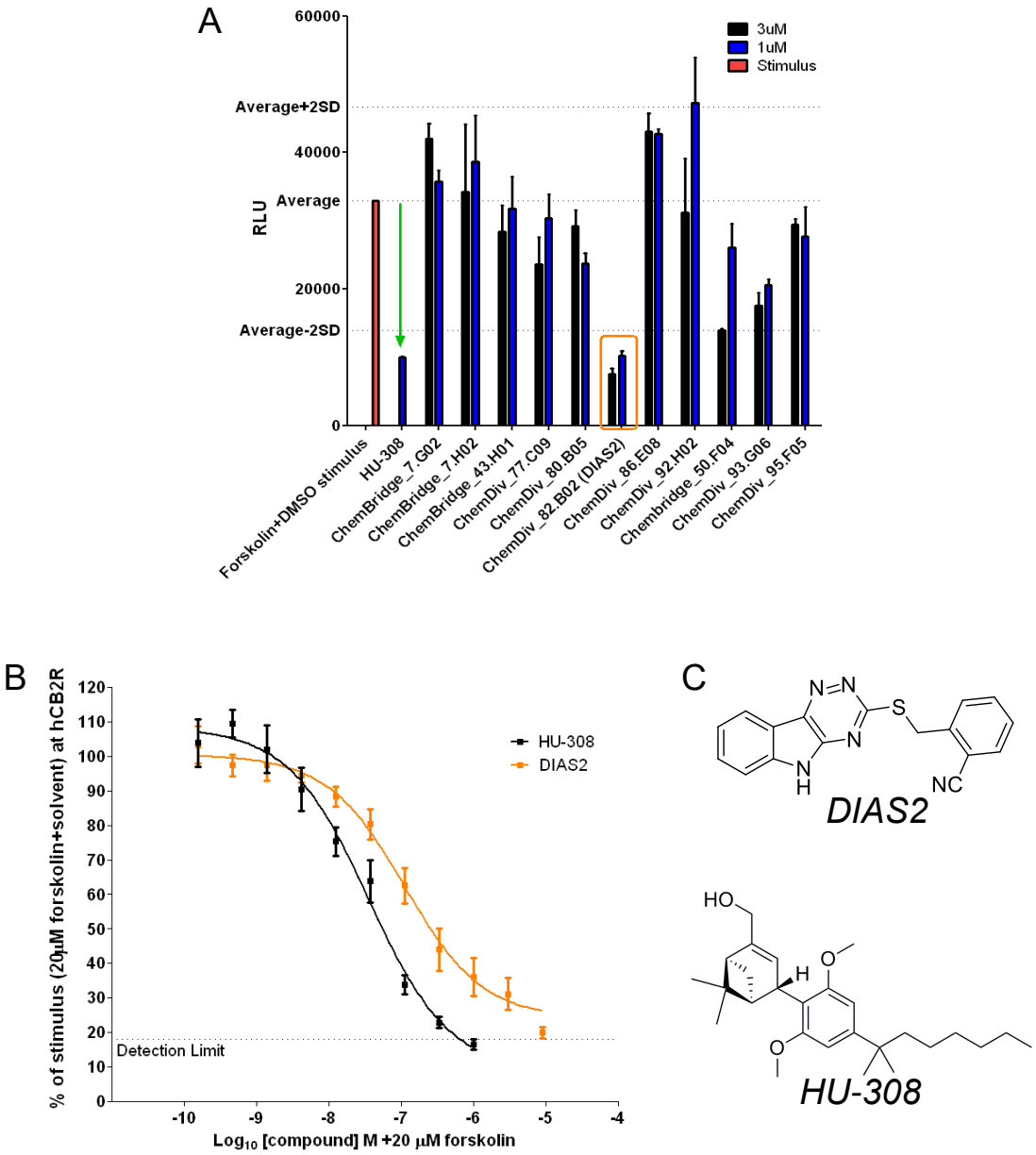

Figure 3.6: Sub-structure search of the tri-cyclic core of DIAS1 within the chemistry library, identifies a second potent CB2R agonist, DIAS2

Searching within the chemistry library for the tri-cyclic core of DIAS1, identified 30 more compounds with the same structural core which were available and had a molecular weight <400. Testing these compounds at 1 and 3 μM in the presence of forskolin in the hCB2R cAMP assay, identified a second potent CB2R agonist (DIAS2) with an EC_{50} of 110 nM in inhibition of cAMP production. A) Screening plate example, error bars=SD, 2 technical replicates, B) Dose-response curve of DIAS2 and HU-308. Pooled data of 3 independent experiments, error bars=SEM.

3.2.4 SAR studies around the novel scaffold of DIAS1 and DIAS2

In collaboration with Matteo Giannella-Borradori, in Dr Russell's group in the Chemistry department, our next goal was to expand the chemical scaffold of DIAS1 and DIAS2 using SAR studies. In the first round of SAR studies (SAR1-43), 9 compounds and a *de novo* synthesised DIAS2 (SAR6 in this series) inhibited the forskolin-induced cAMP production at 1 and 3 μM and were therefore characterised further. Dose-response curves of these compounds are shown in Figure 3.7A and B. In the second round of SAR studies (SAR50-77), 9 more compounds were identified to be potent CB2R agonists (Figure 3.8A and B). Notably, high doses of SAR53 inhibited forskolin-induced cAMP production beyond the detection limit. For EC_{50} values and structures of all the active compounds please refer to Table 3.1. Batch to batch variation of the active compounds' solubility in DMSO and their activity (EC_{50}) in the cAMP assay was minimal (data not shown). For the structures of compounds with low or no activity at hCB2R please refer to Table 3.2. The Markush (generic chemical structure) of this family of CB2R agonists was novel and is now covered by two UK patents applications: P137853GB and P137853GB.

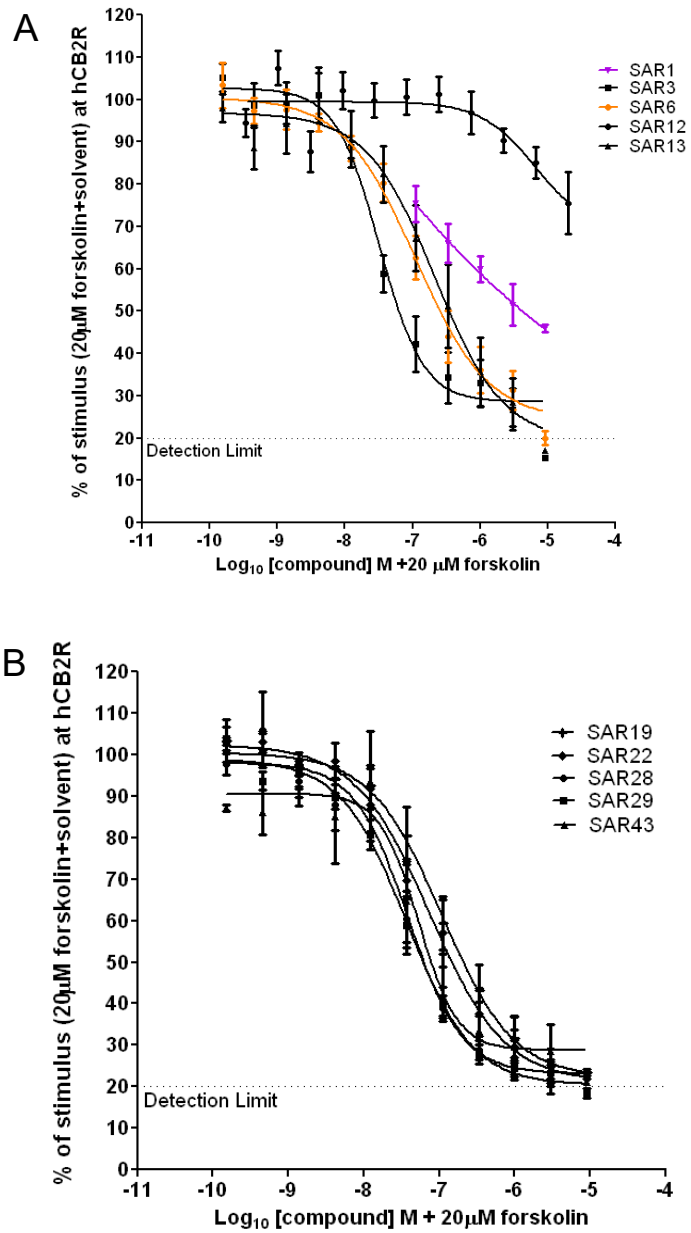

Figure 3.7: Expanding this novel family of CB2R agonists and structure-activity relationships (SAR) for this series: SAR1-43
In collaboration with Matteo Gianella-Borradori, a chemistry PhD student in Dr Russell's group, our efforts were oriented to expand this novel class of CB2R compounds. Screening of compounds synthesised by Matteo was performed using the hCB2R-cAMP assay as in Figure 3.2. From the 43 compounds tested, DIAS2 (SAR6) along with 9 other compounds were identified to be potent CB2R agonists. Dose response curves of A) SAR3, 6 (DIAS2), 12 and 13, B) SAR19, 22, 28, 29 and 43. For both A and B, pooled data are shown from 3 independent experiments, error bars=SEM. For a detailed table of the EC_{50} values please refer to Table 3.1.

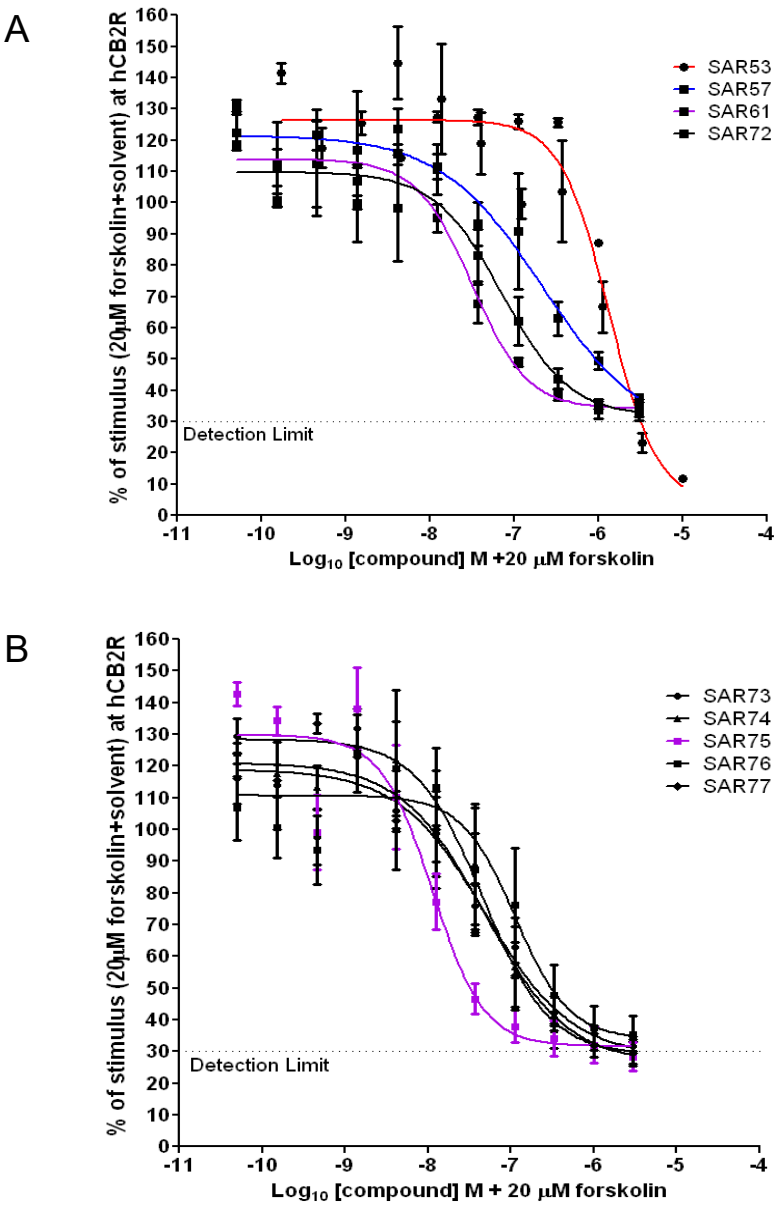

Figure 3.8: Expanding this novel family of CB2R agonists using structure-activity relationships:SAR50-77
In collaboration with Matteo Gianella-Borradori, a chemistry PhD student, our efforts oriented to further expand this novel class of CB2R compounds. Screening was performed using the hCB2R-cAMP assay as in Figure 3.2. From the 37 compounds tested in this round at 1 and 3 µM, 9 more compounds were identified to be potent CB2R agonists with nanomolar activity. Dose response curves of A) SAR53, 57, 61 and 72, B) SAR73, 74, 75 (most potent), 76 and 77. For both A and B, pooled data are shown from 2 independent experiments, error bars=SEM. For a detailed table of the EC_{50} values please refer to Table 3.1.

3.2.5 Selectivity of compounds for CB2R over CB1R

The selectivity of this novel class for CB2R was tested first in hCB1R cAMP assays where ligand activation of CB1R-transfected CHO cells inhibits the production of cAMP induced by forskolin. The highly selective CB1R agonist arachidonyl-2'-chloroethylamide (ACEA) and Δ9-THC were used as positive controls (Figure 3.9). From the 6 SAR compounds tested (including DIAS2), SAR13 was identified as a potent CB1R agonist (EC_{50}=1.55 μM), SAR28 was identified as a weak CB1R agonist (EC_{50}≥ 20 μM) and the rest of the compounds were inactive at the receptor up to 30 μM (Figure 3.9 and Table 3.1).

Radioligand binding assays with membranes expressing hCB1R and hCB2R were employed to assess the affinity of the active compounds for the CB1R and CB2R receptors as well as to confirm with a second independent readout our cAMP results of CB2R activity. Most of the active compounds from the two rounds of SAR studies were tested for affinity to hCB1R and hCB2R using radioligand binding studies performed by CEREP (France) (Table 3.1). From the SAR round 1-43, all tested compounds dose-dependently bound hCB2R by displacing WIN-55212 and only SAR 13, 28 and 43 bound hCB1R with various degrees of affinity (Figure 3.10 and Table 3.1). The active compounds from the second round of SAR 50-77 were also tested for affinity against CB2R and CB1R. Most compounds tested had high affinity for the hCB2R receptor and only two compounds exhibited weak binding for CB1R (Table 3.1). SAR53 was the only compound from the whole SAR studies that demonstrated no binding for hCB2R.

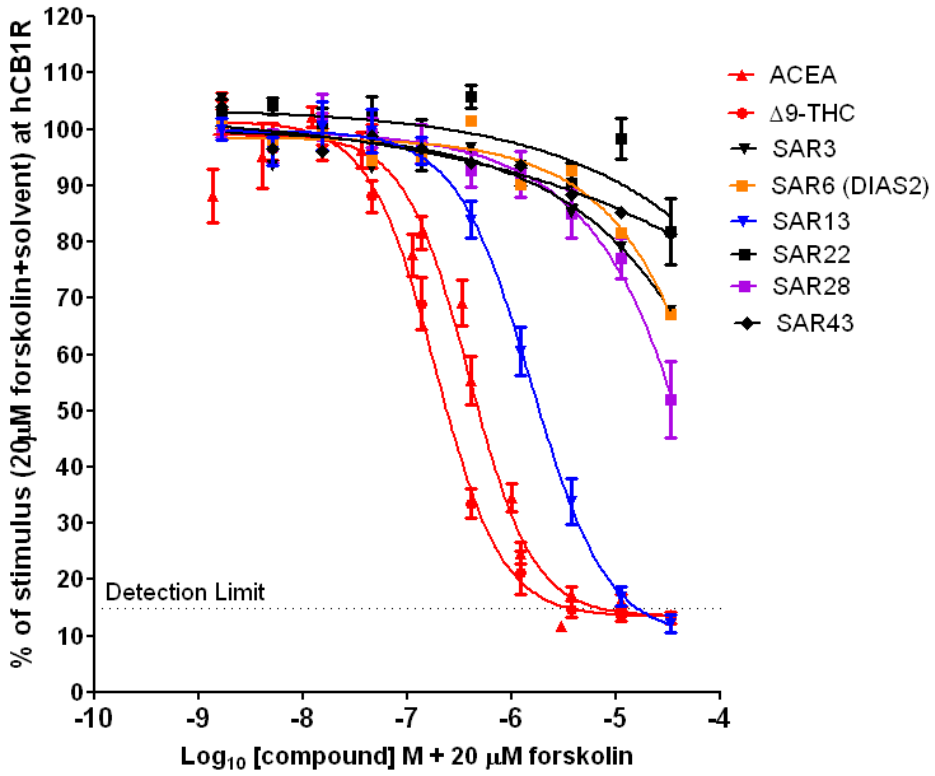

Figure 3.9: Selectivity of our novel CB2R agonists for CB2R over CB1R: CB1R cAMP assay

CB1R is the second cannabinoid receptor which is expressed mainly in the CNS and is responsible for psychoactive effects of Δ9-THC. A CHO-K1 hCB1R cAMP assay (DiscoveRx) was set up in a similar manner to hCB2R cAMP assay (Figure 3.2). ACEA (a selective CB1R agonist) and the phytocannabinoid Δ9-THC (non-selective CB1R/CB2R agonist) were used as positive controls. Δ9-THC, ACEA and SAR13 dose-dependently inhibited cAMP production with EC_{50} of 188, 392 and 1553 nM respectively. SAR28 was a weak CB1R agonist with EC_{50} of approximately 20 μM. Pooled data are shown from 3 independent experiments, error bars=SEM.

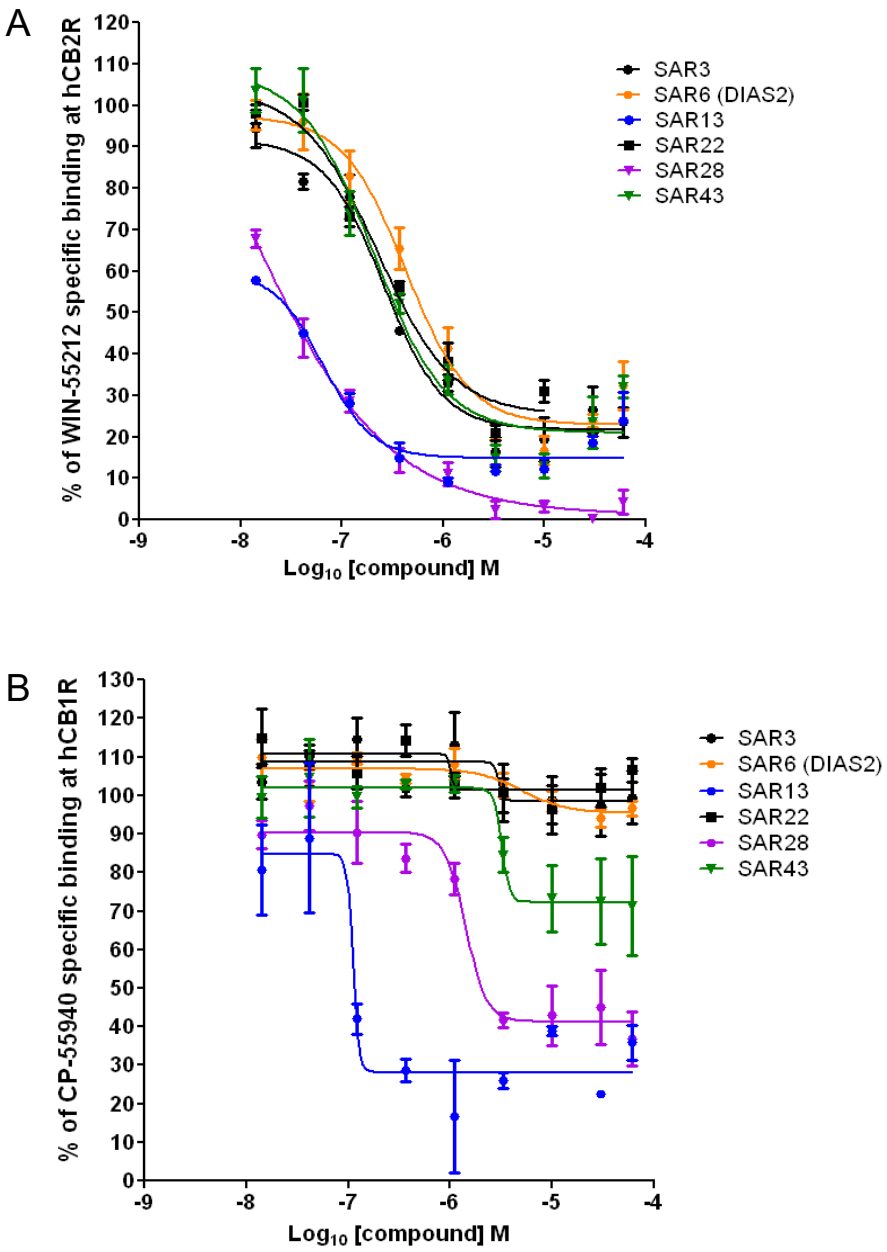

Figure 3.10: Affinity studies confirm the binding of our novel CB2R agonists mainly to hCB2R and not CB1R

Radioligand-binding assays were performed using membranes expressing hCB1R or hCB2R. The radioligands used for CB1R and CB2R, were CP-55940 and WIN-55212 respectively. A) Affinity for hCB2R of SAR 3, 6, 22, 28 and 43. B) Affinity for hCB1R of SAR 3, 6, 22, 28 and 43. For both A and B, pooled data are shown from 2 independent experiments (apart from SAR13 N=1), error bars=SEM. For a detailed table of the EC_{50} values please refer to Table 3.1.

Table 3.1: EC_{50} and K_i values for active members of novel family of CB2R agonists: SAR1-43

SAR number	Structure	CB2		CB1	
		EC_{50} (nM)	K_i (nM)	EC_{50} (nM)	K_i (nM)
1	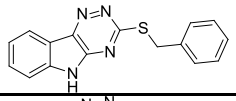	10000	—	—	—
3	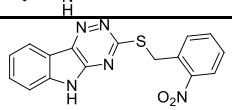	33	155	≥30000	N.D.
6 (*DIAS2*)	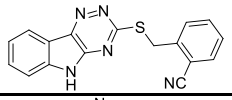	110	355	≥30000	N.D.
12	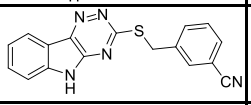	≥10000	—	—	—
13	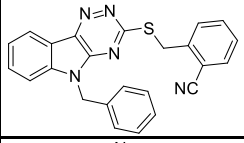	214	11	1553	61
15	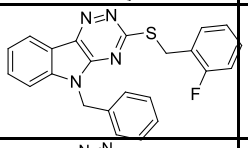	850	215	—	275
19	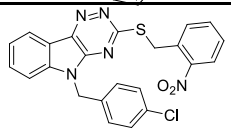	109	—	—	—
22	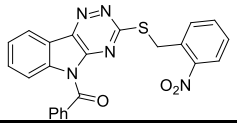	75	235	≥30000	N.D.
28	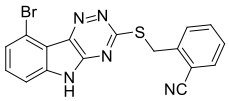	39	22.5	Approx. 20000	3200
29	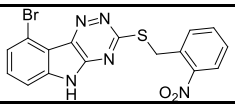	37	—	—	—
43	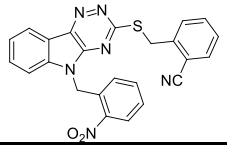	53	290	≥30000	≥50000

N=2-3 independent experiments for EC_{50} and K_i values (apart from N=1 for SAR13 K_i values). For affinity studies if no binding was detected up to 60 μM then it will be entered as N.D.

Table 3.1 (continued): EC_{50} and K_i values for active members of novel family of CB2R agonists: SAR50-77

SAR number	Structure	CB2		CB1	
		EC_{50} (nM)	K_i (nM)	EC_{50} (nM)	K_i (nM)
51	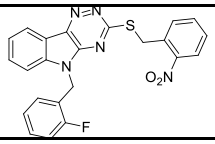	201	—	—	—
53	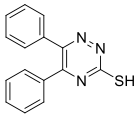	1330	N.D.	—	N.D.
57	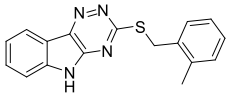	215	≥6000 (partial displacement)	—	N.D.
61	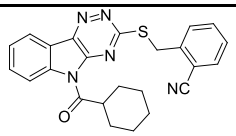	31	30	—	N.D.
72	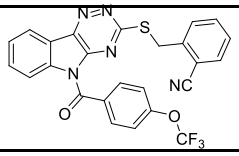	73	380	—	N.D.
73	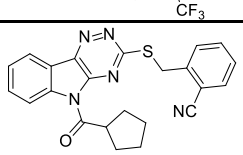	49	320	—	N.D.
74	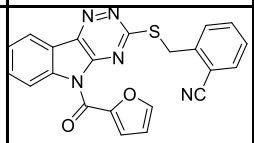	46	490	—	>10000 (partial displacement)
75	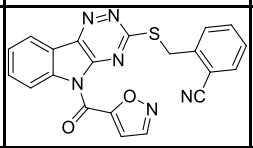	11	45	—	N.D.
76	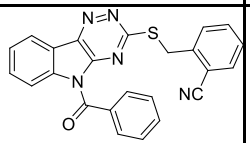	113	300	—	>10000 (partial displacement)
77	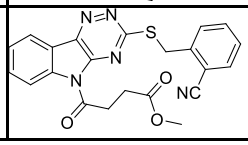	48	360	—	N.D.

N=2-3 independent experiments for EC_{50} values. N=1 for all Ki values. For affinity studies if no binding was detected up to 60 μM then it will be entered as N.D. Highlighted in yellow is SAR53 which was later identified as false positive.

Table 3.2: Compounds with low or no activity at hCB2R: SAR1-43

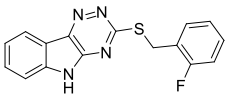 SAR2	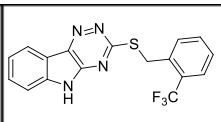 SAR4	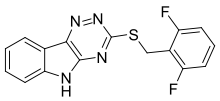 SAR5	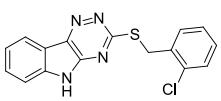 SAR7
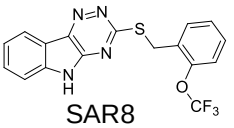 SAR8	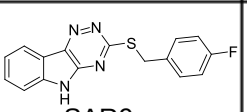 SAR9	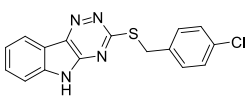 SAR10	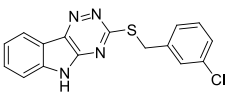 SAR11
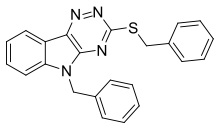 SAR14	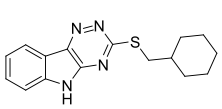 SAR16	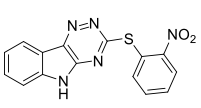 SAR17	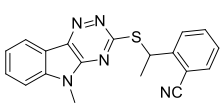 SAR20
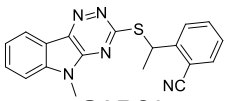 SAR21	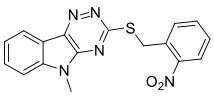 SAR23	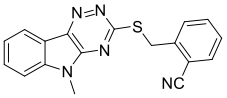 SAR24	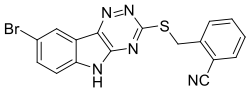 SAR25
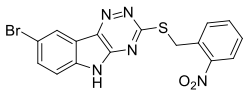 SAR26	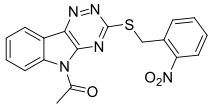 SAR27	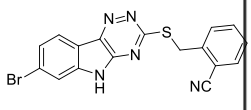 SAR30	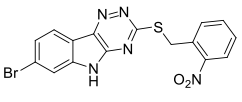 SAR31
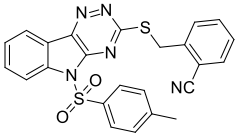 SAR32	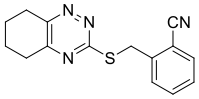 SAR33	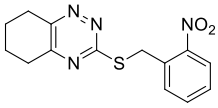 SAR34	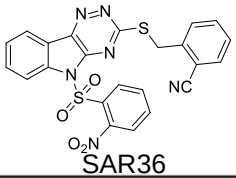 SAR36
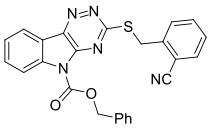 SAR37	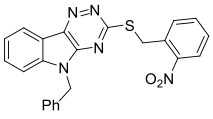 SAR38	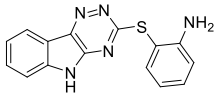 SAR39	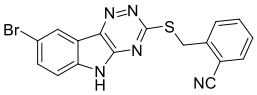 SAR40
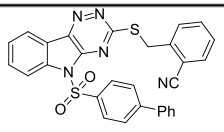 SAR41	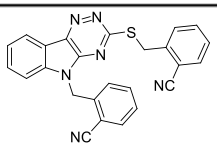 SAR42		

Compounds from the SAR series 1-43 that did not fulfill the goal of a plateau at 1 and 3 μM and were deemed not potent enough to be characterised further.

Table 3.2: Compounds with low or no activity at hCB2R: SAR50-77

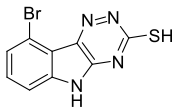 SAR50	SAR52 was re-synthesis of SAR9	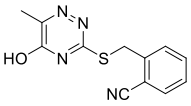 SAR54	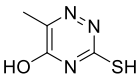 SAR56
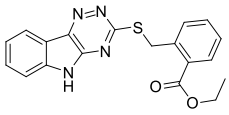 SAR58	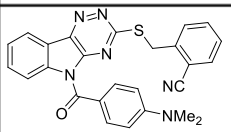 SAR59	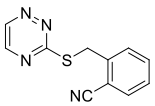 SAR63	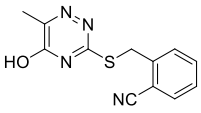 SAR64
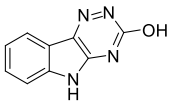 SAR66	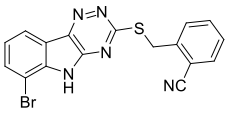 SAR67	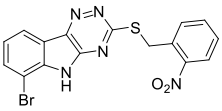 SAR68	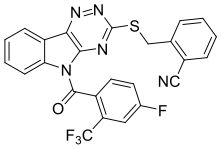 SAR69
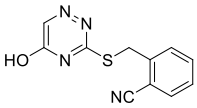 SAR71			

Compounds from the SAR series 50-77 that did not fulfill the goal of a plateau at 1 and 3 μM and were deemed not potent enough to be characterised further.

Taken together with previous data in the CB2R cAMP assay, SAR53 was deemed as a false positive result (Figure 3.8A, highlighted yellow in Table 3.1). Thus in total, our novel class of CB2R agonists includes eight highly selective CB2R agonists (SAR3, 6 (DIAS2), 22, 61, 72, 73, 75 and 77) with no binding to hCB1R at doses up to 60 μM.

The next aim was to test the selectivity of our compounds for CB2R compared to other targets such as GPR55 which has been suggested as a potential cannabinoid receptor. Activation of GPR55 by its ligand L-alpha-lysophosphatidylinositol (LPI) dose-dependently recruited β-arrestin while our CB2R agonists had no effect (Figure 3.11). The second target tested was CXCR2, since patent searching for the Markush indicated some structural similarities with a patented CXCR2 antagonist family. As shown in Figure 3.12, the tested CB2R agonists were neither agonists nor antagonists at human CXCR2.

3.2.6 Inhibition of cAMP levels in primary macrophages by DIAS2

In order to confirm the presence of active CB2 receptors in macrophages and investigate whether DIAS2 is biologically active, the ability of CB2R agonists to inhibit cAMP production in primary murine macrophages was tested. To begin with, a cAMP assay from DiscoveRx was tested but with EC_{50} of 5 nM and detection limit of 200 pM, the assay was not sensitive enough (data not shown). The second assay tested was from Invitrogen and had an EC_{50} of 2 pM (Figure 3.13A). The assay was set up and optimized as shown in Figure 3.13.

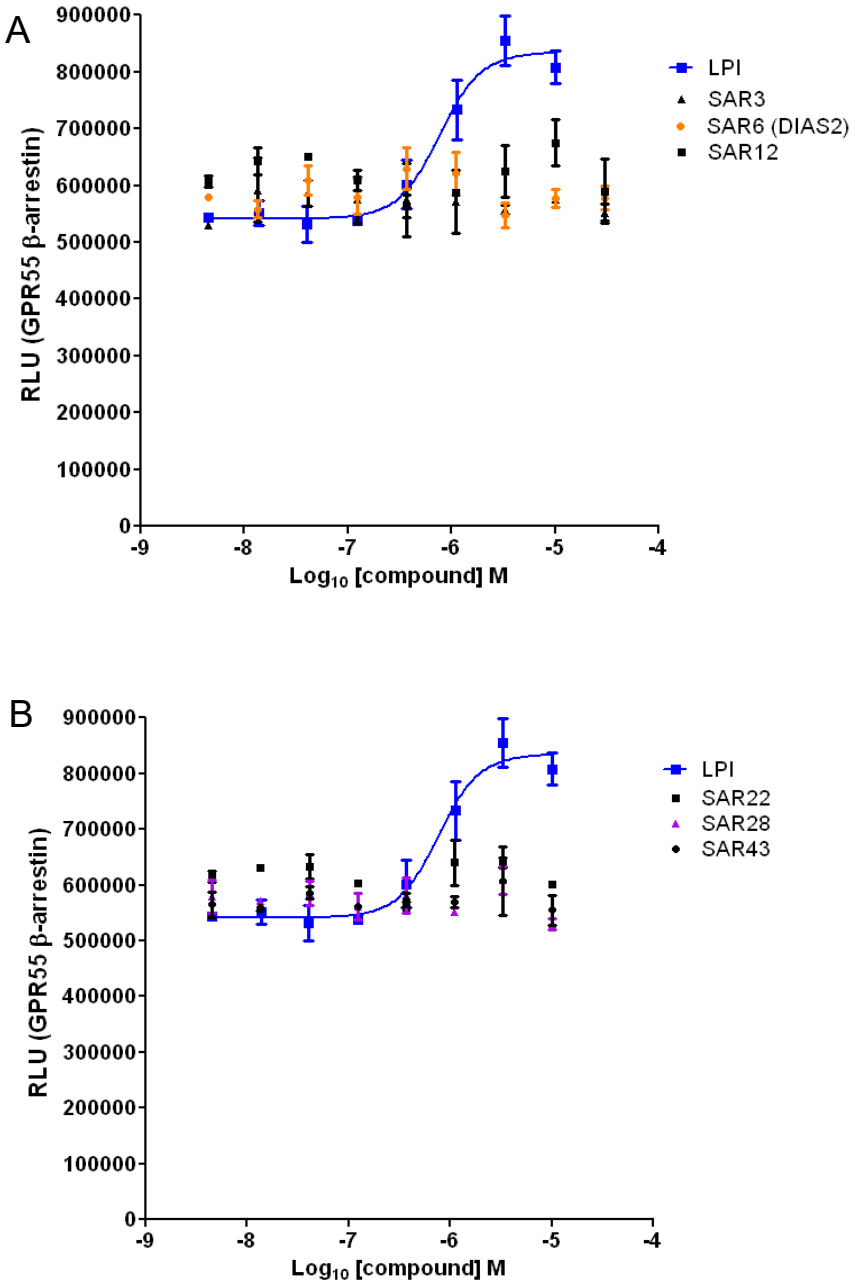

Figure 3.11: SAR compounds do not activate GPR55 to induce β-arrestin recruitment

GPR55 is a putative cannabinoid receptor with LPI as its only known natural ligand. CHO-K1 hGPR55 β-arrestin cells (DiscoveRx) were stimulated as in Fig. 3.2. The data shown are dose response curves of LPI (endogenous ligand) and SAR3, 6, 12, 22, 28 and 43. For all compounds solvent was 0.5% DMSO. Data are from an experiment performed once, 2 technical replicates, error bars=SD

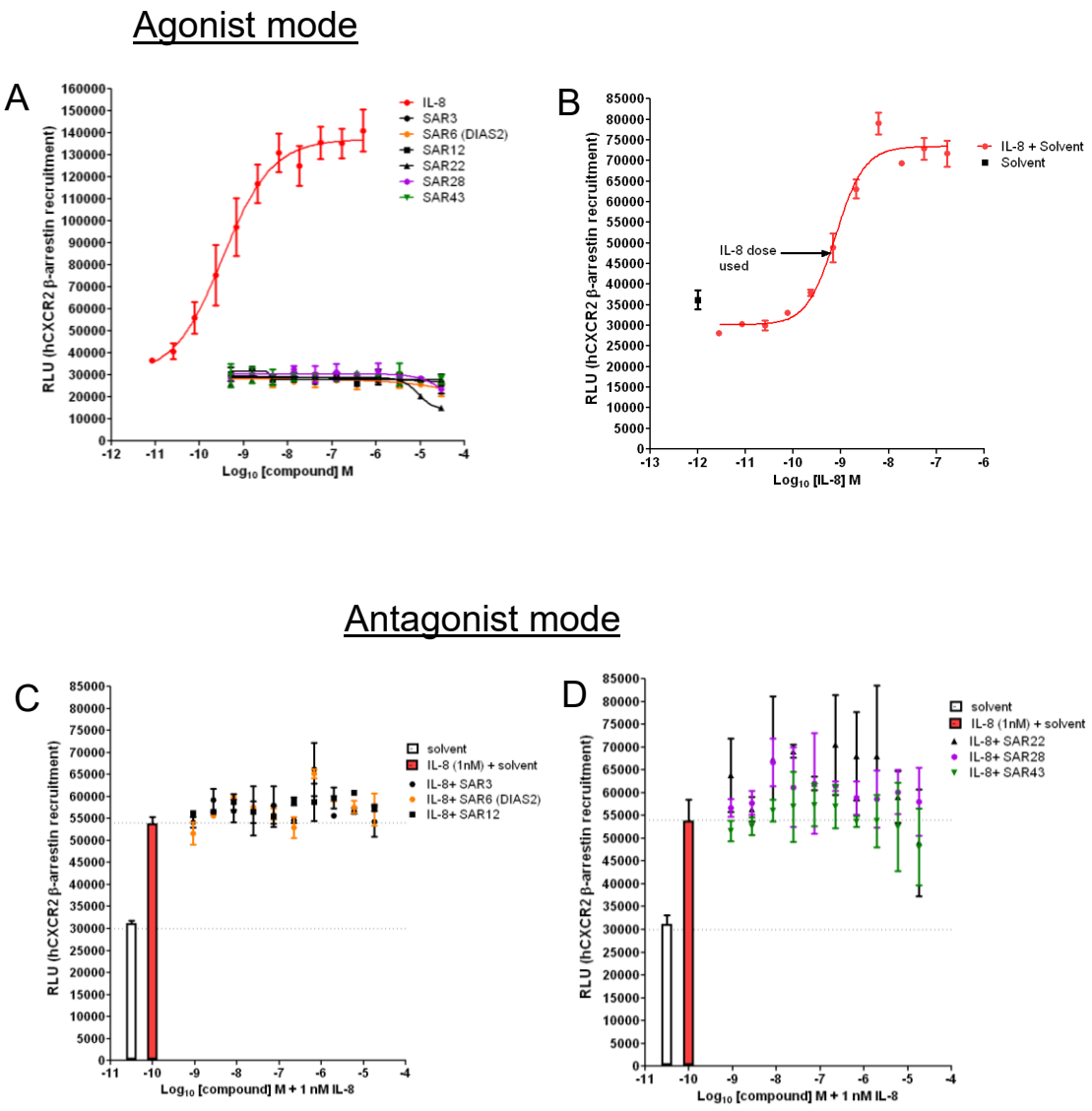

Figure 3.12: SAR compounds do not activate hCXCR2
Patent searching indicated that our SAR compounds have limited structural similarities with a class of CXCR2 antagonists. HEK-hCXCR2 β-arrestin cells (DiscoveRx) were stimulated as in Figure 3.2. A) Dose-response agonist curves of IL-8 and SAR3, 6, 12, 22, 28 and 43. B) Dose-response curve of IL-8 in the present of solvent (0.5%DMSO) and 1 nM dose selected for antagonist studies. C) Compounds SAR 3, 6 and 12 or solvent in the presence of 1 nM IL-8 (antagonist mode). D) Compounds SAR 22, 28 and 43 or solvent in the presence of 1 nM IL-8. Data are from an experiment performed once, 2 technical replicates, error bars=SD

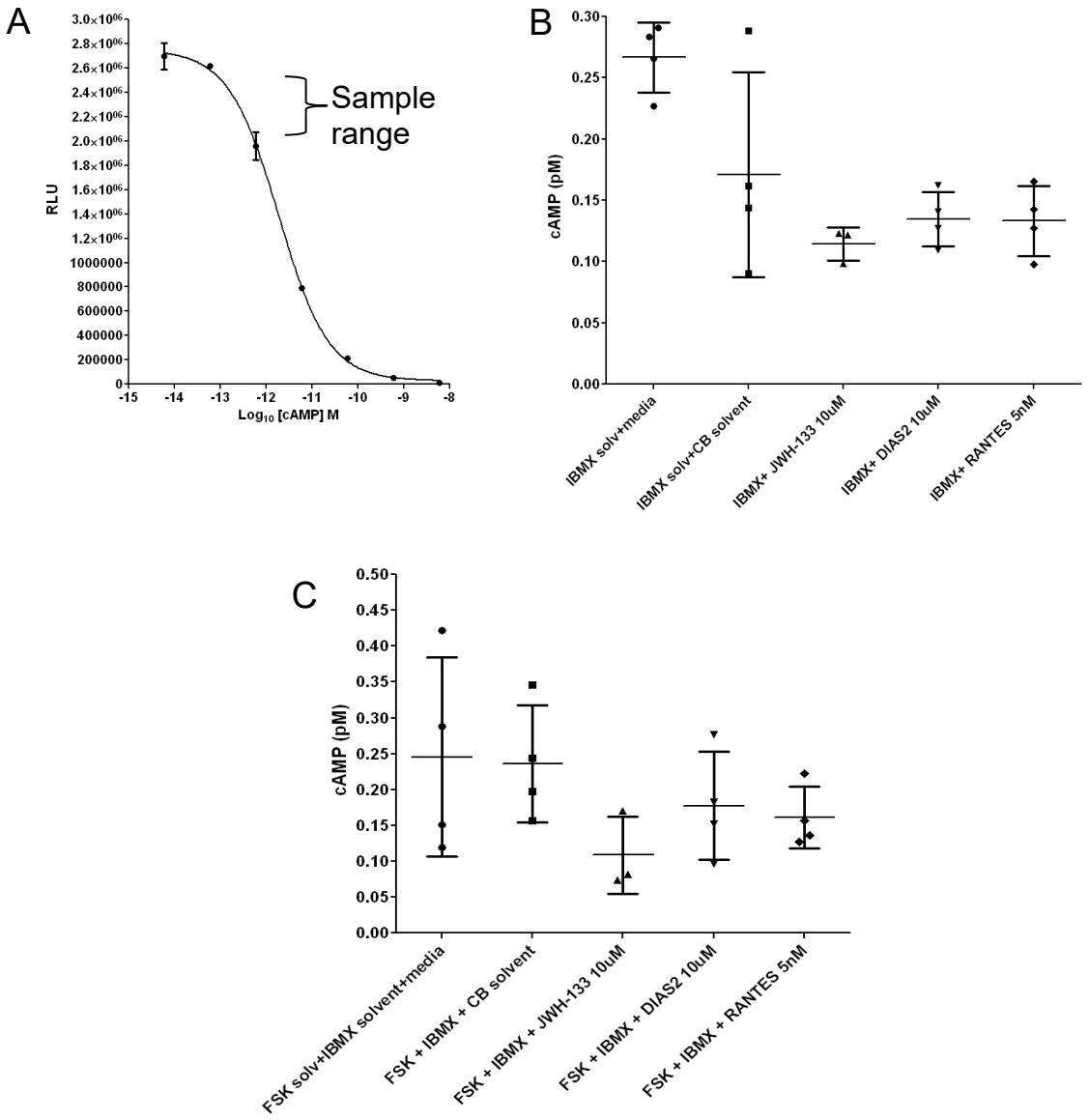

Figure 3.13: Optimization of cAMP assay for primary macrophages
Murine primary Bio-Gel-elicited peritoneal exudate cells (PECs) were plated in a 96-well plate for 1 hour before Bio-Gel beads were washed off and the cells were allowed to recover for 2 hours. The adherent macrophages were then stimulated with the phosphodiesterase inhibitor IBMX for 20 minutes and then activated with 50 μM forskolin or solvent (0.2% DMSO) for 5 minutes. DIAS2, the CB2R agonist JWH-133 or solvent (0.15% DMSO) were added for a further 5 minutes. An Invitrogen cAMP detection kit was then used where the cells were then lysed for 30 minutes with provided lysis buffer and the lysates were incubated on the pre-coated plate for 90 minutes. The plate was then washed and a luminescent substrate was added for 45 minutes before the signal was detected with a luminometer. cAMP values were extracted from the linear part of a cAMP standard curve. A) cAMP levels, B) in the presence of IBMX alone and C) in the presence IBMX and forskolin. Data are from one experimental animal, 4 technical replicates, error bars=SD

The combination of a phosphodiesterase inhibitor (IBMX) added first to decrease the degradation of cAMP followed by forskolin to increase cAMP levels was preferred to IMBX alone to reduce well to well variability. The cAMP levels were extrapolated from the linear part of the cAMP standard curve. Both the lead compound DIAS2 (SAR6) and JWH-133 were able to decrease cAMP production in macrophages (Figure 3.14). The chemokine RANTES was used as a positive control.

3.3 Discussion

In this chapter we report the identification and characterisation of novel class of CB2R agonists. A second messenger assay detecting cAMP production was identified as suitable for screening CB2R agonists. Ligand-based virtual screening successfully identified one compound (DIAS1) with CB2R activity and sub-structure screening within the library led to the identification of a second CB2R agonist with same tri-cyclic core and potency similar to HU-308. Performing SAR expanded the chemical scaffold into a family of novel CB2R agonists. From the compounds tested so far (1-77), 8 compounds were identified as highly selective potent CB2R agonists with no binding to hCB1R up to 60 μM (SAR3, 6 (DIAS2), 22, 61, 72, 73, 75 and 77) and 5 compounds were identified as potent agonists at hCB2R but with varying activity/binding to hCB1R (SAR 13, 15, 28, 43, 74 and 76). Moreover CB2R agonists from this family and our lead compound DIAS2 have no detected activity on GPR55 and CXCR2. Importantly, the lead compound DIAS2 and a well-established CB2R agonist JWH-133 were able to inhibit cAMP production in primary murine macrophages using a highly sensitive cAMP assay.

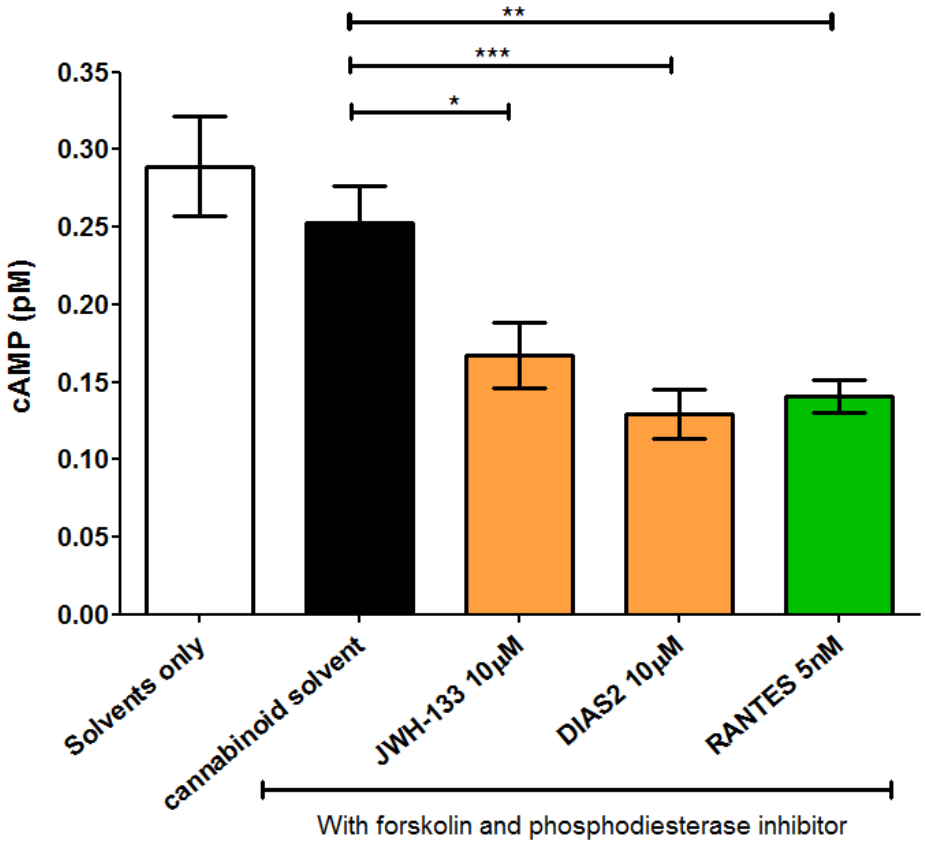

Figure 3.14: DIAS2 (SAR6) inhibits cAMP production in primary macrophages

The assay was performed as in Figure 3.13. Briefly, primary macrophages were activated with IBMX followed by 5 minutes forskolin or solvent and 5 minutes CB2R agonists (JWH-133 and DIAS2) or solvent or chemokine (RANTES). The cells were then lysed and cAMP levels were measured using a cAMP kit (Invitrogen). Pooled data from stimulation of DIAS2 and JWH-133 in the presence of forskolin and IBMX. Pooled data of 4 independent mice are shown, error bars=SEM. One-way ANOVA and Dunnett's multiple comparison test, *P<0.05, **P<0.01, ***P<0.001

3.3.1 Choices and suitability of screening assay

From the two second messenger assays tested, the hCB2R-cAMP assay was able to detect all CB2R agonists tested including the endogenous ligand 2-AG. On the other hand, in the mCB2R β-arrestin assay, only JWH-133 was able to recruit β-arrestin while neither HU-308 nor the endogenous ligand elicited such a response. Another study demonstrated that CP-55940, WIN-55212 and JWH-015 (a less selective CB2R agonist from the same class as JWH-133), but not GW-405833, were able to recruit β-arrestin via CB2R using the same DiscoveRx kit used for our studies (McGuinness *et al.*, 2009). This differential β-arrestin recruitment could represent biased agonism at the CB2R receptor while the inhibition of adenylate cyclase is the characteristic signalling pathway of $G\alpha_i$ receptors. The cAMP assay was selected to avoid false negatives at the earliest stages of drug discovery. cAMP assays have recently being used to discover novel CB2R agonists (Ermann *et al.*, 2008; Zindell *et al.*, 2011) confirming the suitability of our approach.

Importantly we employed a second independent assay to confirm interaction of the compounds with CB2R for most of the CB2R agonists in this class. Radioligand binding assays detect in a cell-free manner binding of both orthosteric agonists and antagonists to the receptor (Markt *et al.*, 2009; Zhang *et al.*, 2012) and rely on a second assay to distinguish between them. It is also challenging to identify binding at an allosteric site, which for example has already been identified for CB1R (Price *et al.*, 2005). Also in this chapter, radioligand binding demonstrated that one of the 14 compounds with CB2R activity was actually a false positive (SAR53). Indication for a

non-specific effect of SAR53 was shown in the cAMP assays since at high doses it appeared to reduce cAMP beyond the detection limit (Figure 3.8B). In one study the lead compound of a novel class of CB2R agonists, which was identified using CB1R and CB2R cAMP assays, was unable to displace the radiolabelled CP-55940 from CB2R with the authors suggesting that the compound may have a different site of binding (Riether *et al.*, 2011) . Since the authors did not confirm their compounds' interaction with CB2R using a second assay, for example GTP-γS, their lead compound could either have a different binding site from CP-55940 as they suggest or have a non-specific effect on the cAMP assays as we observed for SAR53.

3.3.2 Virtual screening and identification of a novel class of CB2R agonists

Virtual screening has identified a novel scaffold for CB2R agonists within the top 60 compounds with high similarity to HU-308. Moreover this novel family of CB2R agonists, extended by SAR studies, has some similarities with the original template HU-308. To begin with, the high selectivity of HU-308 for CB2R over CB1R has been retained. Eight selective CB2R agonists from this class have no binding to CB1R up to 60 μM, similar to HU-308 which has no binding to CB1R up to 10 μM (Hanus *et al.*, 1999). Moreover the potency of HU-308 to activate the CB2R with EC_{50} in the nanomolar range (Figure 3.2. and (Hanus *et al.*, 1999)) has also been retained, if not improved. Some of the discovered CB2R agonists are highly potent like HU-308, such as SAR3 and SAR61, or even 3 fold more potent than HU-308, such as SAR75. Therefore, choosing HU-308 as a highly selective and potent CB2R agonist for the

template played a fundamental role for the discovery of a novel scaffold with high selectivity and nanomolar range activity at CB2R. To date HU-308 has only been used as part of a common-feature pharmacophore model along with other CB2R agonists (Markt *et al.*, 2009), this is the first study to use HU-308 as the sole template for ligand-based virtual screening. However, it is important to note that DIAS2 was ranked >500 of 20,000 compounds in the virtual screening and was only obtained after searching for compounds containing the DIAS1 tricyclic core within the library.

3.3.3 SAR studies and main findings

Although in depth discussion of SAR studies falls outside the scope of this thesis the features found to be important are the following:

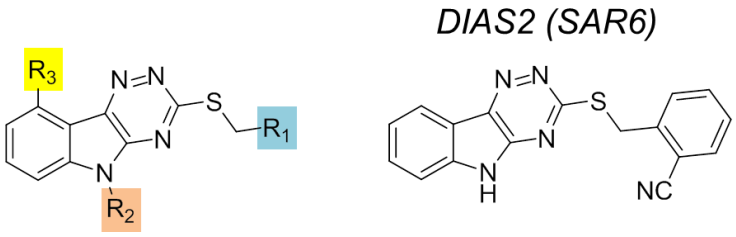

Regarding the R^1 position in the tricyclic core, substitutions around the benzyl group have been investigated. When the benzyl group is un-substituted (SAR1) activity for CB2R is greatly reduced. Instead by functionalization on the *ortho*- position with a nitrite (C $\equiv$ N; SAR6) or a nitro (-NO_2; SAR3), activity and affinity for CB2R is increased. Additionally, selectivity for CB2R is also observed in the range of our novel compounds. Moreover substitutions of the *meta*- and *para*- positions (SAR12

and Table 3.2) led to loss of CB2R activity, indicating *ortho* is a crucial site for interaction with the active site of CB2R.

In the R^2 position, substitutions showed that the carbonyl derivatives (C=O; SAR22, 61, 72-77) had improved potency at CB2R while retaining selectivity for CB2R over CB1R. It was also observed via substitution of the carbonyl (C=O) to a methyl group (CH_2), that the affinity for CB2R increases but compromises the selectivity for CB2R due to increased affinity for CB1R (SAR13, 15, 43). Substitution in the R^3 position of SAR6 with bromide (SAR28), greatly improves the affinity of the compound for CB2R, but it also greatly increases the affinity for CB1R thus reducing the selectivity for CB2R over CB1R. More SAR compounds will be synthesised to investigate this position further.

Currently crystal structures for the CB2R and CB1R receptor are not available. Studies have identified amino acids which are important for binding and selectivity at CB2R (Gouldson *et al.*, 2000; Song *et al.*, 1996; Song *et al.*, 1999). Interestingly mutagenesis studies demonstrated that some amino acids in the CB2R are important for both binding and inhibition of adenylate cyclase (Song *et al.*, 2002), while some others play no role in binding to CB2R but are crucial for signal transduction (Feng *et al.*, 2001). Importantly, several amino acids identified to be important for binding and activating the human CB2R are present in the sequences of rat and mouse CB2R (McPartland *et al.*, 2003). This suggests that it is likely that agonists at hCB2R will retain the same pharmacological properties in murine and rat cells.

3.3.4 Selection of lead compound and cAMP studies in primary murine macrophages

DIAS2 (SAR6) was selected as the lead compound for biological studies because it has potent activity and selectivity for CB2R and it has a low molecular weight (317.07) relative to other active SAR compounds that have higher molecular weight due to additional lipophilic groups which results in reduced solubility in aqueous solutions. SAR3 has similar properties to SAR6, however due its aromatic nitro group it is considered to have potential toxic effects in humans, such as skin sensitisation, immunotoxicity and methaemoglobinaemia (World Health Organization, Nitrobenzene. International Programme on Chemical Safety 230, 2003), as well as liver and kidney toxicity in rats due to reactive metabolites (Hakimelahi *et al.*, 2005) and for these reasons was not selected as our lead compound.

Both DIAS2 (SAR6) and JWH-133 were able to inhibit cAMP production in primary murine macrophages (Figure 3.14). This was important to demonstrate that the lead compound was biologically active in primary cells and that murine primary macrophages express a functional CB2R. The doses used in the cAMP assay with primary cells are in the micromolar range compared to the nanomolar doses used in CHO-cells overexpressing CB2R. These are the doses used in the literature to see CB2R-mediated effects in primary monocytes and macrophages chemotaxis (Montecucco *et al.*, 2008; Sacerdote *et al.*, 2000) and are used in *in vitro* assays in Chapter 5. Theoretically, the dose-response curves of high efficacy agonists are right-shifted as receptor number decreases (Kenakin, 1985), therefore it is likely that higher doses used for the CB2R agonists reflect a lower CB2 receptor expression

than that seen in recombinant systems. Alternatively, the efficiency of coupling to signalling pathways may be different between the human and murine CB2R.

3.3.5 Limitations for this study

The first limitation in this chapter was the size of the medicinal chemical library. Compared to the size of chemical libraries in pharmaceutical companies with hundreds of thousands compounds (Hollinshead *et al.*, 2012; Markt *et al.*, 2009) our library had only 20,000 compounds thus limiting the number of potential hits and novel scaffolds. Moreover, we only screened a total of 94 hits from the total 500 or more virtual screening hits, so it is possible we missed the opportunity to identify more novel scaffolds for CB2R agonists. Ideally we would like to repeat virtual screening in bigger libraries and use DIAS2 as template. Another potential limitation is false negatives due to poor synthesis or degradation of compounds on storage. Possible examples are compounds active at 3 μM but not 1 μM (Figure 3.5). If time permitted, we could have revisited compounds active at 3 μM and re-synthesised.

Using the cAMP assays for screening we discovered novel CB2R agonists that were potent in inducing inhibition of adenylate cyclase via CB2R. However, the limitation of such assays is their reliance on signal inhibition. In this case compounds which interfere with signal detection or induce cell death can be described as positives, while in reality they are false positives. The induction of cell death by compounds could be assessed with cytotoxicity assays while interference with the signal would more difficult to assess. Additionally, $G\alpha_i$-assays mainly identify full and partial

agonists but identification of antagonists can be challenging. It is possible that some of the compounds considered to be inactive at the concentrations tested and not characterised further may have been neutral antagonists and inverse agonists. In principle these compounds could be tested in an assay designed to test for CB2R antagonists or radio-ligand binding assays.

A limitation for the detection of cAMP in primary murine cells is that a very short stimulation time (5 minutes) was used for the GPCR ligands. Although the assay has worked for all 3 ligands tested, it is possible that other ligands with slower receptor kinetics may not have activated the receptor within this time interval. Moreover, the sensitivity of the assay is also a limitation, as it can only detect cAMP changes down to 0.1 pM. In experiments where the cAMP levels in the cells are 0.1 pM or below, the detection of $G\alpha_i$-activity is not possible. Additionally, our compounds can activate both murine and human CB2R but there is a possibility that species specific ligands could not be assessed in primary murine cells. In this case, hCB2R knockin mice could be used for preclinical testing.

Finally, only one assay methodology was used for the primary screen i.e. CHO-cells transfected with hCB2R. Ideally the screen could have been improved by testing compounds in other HTS functional assays such as GTPγ-S.

3.4 Summary

In this chapter we have validated a cAMP assay for screening of CB2R agonists and using ligand-based virtual screening we identified a novel scaffold of CB2R agonists. In collaboration with Dr Russell and Matteo Giannella-Borradori in the Chemistry department of Oxford University, we used SAR studies to identify key pharmacophores in this scaffold which are important for CB2R activity, affinity and selectivity. Moreover we demonstrated that the lead compound DIAS2 is biologyically active in primary murine macrophages by inhibiting cAMP production.

In the next chapter the biological activity of DIAS2 will be tested in the *in vivo* inflammation model of peritonitis.

CHAPTER 4 : In vivo anti-inflammatory effect of novel CB2R agonists

4.1 Introduction

Significant and reproducible anti-inflammatory effects of CB2R agonists have been reported in the ApoE knockout mouse model of atherosclerosis (Hoyer *et al.*, 2011; Steffens *et al.*, 2005) and analgesic effects have been reported in several mouse models of pain such as the CFA-induced inflammatory pain (Giblin *et al.*, 2007; Yao *et al.*, 2008). However, the effects of CB2R agonists reported *in vitro* are less impressive (Steffens *et al.*, 2005). Therefore to assess the biological role of CB2R in inflammation following activation with our novel class of CB2R agonists, it was reasoned that *in vivo* inflammation models could be more informative than *in vitro* experiments. Furthermore *in vivo* experiments not only validate drug targets and provide information regarding the efficacy of treatments as therapeutics, but they also assess the overall effect of the treatment on the complex process of inflammation when the exact cellular mechanism is unclear.

Undeniably animal experiments are more challenging to perform than *in vitro* experiments. They are of relatively smaller scale, higher variability and cost than equivalent cell culture experiments with animal cells. Additionally appropriate drug formulation is important for efficacious *in vivo* administration and in the case of highly lipophilic compounds, such as cannabinoid ligands, it is also important for

maintaining the compound in solution. For example DMSO is one of the most common solvents used in *in vitro* treatments, but it has multiple *in vivo* side effects including vomiting, diarrhoea and hypertension when used at high doses (Santos *et al.*, 2003). For this reason, DMSO is used in very few studies for administration of cannabinoid ligands in mice (Cluny *et al.*, 2010). The most common solvent used *in vivo* is combination of saline with emulsifiers like Cremophor® EL (polyethoxylated castor oil) (Gallily *et al.*, 1997; Howlett *et al.*, 2002; Zimmer *et al.*, 2001). Alternative solvents used in the cannabinoid area are Tocrisolve^{TM} 100 from Tocris Bioscience (Hoyer *et al.*, 2011), 5% milk and methanol (Steffens *et al.*, 2005) and the cyclic oligosaccharides cyclodextrins (Jarho *et al.*, 1996; Mauler *et al.*, 2002). Overall, for *in vivo* experiments with lipophilic compounds the addition of a solvent contributes to higher *in vivo* variability but is essential for solubilising the compounds and maintaining a therapeutic dose of the test compound.

As previously described in the introduction to this thesis, CB2R has been strongly linked with regulation of inflammation, especially through its effects on monocytes and macrophages (Montecucco *et al.*, 2008; Raborn *et al.*, 2008) whereas it has no reported effects on neutrophils (Chouinard *et al.*, 2011; Kraft *et al.*, 2005). Several inflammatory stimuli have been used in mouse models to study acute inflammation but the two well-established and reproducible models of sterile inflammation are zymosan, which is yeast cell wall component, and carrageenan, which is an extract from red algae. Injection of either of these stimuli induces the cardinal signs of inflammation; oedema, pain, redness and heat, which is associated with leukocyte infiltration. In these models leukocyte recruitment is a very dynamic process

consisting of neutrophil influx peaking at 4 hours and followed by monocyte recruitment peaking at approximately 24 hours, with the magnitude and the duration of inflammation depending on the dose of the inflammatory stimulus (Cash *et al.*, 2009; Di Rosa, 1972; Doherty *et al.*, 1985). It has also been demonstrated that in acute inflammation regulation of leukocyte influx can occur by other cells such as mast cells, which release KC and JE and have a pro-inflammatory role, and resident macrophages, which via their release of IL-10 regulate neutrophil influx (Ajuebor *et al.*, 1999). Moreover production of inflammatory mediators is also observed ranging from chemokines, such as JE and KC, to eicosanoids such as leukotrienes and prostaglandins (Ajuebor *et al.*, 1998a; Doherty *et al.*, 1985; García-Ramallo *et al.*, 2002). Importantly these models of acute inflammation played a fundamental role in identifying the anti-inflammatory action of several drugs, including dexamethasone and aspirin (Bonta *et al.*, 1977; Klemm *et al.*, 1995), and therefore provide an excellent system to identify novel treatments for the multicomponent process of inflammation.

4.1.1 Rationale

We have demonstrated in the previous chapter (Figure 3.14) that DIAS2 is biologically active in primary murine macrophages since it inhibited cAMP production in Biogel-elicited peritoneal macrophages. We next wanted to investigate the effect of our novel cannabinoids on CB2R activation *in vivo* where their effects on whole process of inflammation could be observed. From the two widely used acute models of inflammation we chose zymosan-induced peritonitis since the kinetics of this model

have been extensively studied both by our own lab and other groups and it is established that both neutrophils and monocytes are rapidly and prominently recruited within eight hours of zymosan administration, either peritoneally or in an air-pouch (Bannenberg *et al.*, 2005; Cash *et al.*, 2009; Dawson *et al.*, 1991; White *et al.*, 2011). The kinetics of inflammatory cell recruitment in zymosan-induced peritonitis are shown in Figure 4.1. A short-term model of acute inflammation is preferred in our studies since pilot microsomal stability data for DIAS2 and other SAR compounds indicated a liver microsomal half-life of forty minutes or less (Table 4.1).

4.1.2 Experimental aims of this chapter

- Identify an appropriate solvent for *in vivo* administration of cannabinoid ligands by testing three different formulations
- Administer DIAS2 in zymosan-induced peritonitis and assess its effects on inflammatory cell influx
- Compare the effects of DIAS2 (potent agonist, EC_{50}=110 nM at hCB2R) in zymosan-induced peritonitis with SAR1 (weak agonist, EC_{50}=10,000 nM at hCB2R), SAR3 (potent agonist, EC_{50}=33 nM at hCB2R) and JWH-133 (a commercial CB2R agonist, EC_{50}=38 nM at hCB2R)
- Analyse the supernatants from the peritoneal cavity for differences in cytokines and inflammatory mediators

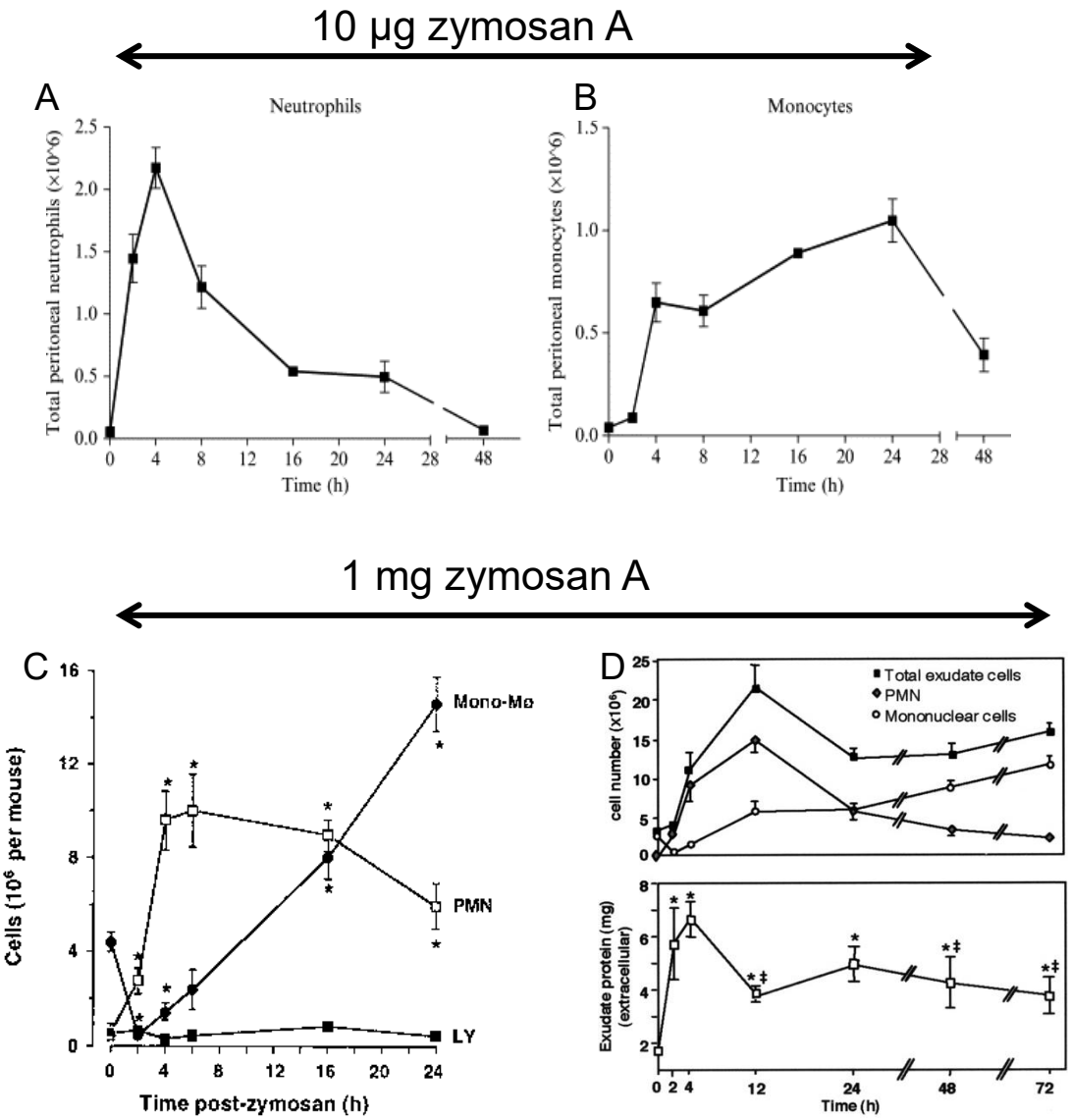

Figure 4.1: Temporal sequence of peritoneal neutrophil and monocyte recruitment following i.p. injection zymosan A in mice

Kinetics of neutrophil and monocyte recruitment in the model of zymosan-induced peritonitis. Kinetics and total number of cells recruited differs between different intraperitoneal doses of zymosan A. Data from Cash *et al*., 2009 (host lab of paper and this thesis) using 10 µg zymosan showing neutrophil (A) and monocyte (B) recruitment. Also data from Ajuebor *et al.* 1998a and Bannenberg et al., 2005 are shown in (C) and (D) respectively, demonstrating kinetics of polymorphonuclear neutrophils (PMN) and monocytes/ macrophages using 1 mg zymosan A. In our studies we used 10 µg zymosan A in this model because it induces moderate instead of severe inflammation, it has faster monocyte kinetics (peak within 24h) and inflammation resolves within 48 hours.

- *Figure 4.1.C from Ajuebor et al 1998 : Republished with permission of Federation of American Societies for experimental Biologiy, from Ajuebor MN, Flower RJ, Hannon R, Christie M, Bowers K, Verity A, et al. : Endogenous monocyte chemoattractant protein-1 recruits monocytes in the zymosan peritonitis model. J Leukoc Biol 63(1): 108-116,1998; permission conveyed through Copyrigt Clearance Center, Inc.*
- *Figure 4.1.D from Bannenberg et al., 2005 : Bannenberg GL, Chiang N, Ariel A, Arita M, Tjonahen E, Gotlinger KH, et al. (2005). Molecular circuits of resolution: formation and actions of resolvins and protectins. J Immunol 174(7): 4345-4355. Copyright 2005. The American Association of Immunologists, Inc.*

SAR compound	Intrinsic clearance (μL/min/mg of protein)	Microsomal stability half life (minutes)
3	32.1	43
6 (DIAS2)	30.3	46
12	39.3	35
13	474	3
22	Solubility issues: Not detected	Solubility issues: Not detected
28	256	5

Table 4.1: Metabolic half-lives for SAR compounds
Metabolic stability studies were contracted to Cyprotex Ltd (UK). Briefly mouse liver microsomes were incubated with 3 μM compounds (0.25% DMSO) at 37^{o}C in the presence of co-factor NADPH. At different points (0, 5, 15, 30, 45 minutes) the microsomes were lysed with methanol and the compound's concentration was detected using liquid chromatography-mass spectrometry (LC-MS/MS). A compound is considered of high clearance when its intrinsic clearance is higher than 48 μL/min/mg protein. Data shown are mean values from a single experiment, triplicate to quadruplicate technical repeats.

4.2 Results

4.2.1 Administration of DIAS2 (in SigmaSolve) in zymosan-induced peritonitis

The first aim of this chapter was to identify an appropriate solvent to solubilise cannabinoids which could be administered *in vivo*. The first solvent used was 90% Saline/ 5% ethanol/ 5% Cremophor®-EL (in this chapter named as SigmaSolve), which is a commonly used solvent for cannabinoids in *in vivo* experiments (Howlett *et al.*, 2002). C57BL/6J male mice were injected i.p. with 10 µg zymosan A or solvent (PBS) at 25 ml/kg for two hours, followed two hours later by i.p. injection of DIAS2 or solvent (SigmaSolve). Four hours after zymosan administration, the mice were culled and their peritoneal cavities were lavaged with cold PBS/ 2mM EDTA. PECs were assessed with flow cytometry while cell-free supernatants were stored at -80^{o}C to be analysed using ELISA assays. Representative flow cytometry plots of PECs in different treatment groups are shown in Figure 4.2 and 4.3. Representative flow cytometry plots (Forward Scatter versus Side Scatter) of the cells in the peritoneal cavity are shown for mice injected with PBS/Solvent and zymosan/solvent (Figure 4.2). Neutrophils are gated as Ly6G^{++}7/4^{++} while monocytes are Ly6G^{-}7/4^{++} (Figure 4.2). This gating strategy agreed well with results from published studies (White *et al.*, 2011). Administration of DIAS2 increased total PECs and total peritoneal neutrophils (Figure 4.4A and B), whereas it decreased total monocytes numbers (Figure 4.4C). It is of note that despite DIAS2 being in solution during i.p. administration, two hours later it was visibly precipitating in the peritoneal cavity's walls.

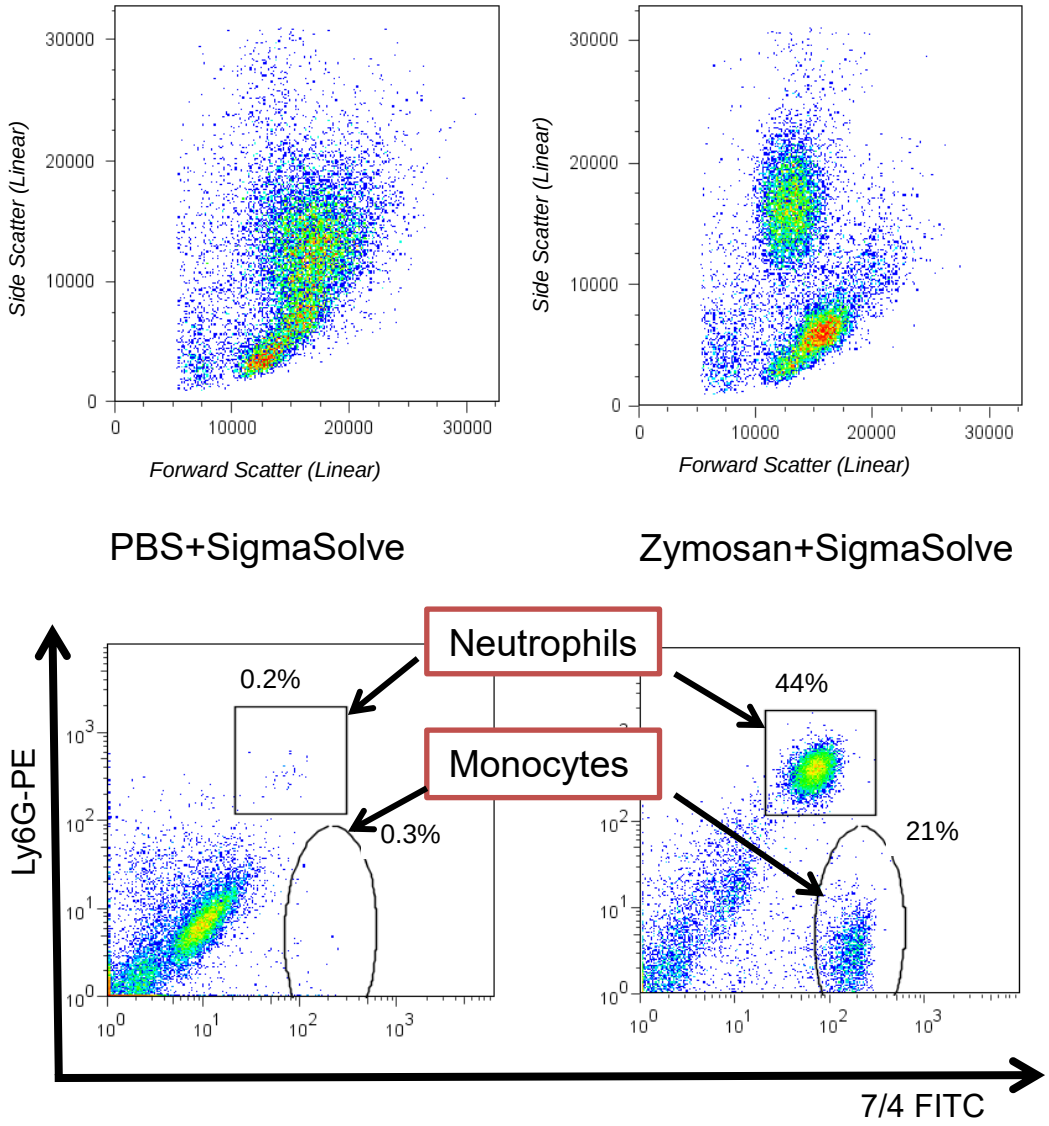

Figure 4.2: Representative flow cytometry examples after solvent administration in zymosan-induced peritonitis
The solvent used for solubilising cannabinoid ligands in this figure was the one most used in the literature, thus 90% Saline/ 5% ethanol/ 5% Cremophor®-EL (in short named SigmaSolve). The model used was i.p. administration of 10 µg of zymosan A (25 ml/kg) or solvent (PBS) and two hours later i.p. administration of SigmaSolve (25 ml/kg). Two hours window for compound or solvent was selected since the microsomal half-life of DIAS2 was ~45 minutes (Table 4.1). Four hours after zymosan A injection, the mice were culled and their peritoneal cavities were lavaged. PECs were assessed by flow cytometry. Representative flow cytometry plots of separate mice are shown (same experiment).

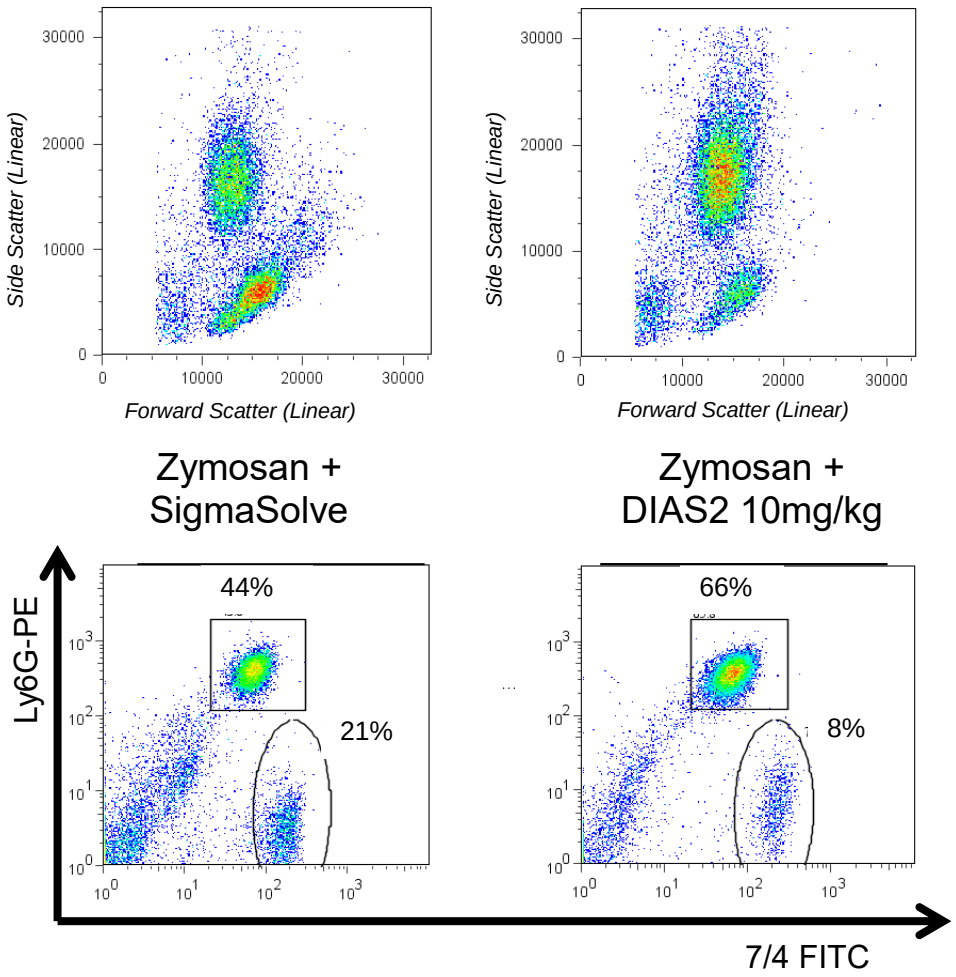

Figure 4.3: Representative flow cytometry examples after DIAS2 administration in the presence of SigmaSolve
Protocol as in Figure 4.2. Administration of 10 µg zymosan A was followed two hours later by injection of DIAS2 (in 90% Saline, 5% ethanol, 5% Cremophor®-EL). Mice were culled four hours after zymosan A administration. It is to be noted that within the two hours of compound administration DIAS2 was coming out of solution and forming visible precipitates in the peritoneal cavity. Neutrophils and monocytes are as gated as in Figure 4.2. Representative flow cytometry plots of separate mice are shown (same experiment).

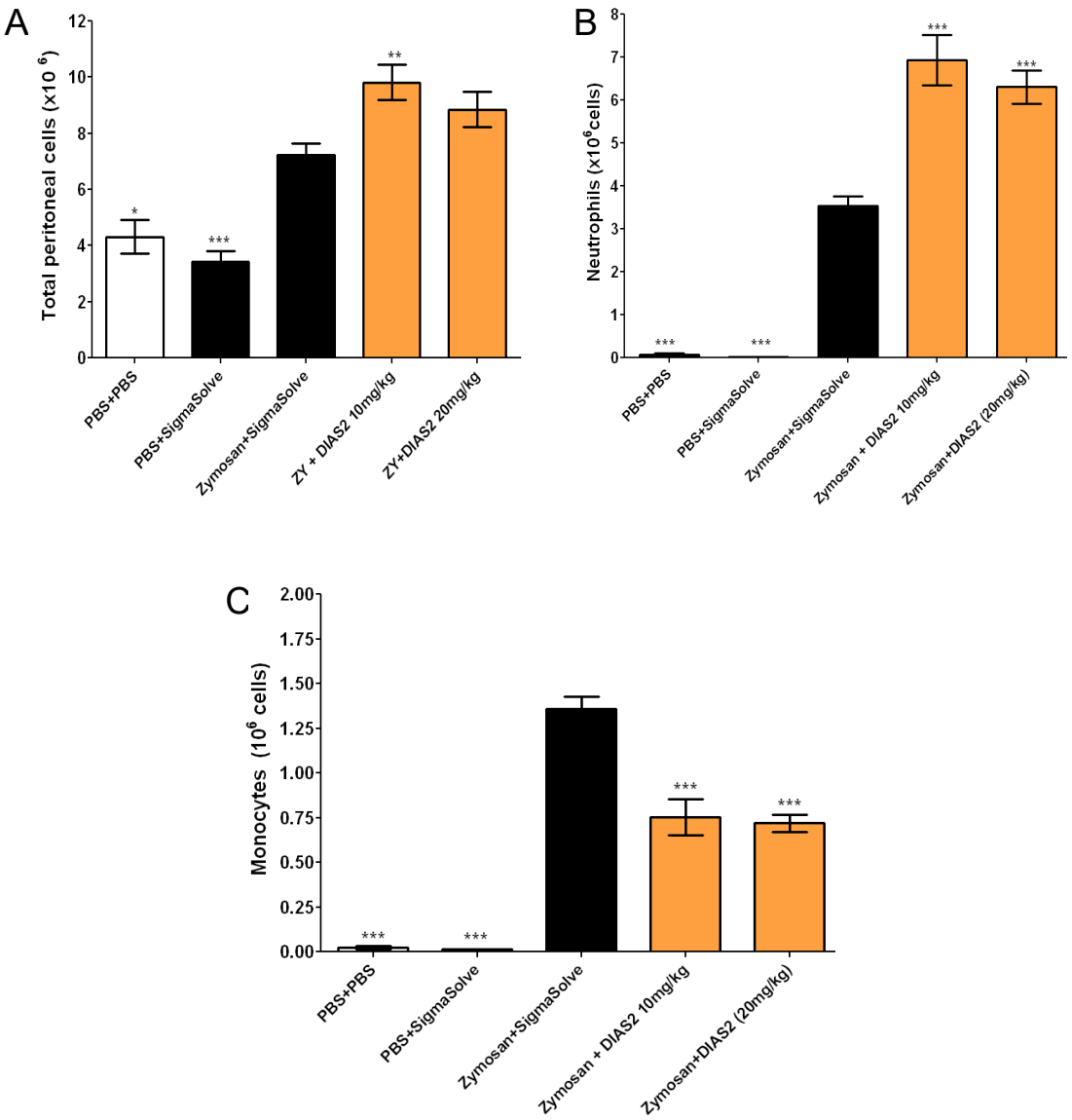

Figure 4.4: DIAS2 (in SigmaSolve) increased total PECs and neutrophils and decreased monocyte total numbers

Protocol as in Figure 4.3. Briefly 10µg zymosan A was administered for two hours, followed by two hours of DIAS2 or solvent before the mice were culled. Total numbers of monocytes and neutrophils per cavity were calculated from multiplication of total numbers in the cavity with the % of each cell type. It is of note that within the two hours of compound administration DIAS2 was coming out of solution and visibly precipitating in the peritoneal cavity. Pooled data of 2-3 independent experiments, 5-10 mice/group, error bars=SEM. One-way ANOVA and Dunnett's multiple comparison test against Zymosan+SigmaSolve, ***P<0.001, **P<0.01, *P<0.05

Overall DIAS2 (dissolved in SigmaSolve) decreased monocytes despite the undesirable solubility problems.

4.2.2 Testing a second solvent (Tocrisolve) in zymosan-induced peritonitis

A second solvent was attempted for solubilising DIAS2. Tocrisolve^{TM} 100 (25% soya oil, 75% water with emulsifier Pluronic F68) has been previously used as solvent for JWH-133 (Hoyer *et al.*, 2011). As above, zymosan A was administered for two hours followed by two hours of solvent alone before the mice were culled. Representative flow cytometry plots are shown in Figure 4.5. Overall, Tocrisolve^{TM} 100 was well tolerated in mice but increased total peritoneal cells (Figure 4.6A), total neutrophils (Figure 4.6B) and total monocytes (Figure 4.6C) in the peritoneal cavity. Moreover Tocrisolve^{TM}-100 has a thick white droplet appearance which made the counting of the total cells under the microscope challenging. Additionally attempts to solubilise DIAS2 in Tocrisolve^{TM} 100 were not conclusive due to the solvent's appearance which made impossible visual assessment whether the compound was dissolved.

4.2.3 DIAS2 dose-dependently inhibits monocyte recruitment in zymosan induced peritonitis

A third type of solvent was then tested which belonged to the class of cyclodextrins (Figure 4.7).

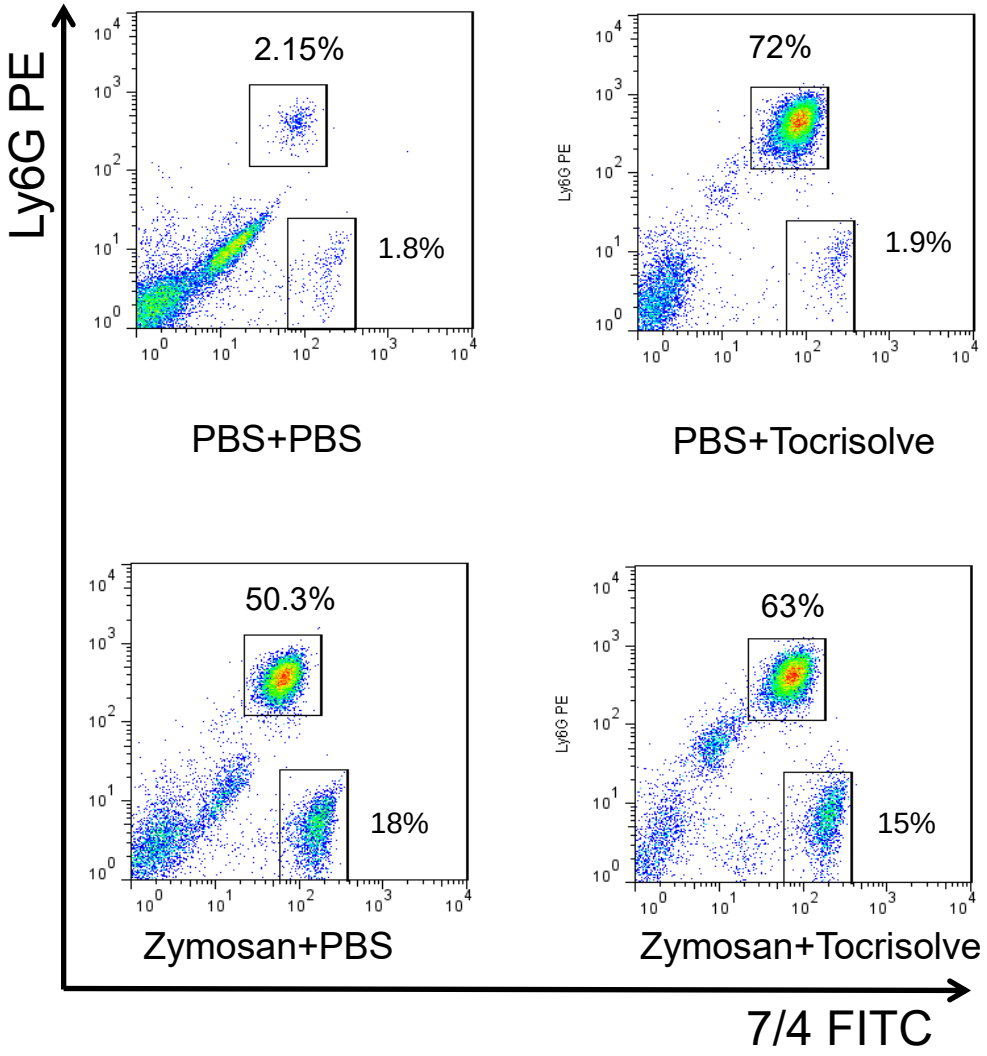

Figure 4.5: Tocrisolve™ 100 administration is tolerated in zymosan-induced peritonitis

SigmaSolve did not adequately solubilise DIAS2 so alternative solvents were tested. Tocrisolve™ 100 (25% soya oil, 75% water with emulsifier Pluronic F68) has been used in the literature as alternative solvent for cannabinoids (Hoyer et al., 2011). The solvent was administered at 25 ml/kg in mice as in the protocol of Figure 4.2. PECs were assessed by flow cytometry. Neutrophils and monocytes are as gated as in Figure 4.2. Representative flow cytometry plots of separate mice are shown (same experiment).

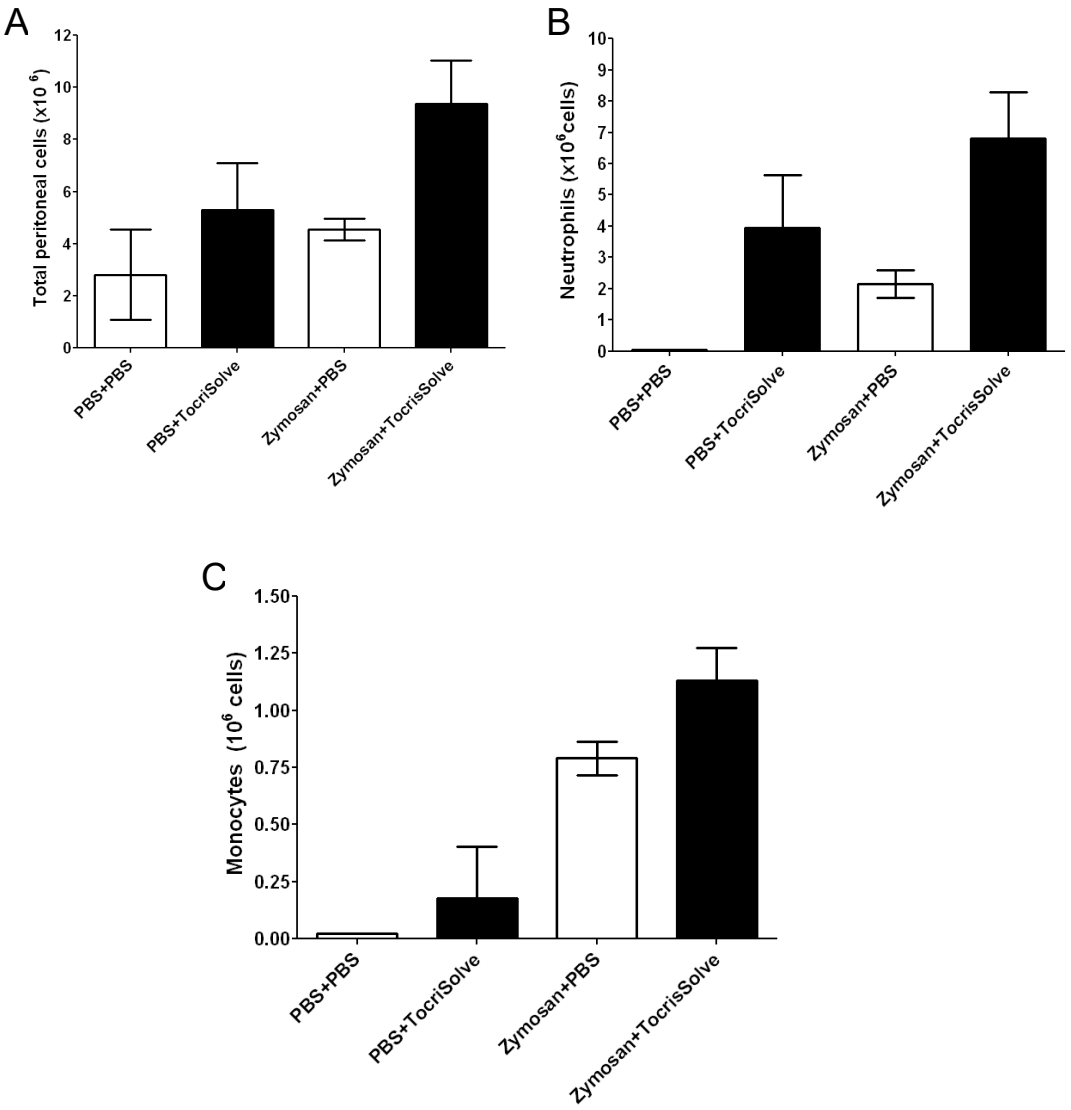

Figure 4.6: Tocrisolve™ 100 is tolerated but increased total PECs, neutrophils and monocytes in zymosan-induced peritonitis

Tocrisolve™ 100 (25% soya oil, 75% water with emulsifier) was administered in mice as in protocol as Figure 4.3. PECs were assessed by flow cytometry. Tocrisolve™ 100 has a thick white droplet appearance and counting total cells was challenging. Data shown are from one experiment, 3-4 mice/group, error bars=SD

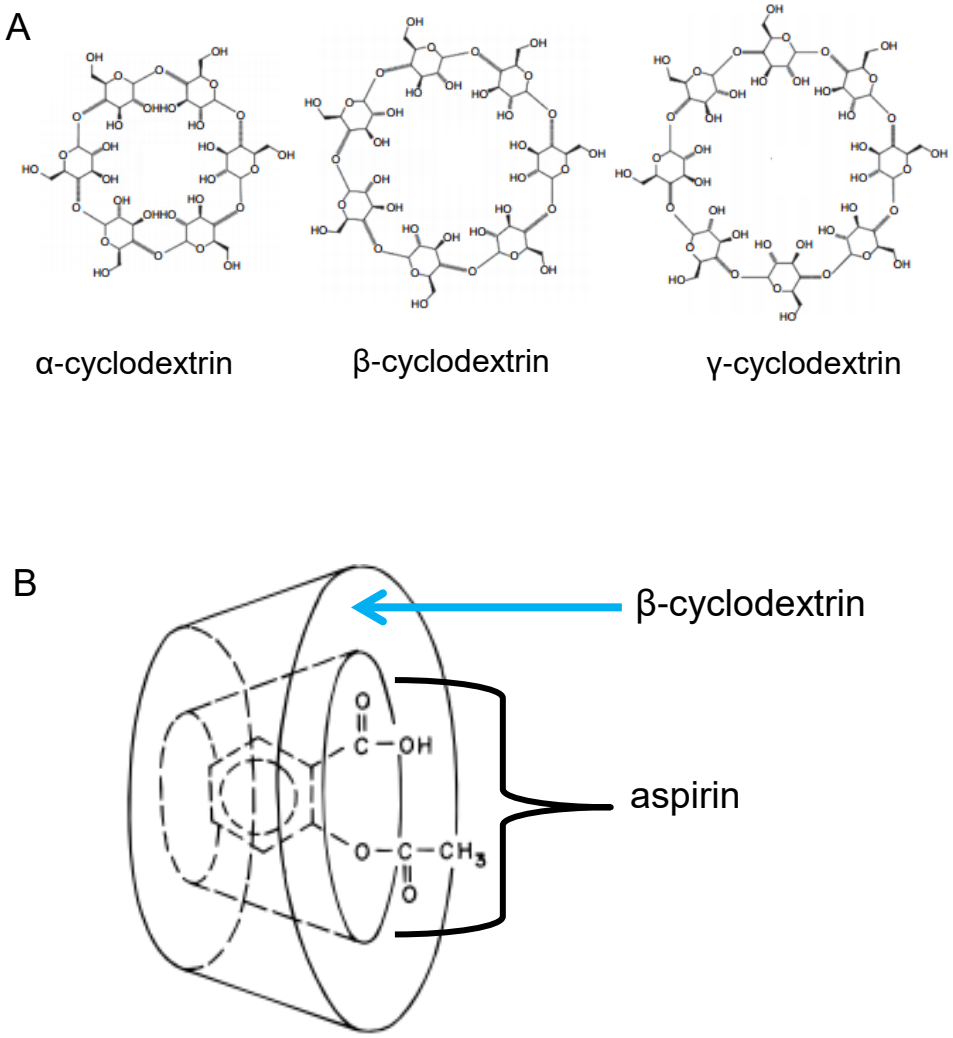

Figure 4.7: Cyclodextrins in drug discovery
Cyclodextrins are cyclic oligosaccharides with a lipophilic core and a hydrophilic exterior (Laza-Kroerr et al., 2010). Depending on the number of glucose units (six, seven or eight) the cyclodextrins are classified as α, β or γ (Figure 4.7A). They are used to enhance solubility of lipophilic compounds in aqueous solutions by forming inclusion complexes with them. Cyclodextrins have also been used as stabilising agents for chemically labile drugs, for example aspirin which in a complex with β-cyclodextrin degrades slower in aqueous solutions (Figure 4.7B) (Loftsson et al., 1996).

Cyclodextrins are cyclic oligosaccharides with a hydrophilic exterior and a lipophilic core and have been used in drug discovery mainly for solubilising lipophilic compounds (Laza-Knoerr *et al.*, 2010; Loftsson *et al.*, 1996). Ten microgram/mouse of zymosan A (25 ml/kg) was administered i.p. for four hours followed by two hours of 5 ml/kg of DIAS2 or solvent (45% w/v 2-hydroxy-propyl cyclodextrin in PBS, HP-β-cyclodextrin, in short named DextrinSolve in this chapter) before the mice were culled. DIAS2 was administered therapeutically (post-zymosan injection) for several reasons. In peritonitis the neutrophils are recruited before monocytes but do not express CB2R (Chouinard *et al.*, 2011) and neither do the resident macrophages (Lee *et al.*, 2001), therefore pre-zymosan DIAS2 administration would not be able to target the key CB2R expressing cell type, thus the recruited monocyte. When DIAS2 was administered at 4 hours post-zymosan the estimated monocyte recruitment in this model from the literature (Cash et al., 2009) would be around $EC_{30\text{-}40}$ and thus could be more modulated than the E_{max} of monocyte recruitment at approximately 24 hours. Additionally in clinical settings anti-inflammatory drugs are administered during inflammation and not prophylactically. Representative flow cytometry plots of the PECs are shown in Figure 4.8. Empirical assessment of the *in vivo* solubility of compounds is challenging when large volumes are collected as is the case for peritoneal lavages (ml volume) compared to blood collection (µl volume). By visual assessment, it appeared that DIAS2 remained in solution *in vivo* throughout the two hour window since no precipitates could be seen in the peritoneal cavity. DIAS2 in DextrinSolve decreased total peritoneal cells at 1 and 5 mg/kg (Figure 4.9A), had no effect on peritoneal neutrophils (Figure 4.9B) and dose-dependently decreased peritoneal monocyte numbers (Figure 4.9C).

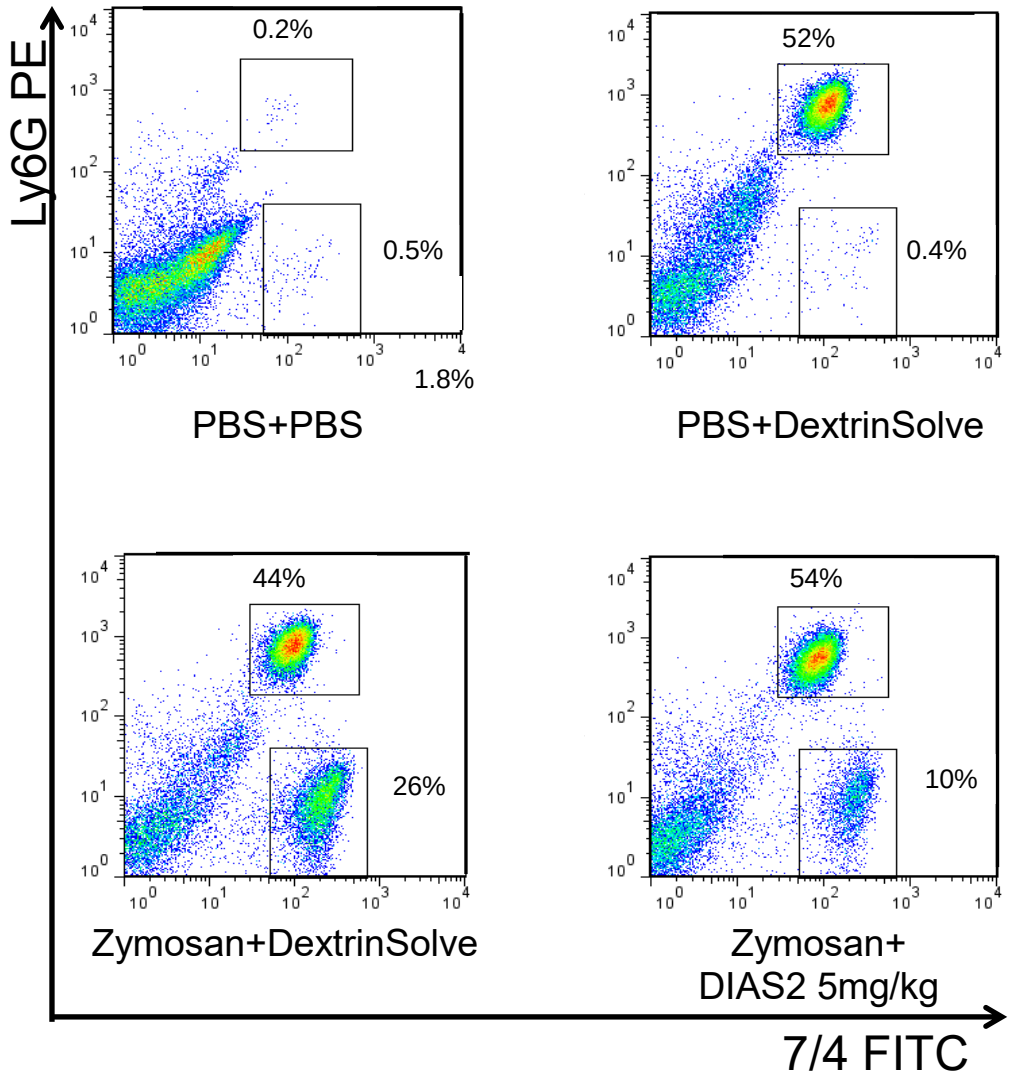

Figure 4.8: Representative flow cytometry example plots after administration of DIAS2 or its solvent HP-β-cyclodextrin
A third solvent was attempted for solubilising cannabinoid ligands. This was 45% w/v 2-hydroxy-propyl cyclodextrin (HP-β-cyclodextrin, in short named DextrinSolve), in PBS administered at 5 ml/kg. The model used was i.p. administration of 10 µg of zymosan A or solvent (PBS) for four hours and followed by i.p. administration of DIAS2 or its solvent (DextrinSolve) for 2 hours. Six hours after zymosan A administration the mice were culled and their cavities were lavaged. PECs were assessed by flow cytometry. Neutrophils and monocytes are as gated as in Figure 4.2. Representative flow cytometry plots are shown from the same experiment.

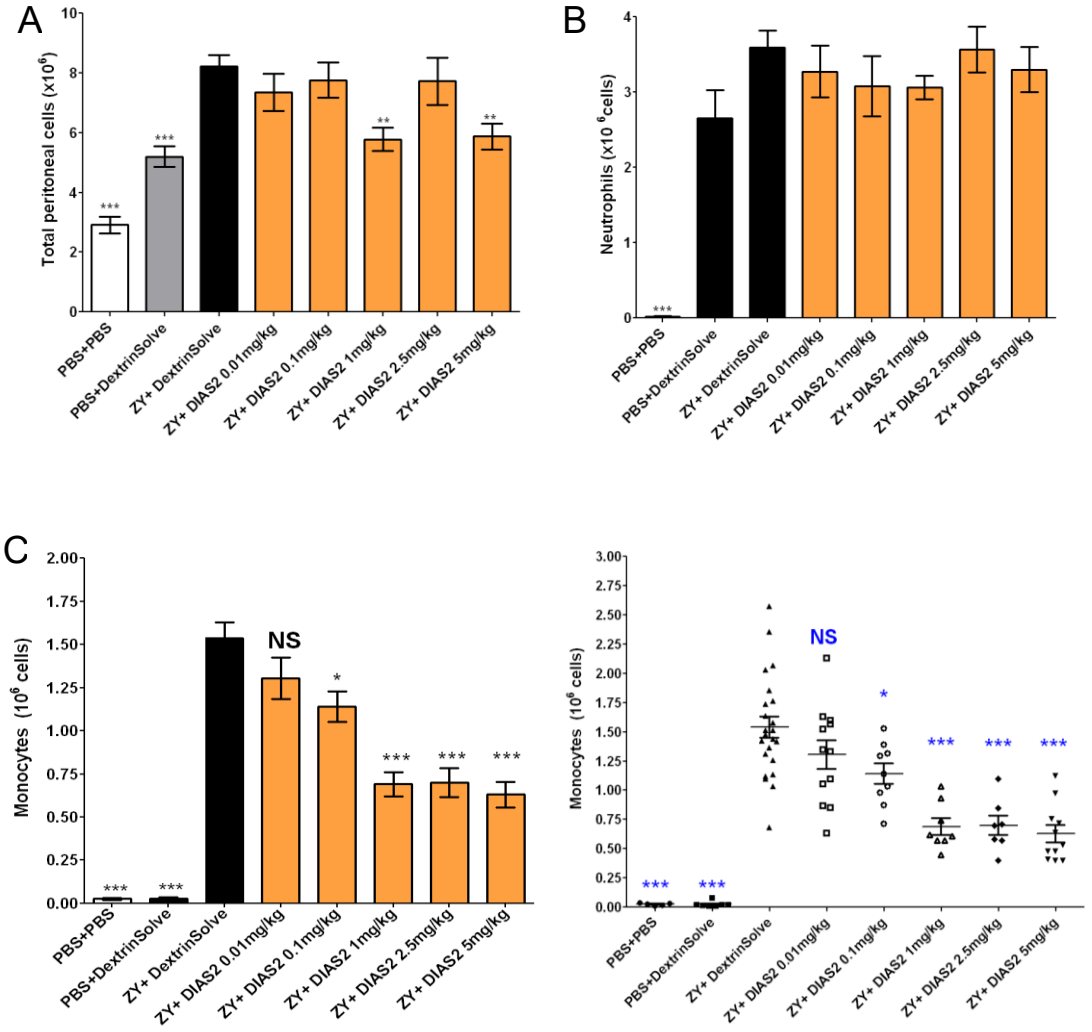

Figure 4.9: Administration of DIAS2 (in HP-β-cyclodextrin) in zymosan-induced peritonitis reduces total monocyte numbers

10 µg of zymosan were administered i.p. for 4 hours followed by 2 hours DIAS2, which was administered *in vivo* as in Figure 4.8. Pooled data from 3-4 independent experiments, 8-10 mice/group, error bars=SEM. One-way ANOVA and Dunnett's multiple comparison test against Zymosan+DextrinSolve, ***P<0.001, **P<0.01, *P<0.05

4.2.4 DIAS2 and SAR3, but not SAR1 and JWH-133 inhibit monocyte recruitment in zymosan-induced peritonitis

Having shown that DIAS2 intraperitoneal administration to a site of on-going inflammation reduced monocyte numbers by 50% but had no effect on neutrophils, the next aim was to compare the biological effect of 5 mg/kg DIAS2 (molecular weight 317.07) with 5 mg/kg dose of SAR1 (weak agonist, EC_{50} = 10,000 nM at hCB2R, molecular weight 293), SAR3 (potent agonist, EC_{50} = 33 nM at hCB2R, molecular weight 337.06) and JWH-133 (a commercial CB2R agonist, EC_{50} = 38 nM at hCB2R, molecular weight 312.49) in zymosan-induced peritonitis. A new batch of zymosan was obtained so a dose-response experiment was performed in the presence of solvent to identify an equipotent inflammatory dose with the previous zymosan batch (Figure 4.10).

At 6 hours higher doses of zymosan had a trend for increased neutrophil numbers (Figure 4.10B) and monocyte numbers (Figure 4.10C). A thirty microgram dose was selected since it recruited a similar number of neutrophils and monocytes within 6 hours compared to the previous batch (Figure 4.9). Thirty microgram of zymosan A was administered per mouse for four hours followed by two hours of 5 mg/kg of DIAS2, SAR1, SAR3, JWH-133 or solvent (DextrinSolve) before the mice were culled. Representative flow cytometry plots of the experiments are shown in Figure 4.11. It was observed that only DIAS2 significantly reduced total cell counts (Figure 4.12A) while none of the four compounds affected the total peritoneal neutrophil numbers (Figure 4.12B).

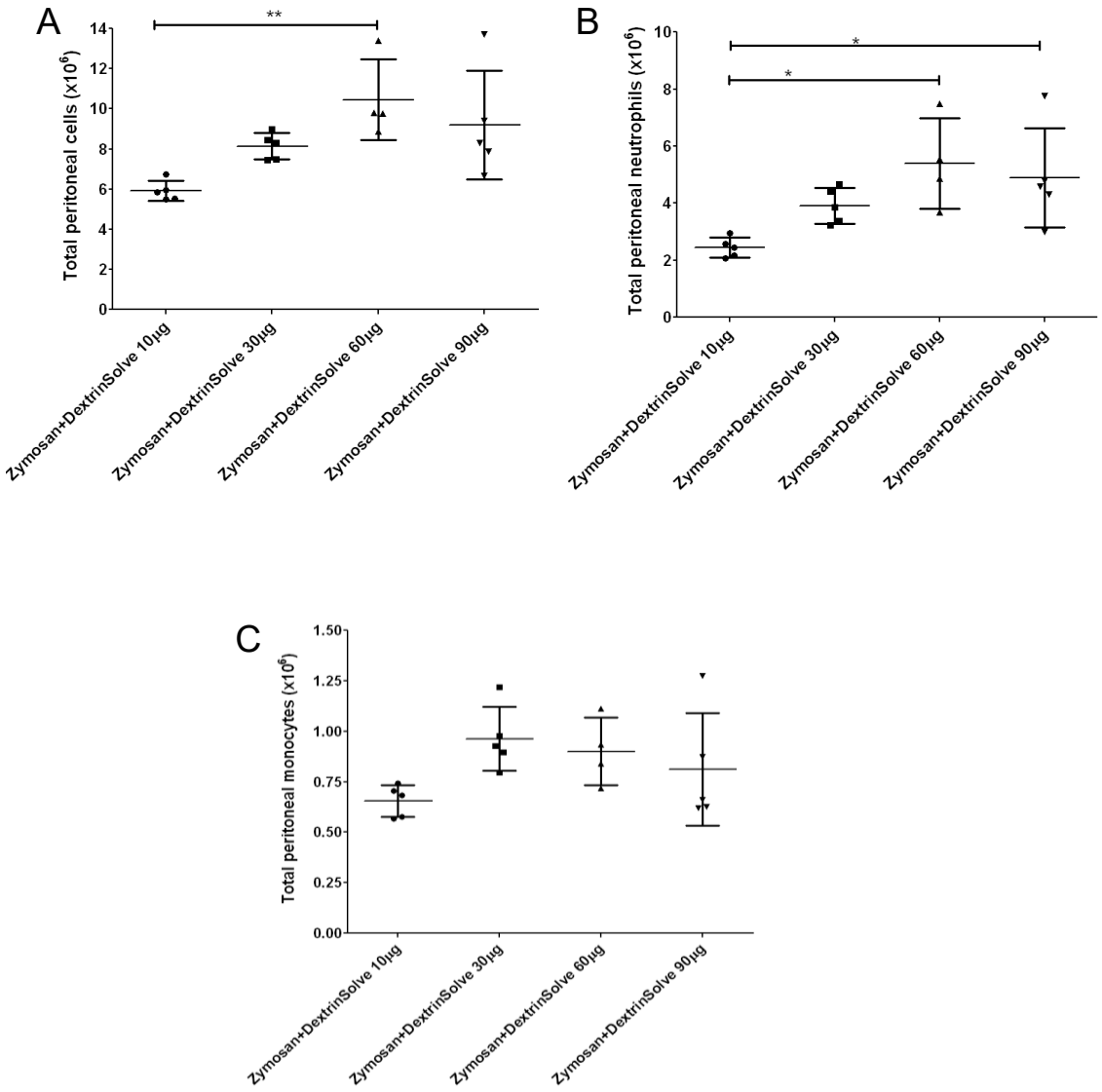

Figure 4.10: Optimizing *in vivo* dose for new batch of zymosan
A new batch of zymosan was obtained and its dose was optimized to match the recruitment of monocytes from the previous batch at the time point of 6 hours. 4-5 mice/group, error bars= SD, One-way ANOVA and Bonferroni's multiple comparison test, **P<0.01, *P<0.05

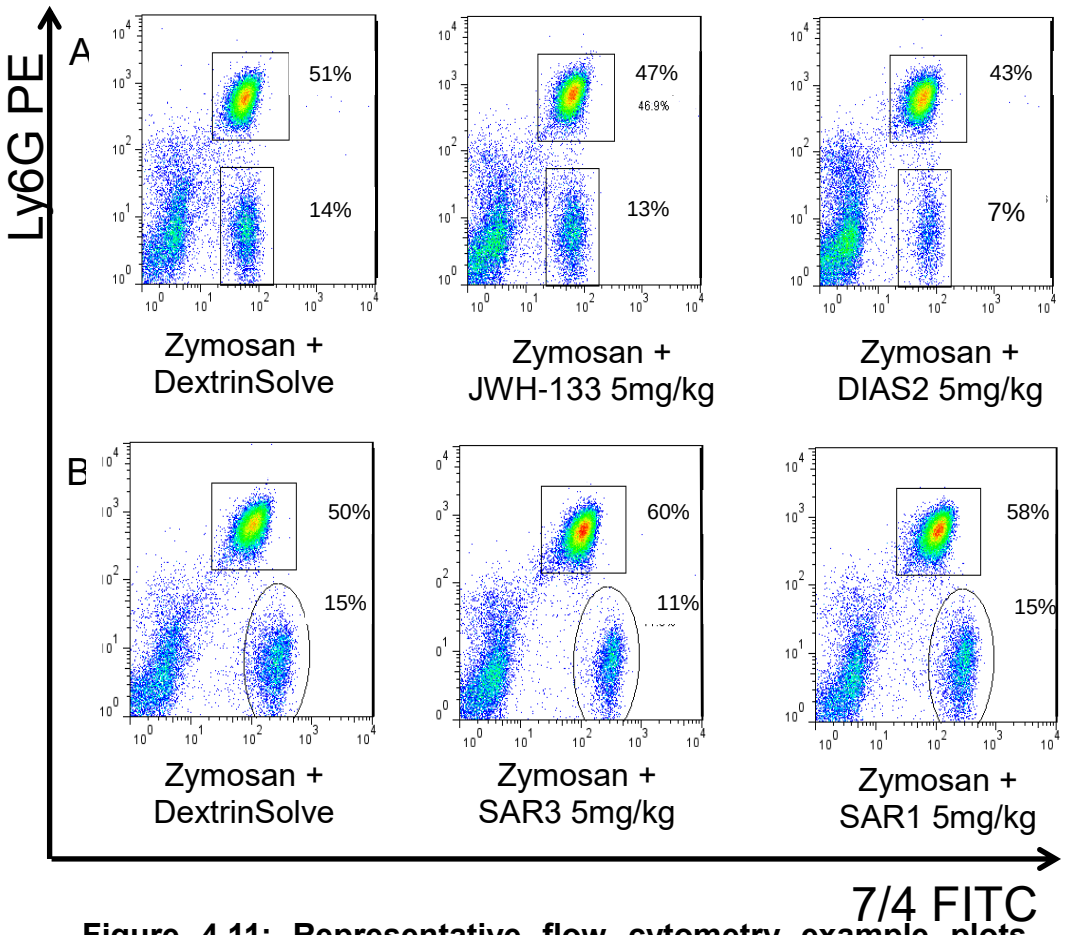

Figure 4.11: Representative flow cytometry example plots after administration of DIAS2, SAR1, SAR3 and JWH-133
30 µg of zymosan were administered i.p. for 4 hours followed by 2 hours of DIAS2, SAR1, SAR3 and JWH-133, which were administered at 5mg/kg in DextrinSolve as in the protocol of Figure 4.8. Neutrophils and monocytes are as gated as in Figure 4.2. Representative flow cytometry plots are shown from two independent experiments (Figure 4.11A and B).

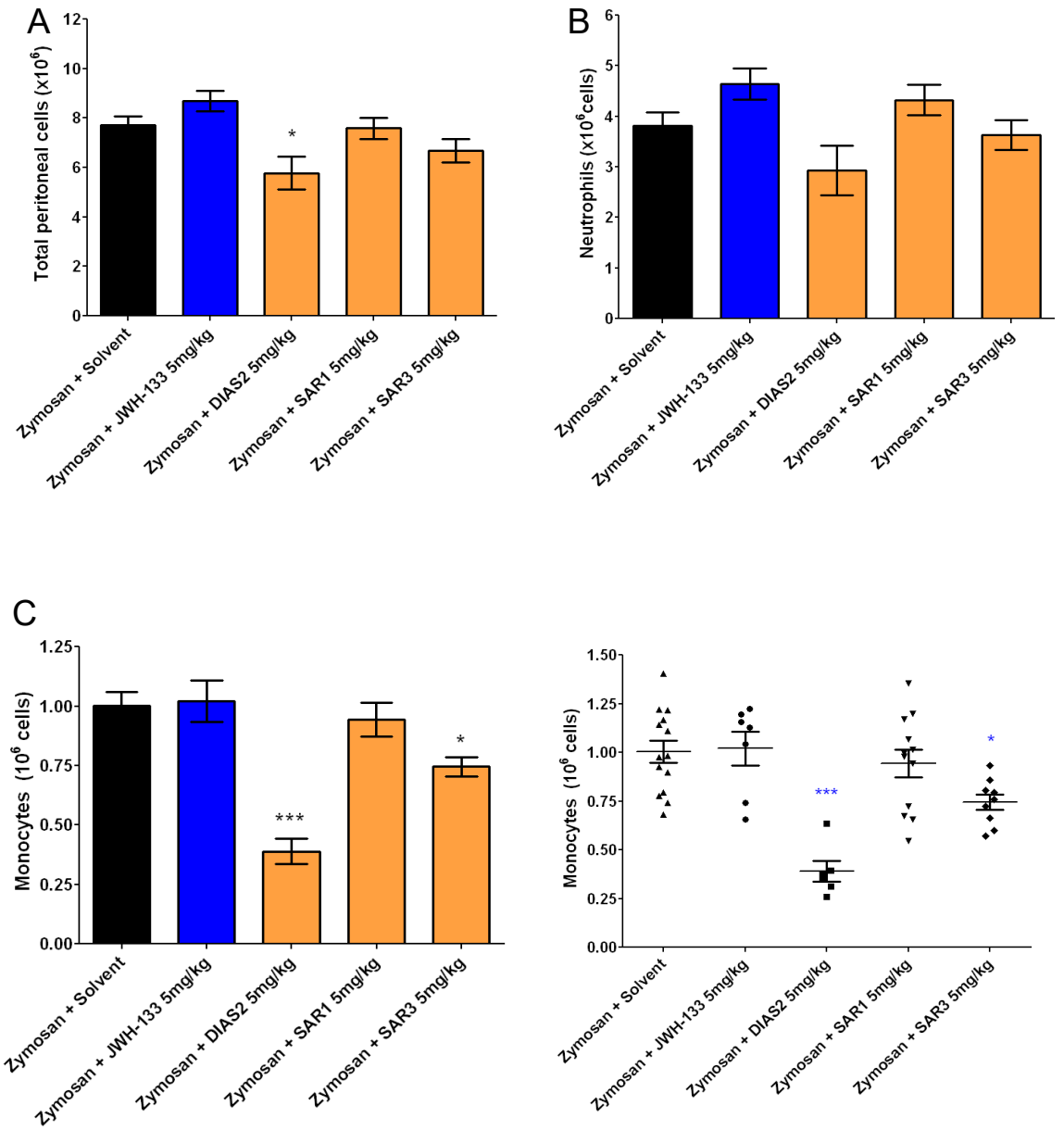

Figure 4.12: Administration of DIAS2 and SAR3 but not JWH-133 and SAR1 in zymosan-induced peritonitis reduced total monocyte numbers
30 µg of zymosan were administered i.p. for 4 hours followed by 2 hours of JWH-133, DIAS2, SAR1 and SAR3 at 5 mg/kg in DextrinSolve (as in Figure 4.9). Pooled data from 2 independent experiments, 6-10 mice/group, error bars=SEM. One-way ANOVA and Dunnett's multiple comparison test against Zymosan+DextrinSolve, ***P<0.001, **P<0.01, *P<0.05

While JWH-133 and SAR1 had no effect on monocyte numbers, both DIAS2 and SAR3 reduced monocyte numbers in zymosan-induced peritonitis (Figure 4.12C). Additional cell markers were used in flow cytometric analysis to distinguish potential effects on other cell types (Table 4.2). None of the compounds tested had any effect on B-cells (Figure 4.13B) and only JWH-133 increased pDCs numbers (Figure 4.13C).

4.2.5 Analysis of peritoneal exudate supernatants from peritonitis experiments

Having demonstrated significant changes in peritoneal cell numbers in vivo, we next studied the peritoneal exudate supernatants using ELISAs to assess whether DIAS2 reduced monocyte numbers due to a modulation of pro-inflammatory or anti-inflammatory mediators. None of the four compounds had any effect on the levels of chemokines JE and MIP-1α (Figure 4.14 A and B). On the other hand, both DIAS2 and SAR3 significantly increased the levels of the CXC chemokine KC (Figure 4.14C). No TNF-α was detected in the same supernatants (detection limit 31.3 pg/ml) (Figure 4.14D). It has been demonstrated in the literature that NO levels modulate KC but not MIP-1α and JE levels in the model of zymosan-induced peritonitis (Ajuebor *et al.*, 1998b). For this reason the NO levels in the supernatants were analysed using a semi-automated-HPLC NO-analyser which detects nitrite/nitrate levels following a series of chemical reactions mentioned in “Methods” chapter. As shown in Figure 4.15B, NO was present in the supernatants but none of

the treatments significantly modulated the NO levels despite DIAS2 having an increasing trend.

Cell type	Markers expressed in zymosan-induced peritoneal cells
Neutrophils	$Ly6G^{++}$ $7/4^{++}$ $CD11b^{++}$ $Ly6C^{+}$ $B220^{-}$
Monocytes	$Ly6G^{-}$ $7/4^{++}$ $CD11b^{++}$ $Ly6C^{++}$ (inflammatory monocytes) $B220^{-}$
B-cells	$Ly6G^{-}$ $7/4^{-}$ $Ly6C^{-}$ $B220^{++}$
Plasmacytoid dendritic cells (pDCs)	$Ly6G^{-}$ $7/4^{-}$ $Ly6C^{+}$ $B220^{++}$

Table 4.2: Markers used for distinguishing cell types in zymosan-induced peritonitis
For more details on methodology and suppliers see methods chapter.

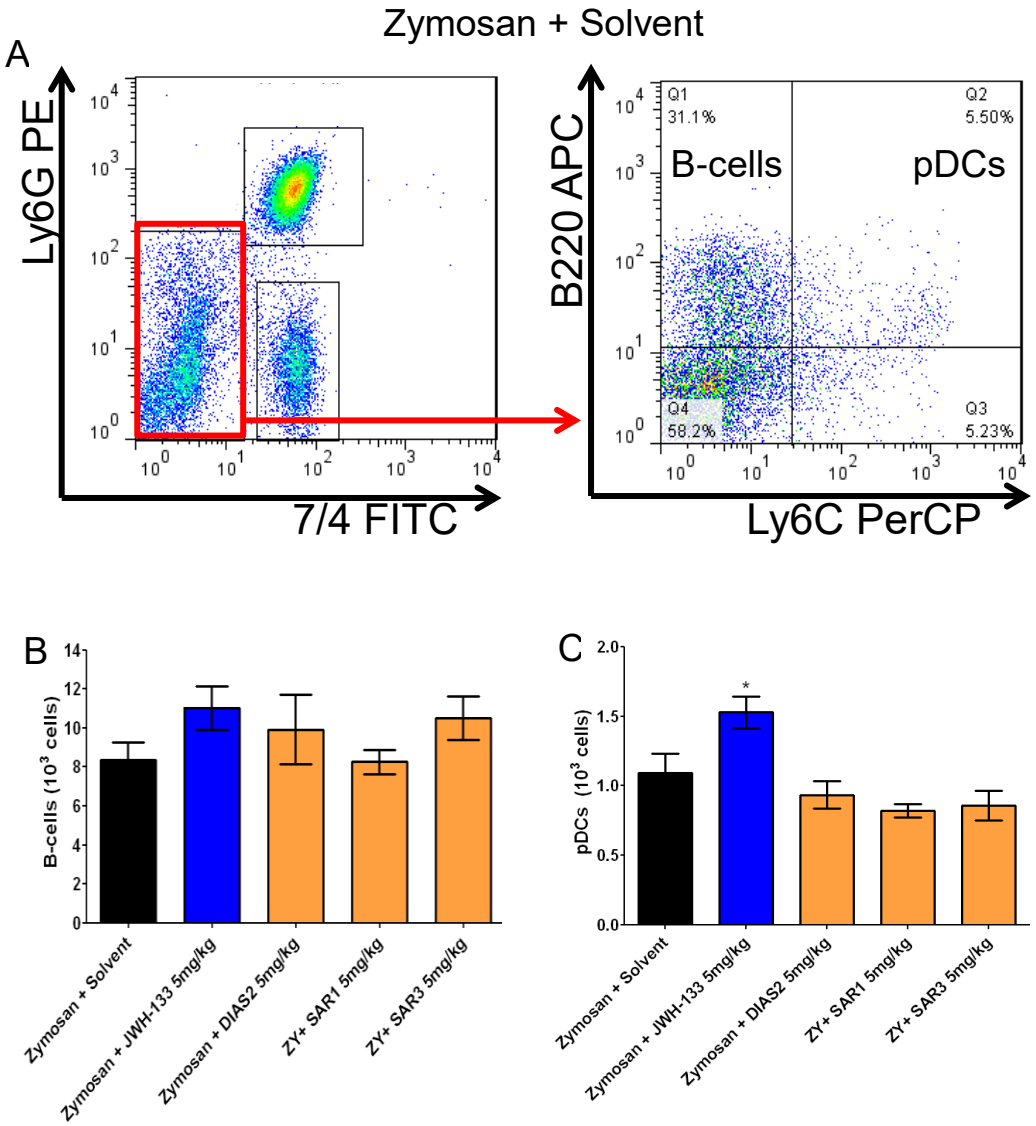

Figure 4.13: Cannabinoid agonists have no effect on peritoneal B-cells and only JWH-133 increased plasmoid dendritic cells

JWH-133, DIAS2, SAR1 and SAR3 were administered at 5mg/kg in DextrinSolve (as in Figure 4.8). B-cells and pDCs were gated as Ly6G 7/4 cells and then further gated according to their expression of B220 and Ly6C (Figure 4.13A). Pooled data from 2 independent experiments, 6-7 mice/group, error bars=SEM. One-way ANOVA and Dunnett's multiple comparison test against Zymosan+DextrinSolve, *P<0.05.

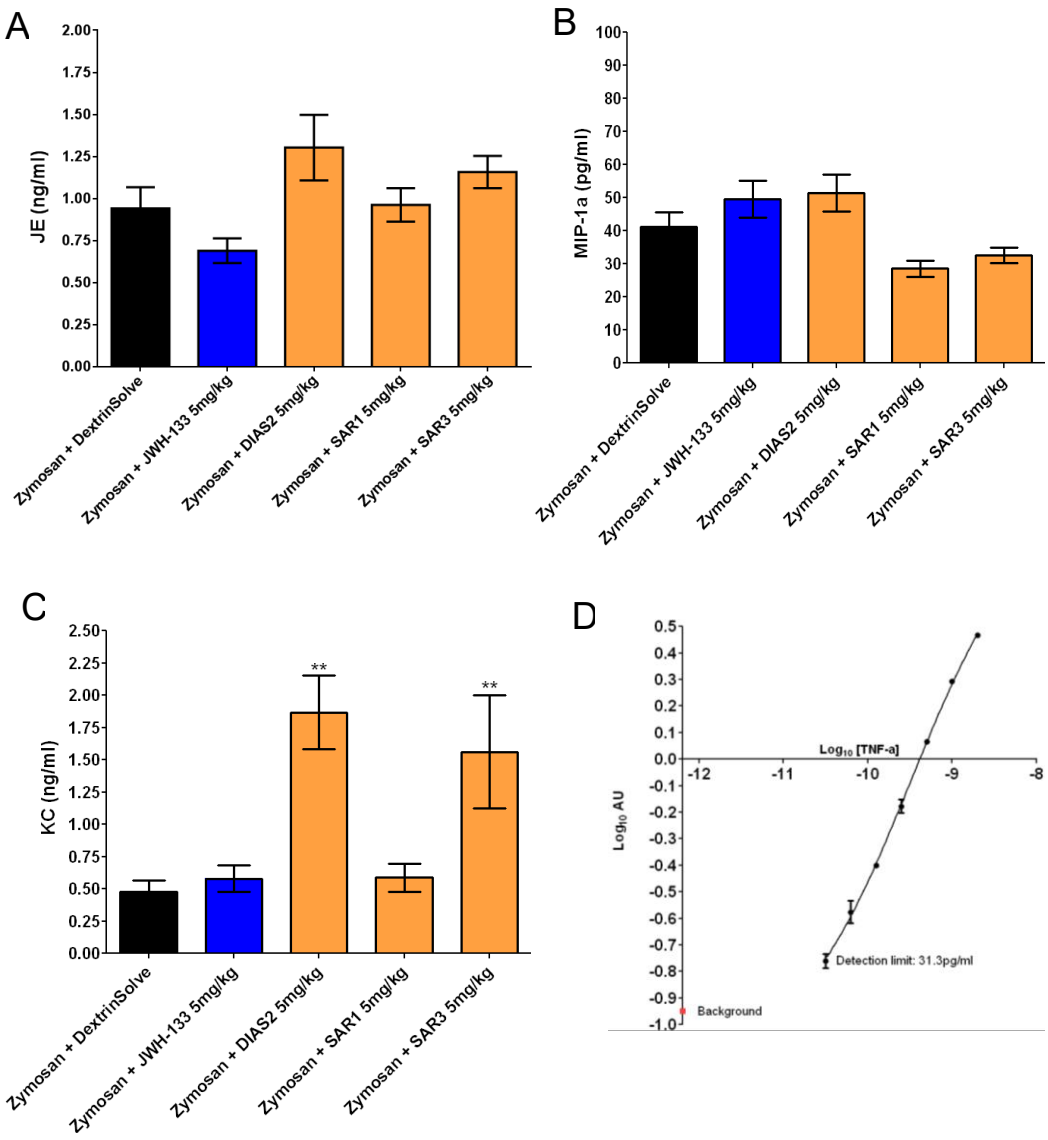

Figure 4.14: Modulation of KC levels by DIAS2 and SAR3 in zymosan-induced peritonitis

Supernatants from the experiment shown in Figure 4.12 were analysed for their levels of TNF-α, KC, MIP-1α and JE using individual ELISA assays. Supernatants were within detection limits for KC, MIP-1α and JE ELISA assays (for detection limits refer to methods chapter). For all samples no TNF-α was detected (below the detection limit of 31 pg/ml (Figure 4.14D). Pooled data from 2 independent experiments, 6-10 mice/group, error bars=SEM. One-way ANOVA and Dunnett's multiple comparison test against Zymosan+DextrinSolve, **P<0.01

4.2.6 Modulation of PECs chemotaxis to RANTES, JE and MIP-1α by JWH-133 and DIAS2

Since no differences were observed in the levels of monocyte/macrophages chemoattractants JE and MIP-1α, the next hypothesis was that cannabinoids may be altering instead the responsiveness of the cells to chemokines. In the literature it was suggested that cannabinoids reduce monocyte chemotaxis to other chemokines by reducing chemokine receptor mRNA (Montecucco *et al*., 2008), for this reason Biogel-elicited PECs were incubated for three hours at 37^{o}C with JWH-133, DIAS2 or solvent (0.3% DMSO). After three hours, chemokines (JE, MIP-1α or RANTES) were added at bottom well of 96-well Boyden-chamber plate (8μm pore) while 400,000 cells were added on top of the filter. Chemotaxis was assessed three hours later by dismounting and fixing the filters. DAPI-stained nuclei on the filters were counted and the fold difference between different treatments over solvent was expressed as a migration index. As shown in Figure 4.16A, neither JWH-133 nor DIAS2 inhibited the chemotaxis of PECs to MIP-1α. RANTES-induced chemotaxis was not influenced by JWH-133 pre-treatment while DIAS2 pre-treatment inhibited PECs chemotaxis to 0.5 nM RANTES by ~40% while PECs chemotaxis to 5 nM was not affected (Figure 4.16B). Also JWH-133 decreased PECs' chemotaxis to 5 nM JE by 50% but had no effect on PECs chemotaxis to 0.5nM JE, while DIAS2 had no effect on PECs chemotaxis to JE (Figure 4.16C).

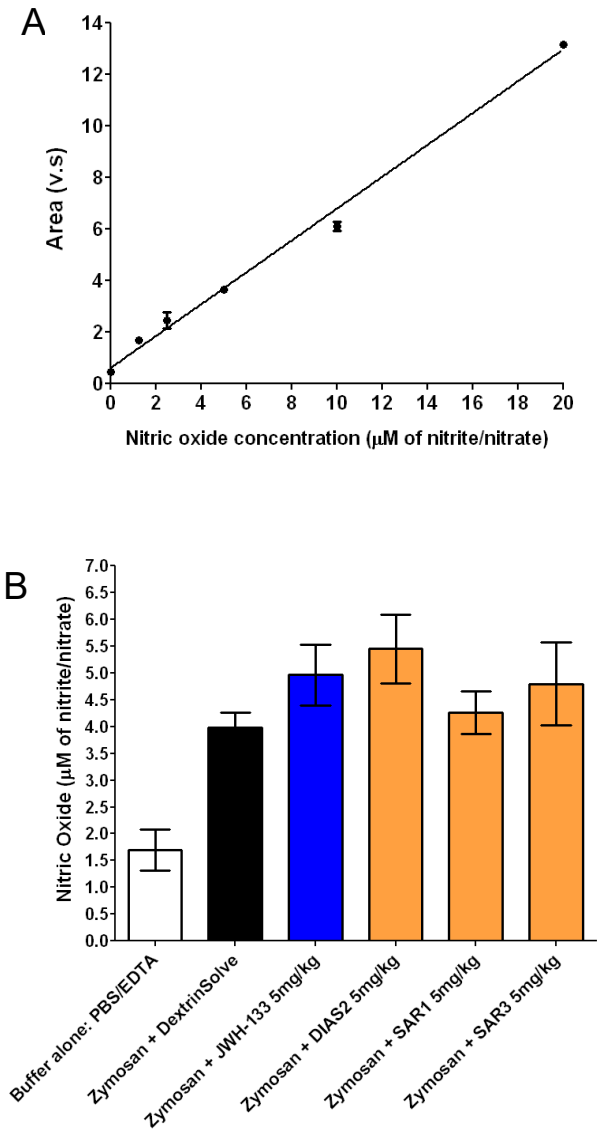

Figure 4.15: Nitric oxide levels were not modulated *in vivo* by cannabinoids
Supernatants from the experiment shown in Figure 4.12 were analysed for their levels of nitrate/nitrite (stable metabolic products of NO) using a semi-automatic-HPLC NO-analyser. Supernatants were within the linear part of the standard curve (Figure 4.15A) and were higher than the nitrate/nitrite levels in the buffer used for peritoneal lavages. Pooled data from 2 independent experiments, 6-10 mice/group, error bars=SEM.

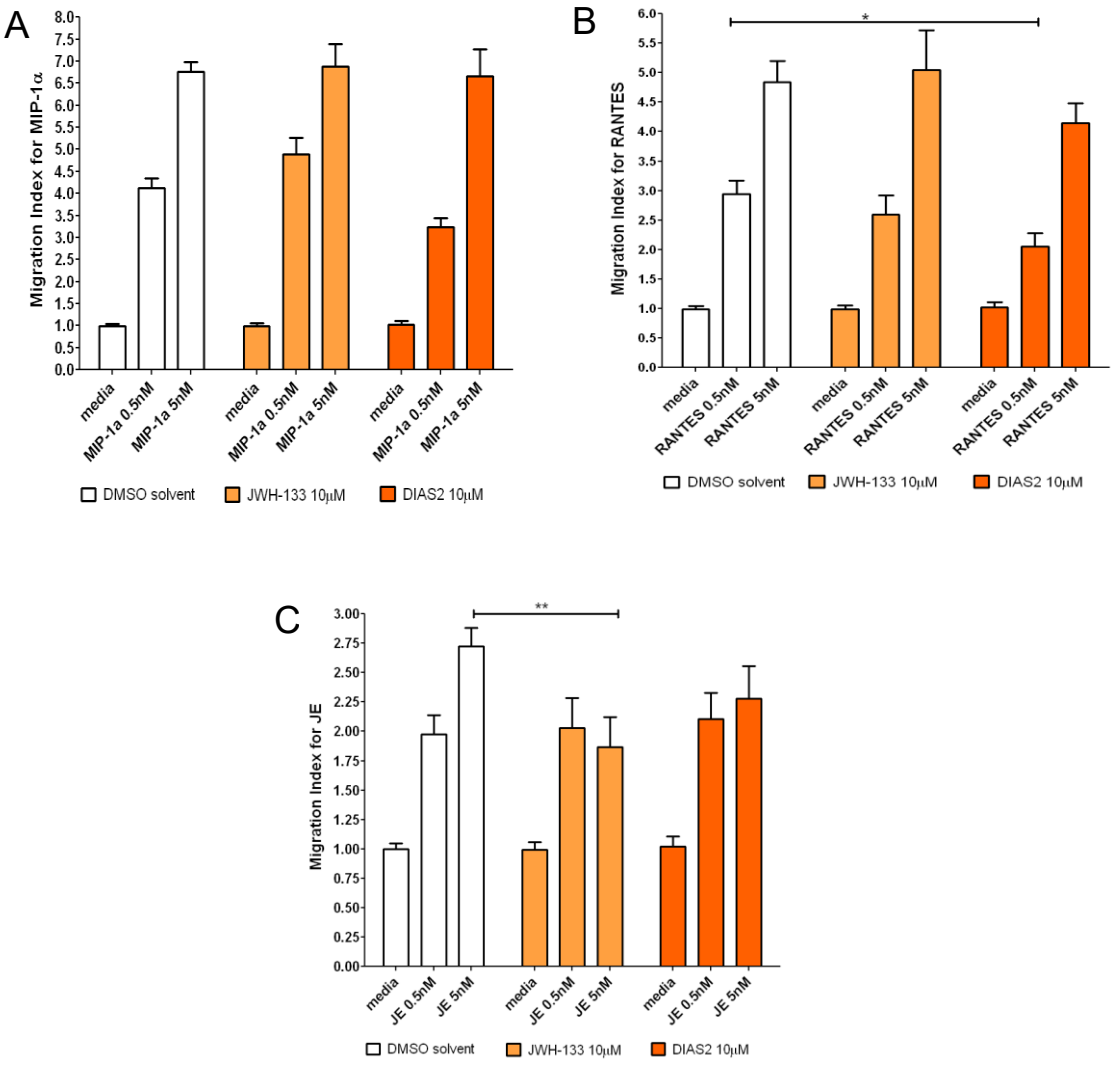

Figure 4.16: Effects of DIAS2 and JWH-133 on PECs chemotaxis to JE, RANTES and MIP-1α

Modulation of chemotaxis to chemokines was assessed *in vitro* as a potential mode of action. Biogel-elicited PECs were incubated for three hours at 37°C with JWH-133, DIAS2 or solvent (0.3% DMSO). After three hours, chemokines (MIP-1α (A),RANTES (B) or JE(C)) were added at bottom well of 96-well Boyden-chamber plate (8 μm pore) while 400,000 cells were added on top of the filter. Chemotaxis was assessed four hours later by counting DAPI-stained nuclei on the filters. Pooled data from 3-4 independent experiments, error bars=SEM. Two-way ANOVA and Bonferroni multiple comparison test against solvent treated cells, **P<0.01, *P<0.05

4.3 Discussion

In this chapter we have identified HP-β-cyclodextrin as a suitable solvent for solubilising the novel CB2R agonists identified in the previous chapter for *in vivo* delivery. Using this solvent, we have demonstrated that DIAS2 dose-dependently decreased inflammatory monocyte numbers by 50% while having no effect on neutrophils in the zymosan-induced peritonitis model. Compared to SAR1, SAR3 and JWH-133, only DIAS2 and SAR3 decreased monocyte numbers while having no effect on neutrophils, B-cells and pDCs in zymosan-induced peritonitis. Although JWH-133 had no significant effect on the numbers of monocytes, neutrophils and B-cells, it modestly increased the pDCs numbers in the inflamed peritoneum. Parallel to the decrease in monocyte numbers induced by DIAS2 and SAR3, an increase of the KC levels was observed with these two CB2R agonists. The decrease in monocytes by DIAS2 was not due to a modulation of MIP1-α, JE or NO levels at the inflammatory site. Additional *in vitro* experiments showed that DIAS2 inhibited PECs' chemotaxis to low but not high doses of RANTES and also did not alter the chemotactic profile of PECs to MIP-1α and JE to suggest this is the mode of action of DIAS2 inhibition of monocyte numbers observed in zymosan-induced peritonitis. Overall, the anti-inflammatory effects of DIAS2 and SAR3 of reducing monocyte numbers are so far linked only with modulation of KC levels.

4.3.1 Suitable solvents for *in vivo* administration

DIAS2 was only adequately dissolved with HP-β-cyclodextrin for the time window of two hours in zymosan-induced peritonitis. Several formulations of saline with

emulsifiers like Cremophor®-EL, for example SigmaSolve, are more commonly used *in vivo* for a range of compounds, from immune-suppressants like cyclosporin to HIV treatments (Strickley, 2004). In our study we had to expose the cavity in order to obtain the cells and hence could visually assess whether the compound remained in solution locally. In contrast in some other studies, such as Hanus *et al.* (1999), HU-308 (dissolved in 18:1:1 of saline: ethanol: emulfor) was administered i.p. in a model of formalin-induced pain and the readout was the number of licks of the formalin-injected paw over an hour period. It is therefore possible that a proportion of HU-308 precipitated out of solution in the peritoneum during the experiment and this was not detected due to the different location of the readout. Conversely cyclodextrins have also been used in *in vivo* studies with cannabinoids (Mauler *et al.*, 2002; Valenzano *et al.*, 2005), where for example GW-405833 dissolved in HP-β-cyclodextrin reduced CFA-induced inflammatory pain with an E_{max} of 1 mg/kg (Valenzano *et al.*, 2005). Unlike SigmaSolve and DextrinSolve, the suitability of Tocrisolve^{TM} 100 as a solvent could not be accurately assessed due to its colour consistency and additionally its droplet formulation made counting of peritoneal cells challenging. Studies, such as Hoyer *et al*. (2011), used JWH-133 pre-dissolved in Tocrisolve^{TM} 100 (available from Tocris Bioscience) in atherosclerosis studies where the readout was atherosclerotic lesion size and is not affected by the solvent consistency. Overall, for our studies in acute inflammation HP-β-cyclodextrin was a suitable, well tolerated solvent and allowed us to successfully investigate the *in vivo* effect of effects of various cannabinoid ligands.

In inflammatory diseases such as atherosclerosis, activation of CB2R has been reported to reduce atherosclerotic lesion size and decrease macrophage lesion content (Hoyer *et al.*, 2011; Steffens *et al.*, 2005). In accordance with these studies, DIAS2 administered in either SigmaSolve or DextrinSolve inhibited monocyte recruitment in zymosan-induced peritonitis (Figure 4.4C and Figure 4.9C respectively), while having no effect on neutrophils when administered in DextrinSolve (Figure 4.9B). Unlike monocytes and macrophages which express CB2R (Montecucco *et al.*, 2008; Raborn *et al.*, 2008), neutrophils express negligible levels of CB2R with no reports of changes in neutrophil function following cannabinoid treatment (Chouinard *et al.*, 2011; Kraft *et al.*, 2005) and therefore a direct effect on neutrophils could be excluded. DIAS2 in SigmaSolve increased neutrophil number while simultaneously decreasing monocyte numbers (Figure 4.4). This increase in neutrophils could be explained as frustrated phagocytosis of the precipitated compound. Only one report exists for assessing the immunological role of cannabinoid ligands in a mouse model of acute inflammation. In this report, female mice were simultaneously injected with thioglycollate (i.p.) and the CB1R/CB2R agonist WIN-55212 (subcutaneously). Four hours later the peritoneal cavity was lavaged and the peritoneal exudates were assessed (Smith *et al.*, 2001). In this report, the authors demonstrated a decrease in neutrophil numbers and no effect on monocyte numbers in the WIN-55212-treated mice compared to solvent-treated mice. However in this model monocyte recruitment is minimal by four hours (Henderson *et al.*, 2003) and WIN-55212 has a high liver microsomal clearance of 1130 µl/min/mg of protein (Richmond *et al.*, 2010). It is therefore possible that there was insufficient WIN-55212 availability for modulation of the subsequent influx of

monocytes. On the other hand, WIN-55212's effect on neutrophils could be due to a receptor other than CB2R since this compound has been reported to also exert non-CB1R/CB2R effects (Curran *et al.*, 2005; Mestre *et al.*, 2006). Moreover, compared to Smith et al. (2001) who used female mice, we have used male mice which mount a greater response to a peritoneal inflammatory stimulus compared to female mice (Scotland *et al.*, 2011) and hence modulation of monocyte numbers could be better observed. Overall our *in vivo* data clearly demonstrate that our lead CB2R agonist DIAS2 is biologically active when given therapeutically in model of acute inflammation by reducing monocyte numbers by 50%.

From the same class of CB2R agonists as DIAS2, SAR1 and SAR3 (as shown at Table 3.1, EC_{50} at human CB2R are 10,000, 33 and 110 nM respectively for SAR1, SAR3 and DIAS2) were also tested *in vivo*. As shown in Figure 4.12C, DIAS2 and to a smaller extent SAR3 significantly inhibited monocyte recruitment while SAR1 had no effect. *In vivo* differences in efficacy between DIAS2 and SAR3 could reflect differences in metabolism (other than liver microsomes, data of Table 4.1) or that DIAS2 is more potent than SAR3 at the murine CB2R. Surprisingly the well-validated selective CB2R agonist JWH-133 had no effect on monocyte numbers (Figure 4.12C), while its only identified effect was a small increase in pDC numbers (Figure 4.13C). The difference in biological activity between the two CB2R agonists, JWH-133 and DIAS2, may be due to several reasons. The microsomal half-life of JWH-133 has not been reported therefore if JWH-133 is of higher metabolic clearance than DIAS2, its concentration in the peritoneal cavity may therefore not have been high enough to observe an effect on the influx of monocytes. Alternatively there are a few

reports of “biased agonism”, also termed as receptor-based “functional selectivity” in the CB2R literature (Shoemaker *et al.*, 2005; Urban *et al.*, 2007). “Biased agonism” refers to the a phenomenon where activation of the same receptor by two different ligands can elicit different signalling transduction pathways, which in turn could lead to a different biological response. Since both DIAS2 and JWH-133 reduced cAMP production in primary macrophages (Figure 3.14), differences in other signalling pathways could be responsible for the observed differences in modulating monocyte recruitment. This subject will be further investigated in experiments presented in Chapter 5.

Notably 1 and 5 mg of DIAS2 consistently decreased total cell count in the peritoneal cavity by two million cells compared to zymosan/solvent treated mice (Figure 4.9 and Figure 4.12). Other drugs with anti-inflammatory action, such as dexamethasone have also been shown to decrease total cell counts in zymosan-induced arthritis (Griffiths *et al.*, 1991). The magnitude of DIAS2-induced decrease in total cell numbers cannot be solely accounted by reduction of monocyte numbers and it is not due to modulation of neutrophil, B-cells or pDCs numbers. Thus DIAS2 could possibly modulate the numbers of other peritoneal cells not studied in this thesis, such as mast cells and T-cells.

The mechanism by which CB2R activation by DIAS2 and SAR3 mediates monocyte recruitment is currently not clear. DIAS2 and SAR3 had no effect on monocyte-recruiting chemokines, JE and MIP-1α (Figure 4.14 A and B). Additionally, TNF-α

levels could not be detected (Figure 4.14D). Surprisingly DIAS2 and SAR3 increased KC levels at six hours zymosan-induced peritonitis (Figure 4.14C). The increase of KC levels I observed in this time point could reflect a delay in the peak of KC levels, as observed in the WIN-55212-treated mice by Smith *et al*. (2001) in the thioglycollate model of acute inflammation. To date known functions of KC (mouse homolog of IL-8) include neutrophil recruitment (Kobayashi, 2008; Zhang *et al.*, 2001), enhancement of monocyte adhesion to inflamed endothelium (Huo *et al.*, 2001) and recovery of endothelial cells after arterial injury (Liehn *et al.*, 2004). Therefore there could be a yet unknown modulating function of KC on monocyte extravasation or alternatively the effect on KC levels could be a side product of a different immunomodulating process since it has been reported that 2-AG and CP-55940 increase IL-8 levels in HL-60 cells via CB2R (Jbilo *et al.*, 1999; Kishimoto *et al.*, 2004). In a report by Ajuebor *et al.* (1998b) it has been demonstrated that in zymosan-induced peritonitis absence of nitric oxide synthase (the enzyme responsible for NO production) led to an earlier peak of KC levels while having no effect on the levels of MIP-1α and JE. Since this could translate to an increase of NO levels leading to a delayed peak of KC levels, a potential explanation could be that DIAS2 and SAR3 modulated monocyte recruitment by increasing NO levels. However as shown in Figure 4.15B, DIAS2 and SAR3 had no effect on peritoneal NO levels. On the whole, only the increased levels of KC correlated with the reduction of monocyte numbers by DIAS2 and SAR3.

In vitro experiments were performed to assess whether PECs chemotaxis to chemokines could be modified by cannabinoids even if only the levels of KC were

increased by DIAS2 *in vivo*. Chemotaxis of PECs to MIP-1α was not altered by either DIAS2 or JWH-133, while only JWH-133 inhibited PECs chemotaxis to 5 nM, but not 0.5 nM, JE by 50% (Figure 4.16A and C). Montecucco *et al.* (2008) demonstrated that 18 hour pre-incubation of human monocytes with 10 μM JWH-015 (same class as JWH-133) could inhibit chemotaxis to 10 nM JE or MIP-1α by approximately 80%. In our experiments, albeit with shorter pre-incubation (three hours instead of eighteen) and murine macrophages instead of human monocytes, we could only reproduce the inhibition of PECs chemotaxis to JE but not MIP-1α. Regarding the effect on MIP-1α, the differences between our studies and Montecucco *et al*. (2008) could be due to different coupling of the CB2R in human and murine cells, or alternatively differences in CB2R coupling in macrophages compared to monocytes. Thus far, no other studies have comprehensively investigated cannabinoid regulation of monocyte/macrophage chemotaxis to JE and MIP-1α. Concerning monocyte/macrophage chemotaxis to RANTES only one report exists, where macrophage chemotaxis to 0.15 nM RANTES is completely abrogated by pre-incubating the cells for three hours (at 4^{o}C) with CP-55940 and Δ9-THC but not solvent (Raborn *et al.*, 2008). Similar to their observed effect, DIAS2 inhibited by 40% macrophage chemotaxis to 0.5 nM RANTES (Figure 4.16B). Similar to the observed difference between DIAS2 and JWH-133 in modulating monocyte numbers (Figure 4.12C), DIAS2 and JWH-133 did not have similar inhibition effects on PECs' chemotaxis to JE and RANTES (Figure 4.16B and C) indicating again to "biased agonism" at CB2R. Finally, although the *in vitro* data suggest that DIAS2 could exert its effect by inhibiting macrophage chemotaxis to low doses of RANTES, RANTES levels were not assessed in the *in vivo* supernatants since it has been shown that at

10 µg zymosan RANTES levels are not up-regulated compared to PBS (Cash *et al.*, 2009) and due to limited sample volume.

Interestingly blocking JE in the zymosan-induced peritonitis only reduces monocyte/macrophage recruitment at 16 hours by 40% (Ajuebor *et al.*, 1998a). Additionally using JE knockout mice in zymosan-induced peritonitis there was approximately 40% reduction in the number of macrophages compared to WT mice 24 hours after zymosan administration, partly due to a compensatory increase of the MCP-3 levels (Takahashi *et al.*, 2009). It is therefore possible that other chemokines apart from JE and MIP-1α are important and non-redundant for monocyte recruitment in zymosan-induced peritonitis, such as MCP-3 and MIP-2. In turn, DIAS2 and SAR3 mode of action could be the reduction of the levels of such unstudied chemokines in order to reduce monocyte recruitment.

4.3.2 Limitations for this study

One of the limitations of the studies presented in this chapter is the metabolism of the compounds (Table 4.1, DIAS2 clearance was 30 µl/min/mg), which could limit the active treatment window to approximately two hours. SAR studies may potentially identify key functional groups with DIAS2 scaffold that are resistant to hepatic metabolism and maintain CB2R activity and selectivity. On the other hand, rimonabant which had a clearance of 200 µl/min/mg in mouse liver microsomes (Richmond *et al.*, 2010), reached Phase II clinical trials where 20 mg/daily dose was more effective than placebo and 5 mg/daily on meeting the primary endpoint of

significant reduction in body weight (Van Gaal *et al.*, 2005). Therefore depending on the endpoint high microsomal clearance could be bypassed by moderately increasing the dose.

A second limitation of this study is the lack of CB2R knockout mice to confirm that the effects of DIAS2 and SAR3 are indeed mediated only via the CB2R receptor. Although CB2R antagonists are commercially available the kinetics of administration of a third intraperitoneal treatment within a six hour window treatment is experimentally challenging and would increase the variability within samples. The CB2R knockout mice have now been ordered but they will not available for testing prior to December 2012. Also other routes of administration apart from intraperitoneal injection could be explored including oral and subcutaneous administration to investigate compound availability via these routes.

A final limitation in this study was the number of analytes (chemokines and cytokines) tested in the supernatants. All the data obtained were from individual ELISA assays. Alternatively Luminex assays are available were up to thirty six selected analytes could be simultaneously tested in each sample. However these assays could not be performed at this stage due to high cost per sample and the limited number of samples that could be tested per kit. However it would have been interesting to investigate the levels of other chemokines, such as MIP-2, MCP-3 and RANTES, as well as other cytokines such as IL-10.

If time had permitted it would have been interesting to test DIAS2 in other models of inflammation including pain and atherosclerosis models. In future experiments it would be interesting to test a wider range of validated CB2R agonists including GW-405833 in the zymosan-induced peritonitis model, since a compound from the same class (GW842166X) reached Phase II clinical trials (Ostenfeld *et al.*, 2011).

4.4 Summary

In this chapter we demonstrated that two compounds from our novel class of CB2R agonists significantly decreased monocyte recruitment by 50% in zymosan-induced peritonitis with no effect on neutrophils. This decrease in monocyte numbers was associated with increased KC levels while the levels of JE, MIP-1α and NO were unchanged. JWH-133, a commercial CB2R agonist, had no effect on monocyte number and we hypothesise this difference in biological activity reflects "biased agonism" at CB2R. We believe further studies characterising the mode of action of DIAS2 are warranted as there are very few current drugs that specifically decrease inflammatory monocyte recruitment. DIAS2 and its derivatives could find application in treatment of inflammatory disease such as atherosclerosis which is characterised by monocyte recruitment with if any neutrophils being present in atherosclerotic plaques. In Chapter 5, further *in vitro* studies on macrophages will be performed with DIAS2 and JWH-133 to investigate the mechanism of action of immunomodulation by DIAS2 and investigate the hypothesis of "biased agonism" at the CB2R.

CHAPTER 5 : Differential activity by CB2R agonists in murine macrophages

5.1 Introduction

In this chapter several CB2R agonists from distinct chemical classes will be tested for their ability to initiate signalling responses and chemotaxis in primary murine macrophages, separate of their ability to inhibit cAMP production demonstrated in Figure 3.14. Actions via the cannabinoid CB2R on primary monocytes/macrophages are confounding, especially since most reports have tested only one class of CB2R agonists throughout their experiments. For example the ability of CB2R agonists to chemoattract these cells is inconsistent, 10 μM JWH-133 has been shown to be chemoattract human monocytes (Montecucco *et al.*, 2008), while up to 1 μM CP-55940 was not only devoid of chemotactic ability but also reduced spontaneous chemotactic activity of rat macrophages (Sacerdote *et al.*, 2000). Importantly in both of the mentioned studies 1 μM of the CB2R antagonist SR 144528 was able to inhibit both JWH-133 and CP-55940 responses, indicating the involvement of CB2R. Such effects via CB2R could suggest bi-phasic effects of CB2R agonists on chemotaxis or the ability of structurally different CB2R to induce distinct signalling responses, a receptor phenomenon known as functional selectivity. Further studies indicating functional selectivity at CB2R will be detailed further in the introduction of this chapter, supporting our interpretation for differential *in vivo* responses on monocyte recruitment between JWH-133 and DIAS2 found in Figure 4.12

5.1.1 Definition and examples of functional selectivity

Functional selectivity, also known as biased agonism, is a receptor phenomenon where different agonists can induce distinct signalling responses via the same receptor in the same cell type (Mailman, 2007; Urban *et al.*, 2007). It is proposed that functional selectivity occurs due to the stabilisation of different conformational shapes by ligands with different functional groups, which in turn could vary the efficacy of recruitment or activation of different effector systems (Galandrin *et al.*, 2007). Thus different receptor conformations can act as switches for the recruitment of signalling effector systems including G-protein dependent and independent signalling, as well as desensitization and endocytosis pathways. A classic example of functional selectivity is activation of the β2 adrenergic receptor by the partial agonists dopamine and salbutamol, versus the full agonists norepinephrine and epinephrine. These different classes of agonists, with the presence of distinct functional groups, have been experimentally shown to stabilise distinct re-arrangements of the transmembrane helixes of the receptor (Swaminath *et al.*, 2005). It has also been demonstrated that structurally distinct ligands of the β2 adrenergic receptor have strikingly different capacities on modulation of AC-mediated cAMP production, MAPK activation and β-arrestin recruitment and these functional effects were not correlated to the compound's strength of binding to the receptor (Drake *et al.*, 2008; Galandrin *et al.*, 2006). It is clear that receptor pharmacology is more complex than previously envisaged, with a ligand's efficacy having to be assessed in additional signalling pathways other than AC modulation and affinity for the receptor.

Remarkably functional selectivity is not only a phenomenon occurring at complex seven-transmembrane GPCRs but has also been reported for dimeric tyrosine kinase receptors. For example binding of the epidermal growth factor (EGF)-receptor homodimers by EGF and transforming growth factor (TGF)-α induces distinct but subtle conformational changes only in subdomain II, which however are adequate to elicit distinct activation of signalling pathways in collaboration with different ECM components, leading to ligand–mediated phenotypically-similar fibroblast migration (Ellis *et al.*, 2007; Wilson *et al.*, 2009). Functional selectivity is therefore a highly fine-tuned process in which even minor changes in the receptor structures could be translated into alternative signalling pathways.

Despite the increasing number of *in vitro* experiments demonstrating functional selectivity at several receptors (DeWire *et al.*, 2011; Kenakin *et al.*, 2010), the therapeutic benefit of drugs demonstrating biased agonism has not yet been demonstrated in clinical trials. However there is one recent *in vivo* study demonstrating physiological differences between equal dosage of two δ-opioid receptor agonists with similar affinity and analgesic properties, but high (compound SNC80) or low (compound ARM390) capacity to induce receptor internalisation (Pradhan *et al.*, 2010). In this study, acute administration of SNC80 induced receptor internalisation and concurrently induced behavioural desensitisation to a second SNC80 dose (12 hours later) in CFA-induced pain in mice. Moreover within 24 hours, SNC80-treated mice were again responsive to the analgesic effects of second dose of SNC80. Conversely mice were responsive to analgesic effects of a second dose of ARM390 administered 12 or 24 hours after the first dose. In fact 5-day daily

dosage of SNC80 greatly down-regulated receptor expression and receptor coupling to G-proteins compared to vehicle-treated animals, thus inducing generalised tolerance to further opiate doses (Pradhan *et al.*, 2010). On the other hand in the same 5-day treatment regime, in the ARM390-treated mice the receptor expression and G-protein coupling were unaltered while only the receptor coupling to voltage-dependent Ca^{2+} channels was affected, thus inducing analgesic tolerance. Therefore evidence from this study suggests that biased agonism towards a signalling pathway could have a physiological significance *in vivo* which in turn could be harnessed for treatment with greater efficacy and/or fewer adverse effects.

5.1.2 Evidence for functional selectivity at the CB2R

Functional selectivity at the CB2R has only been addressed recently since most studies were demonstrating effects with one or two cannabinoid ligands, especially regarding monocytes/macrophages activation (Correa *et al.*, 2005; Montecucco *et al.*, 2008; Steffens *et al.*, 2012). A study by Shoemaker *et al.* (2005) was the first to demonstrate that in CHO-cells overexpressing human CB2R, 2-AG was more potent at inducing ERK1/2 phosphorylation (ED_{50} = 12.4 nM) and required higher doses to induce AC inhibition (ED_{50} = 238 nM). Conversely CP-55940 was more potent at inducing AC inhibition (ED_{50} = 0.4 nM) and required higher doses to induce ERK1/2 phosphorylation (ED_{50} = 2.6 nM). Recently a study by Atwood *et al.* (2012b) has shown evidence for functional selectivity at CB2R using HEK-cells overexpressing rat CB2R. In this study it was demonstrated that cell stimulation with CP-55940, WIN-55212, 2-AG, JWH-133, THC and 2-AG, but not AM-1241, was able to induce

ERK1/2 phosphorylation (120-130% from basal) (Atwood *et al.*, 2012b). From the seven CB2R ligands studied in this paper, only JWH-133 and CP-55940 induced significant receptor internalisation and β-arrestin recruitment. On the whole these two published studies demonstrate evidence for functional selectivity at CB2R *in vitro* in transfected cell lines. To date the effect of CB2R activation on inhibiting macrophage chemotaxis to chemokines has been mainly studied *in vitro* using only one cannabinoid treatment of CP-55940, Δ9-THC or JWH-133 (Correa *et al.*, 2005; Raborn *et al.*, 2008; Steffens *et al.*, 2005), while the ability of individual CB2R agonists to chemoattract monocyte/macrophages is inconsistent as previously mentioned (Montecucco *et al*., 2008; Sacerdote *et al.*, 2000) in the introduction of this chapter. Currently no published study has extended the functional selectivity observation from cells overexpressing the receptor to primary cells with physiological levels of the receptor. Additionally at present the testing of several CB2R agonists within the same experimental setting in primary macrophages for consistency has not been performed.

5.1.3 Rationale

In Chapter 4, we demonstrated that DIAS2 significantly inhibited monocyte recruitment in zymosan-induced peritonitis while JWH-133 had no effect. We hypothesised that this difference in function between JWH-133 and DIAS2 could be due to stabilisation of the CB2R receptor in different conformation states, which in turn activate distinct signalling pathways and hence have a different functional output. Since functional selectivity at CB2R has not been investigated in primary

cells, we decided to investigate functional selectivity in the cell of interest, the primary murine macrophage. To assess potential differential signalling, we investigated several signalling readouts including ERK1/2 and Akt phosphorylation, as well as β-arrestin recruitment and primary macrophage chemotaxis.

5.1.4 Experimental aims of this chapter

- Assess chemotaxis of murine PECs and human monocytes to CB2R agonists JWH-133 and DIAS2
- Evaluate recruitment of β-arrestin by JWH-133, DIAS2 and other SAR compounds
- Investigate different signalling pathways activated in macrophages treated with cannabinoids

Where possible, experiments were performed with primary murine macrophages as a better model for assessing the differences in anti-inflammatory effects between DIAS2 and JWH-133, seen in the *in vivo experiments* of Chapter 4. Moreover we wanted to use a cell type with physiological levels of CB2R expression and physiological coupling.

5.2 Results

5.2.1 mRNA expression of cannabinoid receptors on primary macrophages

In order to confirm the expression of cannabinoid receptors on macrophages, we first investigated the presence of CB1R, CB2R and GPR55 mRNA in BMDM and Biogel-elicited macrophages. Initially the primers were validated by resolving the RT-PCR product from BMDM samples on an agarose gel and confirming the presence of only one product (shown by bands) and of the correct size (Figure 5.1). Real-time PCR was then used with the same primers, this time for Biogel-elicited macrophages since it is a more precise assay, with higher sensitivity and can discriminate smaller differences in copies' numbers. In Real-time PCR mRNA products are shown by amplification curves in the course of 40 cycles. The greater the number of mRNA copies, the smaller the number of PCR cycles needed to obtain an amplification curve. Melting curves were checked to confirm for a second time, that only one peak and thus only product was amplified with the set of primers (data not shown). The housekeeping gene GAPDH was highly expressed in BMDM (Figure 5.1A) shown by the strength of the band, and in the Biogel-elicited macrophages (Figure 5.1B) shown by the amplification of the product starting from 15 PCR cycles. CB2R mRNA was shown to be expressed on both BMDM (Figure 5.1A), albeit the band's intensity was weaker than the GAPDH band; and in Biogel-elicited macrophages (Figure 5.1B) since the product amplified from 22 cycles. On the other hand, CB1R mRNA was not detected in BMDM (Figure 5.1A) since no band was shown and it was not present in Biogel-elicited macrophages (Figure 5.1B) since no product was amplified within 40

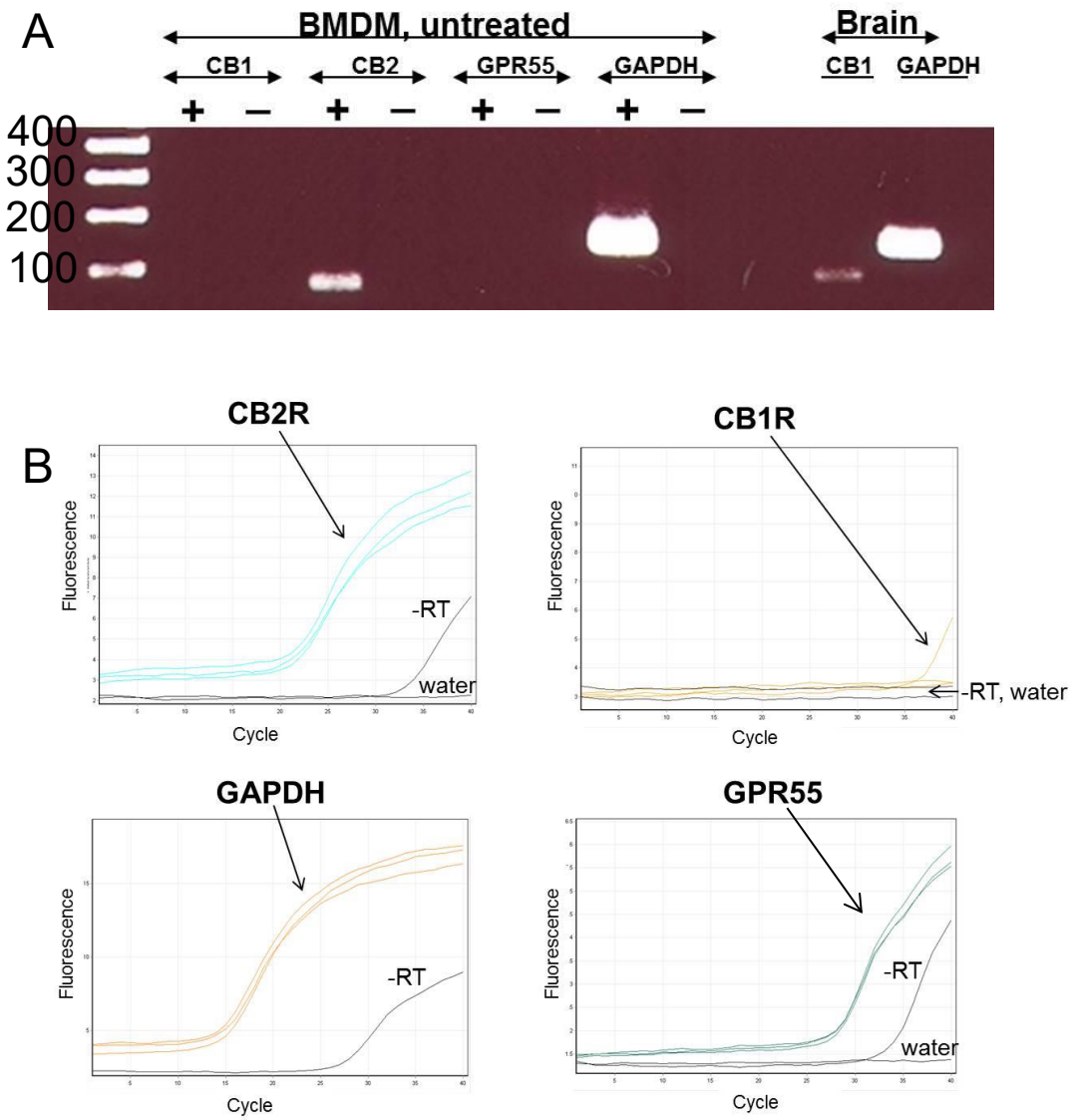

Figure 5.1: CB2R mRNA is expressed on macrophages
Primers for GAPDH, CB1R, CB2R and GPR55 were validated by reverse transcriptase reaction on mRNA samples from untreated bone-marrow derived macrophages (BMDM) resolved in agarose gel. Real time-PCR was then used to test for receptor expression on untreated Biogel-elicited macrophages. Representative traces are shown from 3 independent experiments, 3 biological replicates per RealTime-PCR experiment.

cycles. However CB1R primers were able to detect CB1R mRNA when present, and thus we were able to detected CB1R mRNA in the mouse brain cDNA (Figure 5.1A). Moreover although GPR55 was not detected in BMDM (Figure 5.1A), weak expression of GPR55 mRNA was observed in Biogel-elicited macrophages (Figure 5.1B), although it was close to –RT negative control (reflects presence of genomic DNA rather cDNA from mRNA). Nonetheless, from the cannabinoid receptors tested only CB2R mRNA was present at sufficiently high levels.

5.2.2 Cytotoxicity assays with cannabinoid agonists on primary macrophages

Cytotoxicity assays were performed to assess whether any of the cannabinoid ligands to be used in future assays were cytotoxic to Biogel-elicited macrophages. Biogel-elicited macrophages were cultured in a 96-well plate in chemotaxis buffer and treatments were added for 5 hours. The cells were then washed with chemotaxis buffer and CTG was added to assess ATP production from the cells, which is correlated to cell number/survival. Of the four cannabinoid ligands tested only HU-308 induced 25% cell death within 5 hours, whereas JWH-133, DIAS2, 2-AG and the CB2R antagonist (SR 144528) were not cytotoxic within 5 hours of treatment (Figure 5.2).

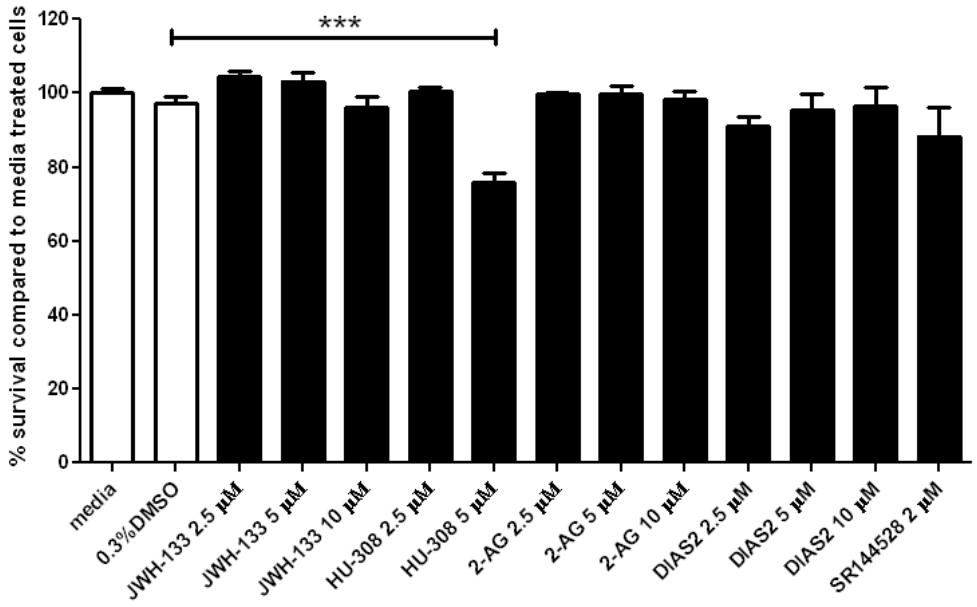

Figure 5.2: Cytotoxicity studies performed with cannabinoid ligands
Biogel-elicited PECs were added in a 96-well plate in chemotaxis buffer, cells were allowed to adhere for 90 minutes prior to washing with warm PBS. The cells were rested for 2 hours prior to removal of medium and addition of treatment for 5 hours. After 5 hours, the treatments were aspirated and the wells were washed twice with chemotaxis media before addition of CTG. Following 2 minute shaking and 10 minute equilibration the luminescence signal was read using a luminometer. Cell survival was normalised to media-treated cells (100%). Pooled data from 2-3 independent experiments, error bars=SEM. One-way ANOVA and Dunnett's post-hoc test against solvent treated cells, ***P<0.001.

5.2.3 Induction of PECs chemotaxis by CB2R agonists

The ability of selective CB2R agonists (HU-308, JWH-133 and DIAS2) to induce Biogel-elicited PECs' chemotaxis was tested in a 96-well modified Boyden chamber (8 μm pore). The chemokine MIP-1α was used as a positive control for chemotaxis (Figure 5.3A). It was observed that JWH-133 dose-dependently induced PECs' chemotaxis (Figure 5.3 B & C) and the chemotaxis was CB2R-dependent since it could be inhibited by 1 μM of the CB2R antagonist SR 144528 (Figure 5.3D). HU-308 significantly induced PECs' chemotaxis at the 2.5 μM dose (Figure 5.3B) but it did not induce significant chemotaxis at the moderately cytotoxic dose of 5 μM. DIAS2 was not chemotactic to PECs at 2.5-10 μM doses (Figure 5.3C).

5.2.4 Assessing homologous desensitization at murine CB2R

Since DIAS2 was not chemotactic for murine PECs in our experiments, it was then assessed whether DIAS2 could at least desensitize CB2R, thus making the receptor unavailable to JWH-133 induced chemotactic responses as in Figure 5.3 it was clearly demonstrated that JWH-133 induced macrophage chemotaxis via CB2R. As shown in Figure 5.4, JWH-133 pre-treatment significantly desensitised the CB2R to a second dose of JWH-133, which was thus unable to induce significant PECs' chemotaxis (Figure 5.4). Interestingly DIAS2 pre-treatment had a non-significant trend on inhibiting JWH-133-induced PECs' chemotaxis.

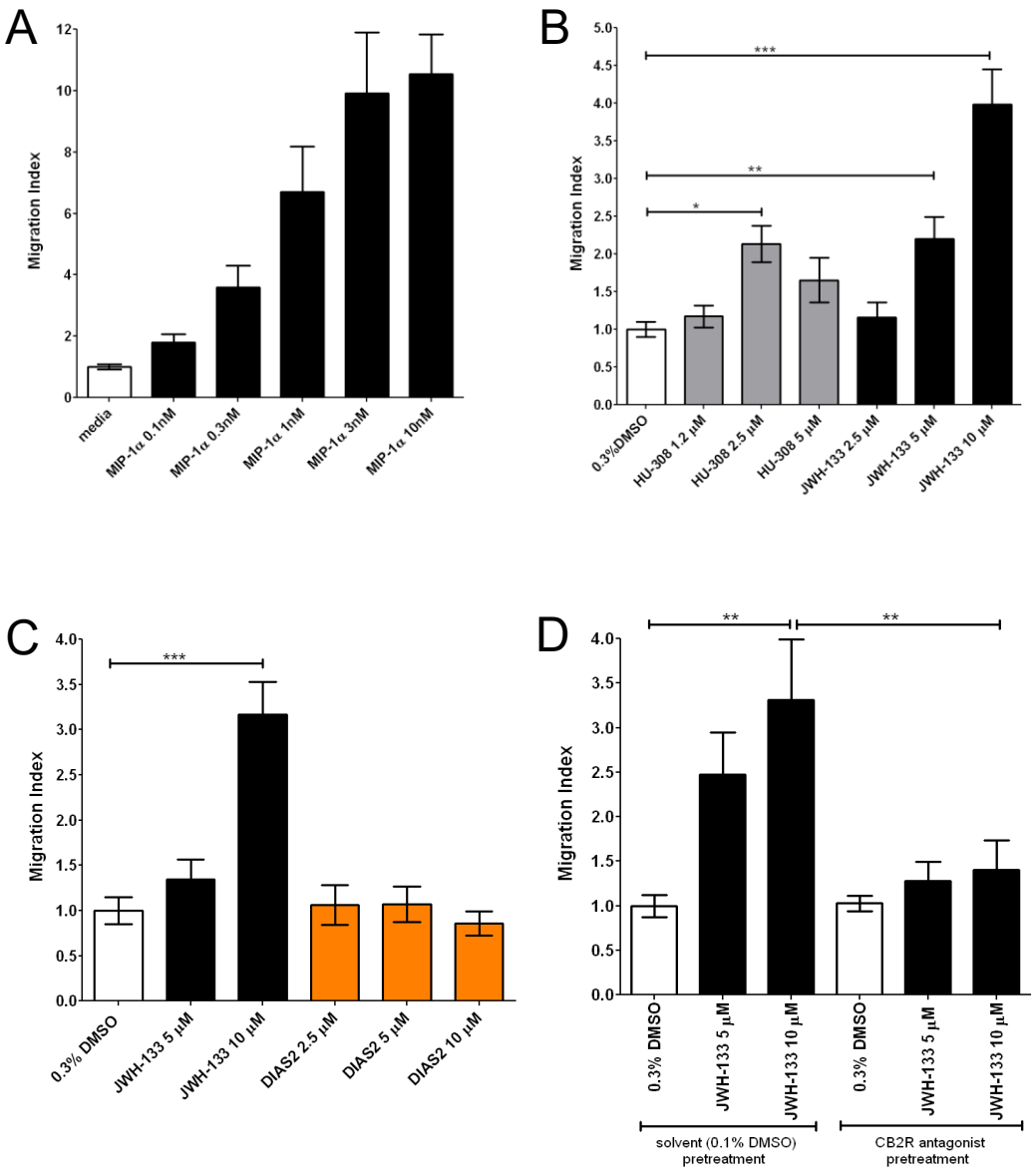

Figure 5.3: Induction of PECs chemotaxis by CB2R agonists and MIP-1α
400,000 Biogel-elicited PECs were added in a modified Boyden chamber with 8 μm pore membrane and allowed to migrate towards solvent (0.3% DMSO for cannabinoids or media for chemokine) or treatment for 4 hours at 37°C, 5% CO_2. In the CB2R antagonist studies, the cells were pre-treated with 1 μM SR144528 or solvent for 30 minutes. Chemotaxis was assessed four hours later by counting DAPI-stained nuclei on the filters. Pooled data from 3 independent experiments, error bars=SEM. One-way ANOVA and Dunnett's post-hoc test against solvent treated cells, ***P<0.001, **P<0.01, *P<0.05

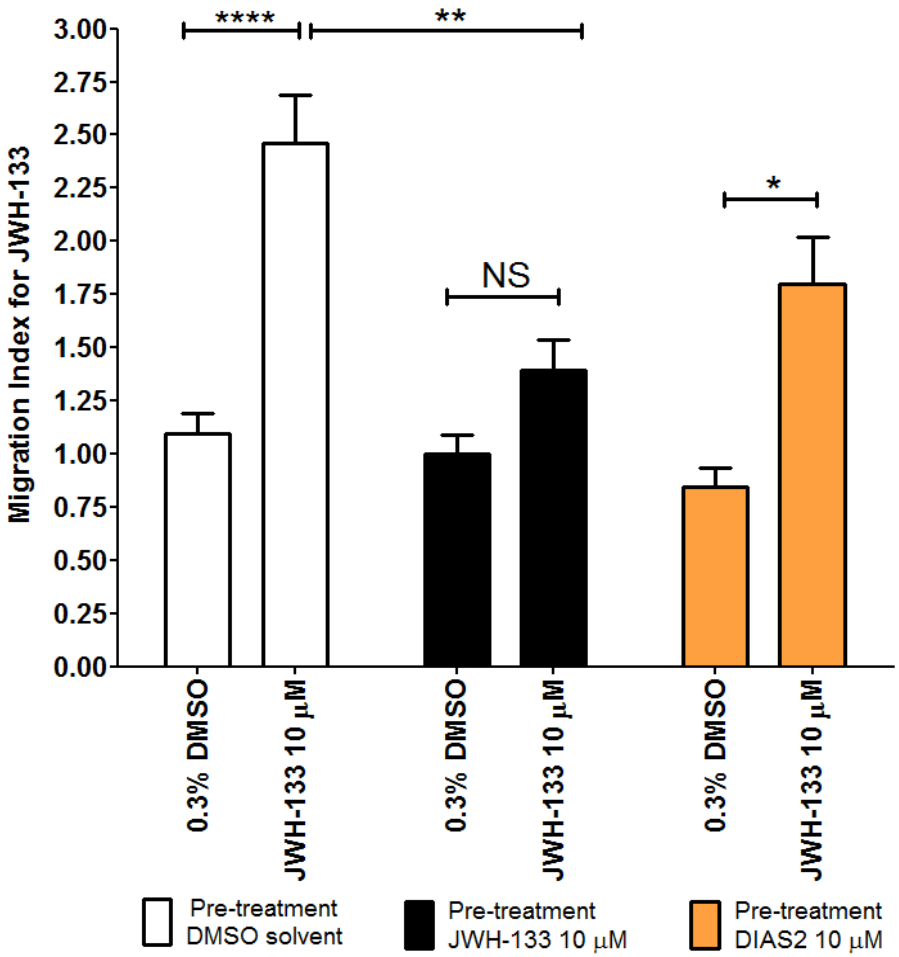

Figure 5.4: Assessing homologous desensitization at CB2R in PECs Biogel-elicited PECs were incubated with JWH-133, DIAS2 or solvent (0.1 % DMSO) for 3 hours at 37°C, 5 % CO_2. Then 400,000 PECs were added in a modified Boyden chamber with 8 µm pore membrane and allowed to migrate to solvent (0.3% DMSO) or 10 µM JWH-133 for 3 hours at 37°C, 5% CO_2. Chemotaxis was assessed three hours later by counting DAPI-stained nuclei on the filters. Pooled data from 3 independent experiments, error bars=SEM. Two-way ANOVA and Bonferroni multiple comparison test against solvent treated cells, ***P<0.001, **P<0.01, *P<0.05

5.2.5 Induction of human monocyte chemotaxis by CB2R agonists

As DIAS2 and the other members of the novel family of CB2R agonists described in Chapter 3 were screened in cells over-expressing the human CB2R, it was possible that DIAS2 might be more potent in cells of human origin, for example WIN-55212 has been shown to have an EC_{50} of 11 and 330 nM in cAMP assays with human and rat CB2R respectively (Mukherjee *et al.*, 2004). It was previously demonstrated by Montecucco *et al.* (2008) that JWH-133 induced chemotaxis in human monocytes in a CB2R-dependent manner. For this reason, human monocytes isolated from leukocyte cones using CD14 positive selection were used in a 5μm pore modified Boyden chamber 96-well assay. In this assay MCP-1 was used a positive chemotactic control (Figure 5.5). It was observed that 10 μM JWH-133 significantly induced chemotaxis in human monocytes, while DIAS2 was not chemotactic in a range of doses (Figure 5.5).

5.2.6 Recruitment of β-arrestin by JWH-133

Since the difference in chemotactic capacity between DIAS2 and JWH-133 observed in murine PECs was reproduced in human monocytes, the effect could not be explained by species differences. For this reason, the possibility of differences in signalling pathways was explored. To begin with, in CHO-K1 cells with mCB2R JWH-133, HU-308 and 2-AG were at least 3-fold more efficacious on recruiting β-arrestin (EC_{50} of 94 nM, 81 nM and 10 μM respectively) than full CB2R agonists SAR3 and SAR6 (DIAS2) (EC_{50} values of 44 and 99 nM respectively) (Figure 5.6).

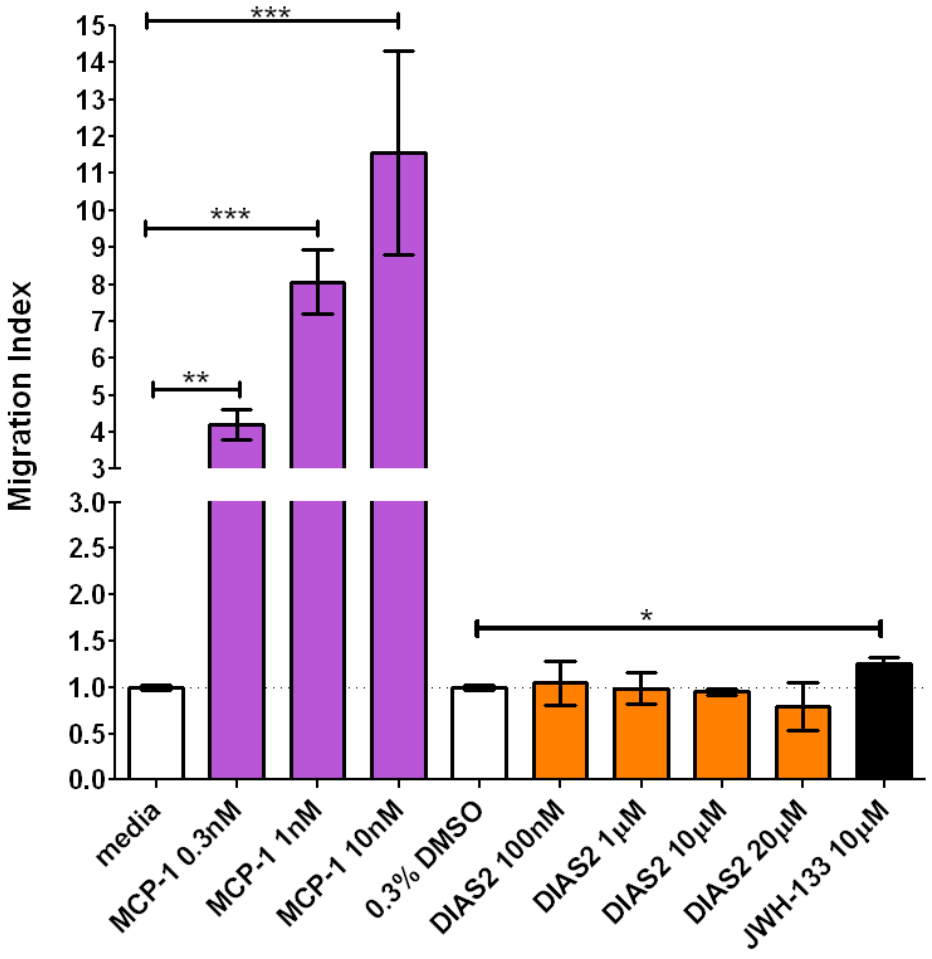

Figure 5.5: Induction of human monocyte chemotaxis by CB2R agonists and MIP-1α

Human monocytes isolated by CD14 positive selection were then added in a modified Boyden chamber with 5 µm pore membrane and allowed to migrate to solvent (0.3% DMSO) or 10 µM JWH-133 for 2 hours at 37^{o}C, 5% CO_2. Chemotaxis was assessed two hours later by CTG. Pooled data from 3 independent experiments, error bars=SEM. One-way ANOVA and Dunnett's posthoc test against solvent treated cells, ***P<0.001, **P<0.01, *P<0.05

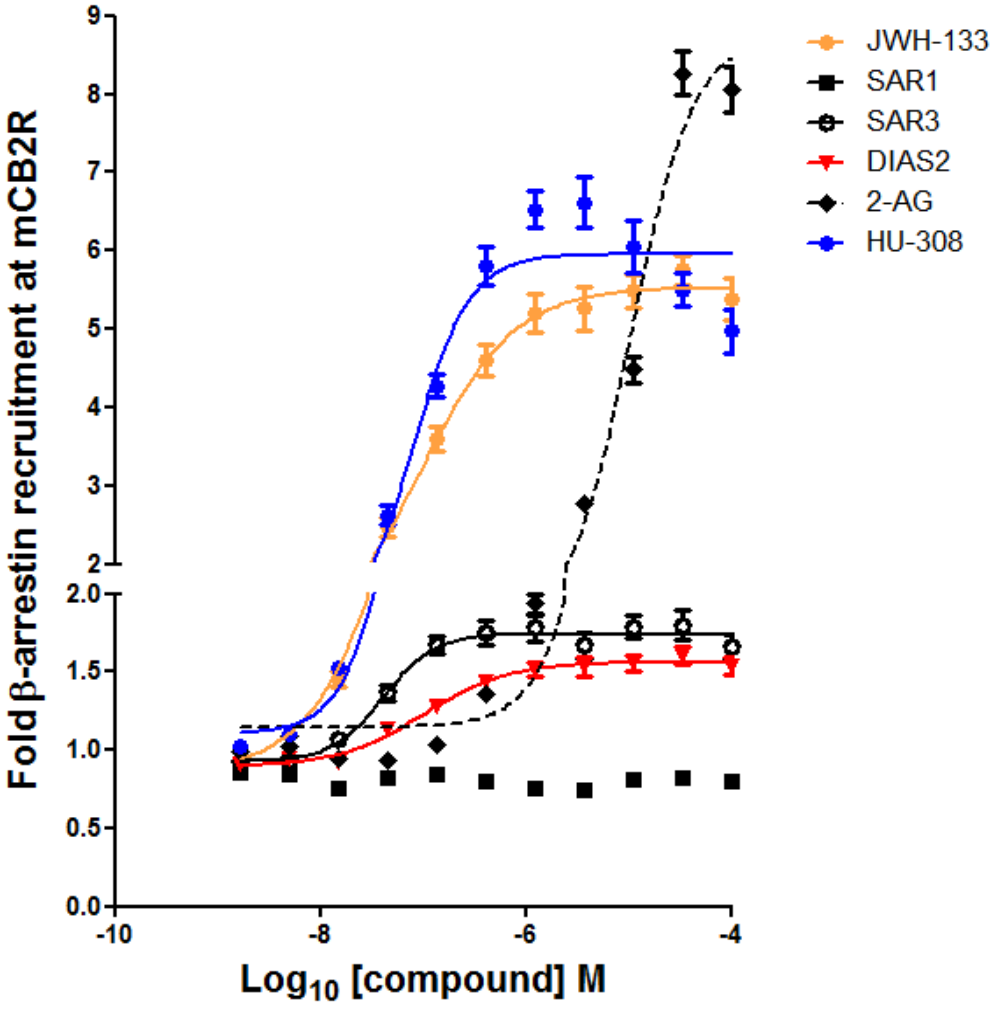

Figure 5.6: Recruitment of β-arrestin at mCB2R after JWH-133 and SAR compounds

CHO-K1 mCB2R β-arrestin2 cells (DiscoveRx) were stimulated with compounds or solvent (0.5% DMSO) for 90 minutes as in Figure 3.2. Data are expressed as the ratio (fold β-arrestin recruitment) of compound treated cells over solvent. Data shown are from 4 independent experiments, error bars = SEM.

On the other, the partial agonist SAR1 failed to recruit β-arrestin at mCB2R (Figure 5.6).

5.2.7 Differential phosphorylation of ERK1/2 by JWH-133 and DIAS2 in primary macrophages

Differences in signalling pathways were further explored in murine Biogel-elicited macrophages. The dose selected for cannabinoid treatment was 10 μM since JWH-133 induced macrophage chemotaxis (Figure 5.3) and inhibition of cAMP production (Figure 3.14) in primary macrophages with this dose. In these experiments, JWH-133 (10 μM) time-dependently induced ERK1/2 phosphorylation by 30 minutes compared to solvent (0.3 % DMSO) (Figure 5.7A). On the other hand, DIAS2 (10 μM) did not induce ERK1/2 phosphorylation at all (Figure 5.7B). Equal loading was ensured in all blots by stripping the membrane and re-blotting with total ERK2.

To extend the observation on the induction of ERK1/2 phosphorylation, the effect of treatment of several cannabinoid ligands was explored at 5 and 30 minutes. As shown in Figure 5.8A none of the ligands induced ERK1/2 phosphorylation at 5 minutes. However 10 μM JWH-133 and HU-308 was capable of inducing ERK1/2 phosphorylation at 30 minutes while DIAS2 and 2-AG had no effect (Figure 5.8B).

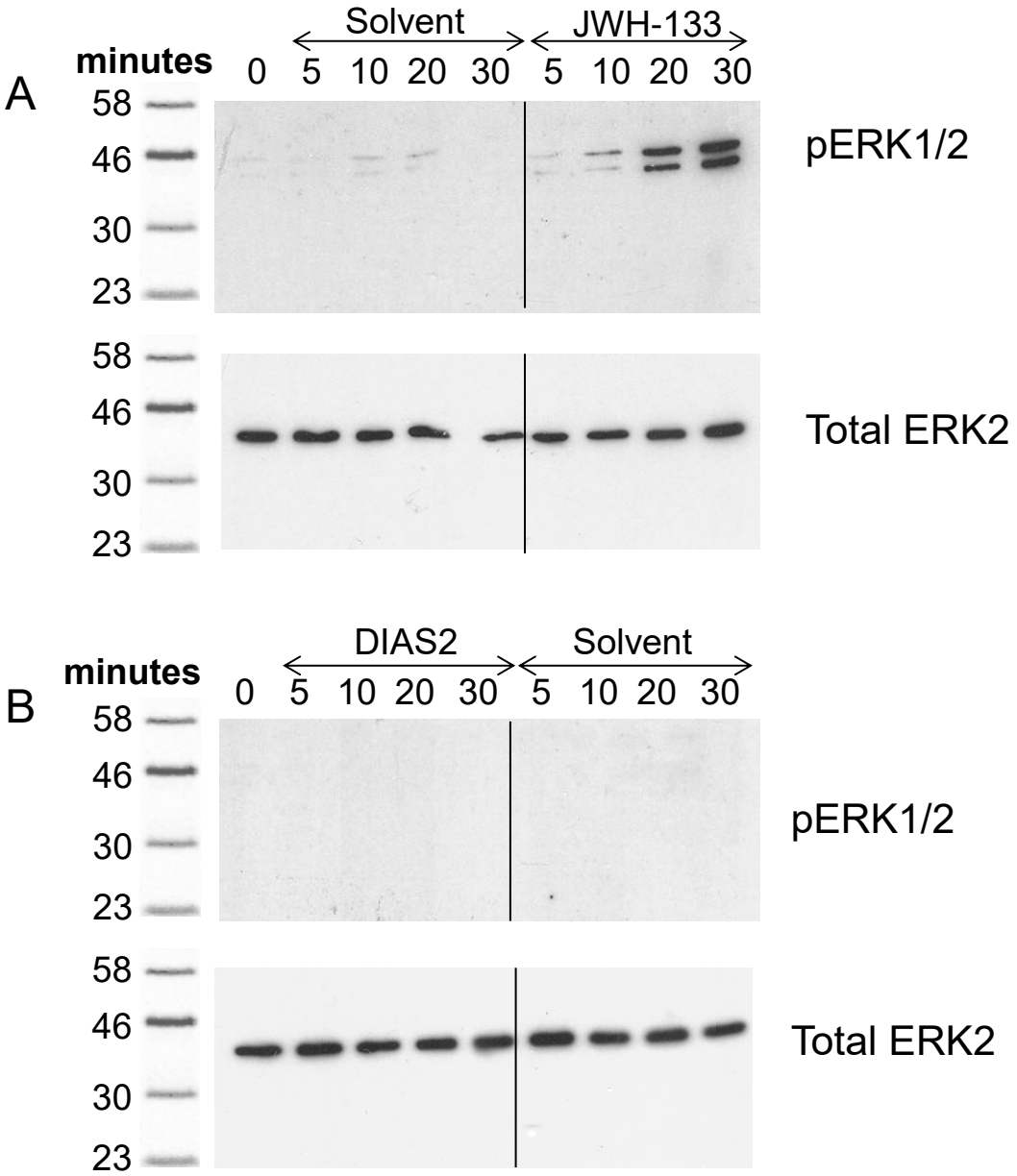

Figure 5.7: Phosphorylation of ERK1/2 by CB2R agonists JWH-133 and DIAS2 on primary murine macrophages

In 6-well plates, Biogel-elicited PECs were plated at 2 million cells/well for 1 hour in chemotaxis buffer at 37^{o}C, 5 % CO_2. Non-adherent cells were removed by washing with warm PBS. The cells were then rested for 2-3 hours and 1 hour before stimulation, the media was replaced (1 ml/well). The macrophages were then stimulated with CB2R agonists or solvent (0.3% DMSO) for the indicated amount of time. Representative blots of 3 independent experiments are shown.

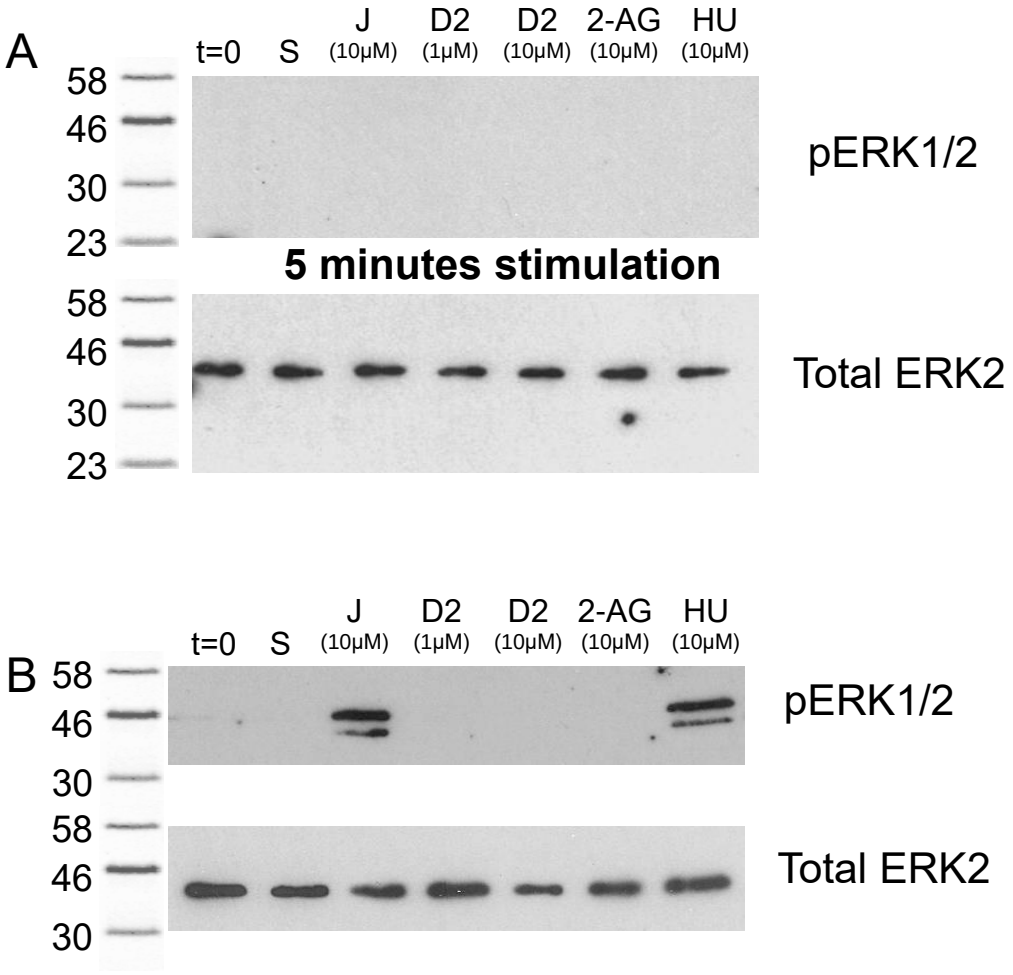

Figure 5.8: Phosphorylation of ERK1/2 by several cannabinoid receptor agonists on primary murine macrophages
Biogel-elicited macrophages were stimulated as in Figure 5.6. with solvent (S, 0.3 % DMSO) or cannabinoid ligands JWH-133 (J), DIAS2 (D2), 2-AG and HU-308 (HU) at the indicated doses for 5 or 30 minutes. Blots shown are representative from 3-4 independent experiments.

5.2.8 Analysis of CB2R agonists signalling using a phosphoarray

A phosphokinase array (R&D) with multiple kinases targets was then used to investigate if further signalling differences exist between JWH-133 and DIAS2 when activating the CB2R receptor on murine Biogel-elicited macrophages. Based on results of experiments in Figure 5.8, we chose the following treatments and time points. Lysates of Biogel-elicited macrophages treated with solvent (0.3% DMSO), JWH-133 or DIAS2 for 20 minutes were created as in the other WB studies. 330 μg of lysate was then loaded per membrane and manufacturer's instructions were followed. Although no loading control was incorporated in the membrane, positive detection controls where included in each membrane at the top and bottom left-hand corner. Following film development, bands' intensity was analysed using by densitometry using ImageJ and the effect of the treatments (JWH-133 and DIAS2) was normalised against the solvent. Remarkably the phosphorylation of JWH-133 was strikingly different from DIAS2 (blots shown in Figure 5.9). Analysis of the phosphorylation targets affected by JWH-133 and DIAS2 is shown in Table 5.1A and B. A common up-regulated phosphorylation target by DIAS2 and JWH-133 was haemopoietic cell kinase (Hck). Unfortunately R&D only commercially sells an antibody for total Hck and not for detection of the phosphorylated protein at the site Y411. In addition no other company sells an antibody against that phosphorylation site of Hck. Consequently a second target from the array was chosen for validation.

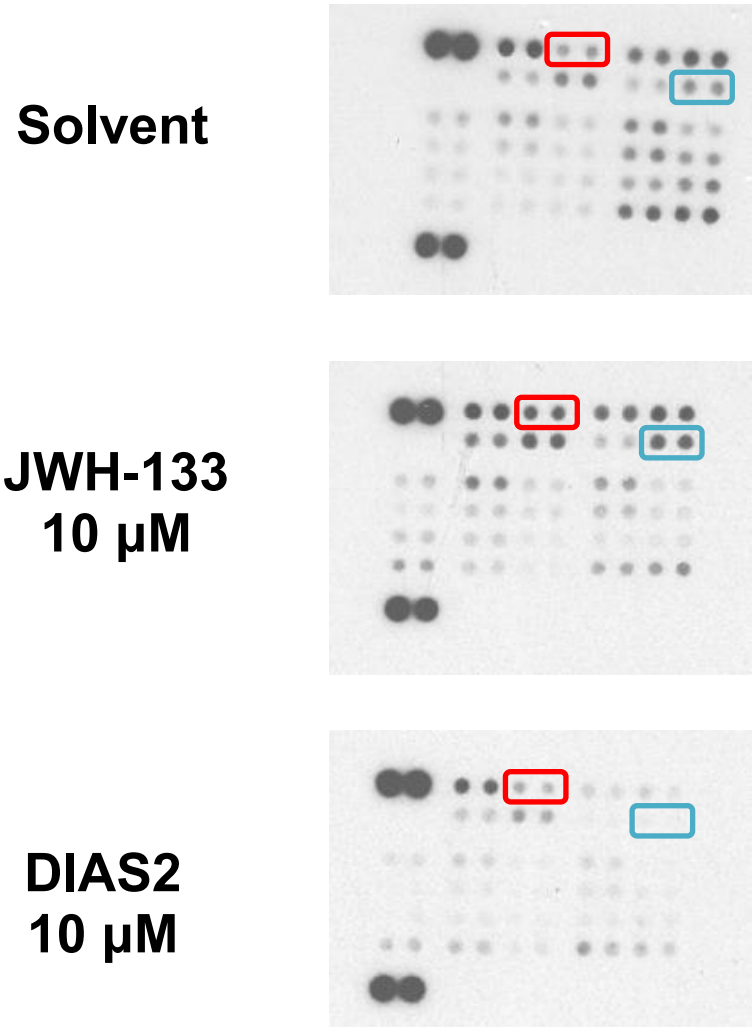

Figure 5.9: Assessment of phosphorylation profile of JWH-133 and DIAS2 on primary murine macrophages
Biogel-elicited macrophages were stimulated as in Figure 5.6. with solvent (0.3 % DMSO) or 10 µM of cannabinoid ligands JWH-133 and DIAS2 for 20 minutes. 330 µg of lysates (concentration found by BCA assay) were then analysed using a phospho-kinase array kit (R&D). Red box: ERK1/2 phosphorylation, Blue box: Akt phosphorylation. Blots shown are from one experiment, each target is represented in two technical replicates.

TARGET	Phosphorylation site	Fold induction JWH-133 10 µM	Fold induction DIAS2 10 µM
MEK 1/2	S218/S222, S222/S226	1.71	0.70
p38a	T180/Y182	1.06	0.89
ERK 1/2	T202/Y204, T185/Y187	1.66	0.70
JNK pan	T183/Y185, T221/Y223	1.10	0.26
GSK3 a/b	S21/S9	1.03	0.22
Akt	S473	1.64	0.18
Hsp27	S78/S82	0.99	0.45
MSK 1/2	S376/S360	1.27	0.65
AMPK-α1	T174	1.09	0.34
AMPK-α2	T172	0.79	0.27
B-catenin	-------	0.60	0.27
CREB	S133	1.31	0.42
Src	Y419	0.82	0.47
TOR	S2448	0.90	0.40

Table 5.1A: Analysis of phosphorylation of proteins by JWH-133 and DIAS2 on primary murine macrophages
Biogel-elicited macrophages were stimulated as in Figure 5.6. with solvent (0.3 % DMSO) or 10 µM of cannabinoid ligands JWH-133 and DIAS2 for 20 minutes. The lysates were then analysed using a phospho-kinase array kit (R&D). The bands' intensity was quantified using ImageJ. For each target, the band's intensity for the cannabinoid treatment was normalised to solvent to obtain fold induction.

TARGET	Phosphorylation site	Fold induction JWH-133 10 µM	Fold induction DIAS2 10 µM
STAT2	Y689	0.58	0.28
STAT3	Y705	0.32	0.27
STAT5a	Y694	0.36	0.26
STAT5b	Y699	0.28	0.20
STAT5 a/b	Y694/Y699	0.59	0.33
STAT6	Y641	0.54	0.53
Chk-2	T68	1.87	2.32
Fgr	Y412	0.75	0.63
Fyn	Y420	1.94	0.62
FAK	Y397	0.68	0.83
Hck	Y411	3.34	2.02
Lyn	Y397	0.99	0.45
Lck	Y394	1.14	0.57
Yes	Y426	2.04	0.91

Table 5.1B: Analysis of phosphorylation of proteins by JWH-133 and DIAS2 on primary murine macrophages
Biogel-elicited macrophages were stimulated as in Figure 5.6. with solvent (0.3 % DMSO) or 10 µM of cannabinoid ligands JWH-133 and DIAS2 for 20 minutes. The lysates were then analysed using a phospho-kinase array kit (R&D). The bands' intensity was quantified using the programme ImageJ. For each target, the band's intensity for the cannabinoid treatment was normalised to solvent to obtain fold induction.

5.2.9 Differential phosphorylation of Akt by CB2R agonists in primary macrophages

Akt was selected as a second target from the kinase array for validation due to its fundamental importance in cell signalling, survival and metabolism. As shown in Figure 5.10A only JWH-133 modestly increased Akt phosphorylation compared to solvent after 5 minutes stimulation of Biogel-elicited macrophages. Furthermore by 30 minutes JWH-133 has induced further and stronger Akt phosphorylation than solvent (Figure 5.10B). Interestingly although DIAS2 had no effect, HU-308 modestly increased Akt phosphorylation (Figure 5.10B, long exposure). 2-AG seemed to cause a slight decrease in Akt phosphorylation, however this data was not highly reproducible between independent experiments and further data has to be obtained in order to establish the effect of 2-AG on Akt phosphorylation.

5.3 Discussion

In this chapter we have presented *in vitro* evidence for functional selectivity at the mCB2R in primary macrophages since different CB2R agonists induce functionally distinct signalling pathways in macrophages. We have shown that non-cytotoxic doses of JWH-133 and HU-308 induce murine PECs' chemotaxis while DIAS2 has no effect. In addition DIAS2 could only partially desensitize CB2R for JWH-133 mediated chemotaxis. The difference in chemotactic capacity of JWH-133 versus DIAS2 was also observed in human monocytes, albeit with lower efficacy.

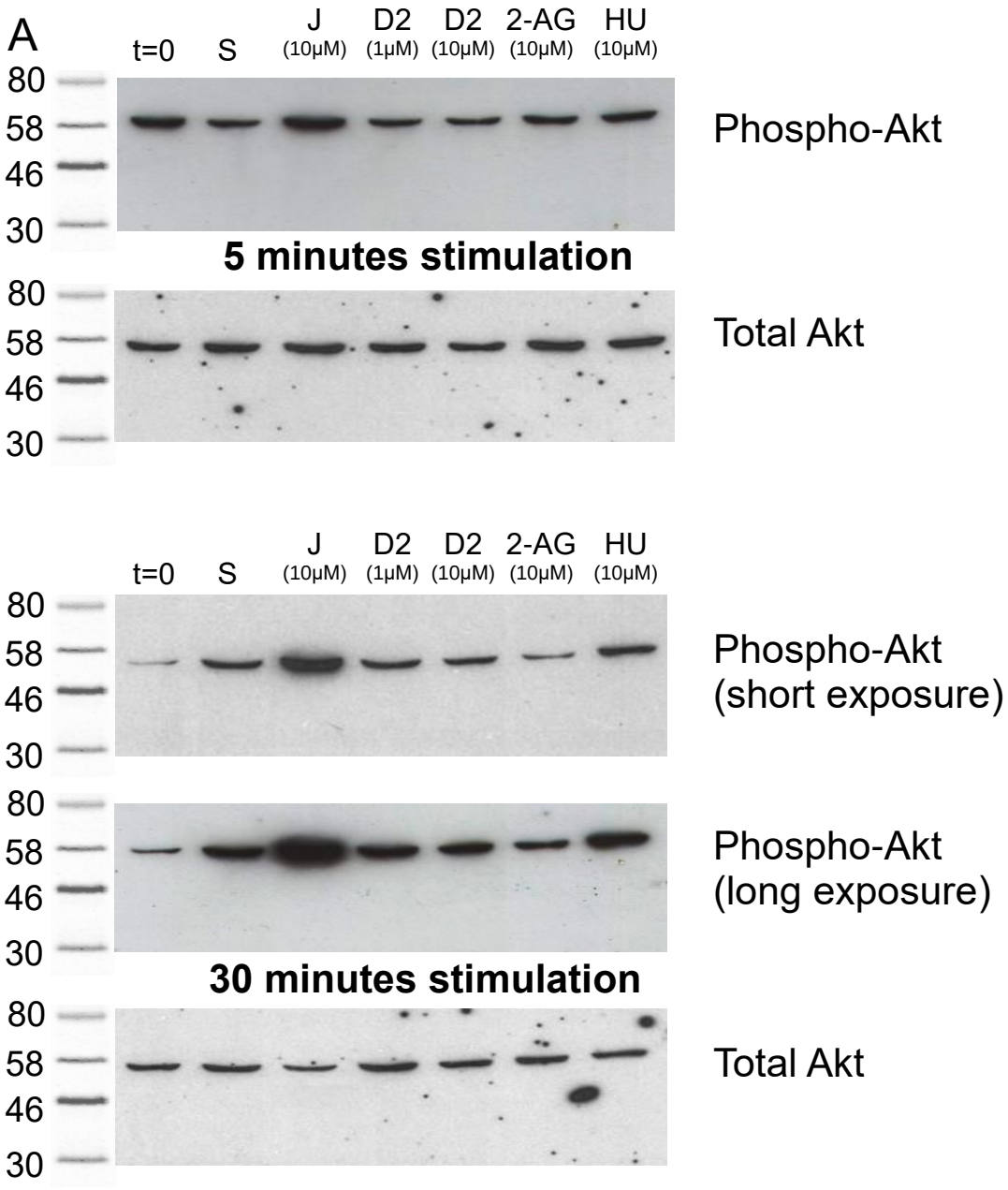

Figure 5.10: Phosphorylation of Akt by several cannabinoid receptor agonists on primary murine macrophages
Biogel-elicited macrophages were stimulated as in Figure 5.6. with solvent (S, 0.3 % DMSO) or cannabinoid ligands JWH-133 (J), DIAS2 (D2), 2-AG and HU-308 (HU) at the indicated doses for 5 or 30 minutes. Blots shown are representative of 3-4 independent experiments.

Interestingly JWH-133 and HU-308 were 3-fold more efficacious at recruiting β-arrestin to the murine CB2R than DIAS2 and SAR3. Moreover both HU-308 and JWH-133 induced ERK1/2 phosphorylation in primary murine macrophages. Remarkably in primary macrophages JWH-133 induced Akt phosphorylation by 5 minutes which intensified by 30 minutes while Akt phosphorylation by HU-308 was only evident by 30 minutes. Phosphorylation of Akt was not affected when macrophages were treated with DIAS2 for 5 or 30 minutes.

In this chapter we demonstrated that macrophages, both bone-marrow derived and Biogel-elicited, express CB2R mRNA (Figure 5.1) and this finding was in line with the literature (Carlisle *et al.*, 2002; Galiegue *et al.*, 1995; Lee *et al.*, 2001). Additionally in the literature it has been reported that CB2R mRNA is also found in monocytes and thioglycollate-induced macrophages but not in resident macrophages (Galiegue *et al.*, 1995; Lee *et al.*, 2001). Therefore CB2R receptor mRNA expression by macrophages appears to be different depending on the cell origin. Once more in line with the literature (Carlisle *et al.*, 2002), CB1R mRNA was not detected in either BMDM or Biogel-elicited macrophages but was detected in a brain cDNA sample (Figure 5.1A & B). Weak expression of GPR55 mRNA was found in Biogel-elicited macrophages (Figure 5.1B) and in related studies low level mRNA expression GPR55 has only been reported so far in human monocytes and osteoclasts (Whyte *et al.*, 2009). Overall from the cannabinoid and cannabinoid-related receptors surveyed, only CB2R mRNA was detected at sufficiently high levels suggesting that the observed effects of cannabinoid treatments on Biogel-elicited macrophages are most likely due to CB2R activation.

5.3.1 Differential modulation of chemotaxis by CB2R agonists

In our chemotaxis studies with Biogel-elicited PECs we observed that JWH-133 and non-cytotoxic doses of HU-308 could induce PECs chemotaxis, while DIAS2 had no effect. Moreover the JWH-133-induced chemotaxis was inhibited by a well validated CB2R antagonist, indicating it was CB2R dependent (Figure 5.3). Only two studies in the literature have directly addressed *in vitro* the effect of cannabinoids on monocyte/macrophage chemotaxis. In a study using the promyelocytic cell line (monocyte-like cell line) HL-60 and human monocytes, it was shown that only the endocannabinoid ligand 2-AG, but not CP-55940 or AEA, was chemotactic in a CB2R-dependent manner (Kishimoto *et al.*, 2003). A second study by Montecucco *et al.* (2008), which only used JWH-133 (and its structurally similar JWH-015), demonstrated that JWH-133 was chemotactic for human monocytes. Therefore our studies not only extended this observation into primary murine macrophages but also by using three different selective CB2R agonists we demonstrated that not all CB2R agonists could induce chemotaxis in macrophages (Figure 5.2). These differences in chemotaxis were the first indication suggesting functional selectivity at the CB2R.

5.3.2 Homologous desensitisation of CB2R

Receptor desensitization can be induced by several mechanisms, including β-arrestins and protein kinases A (PKA) and C (PKC) (Chuang *et al.*, 1996; Hausdorff *et al.*, 1990; Liu *et al.*, 2001). The term homologous desensitization refers to receptor activation by a ligand leading to subsequent recruitment of G-protein coupled receptor kinases and then β-arrestins at the receptor's C-terminus, which in turn targets the receptor for recycling or degradation and hence making only the receptor

unavailable for further immediate signalling responses (Chuang *et al.*, 1996). Therefore our findings could be explained by efficient recruitment of β-arrestin by JWH-133 (Figure 3.2 and Figure 5.6), which desensitized the receptor to further chemotactic responses (Figure 5.4). In contrast, DIAS2 was at least 3-fold less efficacious than JWH-133 and HU-308 in recruiting β-arrestin (Figure 5.6) and this could explain the inability of DIAS2 pre-treatment to significantly desensitise the receptor to subsequent JWH-133-elicited responses (Figure 5.4). In previous β-arrestin recruitment assays I also demonstrated that JWH-133 was more potent than HU-308, 2-AG, Δ9-THC on recruiting β-arrestin at mCB2R (Figure 3.2). At those first experiments HU-308 was not potent as JWH-133 at recruiting β-arrestin, but improved compound handling and warming the aliquot prior use significantly contributed to obtain HU-308 in solution.

Overall CB2R could be more profoundly desensitized by JWH-133 and HU-308 via β-arrestin-2 than DIAS2 as tested in this thesis, and it is therefore possible that effects elicited via these two CB2R agonists could be short-lived if the receptor is promptly targeted for degradation or is slowly recycled following internalisation. Although only the recruitment of β-arrestin-2 has been linked so far with CB2R (Atwood *et al.*, 2012b; Franklin *et al.*, 2012), it is possible that the other tested CB2R ligands, that weakly recruit β-arrestin-2, are more efficient on recruiting other β-arrestin isoforms in order to terminate receptor signalling (β-arrestin-1 and 3). Alternatively, DIAS2 and the other CB2R ligands could activate other desensitisation pathways in conjunction with β-arrestin, as indeed it has been reported for the μ-opioid receptor via protein kinase activation (Kelly *et al.*, 2008) and the angiotensin II type 1 receptor via Rab

GTPases (Esseltine *et al.*, 2011). Overall, the observed differences in β-arrestin recruitment and desensitisation between DIAS2 and JWH-133 provide experimental support for the hypothesis for functional selectivity at CB2R.

5.3.3 Induction of different signalling pathways in primary macrophages: evidence for functional selectivity at CB2R?

In this chapter we have also investigated different signalling pathways stimulated by several CB2R agonists. Interestingly JWH-133 time-dependently increased ERK1/2 phosphorylation (Figures 5.7 and Figure 5.8) and this was replicated by HU-308, while DIAS2 and 2-AG had no effect on ERK1/2 phosphorylation. In the literature ERK1/2 phosphorylation has been linked both to G-protein dependent and independent pathways such as β-arrestin (Luttrell, 2003; Luttrell *et al.*, 2002; Rajagopal *et al.*, 2010) depending on the receptor and the cell type. Of the compounds tested both JWH-133 and HU-308 potently recruited β-arrestin and induced ERK1/2 phosphorylation, then it possible that ERK1/2 phosphorylation observed with these agonists is β-arrestin-dependent in primary macrophages.

On the other hand, phosphorylation of Akt by CB2R agonists appears to be complex. Since both JWH-133 and HU-308 induce Akt phosphorylation, albeit with different kinetics (Figure 5.10), and Akt phosphorylation has been demonstrated to be crucially involved in chemokine-induced chemotaxis in leukocytes (Heit *et al.*, 2002; Zhang *et al.*, 2009), it is possible that Akt phosphorylation is involved in HU-308 and JWH-133 mediated chemotaxis (Figure 5.3). On the other hand, 2-AG appeared to decrease Akt phosphorylation in primary macrophages (Figure 5.10) while in a second

experiment it did not affect Akt phosphorylation. Further data are needed to assess 2-AG effect further but in support of our preliminary findings, one study has demonstrated that ox-LDL-induced down-regulation of Akt phosphorylation was more prominent in WT than CB2R knockout macrophages, thus *endogenous* CB2R activation was involved in inhibition of Akt phosphorylation (Freeman-Anderson *et al.*, 2008). However it is possible that the effect observed could be due to a metabolic product of 2-AG exerting a response through a different receptor as it has been reported in neutrophils (Chouinard *et al.*, 2011). Moreover DIAS2 did not appear to modulate Akt phosphorylation at 5 or 30 minutes (Figure 5.10), despite the result of the phosphoarray indicating that DIAS2 treatment for 20 minutes decreased Akt phosphorylation compared to solvent (Table 5.1A). In summary CB2R activation can modulate Akt phosphorylation depending on the CB2R ligand and the tested CB2R agonists differ in their potency and kinetics on eliciting this response.

5.3.4 Limitations

During the course of this DPhil study we tested two commercial polyclonal CB2R antibodies (from Abcam and Cayman Chemical) in flow cytometry for detection of the receptor. However with neither of them CB2R could be detected in Biogel-elicited macrophages or human monocytes (data not shown), especially after taking into account non-specific binding. As a result we were unable to demonstrate CB2R pattern expression on Biogel-elicited macrophages and human monocytes and I was unable to perform further experiments on receptor recycling/degradation as I propose above.

Due to time constraints we did not have time to test in more independent experiments the effect of 2-AG on Akt phosphorylation in time for this thesis. We also did not have the opportunity to use CB2R antagonists in our signalling assays to confirm that ERK1/2 and Akt phosphorylation by the CB2R agonists was via the CB2R. Moreover if time permitted we would have used Akt and ERK inhibitors to assess the contributions of these signalling cascades to JWH-133 and HU-308 chemotaxis, instead of speculating on their contribution. Also the β-arrestin recruitment assays used in this thesis were performed using CHO-K1 cells with overexpressed mCB2R. It is possible that coupling of the receptor to β-arrestin could be different on different cell types and in systems with more physiological levels of the receptor.

Additionally the 10 μM dose of HU-308 used for signalling studies (up to 30 minutes) is higher than the highest dose used for chemotaxis assays (5 μM) due to the moderate cytotoxicity of the compound for the 4 hour duration of the assay. Moreover all the observations in the phosphorylation of ERK1/2 and Akt are limited to one dose of each agonist and two time-points. It is possible that if DIAS2 was less potent than JWH-133 and HU-308 at inducing Akt phosphorylation, higher doses may have been needed to elicit this response. Again due to time constraints we were not able to test any of the SAR compounds with high affinity and selectivity at the CB2R that we identified in Chapter 3.

5.4 Summary

In this chapter we have presented experimental evidence that structurally distinct CB2R agonists have differential effects on signalling responses and chemotaxis, supporting the hypothesis for functional selectivity at the CB2R in murine primary macrophages. We have demonstrated that only JWH-133 and HU-308 could elicit PECs' chemotaxis while DIAS2 had no effect. JWH-133 and HU-308 activation of murine CB2R also recruited β-arrestin-2 and induced the phosphorylation of both ERK1/2 and Akt in primary macrophages. Conversely treatment of macrophages with DIAS2 did not induce phosphorylation of either ERK1/2 or Akt, similarly treatment with 2-AG did not induced phosphorylation of ERK1/2. These novel data obtained with primary cells provide evidence for functional selectivity at CB2R especially with regard to chemotaxis, β-arrestin recruitment and phosphorylation of ERK1/2 and Akt.

CHAPTER 6 : Final discussion and future directions

At the start of this thesis it had been recently demonstrated that activation of CB2R could inhibit progression of atherosclerosis and reduce chronic inflammatory pain (Cheng *et al.*, 2007; Steffens *et al.*, 2005). The exact mechanism of action had not been elucidated fully and in fact it is still considered complex. Moreover a few classes of CB2R agonists were available at that time with variable degrees of selectivity against CB1R and high lipophilicity which made *in vivo* administration challenging.

6.1 Key findings of this thesis

Using ligand-based virtual screening with the highly CB2R selective HU-308 we discovered a novel class of CB2R agonists with a new chemical scaffold (Chapter 3). Notably members of this class and our current lead compound DIAS2 were shown to be highly selective at CB2R (at least 300-fold) over CB1R in cAMP assays and radioligand binding assays. DIAS2 and JWH-133 were biologically active since they inhibited cAMP production in primary macrophages (Figure 3.14). In Chapter 4 we showed that in the zymosan-induced peritonitis model that DIAS2 and the structurally-similar SAR3 inhibited monocyte recruitment while a commercial CB2R agonist (JWH-133) had no such effect. The reduction of monocyte recruitment was not associated with a reduction in the levels of MIP-1α or JE or NO. *In vitro* studies

on primary macrophages (reported in Chapter 5) we demonstrated that HU-308 and JWH-133 induced macrophage chemotaxis in a CB2R-dependent manner, while DIAS2 was not chemotactic. In our studies showed that only treatment with JWH-133 resulted to phosphorylation of ERK1/2, while 2-AG (an endogenous eCB ligand) and DIAS2 had no such effect. Additionally we demonstrated that both JWH-133 and HU-308 induced Akt phosphorylation while DIAS2 had no effect.

In the literature it has been assumed that the anti-inflammatory effects following administration of CB2R agonists in inflammatory disease models was due to modulation of monocyte/macrophage chemotaxis to other chemokines (Steffens *et al.*, 2005). It has been demonstrated that cannabinoid agonists such as CP-55940 and JWH-133 could inhibit the chemotaxis of monocytes/macrophages towards chemokines such as RANTES, JE and MIP-1α, via CB2R activation (Montecucco *et al.*, 2008; Raborn *et al.*, 2008). I investigated their observations using two doses of chemokines and either DIAS2 or JWH-133 (Figure 4.16) and weak or no effects were observed for JE and MIP-1α induced chemotaxis. However DIAS2 induced a more significant inhibition (~40%) of macrophage chemotaxis to a low dose of RANTES chemotaxis than JWH-133. Our findings suggest that modest modulation of CB2R agonists on macrophage chemotaxis could not account *alone* for the strong anti-inflammatory effect observed in our zymosan peritonitis studies and the atherosclerosis models (Hoyer *et al.*, 2011; Steffens *et al.*, 2005).

6.2 Can the inhibition of cAMP production by CB2R agonists account for inhibition of monocyte inhibition *in vivo*?

Enhancement of cAMP levels, for example by prostaglandin E2 or forskolin, has been shown to inhibit macrophage phagocytosis of pathogens and apoptotic cells and reduce bacterial killing (Aronoff *et al.*, 2004; Aronoff *et al.*, 2005; Chang *et al.*, 1984; Peters-Golden, 2009; Rossi *et al.*, 1998). For example the oral and systemic pathogen *Porphyromonas gingivalis* synergises with complement C5a to substantially raise cAMP levels in macrophages and hence inhibit macrophage function and prolong pathogen survival *in vitro* and *in vivo* (Wang et al., 2010). Moreover increased intracellular cAMP inhibits the NF-κB pathway thus down-regulating production of pro-inflammatory mediators, such as TNF-α and chemokines, while increasing IL-10 levels (Aronoff *et al.*, 2005; Delgado *et al.*, 2001; Wall *et al.*, 2009). In addition, modulation of cAMP levels is involved in the recruitment of leukocytes. Interestingly, in human monocytes the ability of chemokines (RANTES, MCP-1 and MIP-1α) to inhibit cAMP plays a more important role on their induction of chemotaxis than ERK1/2 and PI3K phosphorylation, whereas forskolin-induced increase of cAMP inhibited the chemokine-induced chemotaxis (Fine *et al.*, 2001).

Therefore inhibition of cAMP by CB2R agonists could enhance zymosan or apoptotic neutrophil phagocytosis by monocytes and thus promote resolution of inflammation by release of anti-inflammatory mediators such as TGF-β and lipoxins and resolvins (Fadok *et al.*, 1998; Maderna *et al.*, 2009b; Schwab *et al.*, 2007). A more extensive analysis of analytes with Luminex® and lipidomic techniques could identify if CB2R agonists like DIAS2 increase the production of pro-resolution mediators such as

lipoxins (Nathan *et al.*, 2010; Serhan *et al.*, 2005). In the time point used in these experiments both DIAS2 and JWH-133 inhibited cAMP production in primary macrophages (Figure 3.14) but had different *in vivo* effect (Figure 4.12). Further experiments could assess *in vitro* possible kinetic differences between DIAS2 and JWH-133 on inducing and possibly sustaining cAMP inhibition in primary macrophages. Identification of such differences in the macrophage's cAMP content could account for differences in functional output between DIAS2 and JWH-133.

6.3 Can alternative signalling pathways activated from CB2R agonists account for modulation of macrophage inflammatory responses?

In the experiments presented in Chapter 5 we have demonstrated that HU-308 and JWH-133 induced Akt phosphorylation and that both of these CB2R agonists were chemotactic to macrophages. In contrast DIAS2 did not induce Akt phosphorylation or macrophage chemotaxis. Montecucco *et al.*, (2008) has demonstrated that JWH-133, and the structurally similar JWH-015, could induce human monocyte chemotaxis in PI-3K/Akt and ERK1/2 dependent manner. Our findings, despite using murine macrophages, are in agreement with the findings of the above study. An obvious follow up experiment would be to see if pharmacological inhibition of Akt phosphorylation blocked murine macrophage chemotaxis to CB2R agonists.

The impact of ERK1/2 phosphorylation in macrophages has been linked with atherosclerosis progression. It has been demonstrated that ox-LDL can induce macrophage proliferation in an ERK1/2 dependent manner (Senokuchi *et al.*, 2004) and, in turn, inhibition of nuclear translocation of ERK1/2 by the antidiabetic agent troglitazone was able to inhibit ox-LDL induced macrophage proliferation (Yano *et al.*, 2007). Moreover ERK1/2 activation has been shown to reduce cholesterol efflux from the macrophages and thus promote the formation of foam cells (Zhou *et al.*, 2010). Therefore the induction of ERK1/2 phosphorylation in macrophages by JWH-133 may not account for inhibition of macrophage recruitment and reduction of atherosclerotic lesion size observed in the studies of Hoyer *et al.* (2011). However the increased foam cell formation resulting from ERK1/2 phosphorylation could instead counteract other anti-inflammatory actions of JWH-133, thus reducing the net anti-inflammatory effect.

The impact of Akt phosphorylation on macrophage regulation of inflammation is controversial. Studies have demonstrated that Akt activation was crucial for macrophage survival and hence prevention of the atherosclerotic plaque's progression to necrosis in ApoE knockout mice (Seimon *et al.*, 2009). In fact there are three isoforms of Akt: Akt1, Akt2 and Akt3. Akt1 ablation in ApoE knockout mice has been shown to increase macrophage and endothelial cell apoptosis and increase atherosclerotic lesion size (Fernandez-Hernando *et al.*, 2007). Akt3 is also atheroprotective but through prevention of modified ester uptake and reduced formation of foam cells (Ding *et al.*, 2012). However induction of macrophage apoptosis in early plaque has been shown to reduce disease progression while

induction of macrophage apoptosis in advanced lesions is thought to promote atherosclerosis due to triggering of monocyte recruitment (Gautier *et al.*, 2009). In addition activation of CB2R by endogenous ligands contributes to ox-LDL induced macrophage death due to inhibition of Akt phosphorylation (Freeman-Anderson *et al.*, 2008). Therefore depending on the stage of the atherosclerotic lesion modulation of Akt levels by CB2R agonists could be protective or detrimental.

In future experiments it would be interesting to stain for intracellular ERK1/2 and Akt phosphorylation in monocytes from cannabinoid treated mice in the peritonitis model in order to see whether this reflects the *in vitro* studies in this thesis. Also in the zymosan-induced peritonitis model CB2R knockout mice would have been employed to confirm the role of CB2R in the observed effect and different time points, including 1, 16 and 24 hours would be investigated to assess whether DIAS2 and JWH-133 differ at the duration or the kinetics of inhibiting monocyte recruitment. Finally it would be fascinating to perform experiments in ApoE knockout mice with DIAS2 along JWH-133 and investigate how functional selectivity at CB2R and differential activation of ERK1/2 and Akt can influence the reduction of lesion size and the recruitment of macrophages. Important technical hurdles with such studies would be dosing and pharmacokinetic/ pharmacodynamic studies.

6.4 Impact of this thesis findings on the field of inflammation biology

As mentioned in the introduction, Δ9-THC and JWH-133 administration in ApoE knockout mice reduced atherosclerotic lesion size by 30-40% (Hoyer *et al.*, 2011; Steffens *et al.*, 2005). Conversely administration of JWH-133 in LDLR knockout mice had no effect on atherosclerotic lesion size (Willecke *et al.*, 2011). However LDLR knockout mice develop faster and more advanced lesions than ApoE knockout mice (Ma et al., 2012), therefore a stronger anti-inflammatory effect than the JWH-133 induced response may be needed to observe a reduction in atherosclerosis lesion size in the LDLR knockout mice. Findings from the literature in combination with our peritonitis studies indicate that CB2R agonists could be used therapeutically in atherosclerosis. However our studies also raise the possibility that CB2R activation by structurally different CB2R agonists could influence the outcome or the magnitude of the observed effect on macrophages depending on the signalling downstream target (Figure 6.1).

Working hypothesis

Our working hypothesis for the mechanism by which the CB2R agonist DIAS2 inhibits monocyte recruitment in zymosan-induced peritonitis by a combination of inhibitory pathways on endothelial cells and recruited monocytes (Figure 6.2). According to data by Rajesh *et al.* (2007) the CB2R agonists JWH-133 and HU-308 down-regulated adhesion molecules ICAM-1 and VCAM-1 on endothelial cells, which resulted on reduced monocyte adhesion to the endothelium.

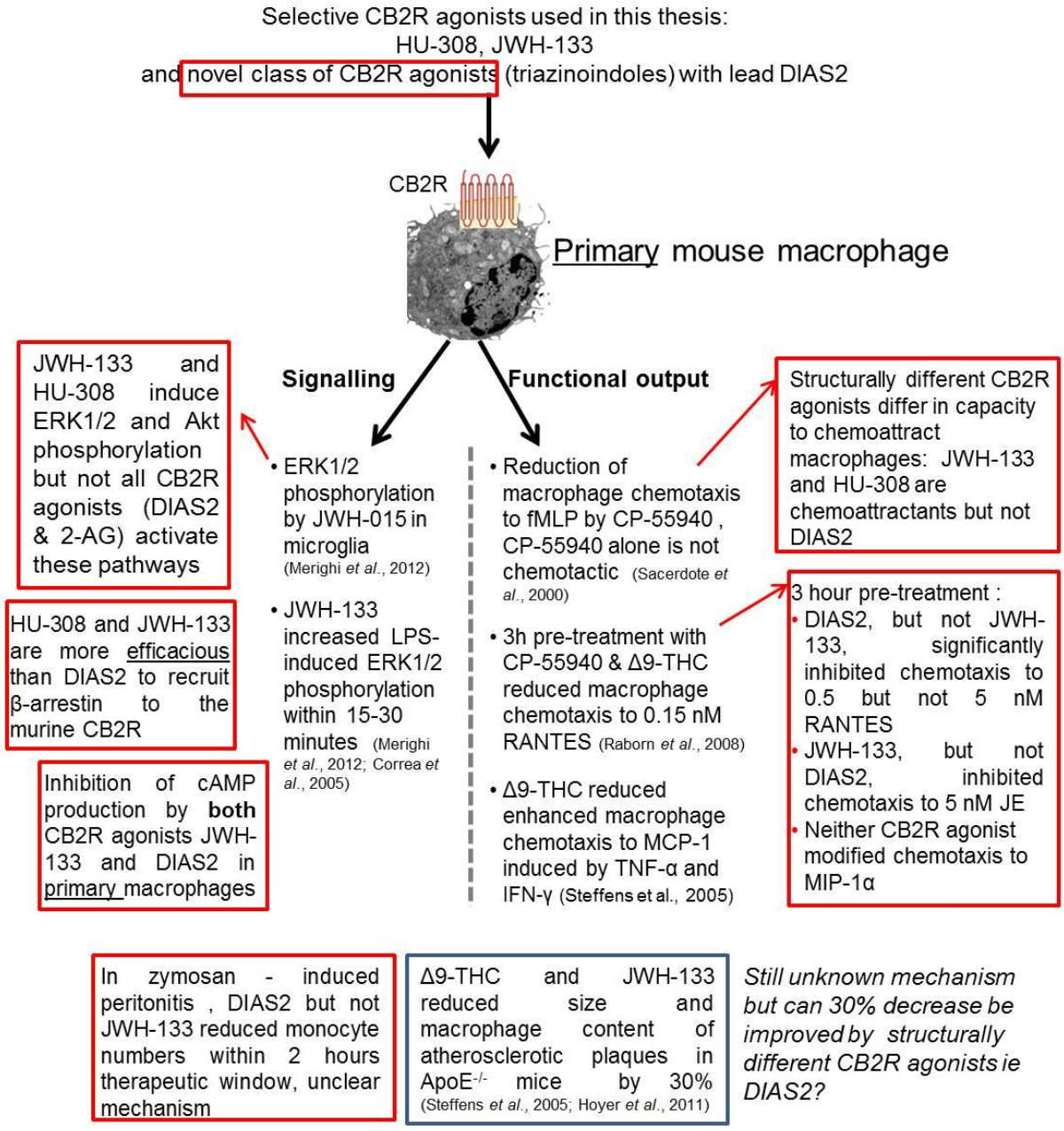

Figure 6.1: Key pathways studied in the macrophage literature about CB2R role and findings from this thesis

This figure is a modification of Figure 1.5 from the Introduction. It indicates the pathways studied in primary (physiological levels of the CB2R and physiological coupling) murine macrophages in the literature regarding the effects of CB2R agonists on these cells. In red boxes the contribution of this thesis to the literature. Structurally different CB2R agonists do not elicit identical responses in primary macrophages

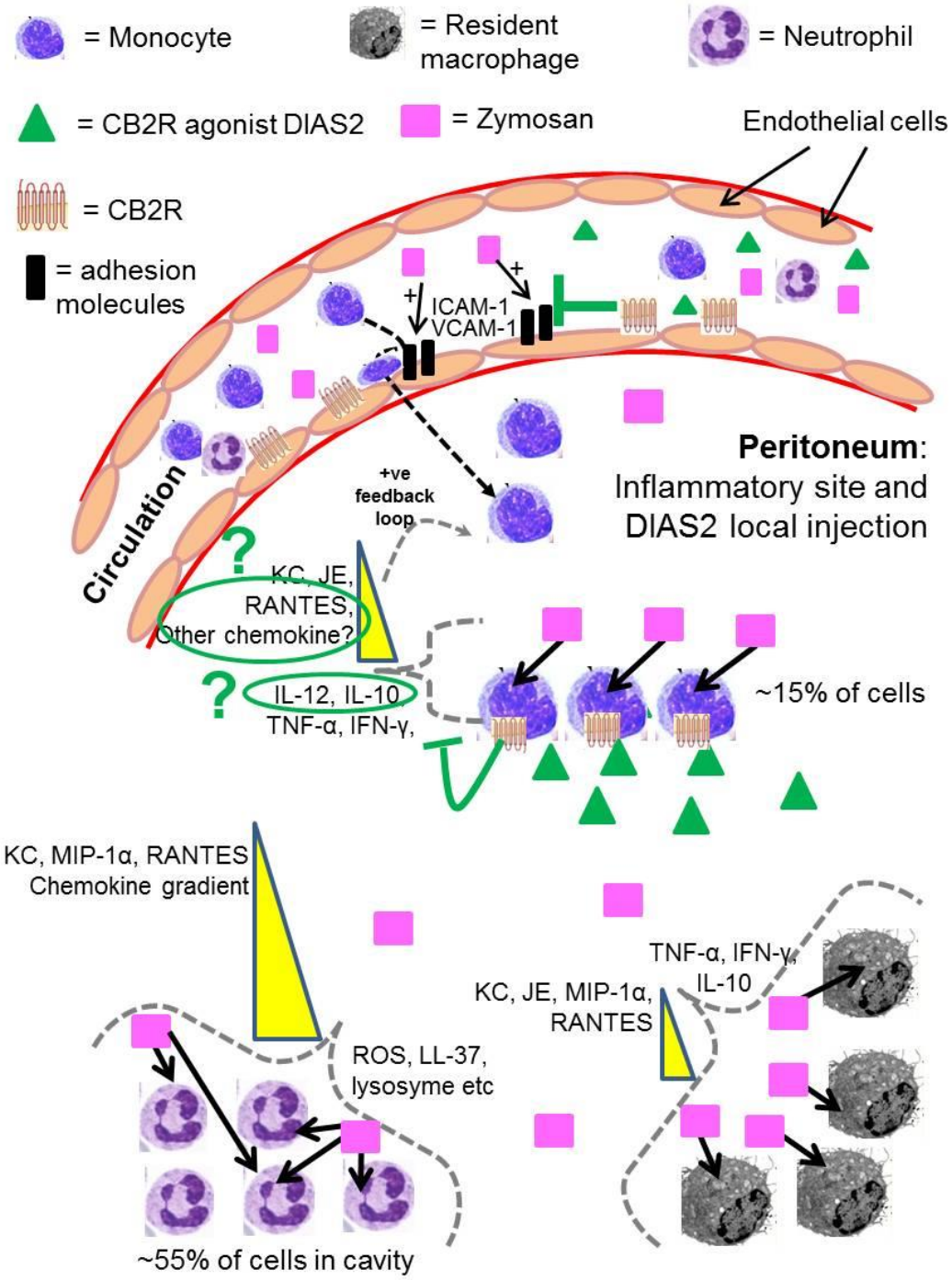

Figure 6.2: Working hypothesis for the anti-inflammatory role of CB2R and DIAS2 in zymosan-induced peritonitis

We hypothesise that the CB2R agonist DIAS2 reduces monocyte recruitment to zymosan-induced peritonitis possibly by a combined effect on reducing adhesion molecule expression on endothelial cells, reducing the positive feedback loop of chemokines by recruited monocytes and also possibly by reducing the levels of pro-inflammatory IL-12 and increasing the levels of IL-10 from the recruited monocytes.

Therefore inhibition of the adhesion cascade by CB2R agonists like DIAS2 could contribute to reduce monocyte influx into the inflamed site. However since JWH-133 had no significant effect on monocyte recruitment at the time window tested alternative inhibitory pathways may also take place to contribute to increase the anti-inflammatory effect on reducing monocyte influx. Such inhibitory effects by CB2R agonists could mainly be exerted on recruited monocytes since neither resident macrophages nor neutrophils express considerable amount of CB2R (Chouinard *et al.,* 2011; Lee *et al*., 2001). Possible effects on recruited monocytes could be to inhibit the release of chemokines, such as JE or RANTES, which would provide a positive feedback loop for further monocyte recruitment. Since JE and MIP-1α levels were not altered by DIAS2 (Figure 4.14), such chemokines could be RANTES or a yet unidentified chemokines with contribution to monocyte recruitment in zymosan induced peritonitis (Ajuebor *et al*., 1998a). Additionally, it is possible that DIAS2 only inhibits monocyte recruitment by 50% because the zymosan-induced chemokine production by recruited neutrophils could not be directly modulated by CB2R agonists, thus only partial decrease of chemokine levels could be achieved. Agonists like DIAS2, which are devoid of chemotactic ability, could have stronger effects on for example RANTES-induced monocyte recruitment, as suggested from our *in vitro* results in Figure 4.16. Apart from chemokine modulation, CB2R agonists have been shown to decrease pro-inflammatory IL-12 production from macrophages, while increasing IL-10 production (Correa *et al.*, 2005). Also increasing IL-10 levels by monocytes has been shown to decrease RANTES production (Marfaing-Koka *et al.*, 1996). It is therefore also possible that DIAS2 inhibited monocyte recruitment due to

increased IL-10 production and via IL-10 induced inhibition of pro-inflammatory cytokine and chemokine production by the recruited monocytes.

So far only one CB2R agonist (GW842166X) has reached clinical trials, however it failed to demonstrate analgesia in acute pain from tooth extraction (Ostenfeld *et al.*, 2011). In the limited literature available for this compound it was reported that GW842166X was selected as the lead CB2R agonist from its class due to its high potency on human and rat cAMP assays, its high selectivity over CB1R and oral ED_{50} of 0.1 mg/kg on inhibition of CFA-induced hyperalgesia to weight bearing with no tolerance observed after 1 or 4 day daily administration (Giblin *et al.*, 2007). No other published data are available for GW842166X.

We selected DIAS2 as our lead compound for similar reasons as GW842166X, i.e. potent activity and selectivity for CB2R and low molecular weight (317.07) relative to other active SAR compounds aiding its solubility. However our findings suggest that more factors need to be considered prior to selection of the lead compound, depending on the desired outcome and the target cell type. For example it has been recently demonstrated that microglia are ontogenically distinct from other macrophage populations (Ginhoux *et al.*, 2010) so our observations supporting functional selectivity at the CB2R in peritoneal macrophages could apply to these cells or may be different due to different coupling in the microglia compared to other macrophages following developmental changes. Therefore more experiments investigating the phenomenon of functional selectivity need to be performed in the preclinical phases prior to using CB2R agonists in clinical studies.

6.5 Future challenges for use of CB2R agonists as therapeutics in inflammation

There are many challenges regarding the use of CB2R agonists in the clinic. Selectivity of CB2R over CB1R remains a key issue due to the psychoactive effects of CB1R which could initiate an addictive behaviour from the patients in long-term treatments. Additionally formulation problems exist due to the high lipophilicity of the compounds making the administration challenging, especially *in vivo*. Apart from these problems in early drug discovery, failure of one company's drug (GW842166X) in one clinical trial setting was enough to discourage pharmaceutical funding in clinical trials using *any* CB2R agonists.

However, CB2R agonists have not been tested in inflammatory conditions such as atherosclerosis or inflammatory pain, such as rheumatic pain in arthritis, in clinical trials. Inflammatory pain and neuropathic pain have different associated pathologies, therefore failure of the CB2R agonist in inducing analgesia in neuropathic pain, cannot predict failure of CB2R agonists as analgesics in inflammatory pain or as an anti-inflammatory treatment in atherosclerosis. Further experiments in disease mouse models with CB2R agonists, alone or in combination with standard treatment, would allow better understanding of the role of CB2R in inflammation and its potential as a therapeutic. Also in order to translate novel CB2R agonists, including our novel class, to drugs several steps are important for proof-of-concept prior to application to animal disease models (Figure 6.3). These steps include a dosing regimen, pharmacokinetic studies, appropriate formulation and toxicology. For example 2-HP-

β-cyclodextrin has been used for oral administration of low hydrophilicity, such as hydrocortisone, with no reported toxicity (Laza-Knoerr *et al.*, 2010; Orlu-Gul *et al.*, 2012).

We think that the key finding from this thesis is that CB2R agonists can modulate monocyte/macrophage recruitment and activation *in vitro* and *in vivo* depending on the activated signalling pathways. Consequently modulation of monocyte influx into atherosclerotic plaques and their transformation into activated macrophages by CB2R agonists could provide a safe and sustainable treatment of atherosclerosis by dampening the on-going inflammation.

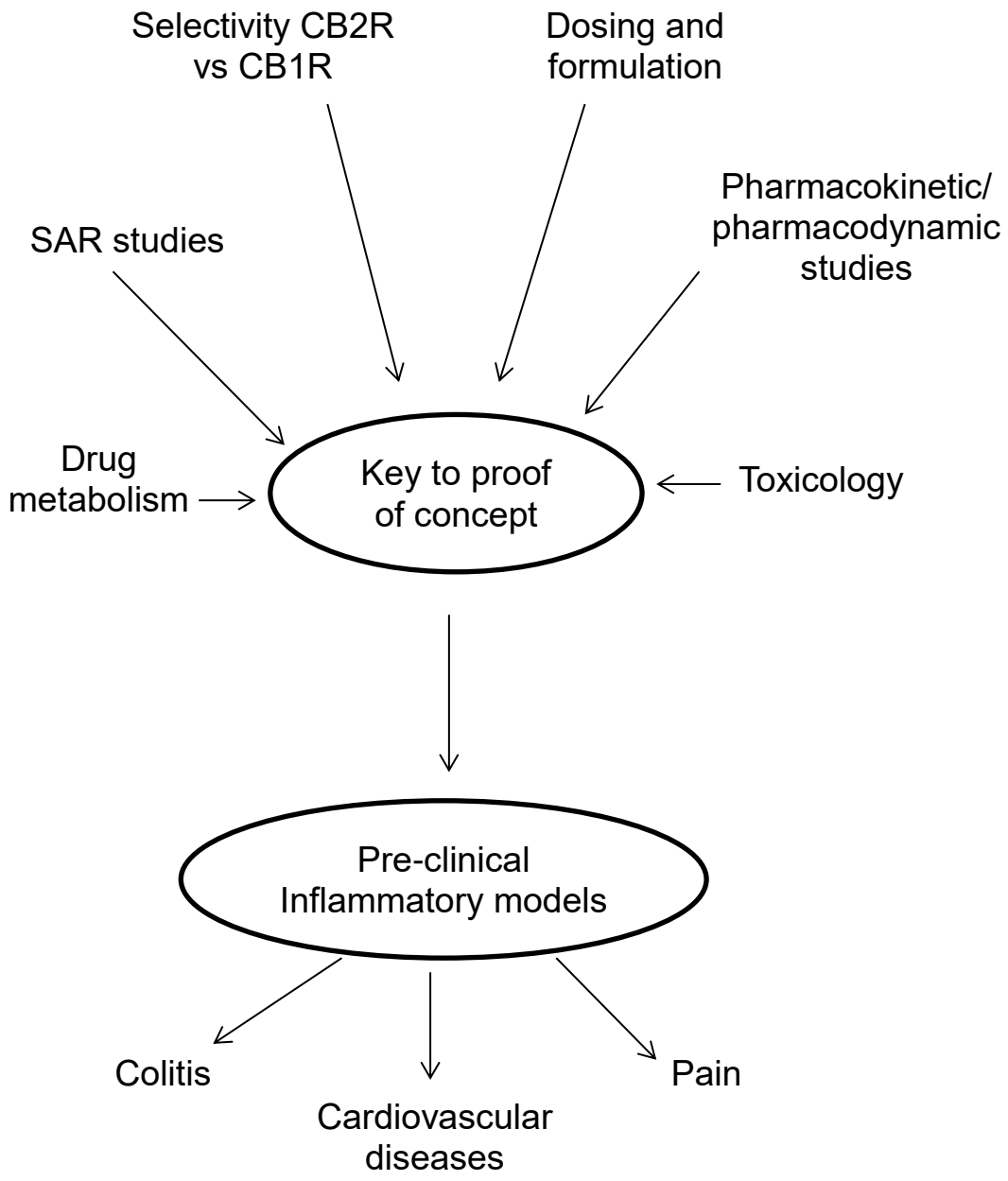

Figure 6.3: Key studies needed for translation of CB2R agonists to drugs
This diagram represent the most important hurdles to overcome in validating any novel CB2R agonist in appropriate pre-clinical/animal models of disease.

BIBLIOGRAPHY

Abdelrahman M, Sivarajah A, Thiemermann C (2005). Beneficial effects of PPAR-gamma ligands in ischemia-reperfusion injury, inflammation and shock. *Cardiovasc Res* 65(4): 772-781.

Agarwal N, Pacher P, Tegeder I, Amaya F, Constantin CE, Brenner GJ*, et al.* (2007). Cannabinoids mediate analgesia largely via peripheral type 1 cannabinoid receptors in nociceptors. *Nat Neurosci* 10(7): 870-879.

Agostini L, Martinon F, Burns K, McDermott MF, Hawkins PN, Tschopp J (2004). NALP3 forms an IL-1beta-processing inflammasome with increased activity in Muckle-Wells autoinflammatory disorder. *Immunity* 20(3): 319-325.

Agudelo M, Newton C, Widen R, Sherwood T, Nong L, Friedman H*, et al.* (2008). Cannabinoid receptor 2 (CB2) mediates immunoglobulin class switching from IgM to IgE in cultures of murine-purified B lymphocytes. *J Neuroimmune Pharmacol* 3(1): 35-42.

Ajuebor MN, Das AM, Virág L, Flower RJ, Szabó C, Perretti M (1999). Role of Resident Peritoneal Macrophages and Mast Cells in Chemokine Production and Neutrophil Migration in Acute Inflammation: Evidence for an Inhibitory Loop Involving Endogenous IL-10. *J. Immunol.* 162(3): 1685-1691.

Ajuebor MN, Flower RJ, Hannon R, Christie M, Bowers K, Verity A*, et al.* (1998a). Endogenous monocyte chemoattractant protein-1 recruits monocytes in the zymosan peritonitis model. *J Leukoc Biol* 63(1): 108-116.

Ajuebor MN, Virag L, Flower RJ, Perretti M, Szabo C (1998b). Role of inducible nitric oxide synthase in the regulation of neutrophil migration in zymosan-induced inflammation. *Immunology* 95(4): 625-630.

An G, Wang H, Tang R, Yago T, McDaniel JM, McGee S*, et al.* (2008). P-selectin glycoprotein ligand-1 is highly expressed on Ly-6Chi monocytes and a major determinant for Ly-6Chi monocyte recruitment to sites of atherosclerosis in mice. *Circulation* 117(25): 3227-3237.

Aronoff DM, Canetti C, Peters-Golden M (2004). Prostaglandin E2 inhibits alveolar macrophage phagocytosis through an E-prostanoid 2 receptor-mediated increase in intracellular cyclic AMP. *J Immunol* 173(1): 559-565.

Aronoff DM, Canetti C, Serezani CH, Luo M, Peters-Golden M (2005). Cutting edge: macrophage inhibition by cyclic AMP (cAMP): differential roles of protein kinase A and exchange protein directly activated by cAMP-1. *J Immunol* 174(2): 595-599.

Atwood BK, Straiker A, Mackie K (2012a). CB(2): Therapeutic target-in-waiting. *Prog Neuropsychopharmacol Biol Psychiatry.* 38(1): 16-20.

Atwood BK, Wager-Miller J, Haskins C, Straiker A, Mackie K (2012b). Functional Selectivity in CB2 Cannabinoid Receptor Signaling and Regulation: Implications for the Therapeutic Potential of CB2 Ligands. *Mol Pharmacol.* 81(2): 250-263.

Bannenberg GL, Chiang N, Ariel A, Arita M, Tjonahen E, Gotlinger KH*, et al.* (2005). Molecular circuits of resolution: formation and actions of resolvins and protectins. *J Immunol* 174(7): 4345-4355.

Basu S, Dittel BN (2011a). Unraveling the complexities of cannabinoid receptor 2 (CB2) immune regulation in health and disease. *Immunol Res.* 51(1): 26-38.

Basu S, Ray A, Dittel BN (2011b). Cannabinoid receptor 2 is critical for the homing and retention of marginal zone B lineage cells and for efficient T-independent immune responses. *J Immunol* 187(11): 5720-5732.

Bayewitch M, Avidor-Reiss T, Levy R, Barg J, Mechoulam R, Vogel Z (1995). The peripheral cannabinoid receptor: adenylate cyclase inhibition and G protein coupling. *FEBS Letters* 375(1-2): 143-147.

Becker EL (1983). Chemotactic factors of inflammation. *Trends Pharmacol Sci.* 4(0): 223-225.

Berdyshev EV, Boichot E, Germain N, Allain N, Anger J-P, Lagente V (1997). Influence of fatty acid ethanolamides and [Delta]9-tetrahydrocannabinol on cytokine and arachidonate release by mononuclear cells. *Eur J Pharmacol.* 330(2-3): 231-240.

Beutler B, Hoebe K, Du X, Ulevitch RJ (2003). How we detect microbes and respond to them: the Toll-like receptors and their transducers. *J Leukoc Biol* 74(4): 479-485.

Bonta IL, Bult H (1977). Effects of anti-inflammatory drugs on the carrageenin-induced hind paw inflammation of rats deprived of endogenous precursors of prostaglandins. *Agents Actions Suppl.* 2: 77-83.

Borregaard N, Cowland JB (1997). Granules of the human neutrophilic polymorphonuclear leukocyte. *Blood* 89(10): 3503-3521.

Bouaboula M, Hilairet S, Marchand J, Fajas L, Le Fur G, Casellas P (2005). Anandamide induced PPARgamma transcriptional activation and 3T3-L1 preadipocyte differentiation. *Eur J Pharmacol* 517(3): 174-181.

Boyden S (1962). The chemotactic effect of mixtures of antibody and antigen on polymorphonuclear leukocytes. *J Exp Med.* 115(3): 453-466.

Branen L, Hovgaard L, Nitulescu M, Bengtsson E, Nilsson J, Jovinge S (2004). Inhibition of tumor necrosis factor-alpha reduces atherosclerosis in apolipoprotein E knockout mice. *Arterioscler Thromb Vasc Biol* 24(11): 2137-2142.

Breslow JL (1996). Mouse models of atherosclerosis. *Science* 272(5262): 685-688.

Buckley NE, McCoy KL, Mezey E, Bonner T, Zimmer A, Felder CC*, et al.* (2000). Immunomodulation by cannabinoids is absent in mice deficient for the cannabinoid CB(2) receptor. *Eur J Pharmacol* 396: 141 - 149.

Byers DE, Holtzman MJ (2011). Alternatively activated macrophages and airway disease. *Chest* 140(3): 768-774.

Cabral GA, Harmon KN, Carlisle SJ (2001). Cannabinoid-mediated inhibition of inducible nitric oxide production by rat microglial cells: evidence for CB1 receptor participation. *Adv Exp Med Biol* 493: 207-214.

Cailhier JF, Partolina M, Vuthoori S, Wu S, Ko K, Watson S*, et al.* (2005). Conditional Macrophage Ablation Demonstrates That Resident Macrophages Initiate Acute Peritoneal Inflammation. *J. Immunol.* 174(4): 2336-2342.

Carayon P, Marchand J, Dussossoy D, Derocq JM, Jbilo O, Bord A*, et al.* (1998). Modulation and functional involvement of CB2 peripheral cannabinoid receptors during B-cell differentiation. *Blood* 92(10): 3605-3615.

Carlisle SJ, Marciano-Cabral F, Staab A, Ludwick C, Cabral GA (2002). Differential expression of the CB2 cannabinoid receptor by rodent macrophages and macrophage-like cells in relation to cell activation. *Int Immunopharmacol* 2(1): 69-82.

Cash JL, White GE, Greaves DR (2009). Chapter 17. Zymosan-induced peritonitis as a simple experimental system for the study of inflammation. *Methods Enzymol* 461: 379-396.

Chang J, Cherney ML, Moyer JA, Lewis AJ (1984). Effect of forskolin on prostaglandin synthesis by mouse resident peritoneal macrophages. *Eur J Pharmacol.* 103(3-4): 303-312.

Chang YH, Lee ST, Lin WW (2001). Effects of cannabinoids on LPS-stimulated inflammatory mediator release from macrophages: involvement of eicosanoids. *J Cell Biochem* 81(4): 715-723.

Chen CC, Rosenbloom CL, Anderson DC, Manning AM (1995). Selective inhibition of E-selectin, vascular cell adhesion molecule-1, and intercellular adhesion molecule-1 expression by inhibitors of I kappa B-alpha phosphorylation. *J Immunol* 155(7): 3538-3545.

Chen M, Lam BK, Kanaoka Y, Nigrovic PA, Audoly LP, Austen KF*, et al.* (2006). Neutrophil-derived leukotriene B4 is required for inflammatory arthritis. *J Exp Med* 203(4): 837-842.

Cheng Y, Hitchcock SA (2007). Targeting cannabinoid agonists for inflammatory and neuropathic pain. *Expert Opin Investig Drugs.* 16(7): 951-965.

Cheung DL, Hart PH, Vitti GF, Whitty GA, Hamilton JA (1990). Contrasting effects of interferon-gamma and interleukin-4 on the interleukin-6 activity of stimulated human monocytes. *Immunology* 71(1): 70-75.

Chouinard F, Lefebvre JS, Navarro P, Bouchard L, Ferland C, Lalancette-Habert M*, et al.* (2011). The Endocannabinoid 2-Arachidonoyl-Glycerol Activates Human Neutrophils: Critical

Role of Its Hydrolysis and De Novo Leukotriene B4 Biosynthesis. *J. Immunol.* 186(5): 3188-3196.

Chuang TT, Iacovelli L, Sallese M, De Blasi A (1996). G protein-coupled receptors: heterologous regulation of homologous desensitization and its implications. *Trends Pharmacol Sci* 17(11): 416-421.

Clark AK, Malcangio M (2012). Microglial signalling mechanisms: Cathepsin S and Fractalkine. *Exp Neurol.* 234(2): 283-292.

Clark ER, Clark EL (1930). Relation of monocytes of the blood to the tissue macrophages. *Am J Anat.* 46(1): 149-185.

Clarke MC, Figg N, Maguire JJ, Davenport AP, Goddard M, Littlewood TD*, et al.* (2006). Apoptosis of vascular smooth muscle cells induces features of plaque vulnerability in atherosclerosis. *Nat Med* 12(9): 1075-1080.

Clarkson S, Newburgh LH (1926). The Relation between Atherosclerosis and Ingested Cholesterol in the Rabbit. *J Exp Med* 43(5): 595-612.

Clayton N, Marshall FH, Bountra C, O'Shaughnessy CT (2002). CB1 and CB2 cannabinoid receptors are implicated in inflammatory pain. *Pain* 96(3): 253-260.

Cluny NL, Keenan CM, Duncan M, Fox A, Lutz B, Sharkey KA (2010). Naphthalen-1-yl-(4-pentyloxynaphthalen-1-yl)methanone (SAB378), a peripherally restricted, cannabinoid CB1/CB2 receptor agonist inhibits gastrointestinal motility, but has no effect on experimental colitis in mice. *J Pharmacol Exp Ther.* : 973-980.

Collins RG, Velji R, Guevara NV, Hicks MJ, Chan L, Beaudet AL (2000). P-Selectin or intercellular adhesion molecule (ICAM)-1 deficiency substantially protects against atherosclerosis in apolipoprotein E-deficient mice. *J Exp Med* 191(1): 189-194.

Coopman K, Smith LD, Wright KL, Ward SG (2007). Temporal variation in CB2R levels following T lymphocyte activation: Evidence that cannabinoids modulate CXCL12-induced chemotaxis. *Int Immunopharmacol.* 7(3): 360-371.

Correa F, Mestre L, Docagne F, Guaza C (2005). Activation of cannabinoid CB2 receptor negatively regulates IL-12p40 production in murine macrophages: role of IL-10 and ERK1/2 kinase signaling. *Br J Pharmacol* 145(4): 441-448.

Cota D, Marsicano G, Tschop M, Grubler Y, Flachskamm C, Schubert M*, et al.* (2003). The endogenous cannabinoid system affects energy balance via central orexigenic drive and peripheral lipogenesis. *J Clin Invest* 112(3): 423-431.

Cravatt BF, Giang DK, Mayfield SP, Boger DL, Lerner RA, Gilula NB (1996). Molecular characterization of an enzyme that degrades neuromodulatory fatty-acid amides. *Nature* 384(6604): 83-87.

Cravatt BF, Lichtman AH (2002). The enzymatic inactivation of the fatty acid amide class of signaling lipids. *Chem Phys Lipids* 121(1-2): 135-148.

Creagh EM, O'Neill LA (2006). TLRs, NLRs and RLRs: a trinity of pathogen sensors that co-operate in innate immunity. *Trends Immunol* 27(8): 352-357.

Curran NM, Griffin BD, O'Toole D, Brady KJ, Fitzgerald SN, Moynagh PN (2005). The Synthetic Cannabinoid R(+)WIN 55,212-2 Inhibits the Interleukin-1 Signaling Pathway in Human Astrocytes in a Cannabinoid Receptor-independent Manner. *J. Biol. Chem.* 280(43): 35797-35806.

Cybulsky MI, Iiyama K, Li H, Zhu S, Chen M, Iiyama M*, et al.* (2001). A major role for VCAM-1, but not ICAM-1, in early atherosclerosis. *J Clin Invest* 107(10): 1255-1262.

da Silva KA, Paszcuk AF, Passos GF, Silva ES, Bento AF, Meotti FC*, et al.* (2011). Activation of cannabinoid receptors by the pentacyclic triterpene alpha,beta-amyrin inhibits inflammatory and neuropathic persistent pain in mice. *Pain* 152(8): 1872-1887.

Dalton D, Pitts-Meek S, Keshav S, Figari I, Bradley A, Stewart T (1993). Multiple defects of immune cell function in mice with disrupted interferon-gamma genes. *Science* 259(5102): 1739-1742.

Damerau B, Grünefeld E, Vogt W (1978). Chemotactic effects of the complement-derived peptides C3a, C3ai and C5a (classical anaphylatoxin) on rabbit and guinea-pig polymorphonuclear leukocytes. *Naunyn Schmiedebergs Arch Pharmacol.* 305(2): 181-184.

Davenport P, Tipping PG (2003). The role of interleukin-4 and interleukin-12 in the progression of atherosclerosis in apolipoprotein E-deficient mice. *Am J Pathol* 163(3): 1117-1125.

Davies JQ, Gordon S (2005). Isolation and culture of murine macrophages. *Methods Mol Biol.* 290: 91-103.

Davignon J, Ganz P (2004). Role of endothelial dysfunction in atherosclerosis. *Circulation* 109(23 Suppl 1): III27-32.

Dawson J, Sedgwick AD, Edwards JC, Lees P (1991). A comparative study of the cellular, exudative and histological responses to carrageenan, dextran and zymosan in the mouse. *Int J Tissue React.* 13(4): 171-185.

de Villiers WJ, Smith JD, Miyata M, Dansky HM, Darley E, Gordon S (1998). Macrophage phenotype in mice deficient in both macrophage-colony-stimulating factor (op) and apolipoprotein E. *Arterioscler Thromb Vasc Biol* 18(4): 631-640.

Delgado M, Ganea D (2001). Inhibition of endotoxin-induced macrophage chemokine production by vasoactive intestinal peptide and pituitary adenylate cyclase-activating polypeptide in vitro and in vivo. *J Immunol* 167(2): 966-975.

Delsing JMD, Leijten PF, Arts K, van Eenennaam H, Garritsen A, Gijbels JJM*, et al.* (2011). Cannabinoid Receptor 2 Deficiency in Haematopoietic cells Aggravates Early Atherosclerosis in LDL Receptor Deficient Mice. *Open Cardiovasc Med J.* 5: 15-21.

Derocq JM, Segui M, Marchand J, Le Fur G, Casellas P (1995). Cannabinoids enhance human B-cell growth at low nanomolar concentrations. *FEBS Lett* 369(2-3): 177-182.

Deusch E, Kraft B, Nahlik G, Weigl L, Hohenegger M, Kress HG (2003). No evidence for direct modulatory effects of delta 9-tetrahydrocannabinol on human polymorphonuclear leukocytes. *J Neuroimmunol* 141(1-2): 99-103.

Devane WA, Dysarz FA, 3rd, Johnson MR, Melvin LS, Howlett AC (1988). Determination and characterization of a cannabinoid receptor in rat brain. *Mol Pharmacol* 34(5): 605-613.

DeWire SM, Violin JD (2011). Biased ligands for better cardiovascular drugs: dissecting G-protein-coupled receptor pharmacology. *Circ Res* 109(2): 205-216.

Di L, Kerns EH (2003). Profiling drug-like properties in discovery research. *Curr Opin Chem Biol.* 7(3): 402-408.

Di Marzo V (2009). The endocannabinoid system: its general strategy of action, tools for its pharmacological manipulation and potential therapeutic exploitation. *Pharmacol Res.* 60(2): 77-84.

Di Marzo V, Bisogno T, De Petrocellis L, Melck D, Orlando P, Wagner JA*, et al.* (1999). Biosynthesis and inactivation of the endocannabinoid 2-arachidonoylglycerol in circulating and tumoral macrophages. *Eur J Biochem.* 264(1): 258-267.

Di Marzo V, Goparaju SK, Wang L, Liu J, Batkai S, Jarai Z*, et al.* (2001). Leptin-regulated endocannabinoids are involved in maintaining food intake. *Nature* 410(6830): 822-825.

Di Rosa M (1972). Biological properties of carrageenan. *J Pharm Pharmacol.* 24(2): 89-102.

Dias R, Timmers LF, Caceres RA, de Azevedo WF, Jr. (2008). Evaluation of molecular docking using polynomial empirical scoring functions. *Curr Drug Targets.* 9(12): 1062-1070.

Ding L, Biswas S, Morton RE, Smith JD, Hay N, Byzova TV*, et al.* (2012). Akt3 deficiency in macrophages promotes foam cell formation and atherosclerosis in mice. *Cell Metab.* 15(6): 861-872.

Dinh TP, Carpenter D, Leslie FM, Freund TF, Katona I, Sensi SL*, et al.* (2002). Brain monoglyceride lipase participating in endocannabinoid inactivation. *Proc Natl Acad Sci U S A* 99(16): 10819-10824.

Doherty DE, Zagarella L, Henson PM, Worthen GS (1989). Lipopolysaccharide stimulates monocyte adherence by effects on both the monocyte and the endothelial cell. *J Immunol* 143(11): 3673-3679.

Doherty NS, Poubelle P, Borgeat P, Beaver TH, Westrich GL, Schrader NL (1985). Intraperitoneal injection of zymosan in mice induces pain, inflammation and the synthesis of peptidoleukotrienes and prostaglandin E2. *Prostaglandins* 30(5): 769-789.

Dol-Gleizes F, Paumelle R, Visentin V, Mares A-M, Desitter P, Hennuyer N*, et al.* (2009). Rimonabant, a Selective Cannabinoid CB1 Receptor Antagonist, Inhibits Atherosclerosis in LDL Receptor-Deficient Mice. *Arterioscler Thromb Vasc Biol* 29(1): 12-18.

Drake MT, Violin JD, Whalen EJ, Wisler JW, Shenoy SK, Lefkowitz RJ (2008). beta-arrestin-biased agonism at the beta2-adrenergic receptor. *J Biol Chem* 283(9): 5669-5676.

Dustin M, Rothlein R, Bhan A, Dinarello C, Springer T (1986). Induction by IL 1 and interferon-gamma: tissue distribution, biochemistry, and function of a natural adherence molecule (ICAM-1). *J Immunol* 137(1): 245-254.

Ehrlich P, Lazarus A (1956). Histology of the Blood. Normal and Pathological. *Myers W [ed and trans]: Cambridge, MA, Cambridge, 1900, reprinted in Himmelweit F (ed): The Collected Papers of Paul Ehrlich. Vol 1. Histology, Biochemistry, and Pathology. New York, NY, Pergamon, 1956*: p 181.

Ekins S, Mestres J, Testa B (2007). In silico pharmacology for drug discovery: methods for virtual ligand screening and profiling. *Br J Pharmacol* 152(1): 9-20.

Ellis IR, Schor AM, Schor SL (2007). EGF AND TGF-alpha motogenic activities are mediated by the EGF receptor via distinct matrix-dependent mechanisms. *Exp Cell Res.* 313(4): 732-741.

Ermann M, Riether D, Walker ER, Mushi IF, Jenkins JE, Noya-Marino B*, et al.* (2008). Arylsulfonamide CB2 receptor agonists: SAR and optimization of CB2 selectivity. *Bioorg Med Chem Lett* 18(5): 1725-1729.

Esseltine JL, Dale LB, Ferguson SS (2011). Rab GTPases bind at a common site within the angiotensin II type I receptor carboxyl-terminal tail: evidence that Rab4 regulates receptor phosphorylation, desensitization, and resensitization. *Mol Pharmacol* 79(1): 175-184.

Fadok VA, Bratton DL, Konowal A, Freed PW, Westcott JY, Henson PM (1998). Macrophages that have ingested apoptotic cells in vitro inhibit proinflammatory cytokine production through autocrine/paracrine mechanisms involving TGF-beta, PGE2, and PAF. *J Clin Invest* 101(4): 890-898.

Fauve RM, Jusforgues H, Hevin B (1983). Maintenance of granuloma macrophages in serum-free medium. *J Immunol Methods* 64(3): 345-351.

Feig JE, Pineda-Torra I, Sanson M, Bradley MN, Vengrenyuk Y, Bogunovic D*, et al.* (2010). LXR promotes the maximal egress of monocyte-derived cells from mouse aortic plaques during atherosclerosis regression. *J Clin Invest* 120(12): 4415-4424.

Feig JE, Quick JS, Fisher EA (2009). The role of a murine transplantation model of atherosclerosis regression in drug discovery. *Curr Opin Investig Drugs.* 10(3): 232-238.

Felder CC, Joyce KE, Briley EM, Mansouri J, Mackie K, Blond O*, et al.* (1995). Comparison of the pharmacology and signal transduction of the human cannabinoid CB1 and CB2 receptors. *Mol Pharmacol.* 48(3): 443-450.

Feng W, Song ZH (2001). Functional roles of the tyrosine within the NP(X)(n)Y motif and the cysteines in the C-terminal juxtamembrane region of the CB2 cannabinoid receptor. *FEBS Lett* 501(2-3): 166-170.

Fernandez-Hernando C, Ackah E, Yu J, Suarez Y, Murata T, Iwakiri Y*, et al.* (2007). Loss of Akt1 leads to severe atherosclerosis and occlusive coronary artery disease. *Cell Metab.* 6(6): 46-457.

Fine JS, Byrnes HD, Zavodny PJ, Hipkin RW (2001). Evaluation of signal transduction pathways in chemoattractant-induced human monocyte chemotaxis. *Inflammation* 25(2): 61-67.

Franklin JM, Vasiljevik T, Prisinzano TE, Carrasco GA (2012). Cannabinoid 2 receptor- and beta Arrestin 2-dependent upregulation of serotonin 2A receptors. *European neuropsychopharmacology* Epub ahead of print.

Freeman-Anderson NE, Pickle TG, Netherland CD, Bales A, Buckley NE, Thewke DP (2008). Cannabinoid (CB2) receptor deficiency reduces the susceptibility of macrophages to oxidized LDL/oxysterol-induced apoptosis. *J. Lipid Res.* 49(11): 2338-2346.

Galandrin S, Bouvier M (2006). Distinct signaling profiles of beta1 and beta2 adrenergic receptor ligands toward adenylyl cyclase and mitogen-activated protein kinase reveals the pluridimensionality of efficacy. *Mol Pharmacol* 70(5): 1575-1584.

Galandrin S, Oligny-Longpre G, Bouvier M (2007). The evasive nature of drug efficacy: implications for drug discovery. *Trends Pharmacol Sci* 28(8): 423-430.

Galiegue S, Mary S, Marchand J, Dussossoy D, Carriere D, Carayon P*, et al.* (1995). Expression of central and peripheral cannabinoid receptors in human immune tissues and leukocyte subpopulations. *Eur J Biochem* 232(1): 54-61.

Galkina E, Ley K (2007). Vascular adhesion molecules in atherosclerosis. *Arterioscler Thromb Vasc Biol* 27(11): 2292-2301.

Gallily R, Breuer A, Mechoulam R (2000). 2-Arachidonylglycerol, an endogenous cannabinoid, inhibits tumor necrosis factor-[alpha] production in murine macrophages, and in mice. *Eur J Pharmacol.* 406(1): R5-R7.

Gallily R, Yamin A, Waksmann Y, Ovadia H, Weidenfeld J, Bar-Joseph A*, et al.* (1997). Protection against septic shock and suppression of tumor necrosis factor alpha and nitric oxide production by dexanabinol (HU-211), a nonpsychotropic cannabinoid. *J Pharmacol Exp Ther* 283(2): 918-924.

García-Ramallo E, Marques T, Prats N, Beleta J, Kunkel SL, Godessart N (2002). Resident Cell Chemokine Expression Serves as the Major Mechanism for Leukocyte Recruitment During Local Inflammation. *J. Immunol.* 169(11): 6467-6473.

Gareau Y, Dufresne C, Gallant M, Rochette C, Sawyer N, Slipetz DM*, et al.* (1996). Structure activity relationships of tetrahydrocannabinol analogues on human cannabinoid receptors. *Bioorg Med Chem Lett* 6(2): 189-194.

Gautier EL, Chow A, Spanbroek R, Marcelin G, Greter M, Jakubzick C*, et al.* (2012). Systemic Analysis of PPARγ in Mouse Macrophage Populations Reveals Marked Diversity in Expression with Critical Roles in Resolution of Inflammation and Airway Immunity. *J Immunol.* 189(5): 2614-2624.

Gautier EL, Huby T, Witztum JL, Ouzilleau B, Miller ER, Saint-Charles F*, et al.* (2009). Macrophage apoptosis exerts divergent effects on atherogenesis as a function of lesion stage. *Circulation* 119(13): 1795-1804.

Geissmann F, Jung S, Littman DR (2003). Blood monocytes consist of two principal subsets with distinct migratory properties. *Immunity* 19(1): 71-82.

Gerrity RG (1981). The role of the monocyte in atherogenesis: I. Transition of blood-borne monocytes into foam cells in fatty lesions. *Am J Pathol* 103(2): 181-190.

Getz GS, Reardon CA (2012). Animal models of atherosclerosis. *Arterioscler Thromb Vasc Biol* 32(5): 1104-1115.

Giblin GM, O'Shaughnessy CT, Naylor A, Mitchell WL, Eatherton AJ, Slingsby BP*, et al.* (2007). Discovery of 2-[(2,4-dichlorophenyl)amino]-N-[(tetrahydro- 2H-pyran-4-yl)methyl]-4-(trifluoromethyl)- 5-pyrimidinecarboxamide, a selective CB2 receptor agonist for the treatment of inflammatory pain. *J Med Chem* 50(11): 2597-2600.

Ginhoux F, Greter M, Leboeuf M, Nandi S, See P, Gokhan S*, et al.* (2010). Fate mapping analysis reveals that adult microglia derive from primitive macrophages. *Science* 330(6005): 841-845.

Glass M, Felder CC (1997). Concurrent stimulation of cannabinoid CB1 and dopamine D2 receptors augments cAMP accumulation in striatal neurons: evidence for a Gs linkage to the CB1 receptor. *J Neurosci* 17(14): 5327-5333.

Gokoh M, Kishimoto S, Oka S, Metani Y, Sugiura T (2005). 2-Arachidonoylglycerol, an endogenous cannabinoid receptor ligand, enhances the adhesion of HL-60 cells differentiated into macrophage-like cells and human peripheral blood monocytes. *FEBS Letters* 579(28): 6473-6478.

Goldstein JL, Brown MS (1987). Regulation of low-density lipoprotein receptors: implications for pathogenesis and therapy of hypercholesterolemia and atherosclerosis. *Circulation* 76(3): 504-507.

Gonsiorek W, Lunn C, Fan X, Narula S, Lundell D, Hipkin RW (2000). Endocannabinoid 2-Arachidonyl Glycerol Is a Full Agonist through Human Type 2 Cannabinoid Receptor: Antagonism by Anandamide. *Mol Pharmacol* 57(5): 1045-1050.

Goparaju SK, Ueda N, Yamaguchi H, Yamamoto S (1998). Anandamide amidohydrolase reacting with 2-arachidonoylglycerol, another cannabinoid receptor ligand. *FEBS Lett* 422(1): 69-73.

Gordon S (2003). Alternative activation of macrophages. *Nat Rev Immunol* 3(1): 23-35.

Gordon S, Martinez FO (2010). Alternative Activation of Macrophages: Mechanism and Functions. *Immunity* 32(5): 593-604.

Gotto AM, Jr., Moon JE (2012). Recent clinical studies of the effects of lipid-modifying therapies. *Am J Cardiol.* 110(1 Suppl): 15A-26A.

Gouldson P, Calandra B, Legoux P, Kerneis A, Rinaldi-Carmona M, Barth F*, et al.* (2000). Mutational analysis and molecular modelling of the antagonist SR 144528 binding site on the human cannabinoid CB(2) receptor. *Eur J Pharmacol* 401(1): 17-25.

Graham ES, Angel CE, Schwarcz LE, Dunbar PR, Glass M (2010). Detailed characterisation of CB2 receptor protein expression in peripheral blood immune cells from healthy human volunteers using flow cytometry. *Int J Immunopathol Pharmacol.* 23(1): 25-34.

Grant I, Cahn BR (2005). Cannabis and endocannabinoid modulators: Therapeutic promises and challenges. *Clin Neurosci Res.* 5(2-4): 185-199.

Gratchev A, Guillot P, Hakiy N, Politz O, Orfanos CE, Schledzewski K*, et al.* (2001). Alternatively activated macrophages differentially express fibronectin and its splice variants and the extracellular matrix protein betaIG-H3. *Scand J Immunol.* 53(4): 386-392.

Griess P (1879). Bemerkungen zu der abhandlung der H.H. Weselsky und Benedikt “Ueber einige azoverbindungen.” *Chem. Ber.* 12: 426-428.

Griffiths RJ, Li SW, Wood BE, Blackham A (1991). A comparison of the anti-inflammatory activity of selective 5-lipoxygenase inhibitors with dexamethasone and colchicine in a model of zymosan induced inflammation in the rat knee joint and peritoneal cavity. *Agents and actions* 32(3-4): 312-320.

Guindon J, Hohmann AG (2008). Cannabinoid CB2 receptors: a therapeutic target for the treatment of inflammatory and neuropathic pain. *Br J Pharmacol* 153(2): 319-334.

Gupta S, Pablo AM, Jiang X, Wang N, Tall AR, Schindler C (1997). IFN-gamma potentiates atherosclerosis in ApoE knock-out mice. *J Clin Invest* 99(11): 2752-2761.

Hagmann WK (2008). The discovery of taranabant, a selective cannabinoid-1 receptor inverse agonist for the treatment of obesity. *Archiv der Pharmazie* 341(7): 405-411.

Hakimelahi GH, Khodarahmi GA (2005). The Identification of Toxicophores for the Prediction of Mutagenicity, Hepatotoxicity and Cardiotoxicity. *Journal of the Iranian Chemical Society* 2(4): 244-267.

Hamilton JA (2008). Colony-stimulating factors in inflammation and autoimmunity. *Nat Rev Immunol* 8(7): 533-544.

Han KH, Lim S, Ryu J, Lee C-W, Kim Y, Kang J-H*, et al.* (2009). CB1 and CB2 Cannabinoid Receptors Differentially Regulate the Production of Reactive Oxygen Species by Macrophages. *Cardiovasc Res* 84(3): 378-386.

Hansson G, Libby P (2006). The immune response in atherosclerosis: a double-edged sword. *Nat Rev Immunol* 6(7): 508-519.

Hanus L, Breuer A, Tchilibon S, Shiloah S, Goldenberg D, Horowitz M*, et al.* (1999). HU-308: A specific agonist for CB2, a peripheral cannabinoid receptor. *Proc Natl Acad Sci U S A.* 96(25): 14228-14233.

Hao M-x, Jiang L-s, Fang N-y, Pu J, Hu L-h, Shen L-H*, et al.* (2010). The cannabinoid WIN55, 212-2 protects against oxidized LDL-induced inflammatory response in murine macrophages. *J. Lipid Res.* 51(8): 2181-2190.

Haringman JJ, Tak PP (2004). Chemokine blockade: a new era in the treatment of rheumatoid arthritis? *Arthritis Res Ther.* 6(3): 93-97.

Harris H (1953). Chemotaxis of monocytes. *Br J Exp Pathol.* 34(3): 276-279.

Harris J, De Haro SA, Master SS, Keane J, Roberts EA, Delgado M*, et al.* (2007). T helper 2 cytokines inhibit autophagic control of intracellular Mycobacterium tuberculosis. *Immunity* 27(3): 505-517.

Hart PH, Ahern MJ, Smith MD, Finlay-Jones JJ (1995). Comparison of the suppressive effects of interleukin-10 and interleukin-4 on synovial fluid macrophages and blood monocytes from patients with inflammatory arthritis. *Immunology* 84(4): 536-542.

Hart R, Greaves DR (2010). Chemerin contributes to inflammation by promoting macrophage adhesion to VCAM-1 and fibronectin through clustering of VLA-4 and VLA-5. *J Immunol* 185(6): 3728-3739.

Hausdorff WP, Caron MG, Lefkowitz RJ (1990). Turning off the signal: desensitization of beta-adrenergic receptor function. *Faseb J* 4(11): 2881-2889.

Heit B, Tavener S, Raharjo E, Kubes P (2002). An intracellular signaling hierarchy determines direction of migration in opposing chemotactic gradients. *J Cell Biol* 159(1): 91-102.

Henderson RB, Hobbs JA, Mathies M, Hogg N (2003). Rapid recruitment of inflammatory monocytes is independent of neutrophil migration. *Blood* 102(1): 328-335.

Herkenham M, Lynn AB, Little MD, Johnson MR, Melvin LS, de Costa BR*, et al.* (1990). Cannabinoid receptor localization in brain. *Proc Natl Acad Sci U S A* 87(5): 1932-1936.

Hervera A, Negrete R, Leanez S, Martin-Campos J, Pol O (2010). The role of nitric oxide in the local antiallodynic and antihyperalgesic effects and expression of delta-opioid and cannabinoid-2 receptors during neuropathic pain in mice. *J Pharmacol Exp Ther* 334(3): 887-896.

Hochrein H, O'Keeffe M, Wagner H (2002). Human and mouse plasmacytoid dendritic cells. *Hum Immunol.* 63(12): 1103-1110.

Hollinshead SP, Astles PC, Chambers MG, Johnson MP, Palmer J, Tidwell MW (2012). Discovery and optimization of novel purines as potent and selective CB2 agonists. *Bioorg Med Chem Lett* 22(15): 4962-4966.

Howlett AC (1987). Regulation of adenylate cyclase in a cultured neuronal cell line by marijuana constituents, metabolites of delta-9-tetrahydrocannabinol, and synthetic analogs having psychoactivity. *NIDA research monograph* 79: 148-157.

Howlett AC, Barth F, Bonner TI, Cabral G, Casellas P, Devane WA*, et al.* (2002). International Union of Pharmacology. XXVII. Classification of cannabinoid receptors. *Pharmacol Rev* 54(2): 161-202.

Howlett AC, Breivogel CS, Childers SR, Deadwyler SA, Hampson RE, Porrino LJ (2004). Cannabinoid physiology and pharmacology: 30 years of progress. *Neuropharmacology* 47 Suppl 1: 345-358.

Hoyer FF, Steinmetz M, Zimmer S, Becker A, Lutjohann D, Buchalla R*, et al.* (2011). Atheroprotection via cannabinoid receptor-2 is mediated by circulating and vascular cells in vivo. *J Mol Cell Cardiol.* 51(6): 1007-1014.

Hu X, Chakravarty SD, Ivashkiv LB (2008). Regulation of interferon and Toll-like receptor signaling during macrophage activation by opposing feedforward and feedback inhibition mechanisms. *Immunol Rev* 226: 41-56.

Huber SA, Sakkinen P, David C, Newell MK, Tracy RP (2001). T helper-cell phenotype regulates atherosclerosis in mice under conditions of mild hypercholesterolemia. *Circulation* 103(21): 2610-2616.

Huestis MA, Gorelick DA, Heishman SJ, Preston KL, Nelson RA, Moolchan ET*, et al.* (2001). Blockade of effects of smoked marijuana by the CB1-selective cannabinoid receptor antagonist SR141716. *Arch Gen Psychiatry.* 58(4): 322-328.

Huo Y, Weber C, Forlow SB, Sperandio M, Thatte J, Mack M*, et al.* (2001). The chemokine KC, but not monocyte chemoattractant protein-1, triggers monocyte arrest on early atherosclerotic endothelium. *J Clin Invest* 108(9): 1307-1314.

Hurst DP, Grossfield A, Lynch DL, Feller S, Romo TD, Gawrisch K*, et al.* (2010). A lipid pathway for ligand binding is necessary for a cannabinoid G protein-coupled receptor. *J Biol Chem* 285(23): 17954-17964.

Huynh J, Nishimura N, Rana K, Peloquin JM, Califano JP, Montague CR*, et al.* (2011). Age-related intimal stiffening enhances endothelial permeability and leukocyte transmigration. *Sci Transl Med.* 3(112): 112-122.

Iiyama K, Hajra L, Iiyama M, Li H, DiChiara M, Medoff BD*, et al.* (1999). Patterns of Vascular Cell Adhesion Molecule-1 and Intercellular Adhesion Molecule-1 Expression in Rabbit and Mouse Atherosclerotic Lesions and at Sites Predisposed to Lesion Formation. *Circ Res.* 85(2): 199-207.

Ishibashi S, Goldstein JL, Brown MS, Herz J, Burns DK (1994). Massive xanthomatosis and atherosclerosis in cholesterol-fed low density lipoprotein receptor-negative mice. *J Clin Invest* 93(5): 1885-1893.

Iversen L (2003). Cannabis and the brain. *Brain* 126(Pt 6): 1252-1270.

Janabi M, Yamashita S, Hirano K, Sakai N, Hiraoka H, Matsumoto K*, et al.* (2000). Oxidized LDL-induced NF-kappa B activation and subsequent expression of proinflammatory genes are defective in monocyte-derived macrophages from CD36-deficient patients. *Arterioscler Thromb Vasc Biol* 20(8): 1953-1960.

Jarho P, Urtti A, Jarvinen K, Pate DW, Jarvinen T (1996). Hydroxypropyl-b-cyclodextrin increases aqueous solubility and stability of anandamide. *Life Sci.* 58(10): 181-185.

Jbilo O, Derocq JM, Segui M, Le Fur G, Casellas P (1999). Stimulation of peripheral cannabinoid receptor CB2 induces MCP-1 and IL-8 gene expression in human promyelocytic cell line HL60. *FEBS Lett* 448(2-3): 273-277.

Jhaveri MD, Sagar DR, Elmes SJ, Kendall DA, Chapman V (2007). Cannabinoid CB2 receptor-mediated anti-nociception in models of acute and chronic pain. *Mol Neurobiol.* 36(1): 26-35.

Jia T, Serbina NV, Brandl K, Zhong MX, Leiner IM, Charo IF*, et al.* (2008). Additive roles for MCP-1 and MCP-3 in CCR2-mediated recruitment of inflammatory monocytes during Listeria monocytogenes infection. *J Immunol* 180(10): 6846-6853.

Jiang L-s, Pu J, Han Z-h, Hu L-h, He B (2009). Role of activated endocannabinoid system in regulation of cellular cholesterol metabolism in macrophages. *Circ Res* 81(4): 805-813.

Johanek LM, Heitmiller DR, Turner M, Nader N, Hodges J, Simone DA (2001). Cannabinoids attenuate capsaicin-evoked hyperalgesia through spinal and peripheral mechanisms. *Pain* 93(3): 303-315.

Jones GE (2000). Cellular signaling in macrophage migration and chemotaxis. *J Leukoc Biol* 68(5): 593-602.

Jorgensen WL (2004). The many roles of computation in drug discovery. *Science* 303(5665): 1813-1818.

Kato H, Sato S, Yoneyama M, Yamamoto M, Uematsu S, Matsui K*, et al.* (2005). Cell type-specific involvement of RIG-I in antiviral response. *Immunity* 23(1): 19-28.

Kawai T, Akira S (2011). Toll-like Receptors and Their Crosstalk with Other Innate Receptors in Infection and Immunity. *Immunity* 34(5): 637-650.

Kelly E, Bailey CP, Henderson G (2008). Agonist-selective mechanisms of GPCR desensitization. *Br J Pharmacol* 153 Suppl 1: S379-388.

Kenakin T, Miller LJ (2010). Seven transmembrane receptors as shapeshifting proteins: the impact of allosteric modulation and functional selectivity on new drug discovery. *Pharmacol Rev* 62(2): 265-304.

Kenakin TP (2009). Cellular assays as portals to seven-transmembrane receptor-based drug discovery. *Nat Rev Drug Discov* 8(8): 617-626.

Kenakin TP (1985). The quantification of relative efficacy of agonists. *J Pharmacol Methods.* 13(4): 281-308.

Kishimoto S, Gokoh M, Oka S, Muramatsu M, Kajiwara T, Waku K*, et al.* (2003). 2-arachidonoylglycerol induces the migration of HL-60 cells differentiated into macrophage-like cells and human peripheral blood monocytes through the cannabinoid CB2 receptor-dependent mechanism. *J Biol Chem* 278(27): 24469-24475.

Kishimoto S, Kobayashi Y, Oka S, Gokoh M, Waku K, Sugiura T (2004). 2-Arachidonoylglycerol, an Endogenous Cannabinoid Receptor Ligand, Induces Accelerated Production of Chemokines in HL-60 Cells. *J Biochem* 135(4): 517-524.

Kitchen DB, Decornez H, Furr JR, Bajorath J (2004). Docking and scoring in virtual screening for drug discovery: methods and applications. *Nat Rev Drug Discov* 3(11): 935-949.

Klemm P, Harris HJ, Perretti M (1995). Effect of rolipram in a murine model of acute inflammation: comparison with the corticoid dexamethasone. *Eur J Pharmacol* 281(1): 69-74.

Kobayashi Y (2008). The role of chemokines in neutrophil biology. *Front Biosci* 13: 2400-2407.

Kopf M, Bachmann MF, Marsland BJ (2010). Averting inflammation by targeting the cytokine environment. *Nat Rev Drug Discov* 9(9): 703-718.

Kovacs JJ, Hara MR, Davenport CL, Kim J, Lefkowitz RJ (2009). Arrestin development: emerging roles for beta-arrestins in developmental signaling pathways. *Dev Cell.* 17(4): 443-458.

Kraft B, Kress HG (2005). Indirect CB2 receptor and mediator-dependent stimulation of human whole-blood neutrophils by exogenous and endogenous cannabinoids. *J Pharmacol Exp Ther* 315(2): 641-647.

Kruth HS (2001). Macrophage foam cells and atherosclerosis. *Front Biosci* 6: D429-455.

LaBuda CJ, Koblish M, Little PJ (2005). Cannabinoid CB2 receptor agonist activity in the hindpaw incision model of postoperative pain. *Eur J Pharmacol* 527(1-3): 172-174.

Lahoute C, Herbin O, Mallat Z, Tedgui A (2011). Adaptive immunity in atherosclerosis: mechanisms and future therapeutic targets. *Nat Rev Cardiol* 8(6): 348-358.

Laza-Knoerr AL, Gref R, Couvreur P (2010). Cyclodextrins for drug delivery. *Journal of drug targeting* 18(9): 645-656.

Ledent C, Valverde O, Cossu G, Petitet F, Aubert JF, Beslot F*, et al.* (1999). Unresponsiveness to cannabinoids and reduced addictive effects of opiates in CB1 receptor knockout mice. *Science* 283(5400): 401-404.

Lee SF, Newton C, Widen R, Friedman H, Klein TW (2001). Differential expression of cannabinoid CB(2) receptor mRNA in mouse immune cell subpopulations and following B cell stimulation. *Eur J Pharmacol* 423(2-3): 235-241.

Ley K, Bullard DC, Arbones ML, Bosse R, Vestweber D, Tedder TF*, et al.* (1995). Sequential contribution of L- and P-selectin to leukocyte rolling in vivo. *J Exp Med* 181(2): 669-675.

Ley K, Laudanna C, Cybulsky MI, Nourshargh S (2007). Getting to the site of inflammation: the leukocyte adhesion cascade updated. *Nat Rev Immunol* 7(9): 678-689.

Liehn EA, Schober A, Weber C (2004). Blockade of keratinocyte-derived chemokine inhibits endothelial recovery and enhances plaque formation after arterial injury in ApoE-deficient mice. *Arterioscler Thromb Vasc Biol* 24(10): 1891-1896.

Liu JG, Anand KJ (2001). Protein kinases modulate the cellular adaptations associated with opioid tolerance and dependence. *Brain Res Brain Res Rev.* 38(1-2): 1-19.

Liu QR, Pan CH, Hishimoto A, Li CY, Xi ZX, Llorente-Berzal A*, et al.* (2009). Species differences in cannabinoid receptor 2 (CNR2 gene): identification of novel human and rodent CB2 isoforms, differential tissue expression and regulation by cannabinoid receptor ligands. *Genes Brain Behav.* 8(5): 519-530.

Liu Y, Cousin JM, Hughes J, Van Damme J, Seckl JR, Haslett C*, et al.* (1999). Glucocorticoids Promote Nonphlogistic Phagocytosis of Apoptotic Leukocytes. *J Immunol* 162(6): 3639-3646.

Loftsson T, Brewster ME (1996). Pharmaceutical applications of cyclodextrins. 1. Drug solubilization and stabilization. *J Pharm Sci.* 85(10): 1017-1025.

Lozovaya N, Mukhtarov M, Tsintsadze T, Ledent C, Burnashev N, Bregestovski P (2011). Frequency-Dependent Cannabinoid Receptor-Independent Modulation of Glycine Receptors by Endocannabinoid 2-AG. *Front Mol Neurosci.* 4: 13.

Lupica CR, Riegel AC, Hoffman AF (2004). Marijuana and cannabinoid regulation of brain reward circuits. *Br J Pharmacol* 143(2): 227-234.

Luttrell LM (2003). 'Location, location, location': activation and targeting of MAP kinases by G protein-coupled receptors. *J Mol Endocrinol* 30(2): 117-126.

Luttrell LM, Lefkowitz RJ (2002). The role of beta-arrestins in the termination and transduction of G-protein-coupled receptor signals. *J Cell Sci* 115(Pt 3): 455-465.

Ma Y, Wang W, Zhang J, Lu Y, Wu W, Yan H*, et al.* (2012). Hyperlipidemia and atherosclerotic lesion development in Ldlr-deficient mice on a long-term high-fat diet. *PLoS One* 7(4): e35835.

Maderna P, Godson C (2009a). Lipoxins: resolutionary road. *Br J Pharmacol.* 158(4): 947-959.

Maderna P, Godson C (2009b). Lipoxins: resolutionary road. *Br J Pharmacol.* 158(4): 947-959.

Mahley RW, Weisgraber KH, Huang Y (2009). Apolipoprotein E: structure determines function, from atherosclerosis to Alzheimer's disease to AIDS. *J Lipid Res* 50 Suppl: S183-188.

Mailman RB (2007). GPCR functional selectivity has therapeutic impact. *Trends Pharmacol Sci* 28(8): 390-396.

Malan TP, Jr., Ibrahim MM, Deng H, Liu Q, Mata HP, Vanderah T*, et al.* (2001). CB2 cannabinoid receptor-mediated peripheral antinociception. *Pain* 93(3): 239-245.

Mantovani A, Sozzani S, Locati M, Allavena P, Sica A (2002). Macrophage polarization: tumor-associated macrophages as a paradigm for polarized M2 mononuclear phagocytes. *Trends Immunol* 23(11): 549-555.

Maresz K, Carrier EJ, Ponomarev ED, Hillard CJ, Dittel BN (2005). Modulation of the cannabinoid CB2 receptor in microglial cells in response to inflammatory stimuli. *J Neurochem* 95(2): 437-445.

Maresz K, Pryce G, Ponomarev ED, Marsicano G, Croxford JL, Shriver LP*, et al.* (2007). Direct suppression of CNS autoimmune inflammation via the cannabinoid receptor CB1 on neurons and CB2 on autoreactive T cells. *Nat Med* 13(4): 492-497.

Marfaing-Koka A, Maravic M, Humbert M, Galanaud P, Emilie D (1996). Contrasting effects of IL-4, IL-10 and corticosteroids on RANTES production by human monocytes. *Int Immunol* 8(10): 1587-1594.

Markt P, Feldmann C, Rollinger JM, Raduner S, Schuster D, Kirchmair J*, et al.* (2009). Discovery of novel CB2 receptor ligands by a pharmacophore-based virtual screening workflow. *J Med Chem* 52(2): 369-378.

Matsuda LA, Lolait SJ, Brownstein MJ, Young AC, Bonner TI (1990). Structure of a cannabinoid receptor and functional expression of the cloned cDNA. *Nature* 346(6284): 561-564.

Mauler F, Mittendorf J, Horvath E, De Vry J (2002). Characterization of the diarylether sulfonylester (-)-(R)-3-(2-hydroxymethylindanyl-4-oxy)phenyl-4,4,4-trifluoro-1-sulfonate (BAY 38-7271) as a potent cannabinoid receptor agonist with neuroprotective properties. *J Pharmacol Exp Ther* 302(1): 359-368.

McGuinness D, Malikzay A, Visconti R, Lin K, Bayne M, Monsma F*, et al.* (2009). Characterizing Cannabinoid CB2 Receptor Ligands Using DiscoveRx PathHunterTM {beta}-Arrestin Assay. *J Biomol Screen* 14(1): 49-58.

McLaughlin RJ, Gobbi G (2012). Cannabinoids and emotionality: a neuroanatomical perspective. *Neuroscience* 204: 134-144.

McPartland JM, Glass M (2003). Functional mapping of cannabinoid receptor homologs in mammals, other vertebrates, and invertebrates. *Gene* 312: 297-303.

Mechoulam R, Ben-Shabat S, Hanus L, Ligumsky M, Kaminski NE, Schatz AR*, et al.* (1995). Identification of an endogenous 2-monoglyceride, present in canine gut, that binds to cannabinoid receptors. *Biochem Pharmacol* 50(1): 83-90.

Melvin LS, Milne GM, Johnson MR, Subramaniam B, Wilken GH, Howlett AC (1993). Structure-activity relationships for cannabinoid receptor-binding and analgesic activity: studies of bicyclic cannabinoid analogs. *Mol Pharmacol* 44(5): 1008-1015.

Mestre L, Correa F, Docagne F, Clemente D, Guaza C (2006). The synthetic cannabinoid WIN 55,212-2 increases COX-2 expression and PGE2 release in murine brain-derived endothelial cells following Theiler's virus infection. *Biochem Pharmacol.* 72(7): 869-880.

Metchnikoff E (1905). Immunity in Infective Diseases. *Book: Eng., Ed. by F. G. Binnie. Cambridge.*

Mikuriya TH (1969). Marijuana in medicine: past, present and future. *California medicine* 110(1): 34-40.

Mills CD, Kincaid K, Alt JM, Heilman MJ, Hill AM (2000). M-1/M-2 macrophages and the Th1/Th2 paradigm. *J Immunol* 164(12): 6166-6173.

Montecucco F, Burger F, Mach F, Steffens S (2008). CB2 cannabinoid receptor agonist JWH-015 modulates human monocyte migration through defined intracellular signaling pathways. *Am J Physiol Heart Circ Physiol* 294(3): H1145-1155.

Moreira FA, Grieb M, Lutz B (2009). Central side-effects of therapies based on CB1 cannabinoid receptor agonists and antagonists: focus on anxiety and depression. *Best Pract Res Clin Endocrinol Metab.* 23(1): 133-144.

Morris DL, Rui L (2009). Recent advances in understanding leptin signaling and leptin resistance. *Am J Physiol Endocrinol Metab.* 297(6): E1247-1259.

Mosser DM, Edwards JP (2008). Exploring the full spectrum of macrophage activation. *Nat Rev Immunol* 8(12): 958-969.

Mukherjee S, Adams M, Whiteaker K, Daza A, Kage K, Cassar S*, et al.* (2004). Species comparison and pharmacological characterization of rat and human CB2 cannabinoid receptors. *Eur J Pharmacol* 505(1-3): 1-9.

Munder M, Eichmann K, Modolell M (1998). Alternative metabolic states in murine macrophages reflected by the nitric oxide synthase/arginase balance: competitive regulation by CD4+ T cells correlates with Th1/Th2 phenotype. *J Immunol* 160(11): 5347-5354.

Munro S, Thomas KL, Abu-Shaar M (1993). Molecular characterization of a peripheral receptor for cannabinoids. *Nature* 365(6441): 61-65.

Murray PJ, Wynn TA (2011). Obstacles and opportunities for understanding macrophage polarization. *J Leukoc Biol* 89(4): 557-563.

Nathan C, Ding A (2010). Nonresolving Inflammation. *Cell* 140(6): 871-882.

Netherland CD, Pickle TG, Bales A, Thewke DP (2010). Cannabinoid receptor type 2 (CB2) deficiency alters atherosclerotic lesion formation in hyperlipidemic Ldlr-null mice. *Atherosclerosis* 213(1): 102-108.

Nikolic T, Dingjan GM, Leenen PJM, Hendriks RW (2002). A subfraction of B220+ cells in murine bone marrow and spleen does not belong to the B cell lineage but has dendritic cell characteristics. *Eur J Immunol.* 32(3): 686-692.

O'Leary DH, Reuwer AQ, Nissen SE, Despres JP, Deanfield JE, Brown MW*, et al.* (2011). Effect of rimonabant on carotid intima-media thickness (CIMT) progression in patients with abdominal obesity and metabolic syndrome: the AUDITOR Trial. *Heart* 97(14): 1143-1150.

Onaivi ES, Ishiguro H, Gong JP, Patel S, Perchuk A, Meozzi PA*, et al.* (2006). Discovery of the presence and functional expression of cannabinoid CB2 receptors in brain. *Ann N Y Acad Sci* 1074: 514-536.

Onaivi ES, Ishiguro H, Gu S, Liu QR (2012). CNS effects of CB2 cannabinoid receptors: beyond neuro-immuno-cannabinoid activity. *J Psychopharmacol* 26(1): 92-103.

Orlu-Gul M, Fisco G, Parmar D, Gill H, Tuleu C (2012). A new reconstitutable oral paediatric hydrocortisone solution containing hydroxypropyl-beta-cyclodextrin. *Drug development and industrial pharmacy*.

Osei-Hyiaman D, DePetrillo M, Pacher P, Liu J, Radaeva S, Batkai S*, et al.* (2005). Endocannabinoid activation at hepatic CB1 receptors stimulates fatty acid synthesis and contributes to diet-induced obesity. *J Clin Invest* 115(5): 1298-1305.

Ostenfeld T, Price J, Albanese M, Bullman J, Guillard F, Meyer I*, et al.* (2011). A Randomized, Controlled Study to Investigate the Analgesic Efficacy of Single Doses of the Cannabinoid Receptor-2 Agonist GW842166, Ibuprofen or Placebo in Patients With Acute Pain Following Third Molar Tooth Extraction. *Clin J Pain.* 27(8): 668-676.

Pacher P, Batkai S, Kunos G (2006). The endocannabinoid system as an emerging target of pharmacotherapy. *Pharmacol Rev* 58(3): 389-462.

Patel S, Hillard CJ (2006). Pharmacological evaluation of cannabinoid receptor ligands in a mouse model of anxiety: further evidence for an anxiolytic role for endogenous cannabinoid signaling. *J Pharmacol Exp Ther* 318(1): 304-311.

Pereira A, Pfeifer TA, Grigliatti TA, Andersen RJ (2009a). Functional cell-based screening and saturation transfer double-difference NMR have identified haplosamate A as a cannabinoid receptor agonist. *ACS Chem Biol.* 4(2): 139-144.

Pereira JP, An J, Xu Y, Huang Y, Cyster JG (2009b). Cannabinoid receptor 2 mediates the retention of immature B cells in bone marrow sinusoids. *Nat Immunol* 10(4): 403-411.

Pertwee RG (2006). Cannabinoid pharmacology: the first 66 years. *Br J Pharmacol* 147 Suppl 1: S163-171.

Pestonjamasp VK, Burstein SH (1998). Anandamide synthesis is induced by arachidonate mobilizing agonists in cells of the immune system. *Biochim Biophys Acta* 1394(2-3): 249-260.

Peter C, Waibel M, Radu CG, Yang LV, Witte ON, Schulze-Osthoff K*, et al.* (2008). Migration to Apoptotic "Find-me" Signals Is Mediated via the Phagocyte Receptor G2A. *J Biol Chem.* 283(9): 5296-5305.

Peters-Golden M (2009). Putting on the brakes: cyclic AMP as a multipronged controller of macrophage function. *Sci Signal.* 2(75): pe37.

Potteaux S, Gautier EL, Hutchison SB, van Rooijen N, Rader DJ, Thomas MJ*, et al.* (2011). Suppressed monocyte recruitment drives macrophage removal from atherosclerotic plaques of Apoe-/- mice during disease regression. *J Clin Invest* 121(5): 2025-2036.

Power CA (2003). Knock out models to dissect chemokine receptor function in vivo. *J Immunol Methods* 273(1-2): 73-82.

Pradhan AA, Walwyn W, Nozaki C, Filliol D, Erbs E, Matifas A*, et al.* (2010). Ligand-directed trafficking of the delta-opioid receptor in vivo: two paths toward analgesic tolerance. *J Neurosci* 30(49): 16459-16468.

Price MR, Baillie GL, Thomas A, Stevenson LA, Easson M, Goodwin R*, et al.* (2005). Allosteric modulation of the cannabinoid CB1 receptor. *Mol Pharmacol* 68(5): 1484-1495.

Prospective Studies C, Lewington S, Whitlock G, Clarke R, Sherliker P, Emberson J*, et al.* (2007). Blood cholesterol and vascular mortality by age, sex, and blood pressure: a meta-analysis of individual data from 61 prospective studies with 55,000 vascular deaths. *Lancet* 370(9602): 1829-1839.

Raborn E, Marciano-Cabral F, Buckley N, Martin B, Cabral G (2008). The Cannabinoid Delta-9-tetrahydrocannabinol Mediates Inhibition of Macrophage Chemotaxis to RANTES/CCL5: Linkage to the CB2 Receptor. *J Neuroimmune Pharmacol.* 3(2): 117-129.

Rajagopal S, Rajagopal K, Lefkowitz RJ (2010). Teaching old receptors new tricks: biasing seven-transmembrane receptors. *Nat Rev Drug Discov* 9(5): 373-386.

Rajavashisth T, Qiao JH, Tripathi S, Tripathi J, Mishra N, Hua M*, et al.* (1998). Heterozygous osteopetrotic (op) mutation reduces atherosclerosis in LDL receptor- deficient mice. *J Clin Invest* 101(12): 2702-2710.

Rajesh M, Mukhopadhyay P, Batkai S, Hasko G, Liaudet L, Huffman JW*, et al.* (2007). CB2-receptor stimulation attenuates TNF-{alpha}-induced human endothelial cell activation, transendothelial migration of monocytes, and monocyte-endothelial adhesion. *Am J Physiol Heart Circ Physiol* 293(4): H2210-2218.

Rajesh M, Mukhopadhyay P, Hasko G, Huffman JW, Mackie K, Pacher P (2008). CB2 cannabinoid receptor agonists attenuate TNF-alpha-induced human vascular smooth muscle cell proliferation and migration. *Br J Pharmacol* 153(2): 347-357.

Ramos CL, Huo Y, Jung U, Ghosh S, Manka DR, Sarembock IJ*, et al.* (1999). Direct demonstration of P-selectin- and VCAM-1-dependent mononuclear cell rolling in early atherosclerotic lesions of apolipoprotein E-deficient mice. *Circ Res* 84(11): 1237-1244.

Rao GK, Zhang W, Kaminski NE (2004). Cannabinoid receptor-mediated regulation of intracellular calcium by D9-tetrahydrocannabinol in resting T cells. *J Leukoc Biol.* 75(5): 884-892.

Ravinet Trillou C, Delgorge C, Menet C, Arnone M, Soubrie P (2004). CB1 cannabinoid receptor knockout in mice leads to leanness, resistance to diet-induced obesity and enhanced leptin sensitivity. *Int J Obes Relat Metab Disord.* 28(4): 640-648.

Reiser R, Sorrels MF, Williams MC (1959). Influence of high levels of dietary fats and cholesterol on atherosclerosis and lipid distribution in swine. *Circ Res* 7: 833-846.

Reitman JS, Mahley RW, Fry DL (1982). Yucatan miniature swine as a model for diet-induced atherosclerosis. *Atherosclerosis* 43(1): 119-132.

Richmond W, Wogan M, Isbell J, Gordon WP (2010). Interstrain differences of in vitro metabolic stability and impact on early drug discovery. *J Pharm Sci.* 99(11): 4463-4468.

Ridker PM, Danielson E, Fonseca FA, Genest J, Gotto AM, Jr., Kastelein JJ*, et al.* (2008). Rosuvastatin to prevent vascular events in men and women with elevated C-reactive protein. *N Engl J Med.* 359(21): 2195-2207.

Riether D, Wu L, Cirillo PF, Berry A, Walker ER, Ermann M*, et al.* (2011). 1,4-Diazepane compounds as potent and selective CB2 agonists: optimization of metabolic stability. *Bioorg Med Chem Lett* 21(7): 2011-2016.

Ripphausen P, Nisius B, Bajorath J (2011). State-of-the-art in ligand-based virtual screening. *Drug Discov Today* 16(9-10): 372-376.

Rollins BJ (1997). Chemokines. *Blood* 90(3): 909-928.

Ross R (1999). Atherosclerosis--an inflammatory disease. *N Engl J Med.* 340(2): 115-126.

Ross RA (2003). Anandamide and vanilloid TRPV1 receptors. *Br J Pharmacol* 140(5): 790-801.

Ross RA (2009). The enigmatic pharmacology of GPR55. *Trends Pharmacol Sci.* 30(3): 156-163.

Ross RA, Brockie HC, Pertwee RG (2000). Inhibition of nitric oxide production in RAW264.7 macrophages by cannabinoids and palmitoylethanolamide. *Eur J Pharmacol.* 401(2): 121-130.

Ross RA, Brockie HC, Stevenson LA, Murphy VL, Templeton F, Makriyannis A*, et al.* (1999). Agonist-inverse agonist characterization at CB1 and CB2 cannabinoid receptors of L759633, L759656, and AM630. *Br J Pharmacol* 126(3): 665-672.

Rossi AG, McCutcheon JC, Roy N, Chilvers ER, Haslett C, Dransfield I (1998). Regulation of macrophage phagocytosis of apoptotic cells by cAMP. *J Immunol* 160(7): 3562-3568.

Rovai LE, Herschman HR, Smith JB (1998). The murine neutrophil-chemoattractant chemokines LIX, KC, and MIP-2 have distinct induction kinetics, tissue distributions, and tissue-specific sensitivities to glucocorticoid regulation in endotoxemia. *J Leukoc Biol* 64(4): 494-502.

Ryan GB, Majno G (1977). Acute inflammation. A review. *Am J Pathol* 86(1): 183-276.

Sacerdote P, Massi P, Panerai AE, Parolaro D (2000). In vivo and in vitro treatment with the synthetic cannabinoid CP55,940 decreases the in vitro migration of macrophages in the rat: involvement of both CB1 and CB2 receptors. *J Neuroimmunol.* 109(2): 155-163.

Salo OM, Raitio KH, Savinainen JR, Nevalainen T, Lahtela-Kakkonen M, Laitinen JT*, et al.* (2005). Virtual screening of novel CB2 ligands using a comparative model of the human cannabinoid CB2 receptor. *J Med Chem* 48(23): 7166-7171.

Santos NC, Figueira-Coelho J, Martins-Silva J, Saldanha C (2003). Multidisciplinary utilization of dimethyl sulfoxide: pharmacological, cellular, and molecular aspects. *Biochem Pharmacol* 65(7): 1035-1041.

Savill J, Dransfield I, Gregory C, Haslett C (2002). A blast from the past: clearance of apoptotic cells regulates immune responses. *Nat Rev Immunol* 2(12): 965-975.

Scannell M, Flanagan MB, deStefani A, Wynne KJ, Cagney G, Godson C*, et al.* (2007). Annexin-1 and Peptide Derivatives Are Released by Apoptotic Cells and Stimulate Phagocytosis of Apoptotic Neutrophils by Macrophages. *J Immunol* 178(7): 4595-4605.

Schaub FJ, Han DK, Liles WC, Adams LD, Coats SA, Ramachandran RK*, et al.* (2000). Fas/FADD-mediated activation of a specific program of inflammatory gene expression in vascular smooth muscle cells. *Nat Med* 6(7): 790-796.

Schebesch C, Kodelja V, Muller C, Hakij N, Bisson S, Orfanos CE*, et al.* (1997). Alternatively activated macrophages actively inhibit proliferation of peripheral blood lymphocytes and CD4+ T cells in vitro. *Immunology* 92(4): 478-486.

Schneider WJ, Kovanen PT, Brown MS, Goldstein JL, Utermann G, Weber W*, et al.* (1981). Familial dysbetalipoproteinemia. Abnormal binding of mutant apoprotein E to low density lipoprotein receptors of human fibroblasts and membranes from liver and adrenal of rats, rabbits, and cows. *J Clin Invest* 68(4): 1075-1085.

Schomberg D, Olson JK (2012). Immune responses of microglia in the spinal cord: contribution to pain states. *Exp Neurol.* 234(2): 262-270.

Schultz RM, Kleinschmidt WJ (1983). Functional identity between murine gamma interferon and macrophage activating factor. *Nature* 305(5931): 239-240.

Schwab JM, Chiang N, Arita M, Serhan CN (2007). Resolvin E1 and protectin D1 activate inflammation-resolution programmes. *Nature* 447(7146): 869-874.

Schwarz H, Blanco FJ, Lotz M (1994). Anadamide, an endogenous cannabinoid receptor agonist inhibits lymphocyte proliferation and induces apoptosis. *J Neuroimmunol* 55(1): 107-115.

Scotland RS, Stables MJ, Madalli S, Watson P, Gilroy DW (2011). Sex differences in resident immune cell phenotype underlie more efficient acute inflammatory responses in female mice. *Blood* 118(22): 5918-5927.

Seimon TA, Wang Y, Han S, Senokuchi T, Schrijvers DM, Kuriakose G*, et al.* (2009). Macrophage deficiency of p38alpha MAPK promotes apoptosis and plaque necrosis in advanced atherosclerotic lesions in mice. *J Clin Invest* 119(4): 886-898.

Senokuchi T, Matsumura T, Sakai M, Matsuo T, Yano M, Kiritoshi S*, et al.* (2004). Extracellular signal-regulated kinase and p38 mitogen-activated protein kinase mediate macrophage proliferation induced by oxidized low-density lipoprotein. *Atherosclerosis* 176(2): 233-245.

Serhan CN, Savill J (2005). Resolution of inflammation: the beginning programs the end. *Nat Immunol* 6(12): 1191-1197.

Sharir H, Abood ME (2010). Pharmacological Characterization of GPR55, A Putative Cannabinoid Receptor. *Pharmacol Ther.* 126(3): 301-313.

Shearer BG, Billin AN (2007). The next generation of PPAR drugs: do we have the tools to find them? *Biochim Biophys Acta* 1771(8): 1082-1093.

Shim JY (2010). Understanding functional residues of the cannabinoid CB1. *Curr Top Med Chem.* 10(8): 779-798.

Shoemaker JL, Ruckle MB, Mayeux PR, Prather PL (2005). Agonist-Directed Trafficking of Response by Endocannabinoids Acting at CB2 Receptors. *J Pharmacol Exp Ther* 315(2): 828-838.

Sigel E, Baur R, Racz I, Marazzi J, Smart TG, Zimmer A*, et al.* (2011). The major central endocannabinoid directly acts at GABA(A) receptors. *Proc Natl Acad Sci U S A* 108(44): 18150-18155.

Silva MT (2010). When two is better than one: macrophages and neutrophils work in concert in innate immunity as complementary and cooperative partners of a myeloid phagocyte system. *J Leukoc Biol* 87(1): 93-106.

Slipetz DM, O'Neill GP, Favreau L, Dufresne C, Gallant M, Gareau Y*, et al.* (1995). Activation of the human peripheral cannabinoid receptor results in inhibition of adenylyl cyclase. *Mol Pharmacol* 48(2): 352-361.

Smith JA (1994). Neutrophils, host defense, and inflammation: a double-edged sword. *J Leukoc Biol.* 56(6): 672-686.

Smith PB, Compton DR, Welch SP, Razdan RK, Mechoulam R, Martin BR (1994). The pharmacological activity of anandamide, a putative endogenous cannabinoid, in mice. *J Pharmacol Exp Ther* 270(1): 219-227.

Smith SR, Denhardt G, Terminelli C (2001). The anti-inflammatory activities of cannabinoid receptor ligands in mouse peritonitis models. *Eur J Pharmacol.* 432(1): 107-119.

Soehnlein O, Lindbom L (2010). Phagocyte partnership during the onset and resolution of inflammation. *Nat Rev Immunol* 10(6): 427-439.

Soehnlein O, Zernecke A, Eriksson EE, Rothfuchs AG, Pham CT, Herwald H*, et al.* (2008). Neutrophil secretion products pave the way for inflammatory monocytes. *Blood* 112(4): 1461-1471.

Song ZH, Bonner TI (1996). A lysine residue of the cannabinoid receptor is critical for receptor recognition by several agonists but not WIN55212-2. *Mol Pharmacol* 49(5): 891-896.

Song ZH, Feng W (2002). Absence of a conserved proline and presence of a conserved tyrosine in the CB2 cannabinoid receptor are crucial for its function. *FEBS Lett* 531(2): 290-294.

Song ZH, Slowey CA, Hurst DP, Reggio PH (1999). The difference between the CB(1) and CB(2) cannabinoid receptors at position 5.46 is crucial for the selectivity of WIN55212-2 for CB(2). *Mol Pharmacol* 56(4): 834-840.

Steffens S, Pacher P (2012). Targeting cannabinoid receptor CB(2) in cardiovascular disorders: promises and controversies. *Br J Pharmacol* 167(2): 313-323.

Steffens S, Veillard NR, Arnaud C, Pelli G, Burger F, Staub C*, et al.* (2005). Low dose oral cannabinoid therapy reduces progression of atherosclerosis in mice. *Nature* 434(7034): 782-786.

Strickley RG (2004). Solubilizing excipients in oral and injectable formulations. *Pharm Res.* 21(2): 201-230.

Sugamura K, Sugiyama S, Nozaki T, Matsuzawa Y, Izumiya Y, Miyata K*, et al.* (2009). Activated Endocannabinoid System in Coronary Artery Disease and Antiinflammatory Effects of Cannabinoid 1 Receptor Blockade on Macrophages. *Circulation* 119(1): 28-36.

Sugiura T, Kodaka T, Nakane S, Kishimoto S, Kondo S, Waku K (1998). Detection of an endogenous cannabimimetic molecule, 2-arachidonoylglycerol, and cannabinoid CB1

receptor mRNA in human vascular cells: is 2-arachidonoylglycerol a possible vasomodulator? *Biochem Biophys Res Commun* 243(3): 838-843.

Sukumar N, Das S (2011). Current trends in virtual high throughput screening using ligand-based and structure-based methods. *Comb Chem High Throughput Screen.* 14(10): 872-888.

Swaminath G, Deupi X, Lee TW, Zhu W, Thian FS, Kobilka TS*, et al.* (2005). Probing the beta2 adrenoceptor binding site with catechol reveals differences in binding and activation by agonists and partial agonists. *J Biol Chem* 280(23): 22165-22171.

Swirski FK, Libby P, Aikawa E, Alcaide P, Luscinskas FW, Weissleder R*, et al.* (2007). Ly-6Chi monocytes dominate hypercholesterolemia-associated monocytosis and give rise to macrophages in atheromata. *J Clin Invest* 117(1): 195-205.

Szabo G, Kiss R, Payer-Lengyel D, Vukics K, Szikra J, Baki A*, et al.* (2009). Hit-to-lead optimization of pyrrolo[1,2-a]quinoxalines as novel cannabinoid type 1 receptor antagonists. *Bioorg Med Chem Lett* 19(13): 3471-3475.

Tabas I (2004). Apoptosis and plaque destabilization in atherosclerosis: the role of macrophage apoptosis induced by cholesterol. *Cell Death Differ.* 11 Suppl 1: S12-16.

Tacke F, Alvarez D, Kaplan TJ, Jakubzick C, Spanbroek R, Llodra J*, et al.* (2007). Monocyte subsets differentially employ CCR2, CCR5, and CX3CR1 to accumulate within atherosclerotic plaques. *J Clin Invest* 117(1): 185-194.

Takahashi M, Galligan C, Tessarollo L, Yoshimura T (2009). Monocyte chemoattractant protein-1 (MCP-1), not MCP-3, is the primary chemokine required for monocyte recruitment in mouse peritonitis induced with thioglycollate or zymosan A. *J Immunol* 183(5): 3463-3471.

Topol EJ, Bousser MG, Fox KA, Creager MA, Despres JP, Easton JD*, et al.* (2010). Rimonabant for prevention of cardiovascular events (CRESCENDO): a randomised, multicentre, placebo-controlled trial. *Lancet* 376(9740): 517-523.

Urban JD, Clarke WP, von Zastrow M, Nichols DE, Kobilka B, Weinstein H*, et al.* (2007). Functional Selectivity and Classical Concepts of Quantitative Pharmacology. *J Pharmacol Exp Ther.* 320(1): 1-13.

Vachal P, Fletcher JM, Fong TM, Huang CC, Lao J, Xiao JC*, et al.* (2009). 1-Sulfonyl-4-acylpiperazines as selective cannabinoid-1 receptor (CB1R) inverse agonists for the treatment of obesity. *J Med Chem* 52(8): 2550-2558.

Valenzano KJ, Tafesse L, Lee G, Harrison JE, Boulet JM, Gottshall SL*, et al.* (2005). Pharmacological and pharmacokinetic characterization of the cannabinoid receptor 2 agonist, GW405833, utilizing rodent models of acute and chronic pain, anxiety, ataxia and catalepsy. *Neuropharmacology* 48(5): 658-672.

van der Meer IM, de Maat MP, Bots ML, Breteler MM, Meijer J, Kiliaan AJ*, et al.* (2002). Inflammatory mediators and cell adhesion molecules as indicators of severity of atherosclerosis: the Rotterdam Study. *Arterioscler Thromb Vasc Biol* 22(5): 838-842.

van Furth R, Cohn ZA (1968). The origin and kinetics of mononuclear phagocytes. *J Exp Med* 128(3): 415-435.

Van Gaal LF, Rissanen AM, Scheen AJ, Ziegler O, Rossner S, Group RI-ES (2005). Effects of the cannabinoid-1 receptor blocker rimonabant on weight reduction and cardiovascular risk factors in overweight patients: 1-year experience from the RIO-Europe study. *Lancet* 365(9468): 1389-1397.

van Gils JM, Derby MC, Fernandes LR, Ramkhelawon B, Ray TD, Rayner KJ*, et al.* (2012). The neuroimmune guidance cue netrin-1 promotes atherosclerosis by inhibiting the emigration of macrophages from plaques. *Nat Immunol* 13(2): 136-143.

Varga K, Wagner JA, Bridgen DT, Kunos G (1998). Platelet- and macrophage-derived endogenous cannabinoids are involved in endotoxin-induced hypotension. *FASEB J.* 12(11): 1035-1044.

Varin A, Gordon S (2009). Alternative activation of macrophages: Immune function and cellular biology. *Immunobiology* 214(7): 630-641.

Virchow R (1856). Phlogose und Thrombose in Gefassystem, gesammelte Abhandlungen zur wissenschaftlichen Medicin *Meidinger, Frankfurt-am-Main*: 458.

Wall EA, Zavzavadjian JR, Chang MS, Randhawa B, Zhu X, Hsueh RC*, et al.* (2009). Suppression of LPS-induced TNF-alpha production in macrophages by cAMP is mediated by PKA-AKAP95-p105. *Sci Signal.* 2(75): ra28.

Wang M, Krauss JL, Domon H, Hosur KB, Liang S, Magotti P*, et al.* (2010). Microbial hijacking of complement-toll-like receptor crosstalk. *Sci Signal.* 3(109): ra11.

Weissman A, Milne GM, Melvin LS, Jr. (1982). Cannabimimetic activity from CP-47,497, a derivative of 3-phenylcyclohexanol. *J Pharmacol Exp Ther* 223(2): 516-523.

White GE, McNeill E, Christou I, Channon KM, Greaves DR (2011). Site-Directed Mutagenesis of the CC Chemokine Binding Protein 35K-Fc Reveals Residues Essential for Activity and Mutations That Increase the Potency of CC Chemokine Blockade. *Mol Pharmacol.* 80(2): 328-336.

White GE, Tan TC, John AE, Whatling C, McPheat WL, Greaves DR (2010). Fractalkine has anti-apoptotic and proliferative effects on human vascular smooth muscle cells via epidermal growth factor receptor signalling. *Cardiovasc Res* 85(4): 825-835.

Whyte LS, Ryberg E, Sims NA, Ridge SA, Mackie K, Greasley PJ*, et al.* (2009). The putative cannabinoid receptor GPR55 affects osteoclast function in vitro and bone mass in vivo. *Proc Natl Acad Sci U S A* 106(38): 16511-16516.

Wiktor-Jedrzejczak WW, Ahmed A, Szczylik C, Skelly RR (1982). Hematological characterization of congenital osteopetrosis in op/op mouse. Possible mechanism for abnormal macrophage differentiation. *J Exp Med* 156(5): 1516-1527.

Willecke F, Zeschky K, Ortiz Rodriguez A, Colberg C, AuwÃ¤rter V, Kneisel S*, et al.* (2011). Cannabinoid Receptor 2 Signaling Does Not Modulate Atherogenesis in Mice. *PLoS One* 6(4): e19405.

Williams C (2004). cAMP detection methods in HTS: selecting the best from the rest. *Nat Rev Drug Discov* 3(2): 125-135.

Williams MR, Azcutia V, Newton G, Alcaide P, Luscinskas FW (2011). Emerging mechanisms of neutrophil recruitment across endothelium. *Trends Immunol* 32(10): 461-469.

Wilson KJ, Gilmore JL, Foley J, Lemmon MA, Riese DJ, 2nd (2009). Functional selectivity of EGF family peptide growth factors: implications for cancer. *Pharmacol Ther* 122(1): 1-8.

Wink DA, Hines HB, Cheng RY, Switzer CH, Flores-Santana W, Vitek MP*, et al.* (2011). Nitric oxide and redox mechanisms in the immune response. *J Leukoc Biol* 89(6): 873-891.

Wintergerst ES, Jelk J, Rahner C, Asmis R (2000). Apoptosis induced by oxidized low density lipoprotein in human monocyte-derived macrophages involves CD36 and activation of caspase-3. *Eur J Biochem* 267(19): 6050-6059.

Witting A, Walter L, Wacker J, Moller T, Stella N (2004). P2X7 receptors control 2-arachidonoylglycerol production by microglial cells. *Proc Natl Acad Sci U S A* 101(9): 3214-3219.

Wotherspoon G, Fox A, McIntyre P, Colley S, Bevan S, Winter J (2005). Peripheral nerve injury induces cannabinoid receptor 2 protein expression in rat sensory neurons. *Neuroscience* 135(1): 235-245.

Xiong W, Cui T, Cheng K, Yang F, Chen S-R, Willenbring D*, et al.* (2012). Cannabinoids suppress inflammatory and neuropathic pain by targeting α3 glycine receptors. *J Exp Med.* 209(6): 1121-1134.

Yan YX, Boldt-Houle DM, Tillotson BP, Gee MA, D'Eon BJ, Chang XJ*, et al.* (2002). Cell-based high-throughput screening assay system for monitoring G protein-coupled receptor activation using beta-galactosidase enzyme complementation technology. *J Biomol Screen* 7(5): 451-459.

Yano M, Matsumura T, Senokuchi T, Ishii N, Motoshima H, Taguchi T*, et al.* (2007). Troglitazone inhibits oxidized low-density lipoprotein-induced macrophage proliferation: impact of the suppression of nuclear translocation of ERK1/2. *Atherosclerosis* 191(1): 22-32.

Yao BB, Hsieh GC, Frost JM, Fan Y, Garrison TR, Daza AV*, et al.* (2008). In vitro and in vivo characterization of A-796260: a selective cannabinoid CB2 receptor agonist exhibiting analgesic activity in rodent pain models. *Br J Pharmacol* 153(2): 390-401.

Yao BB, Mukherjee S, Fan Y, Garrison TR, Daza AV, Grayson GK*, et al.* (2006). In vitro pharmacological characterization of AM1241: a protean agonist at the cannabinoid CB2 receptor? *Br J Pharmacol* 149(2): 145-154.

Yiangou Y, Facer P, Durrenberger P, Chessell IP, Naylor A, Bountra C*, et al.* (2006). COX-2, CB2 and P2X7-immunoreactivities are increased in activated microglial cells/macrophages of multiple sclerosis and amyotrophic lateral sclerosis spinal cord. *BMC neurology* 6: 12.

Zhang B, Ma Y, Guo H, Sun B, Niu R, Ying G*, et al.* (2009). Akt2 is required for macrophage chemotaxis. *Eur J Immunol* 39(3): 894-901.

Zhang R, Xie X (2012). Tools for GPCR drug discovery. *Acta Pharmacol Sin* 33(3): 372-384.

Zhang SH, Reddick RL, Piedrahita JA, Maeda N (1992). Spontaneous hypercholesterolemia and arterial lesions in mice lacking apolipoprotein E. *Science* 258(5081): 468-471.

Zhang XW, Liu Q, Wang Y, Thorlacius H (2001). CXC chemokines, MIP-2 and KC, induce P-selectin-dependent neutrophil rolling and extravascular migration in vivo. *Br J Pharmacol* 133(3): 413-421.

Zhao Y, Liu Y, Zhang W, Xue J, Wu YZ, Xu W*, et al.* (2010a). WIN55212-2 ameliorates atherosclerosis associated with suppression of proinflammatory responses in ApoE-knockout mice. *Eur J Pharmacol.* 649(1-3): 285-292.

Zhao Y, Yuan Z, Liu Y, Xue J, Tian Y, Liu W*, et al.* (2010b). Activation of Cannabinoid CB2 Receptor Ameliorates Atherosclerosis Associated with Suppression of Adhesion Molecules. *J Cardiovasc Pharmacol* 55(3): 292-298.

Zheng Z-M, Specter SC (1996). Delta-9-tetrahydrocannabinol suppresses tumor necrosis factor [alpha] maturation and secretion but not its transcription in mouse macrophages. *Int J Immunopharmacol.* 18(1): 53-68.

Zhou X, Yin Z, Guo X, Hajjar DP, Han J (2010). Inhibition of ERK1/2 and activation of liver X receptor synergistically induce macrophage ABCA1 expression and cholesterol efflux. *J Biol Chem* 285(9): 6316-6326.

Zhu W, Friedman H, Klein TW (1998). Delta 9-Tetrahydrocannabinol Induces Apoptosis in Macrophages and Lymphocytes: Involvement of Bcl-2 and Caspase-1. *J Pharmacol Exp Ther* 286(2): 1103-1109.

Zimmer A, Valjent E, Konig M, Zimmer AM, Robledo P, Hahn H*, et al.* (2001). Absence of delta -9-tetrahydrocannabinol dysphoric effects in dynorphin-deficient mice. *J Neurosci* 21(23): 9499-9505.

Zimmer A, Zimmer AM, Hohmann AG, Herkenham M, Bonner TI (1999). Increased mortality, hypoactivity, and hypoalgesia in cannabinoid CB1 receptor knockout mice. *Proc Natl Acad Sci U S A* 96(10): 5780-5785.

Zindell R, Walker ER, Scott J, Amouzegh P, Wu L, Ermann M*, et al.* (2011). Aryl 1,4-diazepane compounds as potent and selective CB2 agonists: optimization of drug-like properties and target independent parameters. *Bioorg Med Chem Lett* 21(14): 4276-4280.

Ziring D, Wei B, Velazquez P, Schrage M, Buckley NE, Braun J (2006). Formation of B and T cell subsets require the cannabinoid receptor CB2. *Immunogenetics* 58(9): 714-725.

Zoerner AA, Gutzki FM, Batkai S, May M, Rakers C, Engeli S*, et al.* (2011). Quantification of endocannabinoids in biological systems by chromatography and mass spectrometry: a comprehensive review from an analytical and biological perspective. *Biochim Biophys Acta* 1811(11): 706-723.

APPENDIX 1: Solutions

Chemotaxis Buffer: 0.25 % BSA, 25 mM HEPES, RPMI 1640

BMDM media: 10% FCS, 15% L929 media, 2 mM Glutamine, Penicillin/ Streptomycin (P/S), RPMI 1640

Culture media for mRNA: OptiMEM® + P/S + 2mM Glutamine

DextrinSolve: 45% 2-hydroxylpropyl cyclodextrin in PBS. The solution of compound and DextrinSolve was warmed up for 30 minutes in a 37^{o}C water bath and then sonicated in pulses of 5 minutes in a 37^{o}C water bath until a homogenous solution was obtained.

FACS buffer 1: 2% FCS, 5mM EDTA, 25mM HEPES in PBS

FACS Buffer 2 (*in vivo*): 5% heat-inactivated rabbit serum, 0.5% BSA, 5 mM EDTA, 2mM NaN_3 in PBS

ELISA wash buffer: 0.05% Tween® 20 in PBS

ELISA dilution and blocking buffer: 1% BSA in PBS

(4x) Loading Dye (Laemmli Buffer): 63 mM Tris-HCl (pH 6.8), 10% glycerol, 2% SDS, 5% 2-mercaptoethanol, few grains of bromophenol blue

MACS Buffer: 2 mM EDTA, 0.5 % BSA in PBS

Western blot lysis buffer: 150 mM NaCl, 0.8 mM $MgCl_2$, 5 mM EGTA, 50 mM HEPES. Immediately before use: 1 tablet of protease inhibitor cocktail (Table 2.3)

was added to 10 ml of Lysis buffer. 1% IGEPAL (CA-630), 1% Phosphatase inhibitor cocktail 2 were then added to the required volume (Table 2.3)

(5x) Running Buffer: 0.24 M Tris (base), 1.86 M glycine, 1% SDS

(10x) Transfer Buffer: 0.24 M Tris (base), 1.92M glycine

Stripping Buffer: 67 mM Tris (base), 2 % SDS, 100 mM β-mercaptoethanol

TBS-T: 10 mM Tris-HCl, 68 mM NaCl, 0.05% Tween® 20, pH 7.5